Universidade do Minho
Escola de Engenharia

Carla Filipa Melo Silva Antunes

Dynamic Vulcanisation of EPDM/PP blends: Effect of Viscosity Ratio, Composition and Cross-linking on Morphology Development

Agosto de 2010

Dynamic Vulcanisation of EPDM/PP blends: Effect of Viscosity Ratio, Composition and Cross-linking on Morphology Development
Carla Filipa Melo Silva Antunes
UMinho | 2010


POPH


QUADRO
DE REFERÊNCIA
ESTRATÉGICO
NACIONAL
PORTUGAL 2007.2013


UNIÃO EUROPEIA
Fundo Social Europeu

Universidade do Minho
Escola de Engenharia

Carla Filipa Melo Silva Antunes

Dynamic Vulcanisation of EPDM/PP blends: Effect of Viscosity Ratio, Composition and Cross-linking on Morphology Development

Tese de Doutoramento
Ciência e Tecnologia de Materiais

Trabalho efectuado sob a orientação da
Professora Doutora Ana Vera Machado

Agosto de 2010

To my daughter

Ana

"Nada na vida deve ser receado. Tem apenas que ser compreendido".

Marie Curie (1867-1934)

ACKNOWLEDGEMENTS

The work presented here was carried out between 2005 and 2010 in the Department of Polymer Engineering of the University of Minho. Its conclusion would not have been possible without the support of several persons and institutions, which I am and will be always very grateful.

I start by expressing my gratitude to my supervisor, Ana Vera Machado, without whom I would never be able to go so far. "Many Thanks!" for your dedication, support, suggestions and our countless meetings!

To Martin van Duin for all the support, scientific guidance and valuable suggestions. Thanks!! I am also grateful for all his effort to make my stay at DSM Research as best as possible.

To DSM Research where part of this work was performed, for the facilities, equipment provided and the kind hospitality.

I would like to thank António Gaspar Cunha that, in the beginning of this journey, seriously enriched my familiarity with his insightful conversations on polymer engineering.

To my colleague Jorge Silva that shared his *know how* on rheology and gave me all the technical support in the rheology laboratory.

To my colleagues that work with me in the department, along these 5 years. We share good and less good moments. I would like to thank Patrícia, José Carlos, Célio, Marta, Nuno, Cristina, Fátima, Sílvia and Sílvia Santos.

To academic staff, researchers, technicians and administrative staff of the Department of Polymer Engineering of the University of Minho that aided me along this journey. My special "Thanks!" to our technician João Paulo and Mauricio.

I want also to acknowledge the technical support given by Elsa Ribeiro and Nuno Martins, for SEM and Pierre Alcouffe for TEM analysis.

I hereby acknowledge Fundação para a Ciência e Tecnologia, for financial support through the PhD grant (SFRH/BD/ 19536/2004) and scientific project (PPCDT /CTM/60454/2004).

I desire to express my deepest gratitude to my special friend, Sónia. She is the friend for all moments, with whom I shared ideas, opinions, victories, but also my concerns and disappointments. And when I have most needed, she was always there for encouraging and supporting. Thanks for being around!

I would like to thank my family, especially to my mother for her concern and love. And also to my father, his strength and remarkable capacity to go through the difficulties in life have been a great reference in my entire life.

At least I would like to dedicate one chapter of this thesis to express my gratefulness to someone extremely special to me. So, thank you Pedro for your true love!

Finally, to my beloved daughter that, without knowing it, helped me so much with her ability to convert my bad moments to good ones with her smile and shine!

Dynamic Vulcanisation of EPDM/PP Blends: Effect of Viscosity Ratio, Composition and Cross-linking on Morphology Development

ABSTRACT

Thermoplastic vulcanisates (TPVs) are the most magnificent examples of immiscible polymer blends. These materials exhibit the performance of thermoset rubber along with the processability and recyclability of thermoplastic polymers. Their final morphology consists of finely dispersed cross-linked rubber particles in a thermoplastic matrix. The rubber is cross-linked as it melts and mixes with the thermoplastic phase, which is known as dynamic vulcanisation. EPDM/PP – based TPVs have become the most commercial thermoplastic elastomer due to the structural compatibility of the EPDM and PP, which allow to achieve fine morphologies without compatibilisation.

The high performance of the TPVs depends mainly on the cross-linking degree and final morphology. Controlling/understanding both parameters and their intrinsic relationship is required to optimize the dynamic vulcanisation process and the product properties.

The main goal of this thesis is to obtain new insights into chemical and physical phenomena that occur during TPV production. The morphology development mechanism and its relationship with the cross-linking reaction, composition and viscosity ratio are emphasized.

Several EPDM/PP blends and respective TPVs with different weight ratios, in a range of viscosity ratios between 1.6×10^{-3} and 3.6×10^{2}, were prepared in a Haake batch mixer under the same operation conditions using resole/$SnCl_2.2H_2O$ as cross-linking agents. The morphology of the collected samples was studied by scanning and/or transmission electron microscopy and, in the case of blends, the co-continuity was determined by extraction. The cross-linking degree was evaluate by measurements of EPDM gel content and equilibrium swelling degree.

The morphological results obtained for all blends and TPVs allowed to make phase morphology diagrams, which contains the phase inversion region as a function of EPDM/PP viscosity ratio and composition. Several semi-empirical and empirical models, developed to predict the phase inversion composition of immiscible blends, were applied to the experimental results of EPDM/PP blends. These models were not able to predict the phase inversion composition, especially at very low viscosity ratios. Therefore, a new empirical model that fits the experimental data was developed. While the phase inversion composition

of the EPDM/PP blends depends on both composition and viscosity ratio, the phase inversion composition of TPVs is mainly determined by the composition.

A typical EPDM/PP TPV morphology (where the EPDM is dispersed in the PP phase) was obtained in the range of all EPDM/PP viscosity ratios used for TPVs with 70 and 50 wt. % of PP and only at very low viscosity ratios for TPVs with 30 wt. % of PP. Thus, it was shown that phase inversion occurs even at very low viscosity ratios. These results suggest that phase inversion is not only a consequence of cross-linking but also a result of the melt elasticity difference between PP and EPDM phases.

When very low Mw EPDM was used, the cross-linking reaction was slowdown when compared to the reaction with high Mw EPDM. Consequently, it was possible to monitor the morphology development, which allowed to establish a morphological mechanism during dynamic vulcanization, including the phase inversion process.

Vulcanização Dinâmica de misturas de EPDM/PP: Efeito da Razão de Viscosidades, da Composição e da Reticulação no Desenvolvimento Morfológico

RESUMO

Os Termoplásticos Vulcanizados (TPVs) são um exemplo de sucesso de materiais preparados a partir da mistura de polímeros imiscíveis. Os Termoplásticos Vulcanizados combinam o desempenho das borrachas com a facilidade de processamento e a reciclabilidade dos polímeros termoplásticos. Esta característica, está relacionada com a morfologia destes materiais, que consiste em pequenas partículas de borracha reticulada dispersas numa matriz termoplástica. A reticulação da borracha ocorre durante o processamento, em simultâneo com a mistura desta com o termoplástico, processo que se designa por vulcanização dinâmica. Os TPVs produzidos a partir das misturas destes materiais (EPDM e PP) são os mais usados comercialmente, devido à compatibilidade entre PP e EPDM, que permite atingir morfologias finas sem recorrer à compatibilização química.

O elevado desempenho dos TPVs dependente, principalmente, do grau de reticulação do elastómero e da morfologia final. Desta forma, o controlo/conhecimento destes parâmetros e da sua relação intrínseca é essencial para optimizar o processo produtivo. Assim, este trabalho tem como objectivo aprofundar os conhecimentos sobre os fenómenos químicos e físicos que ocorrem durante a produção dos TPVs. Mais especificamente, é estudado o desenvolvimento morfológico e a sua relação com a reacção de reticulação, a composição e a razão de viscosidades.

Misturas com diferentes percentagem de EPDM/PP, com e sem reticulação do EPDM, numa gama de razões de viscosidade entre $1{,}6 \times 10^{-3}$ - $3{,}6 \times 10^{2}$, foram preparadas num misturador intensivo nas mesmas condições de processamento, usando como sistema de reticulação resole/$SnCl_2.2H_2O$. A morfologia das amostras recolhidas foi analisada através da microscopia electrónica de varrimento e/ou transmissão. A co-continuidade das misturas físicas foi também estudada por extracção de uma das fases utilizando solventes adequados. O grau de reticulação do EPDM foi estimado através de ensaios de determinação de conteúdo gel e inchamento.

Os resultados obtidos para as várias misturas de EPDM/PP, com e sem reticulação do EPDM, com diferentes composições e razões de viscosidades, permitiram construir diagramas de morfologia, expressos através da razão da viscosidade em função da composição da mistura, onde é evidenciada a região de inversão de fase. Aos resultados experimentais obtidos para as

misturas de EPDM/PP foram ajustados alguns modelos semi-empíricos e empíricos existentes na literatura, os quais foram desenvolvidos para prever a composição à qual ocorre a inversão de fase. Verificou-se que nenhum dos modelos disponíveis se ajusta satisfatoriamente aos resultados experimentais, sendo os desvios mais acentuados para razões de viscosidades mais baixas. Por isso, desenvolveu-se uma nova relação empírica, que se ajustasse satisfatoriamente aos resultados experimentais, para a determinação da composição à qual inversão de fase ocorre em função da razão de viscosidades. No caso dos TPVs constatou-se que a composição à qual ocorre a inversão de fase é, praticamente, independente da razão de viscosidades e dependendo apenas da composição da mistura.

Para os TPVs preparados com composições de 70 e 50 % em massa de PP, a morfologia típica dos TPVs (EPDM disperso numa matriz de PP) foi observada em toda a gama de razões de viscosidades. No caso da composição com 30 % de PP, esta morfologia foi obtida apenas para razões de viscosidade muito baixas. Estes resultados evidenciam, ao contrário do que seria de esperar, que a inversão de fase pode ocorrer para razões de viscosidade muito baixas. Isto sugere que a inversão de fases não é apenas favorecida pela reticulação do EPDM, mas também pela significativa diferença de elasticidade entre as fases do PP e do EPDM.

Verificou-se ainda, que o uso de um EPDM de massa molecular muito baixa diminuiu a progressão da reacção de reticulação relativamente a um EPDM de massa molecular elevada. Consequentemente, o desenvolvimento da morfologia durante o processo de vulcanização dinâmica do EPDM de massa molecular muito baixa foi mais lento, o que permitiu a sua monitorização. Deste modo, foi possível propor um mecanismo de desenvolvimento morfológico, que inclui o processo de inversão fase, durante a vulcanização dinâmica.

CONTENTS

LIST OF ABBREVIATION AND SYMBOLS

Abbreviations

ACM	Acrylate rubber
ABS	Acrylonitrile butadiene styrene
AFM	Atomic force microscopy
BR	Butadiene rubber
CM	Chlorinated polyethylene
CR	Polychloroprene
^{13}C-NMR	Carbon-13 nuclear magnetic resonance
DCPD	Dicyclopentadiene
E-EA-MA	Ethylene-ethyl acrylate-maleic anhydride terpolymer
EMA	Ethylenemaleic anhydride copolymer
E-MA-GMA	Ethylene–methyl acrylate–glycidyl methacrylate terpolymer
EPDM	Ethylene - propylene diene monomer
EPM	Ethylene - propylene monomer
EPR	Ethylene propylene rubber
ENB	Ethylidene norbornene
EVA	Ethylene vinyl acetate
EPDM-g-MA	Maleic anhydride grafting in ethylene–propylene diene monomer
EDS	Energy Dispersive X-ray Spectroscopy
FIB	Focused ion beam
HD	1,4-hexadiene
HPC	Hydroxypropylcellulose
HDPE	High density polyethylene
IIR	Butyl rubber
LVSEM	Low voltage scanning electron microscopy
Mw	Molecular Weight
MFI	Melt flow index
NR	Natural rubber
NBR	Nitrile rubber
PP	Polypropylene
PVC	Polyvinyl chloride
PE	Polyethylene
PS	Polystyrene
PMMA	Polymethyl methacrylate
PBT	Polybutylene terephthalate
PA	Polyamide
PC	Polycarbonate
PVDF	Polyvinylidene fluoride
PSAN	Poly(styrene-co-acrylonitrile)
PDMS	Polydimethylsiloxane
PET	Polyethylene terephthalate

phr	Parts per hundred
rpm	Rotation per minute
BC	Styrene block-copolymer
SBR	Styrene-butadiene-rubber
SAN	Styrene acrylonitrile
SEM	Scanning electron microscopy
SEM-BSE	Scanning electron microscopy back-scattering mode
TPEt	Polyether block-copolymer
TPE	Thermoplastic elastomer
TPV	Thermoplastic vulcanisate
TPU	Thermoplastic polyurethane
TPA	Thermoplastic polyamide
TPO	Thermoplastic olefin
TEM	Transmission electron microscopy
TMAFM	Tapping mode atomic force microscopy
VNB	Vinylidene norbornene
vol.%	Volume fractions in percentage
wt.%	Weight fraction in percentage

Symbols

Ca	Capillary number
Ca_{cr}	Critical capillary number
cc_{EPDM}	Co-continuity index of the EPDM phase
f_1	Frequency of droplet breakup
g	Gear ratio
l	Distortion wavelength
M	Consistency of polymer
n	Power law index
$N_{2,d}$	Second normal stress difference of the dispersed phase
$N_{2,m}$	Second normal stress difference of the matrix
$N_{1,d}$	First normal stress difference of the dispersed phase
$N_{1,m}$	First normal stress difference of the matrix
Nc	Critical entanglement spacing
$p_{G'}$	Storage modulus ratio
$p_{tan\delta}$	Loss angle ratio
$p_{G''}$	Loss modulus ratio
q	Growth rate parameter of the sinusoidal distortion
R	Droplet radius
R_0	Minimum filament radius
Ri	Effective hydrodynamic radius
Re	Chamber internal radius
w_i	Weight of the EPDM phase present in the original blend
w_f	Weight of the EPDM phase in the sample after solvent extraction

$\tan \delta_i$	Loss angle
t	Time
R_0	Initial thread radius
ΔGm	Free mixing energy
ø	Composition
ΔS_m	Mixing entropy
ΔH_m	Mixing enthalpy
ϕ_{disp}	Volume fraction of the minor component
ϕ_d	Volume fraction of the dispersed phase
ϕ_m	Volume fraction of the matrix
ϕcr	Critical volume fraction
Φ_i	Co-continuity index or degree of co-continuity
η_m	Matrix viscosity
η_d	Viscosity of the dispersed phase
λ	Viscosity ratio
$\dot{\gamma}$	Shear rate
σ	Interfacial tension
σ^*	Dynamic interfacial tension
η_b	Blend viscosity
θ	Probability of droplets coalesce after collision
Δγ	Wetting surface tension difference
ϕc	Fraction of thermoplastic cristallinity
τ(t)	Shear stress
$\eta^r(t)$	Shear viscosity of the reactive system
$\eta_e{}^r(t)$	Elongational viscosity of the reactive system
σ(t)	Elongation stress
$\dot{\varepsilon}$	Strain rate
ϕ_{PI}	Volume fraction at phase inversion
ϕ_m	Maximum packing volume fraction
Γ	Torque
$[\eta]$	Intrinsic viscosity
$G'_i(\omega)$	Storage modulus
α	Distortion amplitude
α_0	Amplitude of initial distortion
$\Omega(l, \lambda)$	Tomokita function

LIST OF FIGURES

Chapter 1

Chapter 2

Chapter 3

Chapter 4

Chapter 5

Chapter 6

LIST OF TABLES

Chapter 2

Chapter 3

Chapter 4

Chapter 5

Chapter 6

Chapter 1: Introduction

This chapter starts with a brief overview of the production, properties and applications of thermoplastic vulcanisates (TPVs) with an emphasis on EPDM/PP-based vulcanisates. The general introduction of the thesis continues with the motivation of the present work and the structure of the thesis. Next, an introduction of polymer blends, miscibility, phase morphology and morphology development are addressed. This state of the art research on thermoplastic vulcanisates focuses on dynamic vulcanisation, resole cross-linking chemistry, morphology, rheology and processing, solid-state properties and morphology development.

1. Overview of the thesis

1.1. Background

Thermoplastic elastomers (TPEs) are generally characterized by the combination of the processing characteristics of thermoplastics materials in the molten state and the elastic-mechanical properties of vulcanised rubbers in the solid state [1-3]. TPE families are formed from two major groups: block-copolymers, which are styrene (SBC), polyurethane (TPU), polyether (TPEt) and polyamide (TPA), and polymer blends, which include thermoplastic olefin blends (TPO) and thermoplastic vulcanisates (TPV) [2].

The TPEs are phase-separated systems that belong to the group of copolymers. They consist of a soft phase and a hard phase that are thermodynamically immiscible and present as heterogeneous [4]. The crystalline or amorphous hard segments work as thermally reversible network points in a soft matrix. They melt the crystalline and soften the amorphous phases at elevated temperatures, which allow this TPE group to be processed by conventional techniques as a thermoplastic material.

The TPOs and TPVs are blends of an elastomer and a thermoplastic. The main difference between TPOs and TPVs is that, in the latter, the rubber is selectively cross-linked during the melt blending process: dynamic vulcanisation [5-8]. As a result of cross-linking, the TPV final morphology consists of finely dispersed cross-linked rubber particles (major phase) in the thermoplastic matrix (minor phase). The thermoplastic matrix enables TPVs to be processed with common techniques [9], such as extrusion, injection moulding, blow moulding, vacuum forming and calendaring.

TPEs blends have gained significant relevance recently. The most commercially relevant TPVs are based on EPDM/PP blends because this pair of polymers has a low interfacial tension that results in a finely blended dispersion without adding compatibilizers. Moreover, EPDM/PP-based TPVs have excellent stability against heat, oxygen and ozone because of their saturated main chain of EPDM and high heat and oil resistance because of their polypropylene high melting point and high crystallinity. Generally, commercial TPVs contain large quantities of extender oil to improve melt processability and reduce hardness.

TPVs emerged commercially in 1978 after studies by Coran et al. [7, 8] on the morphology, tensile properties, compression set and solvent swelling characteristics of sulfur cured EPDM/PP blends. EPDM/PP-based TPVs showed significant improved properties over simple blends, such as stable phase morphology, higher ultimate tensile strength, high

temperature resistance, fatigue and swelling with fluids [8]. Full vulcanisation and small elastomeric particles (between 1 and 1.5 μm) are also requisites to achieve high performance TPVs [8], i.e., low modulus and hardness, improved elongation at break and enhanced elasticity.

The combination of improved properties, low production costs and ability to recycle scrap makes TPVs one of the fastest growing members of the TPE family in the rubber market. TPVs have replaced the PVC and thermoset cross-linking rubbers in automotive applications. TPVs products can also be found in car exteriors, such as the boot and bellows, trims, fuel seals and air management systems, as well as in interior car components, such as airbag covers and dashboard foils. TPV products have also been applied in other markets: building and construction (e.g., doors and window profiles and roof sheeting); electronics and electrics (e.g., cable and wire insulation); consumer goods (e.g., in grips for many types of tools and equipment); and medical and food (e.g., stoppers for flasks and syringe plungers).

1.2. Motivation

The commercial relevance of TPVs and its growth in the market since the 1970's justifies the large number of studies that have been published describing the production of TPVs with desired properties. However, the chemical and physical phenomena that take place during dynamic vulcanisation are still not well understood, and TPV production is based on trial-error operations. Thus, the main goal of this thesis is to obtain new insights into dynamic vulcanisation process, mainly to understand the effects of cross-linking, viscosity ratio and composition on phase inversion and the relationship between cross-linking and morphology development. The knowledge build up can be used for the optimisation of TPVs production and respective properties.

1.3.Thesis Outline

This thesis is organized as follows:

Chapter 1 is a general overview of Polymer Blends and Thermoplastic Vulcanisates that emphasizes morphology development and phase morphology. A short review of dynamic vulcanisation, resole cross-link chemistry, the structure-property relationship of TPVs and, and the rheology and processing for TPVs are also given.

Chapter 2 starts with a short review of the processing equipment used (a batch mixer) and describe the method used to estimate the shear rate inside the mixer. Then, since it was necessary to modify commercial materials (EPDM and PP) an experimental study on branching/cross-linking and degradation behaviour of the EPDM and EPM elastomers and PP is presented. At end, the properties of the all the materials used in this work are given.

Chapter 3 describes the dynamic vulcanisation of EPDM/PP blends with resole/$SnCl_2.2H_2O$ in the batch mixer with an emphasis on the evolution of the cross-linking reaction as a function of reaction time. Different EPDM/PP weight ratios and processing temperatures are used to determine their influence on cross-linking. EPDM without PP was dynamic and static when vulcanised at different processing temperatures to investigate the effect of shear and temperature on the cross-linking reaction.

Chapter 4 reports the morphology of the EPDM/PP blend (without cross-linking). The phase morphology of EPDM/PP blends is explored by scanning electron microscopy (SEM) and extractions. Blend phase morphology is characterised as a function of composition and viscosity ratio. The study mainly focuses on phase inversion phenomena. Empirical and semi-empirical models that predict phase inversion composition of immiscible polymer blends were applied to experimental results, and the influence of composition, melt viscosity and elasticity ratios, and melt viscosity and elasticity of each polymer on phase inversion are discussed.
This investigation is needed to understand the effect of cross-linking on EPDM/PP phase morphology and phase inversion behaviour.

Chapter 5 is devoted to the study of EPDM/PP TPV morphology as a function of composition and viscosity ratio. The TPV morphology is analysed by electron microscopy (SEM and TEM) and the cross-linking degree based on EPDM gel content. TPV morphology is investigated as a function of composition and viscosity ratio. The morphology and phase morphology behaviour of the TPVs are compared with the respective blends (characterised in Chapter V) to evaluate the effect of cross-linking on phase inversion. The effect of dynamic vulcanisation on the domain size of the EPDM/PP blends at certain viscosity ratios is also addressed.

Chapter 6 describes the study of morphology development during dynamic vulcanisation and its correlation with cross-linking reaction. The effect of Mw EPDM on cross-linking and the morphological mechanism development were investigated. The influence of PP viscosity and composition on morphology evolution was also evaluated. The main goal of this chapter is to obtain new insights on morphology development during dynamic vulcanisation, which is successfully achieved due to the use of a very low-molecular weight EPDM that slowed the cross-linking reaction.

Chapter 7 contains the general conclusions regarding the work carried out in this thesis as well as some recommendations for future work.

2. Polymer Blends

2.1. Introduction

Polymer blends, by definition, consist of a combination of two or more polymers/copolymers that are used to generate materials with specific properties that are not achievable with the individual components. Polymer blend properties can be attained only by changing the blend composition and/or viscosity ratio of the components. One major question to be addressed in any polymer blend system is whether the constituents are miscible or immiscible. Miscible blends involve thermodynamic solubility and are characterised by a single phase system over the whole concentration range under isothermal conditions and a single glass transition temperature [10]. Immiscible blends are phase separated, exhibiting the glass transition temperatures and/or melting temperatures of each component [10]. Miscibility is governed by the concentration dependency of the free energy of mixing (ΔGm). The following two requirements should be fulfilled for a binary mixture to be miscible at any composition (ø) [11]:

- The free energy of mixing is negative:

$$\Delta G_m = \Delta H_m - T\Delta S_m < 0 \quad (1)$$

- The second derivative of the free energy of mixing is positive.

$$\frac{\partial^2 G_m}{\partial^2 \emptyset^2} > 0 \quad (2)$$

To satisfy equation (1), the entropy of mixing (ΔS_m) must be larger than the enthalpy of mixing (ΔH_m), or if the entropy of mixing is small, the mixing enthalpy must be negative. Because polymers consist of long molecules with high molecular weight, mixing them is thermodynamically unfavourable, i.e., the gain in entropy is negligible, and as a result, the mixing free energy can only be negative if the enthalpy of mixing is negative. Thus, the mixing must be exothermic, which requires specific interactions, such as hydrogen bonding, ion-dipole, dipole-dipole and donor-acceptor interactions, between the blend components [10]. However, Van der Waals interactions are the most common between polymer chains of the blend components, and consequently, polymer blends are usually immiscible.

Hopefully, polymer blends do not have to be miscible to be functional. Incompatible blends exhibiting coarse morphologies and poor adhesion between the blend phases can be compatibilised. Compatibilisation can be achieved by several methods, such as, addition of a graft or block copolymers, a low molecular weight coupling agent or "in-situ" formation of a graft copolymer (reactive blending) [12].

2.2. Phase Morphology of Immiscible Blends

Polymer blends are prepared by an intensive mechanical mixing process, usually single and twin extruders are used in a commercial scale and internal mixer at lab scale. If the blend is immiscible, heterogeneous morphologies are obtained that are characterized by the shape, size and distribution of the phases. Depending on the rheological properties of the blend components, interfacial tension, blend composition and processing conditions (temperature, screw speed and configuration), different morphologies can be achieved [13]. Fig. 1.1 exhibits a typical morphology of immiscible polymer blends, which can be co-continuous, matrix-dispersed phase and matrix-fibers.

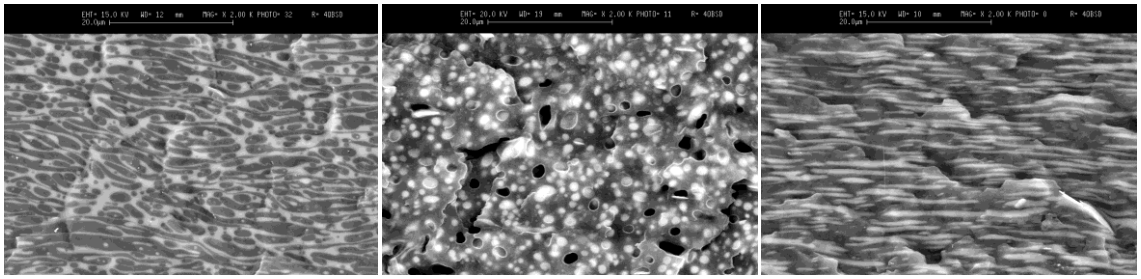

co-continuous matrix - dispersed matrix - fiber

Fig. 1.1. Typical morphologies of the EPDM/PP blends.

Controlling the morphology of polymer blends is an important research area because the solid-state properties significantly depend on it. In addition, the morphology also influences the rheological properties of the blend, which affects the processing that determines the morphology. Understanding the complex interrelationship between morphology, rheology and processability is required to design a product successfully.

Blend composition is one of the most significant parameters that govern morphology. When a polymer A is added to a polymer B at low concentrations of A (minor phase), a dispersion of polymer A in polymer B (the major phase that forms the matrix) is expected to form. Increasing the amount of polymer A leads to the formation of an intermediate morphology, where polymer A can be found as partially continuous and dispersed until both polymers became fully continuous. According to Utracki [14] and Lyngaae-Jørgensen et al. [15, 16] co-continuous morphology is achieved when the minor phase starts to have a continuous portion until it becomes fully continuous. The volume fraction at which the minor phase is no longer fully dispersed is the critical volume fraction, ϕcr, or percolation threshold (15.6 vol. % for a system composed by rigid spheres) [14 - 16]. The fraction of a component that is part of the percolation structure can be determined by the co-continuity index (Φ_i) or degree of co-

continuity, as shown schematically in Fig. 1.2. Usually, the term "co-continuous" is used when both polymers form a full continuous structure, i.e., when the co-continuity index of both polymers is 1.

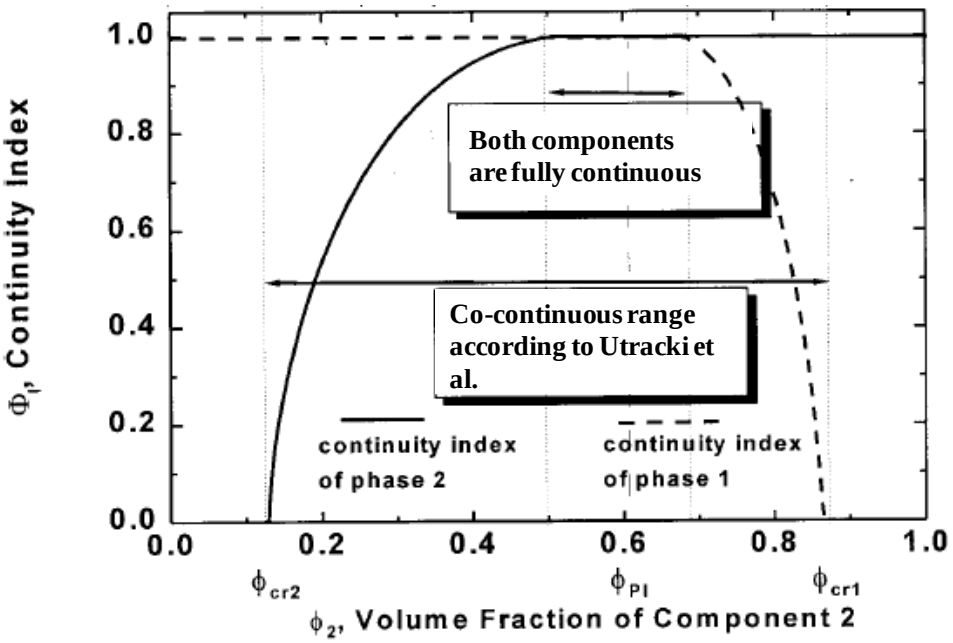

Fig. 1.2. Co-continuous composition range measured by the co-continuous index as a function of volume fraction of the component 2. (Adapted from reference [17])

Co-continuous morphology can be formed over a certain interval of volume fractions and at low volume fractions of the minor phase, as been shown by several authors [18-29]. The range of volume fractions at which co-continuous structures can be formed is related to the rheological properties of the blend components, interfacial tension and processing conditions. The formation of co-continuous structures at low volume fractions of the minor component is acquired by the existence of elongated and interconnected network structures. Willemse et al. [19] developed a semi-empirical model that predicts the lower and upper limits of co-continuous structures:

$$\frac{1}{\phi_{disp}} = 1.38 + 0.0213\left(\frac{\eta_m \dot{\gamma}}{\sigma} R_0\right)^{4.2} \quad (3)$$

The equation (3) relates the critical volume fraction of the minor component (ϕ_{disp}) as a function of the matrix viscosity (η_m), shear rate ($\dot{\gamma}$), interfacial tension (σ) and minimum filament radius (R_0) using unity for the capillary number. By addressing the geometric requirements of the shape of the dispersed phase for the formation of co-continuity structures, this model takes into account the dependence of the formation of co-continuous morphology

on the material properties and processing conditions. The model shows that high shear rate, high matrix viscosity and low interfacial tension or high R_0 contributes to the formation of co-continuous structures at low volume fractions of the minor component.

Although co-continuous morphologies are not formed only at a single volume fraction, phase inversion is believed to occur through co-continuous structures. Thus, determining the phase inversion composition has been a research topic of interest. Phase inversion is defined as the point at which the blend components shift their functions: the dispersed phase becomes the matrix and vice-versa. The rheological properties of the blend components, mainly the viscosity ratio, have been used to predict the phase inversion composition. Avgeropoulos et al. [30] were the first to confirm the rheology-morphology relationship in the control of phase morphology experimentally by examining the torque ratio as a function of volume fraction. The results are represented schematically in Fig. 1.3. It can be observed that the phase with the lowest viscosity and/or the highest volume fraction becomes the matrix and that the phase with the highest viscosity and/or the lowest volume fraction becomes the dispersed phase [30]. At similar viscosities and/or equal volume fractions co-continuous morphology is obtained. Several empirical and semi-empirical models, based on the relationship between viscosity, elasticity ratios and composition, have been developed [14,17, 30 – 40] to estimate phase inversion composition. The most general models are discussed in detail in chapter IV of this thesis.

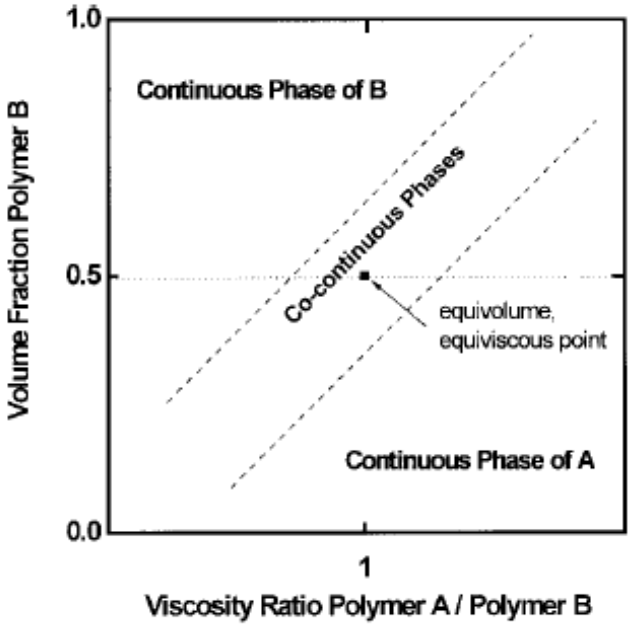

Fig. 1.3. Schematic representation of the co-continuous range as a function of viscosity ratio and volume fraction [17].

2.3. Morphology Development

Morphology development from the material pellets to the micrometer droplet size has been investigated by several researchers [41-52]. Shih et al. [43] identified four rheological characteristic classes: elastic solid pellets, deformable solid pellets, transition material, and viscoelastic fluid. The melting transition regime is characterized by the highest stresses generated during mixing that are a result of the high viscosity of polymers in this stage and the velocity gradients generated due to the presence of un-molten material. Consequently, complex morphologies are formed during this process. Furthermore, a significant reduction of domain size has been reported to occur during melting (or softening) [52-55]. Thus, it has been observed that morphology [56, 57] can be established quite soon for several blends. An initial mechanism of morphology development during polymer blending has been proposed by Scott et al. [52], which is shown in Fig. 1.4. In their experiments, several reactive and non-reactive blend systems were used. They observed a reduction of the size of the dispersed after the formation of sheets or ribbons. As the sheet becomes thinner, holes are formed due to the interfacial and flow forces, resulting in a lace structure. Then the lace structure breaks, which leads to the formation of irregular domains that continue to break into small particles. This sheet mechanism has been observed in batch mixers and twin-extruders where the principal melting mechanism is dissipative mix-melting [45].

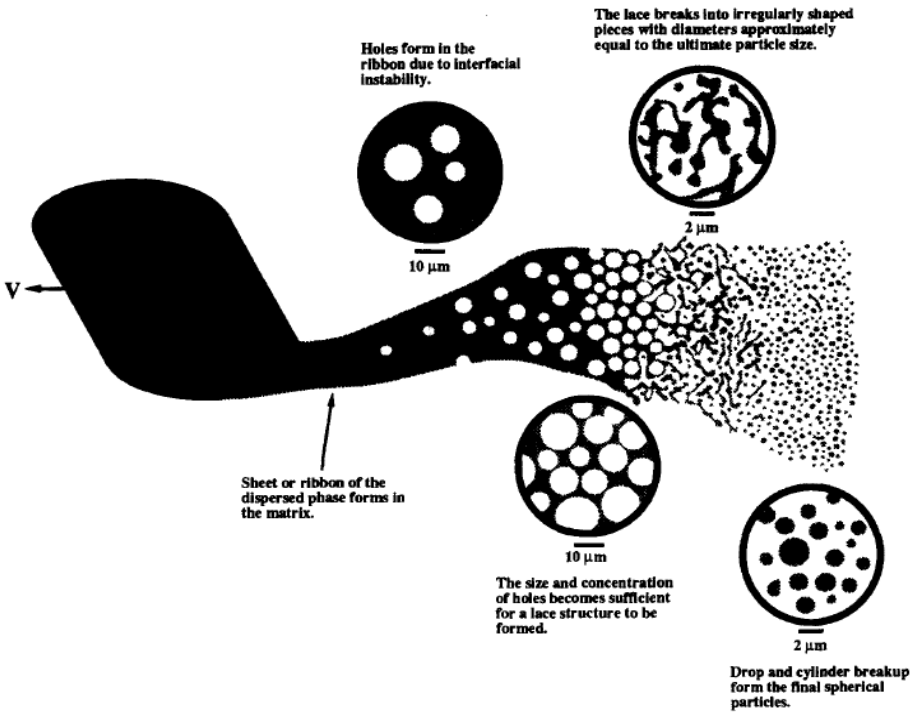

Fig. 1.4. Mechanism of morphology development in polymer blends [52].

Phase inversion at this initial stages has also been observed [48-51] when the minor phase melts (or softens) first and becomes a continuous phase that covers the solid pellets of the major phase as the major phase melt (or soft) phase inversion occurs. The major phase becomes the matrix and the minor phase the dispersed phase. Sundararaj et al. [51] have proposed a mechanism that couples the sheeting mechanism and phase inversion, which is illustrated in Fig. 1.5. The mechanism comprises four steps: (a) the formation of major phase sheets by pulling the softening pellets off near the major component's transition temperature, (b) the sheets become lamellar domains inside the minor phase; (c) the lamellar structures break into irregular pieces; (d) the major phase becomes the continuous phase through coalescence of the major phase domains and the minor phase becomes the dispersed phase with trapped particles of the major phase inside [51].

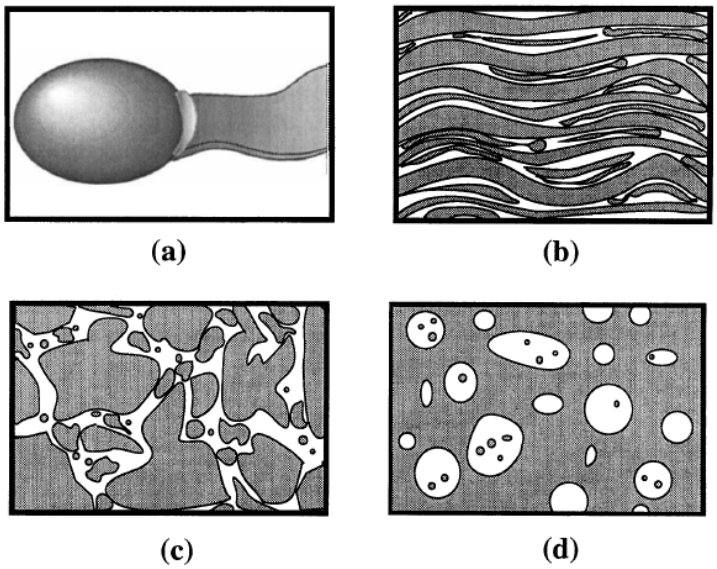

Fig. 1.5. Mechanism for inversion of phase continuity during a melting regime [51].

After entering the melting (or softening) flow regime, the morphology development is controlled by deformation, breakup and coalescence. If a matrix-dispersed morphology is obtained, it is expected that the domains of the dispersed phase are deformed by shear and elongational stresses imposed by the flow field. At sufficiently strong stresses, the domains break up into smaller ones. Simultaneously, the domains of the dispersed phase can collide, and coalescence may occur. The basic fundamentals of the physics of deformation and break up are based on the studies made on Newtonian systems in simple shear flow and pure elongational flow. Taylor [58, 59] investigated the droplet deformation of an oil-water

system; according to his observations, he derived equation (4), which represents the dimensionless number, or capillary number (Ca):

$$Ca = \frac{\eta_m \dot{\gamma} R}{\sigma} \quad (4)$$

where η_m is the matrix viscosity, $\dot{\gamma}$ is the shear rate, R is the radius of the droplet and σ is the interfacial tension. The capillary number represents the balance between the deforming stress ($\eta_m \dot{\gamma}$) imposed by the flow and the interfacial stress (σ/R). If the interfacial stress dominates, then the capillary number is small, and a stable drop shape is developed. As the capillary number becomes larger than a critical capillary number (Ca_{cr}) droplets start to deform and break up. The critical capillary number is a function of the viscosity ratio, λ, (ratio between the viscosity of dispersed phase (η_d) and the viscosity of the matrix), and it is given by equation (5) for Newtonian fluids under simple shear flow [60]; coalescence effects are not taken into account:

$$Ca_{cr} = \frac{1}{2}\frac{16\lambda + 16}{19\lambda + 16} = \frac{\eta_m \dot{\gamma} R}{\sigma} \quad (5)$$

The equation (5) shows that the morphology of the Newtonian fluids is governed by viscosity ratio, shear stress, interfacial tension and droplet radius. As generalized by Cox [61], droplet deformation is a function of the capillary number and viscosity ratio. This relationship is also valid for elongational flow, where the critical capillary number is half than in shear. The studies by Taylor [58, 59] and Grace [60] demonstrated that an elongational flow field is much more efficient than a uniform shear flow field for droplet break up. Grace [60] studied the deformation and breakup of single drops performed in both shear and elongational flows and developed the Grace curve, which describes the critical capillary number as a function of viscosity ratio. The main conclusions are the following: i) droplets are stable when their capillary number is below the critical value; ii) deformation and break up take place most easily if the viscosity ratio is between 0.25 and 1 in shear flow; iii) at viscosity ratios higher than approximately 4, droplet break up is not possible in a simple shear flow; iv) elongational flow is more effective for breakup than shear flow.

Several studies have been performed for Newtonian droplet breakup in a shear flow that suggest a lower and upper limit of the viscosity ratio within which droplet break up can occur must exist [62,63]. Rumscheidt and Mason [63] observed different deformation and break up of fluid droplets of an emulsion in shear and hyperbolic flow. In shear flow, they found that at viscosity ratios higher than approximately 6, no droplet breakup occurs. For viscosity ratios around 1, droplets deform and break up into identical droplets and three satellite droplets also

occurs. If the viscosity ratio is approximately 0.7, the drops enlarge into a long cylindrical filament and then fall apart into single droplets. At a low viscosity ratio of 2×10^{-4}, it was found that the droplets assumed a sigmoidal shape and small droplets detached from the deformed structure at the tip, which is a process called tip streaming.

Two mechanisms are dominant during dispersion of a Newtonian liquid in a Newtonian matrix: droplet splitting and droplet deformation into a cylindrical fibril that then falls apart into single droplets [13].

The disintegration of a Newtonian thread embedded in a quiescent Newtonian continuous phase has been described by Tomokita [64] based on the Rayleigh mechanism. According to him, the Newtonian thread surrounded by a Newtonian matrix breaks up due to instabilities driven by the interfacial tension. Although these relationships were developed under quiescent conditions and for a Newtonian system, Elmendorp [65] found good agreement for viscoelastic polymers. An example of a polymer thread breakup in a polymer matrix is shown in Fig.1.6. Tomokita's model will be discussed in more detail in chapter 6 of this thesis.

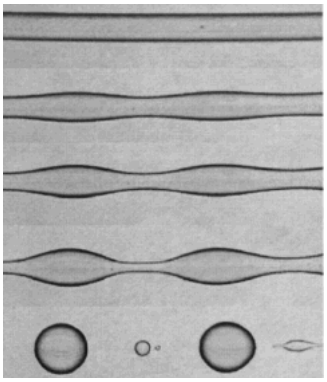

Fig. 1.6. General representation of a polymer thread breakup in a polymer matrix (adapted from [66]).

Because polymer blends are commonly viscoelastic fluids, droplets experience both dissipative (viscous) forces and deformation-resisting forces that arise from the elasticity [67]. Van Oene [68, 69] reported that in viscoelastic fluids, elasticity also accounts for droplet deformation. The contribution of the dispersed and continuous phases of elasticity measured by the second normal stress difference can be accounted for using the dynamic interfacial tension (σ^*) shown in Van Oene's equation (6),

$$\sigma^* = \sigma + \left(\frac{R}{6}\right)(N_{2,d} - N_{2,m}) \tag{6}$$

where σ is the interfacial tension in absence of flow, R is the droplet radius, and $N_{2,d}$ and $N_{2,m}$ are the second normal stress difference of the dispersed phase and of the matrix, respectively.

It has been shown [70,71] that the droplet elasticity tends to have a stabilizing effect during deformation. Consequently, the dispersion in viscoelastic blends is more difficult to attain than in Newtonian blends. Sundararaj et al. [72] modified the capillary number by introducing the first normal stress difference to obtain the "forces" that resist deformation. Ghodgaonkar et al. [73] further modified the approach by introducing the first normal stress difference of the matrix ($N_{1,m}$) and the first normal stress difference of the dispersed phase ($N_{1,d}$), as shown in equation (7):

$$Ca = \frac{(\eta_m \dot{\gamma} + N_{1,m} - N_{1,d})R}{\sigma} \tag{7}$$

This equation, which results from the balance between the forces that resist deformation (interfacial tension and first normal stress of the dispersed phase) and the forces that deform the droplet (shear forces and the matrix first normal stress), was used as an initial approximation to predict the particle size of several systems under different operating conditions [73].

Wu [74] performed a study on polyamide/rubber blends by varying the viscosity ratio and interfacial tension, and he found that droplets can break up during extrusion (in a twin-extruder) at viscosity ratios higher than 4. Because extruder elongational flows were also present, it was not possible to determine if this observation is related to the elasticity effects or to the flow profile in the extruder. Wu [74] obtained the following empirical equation (8) by fitting the capillary master curve:

$$Ca = \frac{\eta_m \dot{\gamma} R}{\sigma} = 4\left(\frac{\eta_d}{\eta_m}\right)^{\pm 0.84} \tag{8}$$

In this equation, the exponent (0.84) is positive if the viscosity ratio is higher than 1 and negative if the viscosity ratio is smaller than 1. Wu's relation suggests a minimum particle size when the viscosities of the two phases are closely matched. Conversely, Favis et al. [75, 76] studied PP/PC blends and determine the minimum size of PC particles at a viscosity ratio of 0.15. Serpe et al. [77] found good agreement between their experimental observations and Wu's results. Nevertheless, they developed a new relation using the blend viscosity (η_b) instead of the matrix viscosity and introduced another term that takes into account the volume fraction of the blend components, as shown in equation (9):

$$\frac{\eta_b \dot{\gamma} R}{\sigma}(1 - (4\phi_d\phi_m)^{0.8} = 4\left(\frac{\eta_d}{\eta_m}\right)^{\pm 0.84} \tag{9}$$

This equation is believed to account for the coalescence effects. Coalescence is an important factor that influences the dispersed phase morphology. Since dispersion and coalescence are simultaneous processes during melt mixing. Coalescence depends on the concentration of the dispersed phase, the average particle size and the molecular mobility of the interface between the matrix and dispersed phase [67]. Therefore, coalescence can be reduced if the matrix becomes highly viscous [72,78]. It has also been reported [72] that the contact time required for coalescence increases as the droplet diameter increases or with an increasing difference in density between the droplets and the matrix. Fortelný et al. [79,80] developed equation (10) to predict the final droplet radius that takes into account the breakup and coalescence phenomena:

$$R = R_{cri} + \left(\frac{\sigma\,\theta}{\eta_m\, f_1}\right)\phi_d \tag{10}$$

where R_{cri} is the critical radius determined from the critical capillary number, θ is the probability that droplets coalesce after collision and f_1 is the slope of the function that represents the frequency of droplet breakup at critical capillary number.

In addition to the above studies, finding a general model to predict the particle size of polymer blends is not straightforward because several parameters have to be taken into account, such as melt viscosity and elasticity, viscosity ratio, blend composition and interfacial tension. In addition, different processing equipment and conditions and different methodologies to determine the particle size and viscosity ratio also affect the results found in literature.

3. Thermoplastic Vulcanisates

3.1. Dynamic Vulcanisation

The term *dynamic vulcanisation* was first introduced by Glesser [5] for the production of high-impact rubber/thermoplastic blends by partially cross-linking the minor rubber phase. He started by joining the elastomer (chlorobutyl), the thermoplastic (PP) and the cross-linking agent. Then, the elastomer was partially vulcanised, and the PP melted under continuous mixing and heating. Fischer [6] was the first to make soft rubberlike materials by partially cross-linking the EPDM phase in EPDM/PP blends at different ratios. However, true dynamic vulcanisate products (TPVs) and their potential utility were developed by Coran et al. [7,81-88].

Dynamic vulcanisation is usually defined as a process in which the thermoplastic phase, the elastomer phase and other ingredients (e.g., filler, plasticizer, oil, and a stabilizer) are first melt-mixed until a homogeneous blend is formed; then, the cross-linking agents are added, and the elastomer phase is selectively cross-linked under continuous mixing and heating. Therefore, a fine dispersion of the highly vulcanised elastomer particles in the thermoplastic phase is obtained. The term *highly vulcanised* means that the elastomer cross-linking density is at least 7×10^{-5} mol/ml (determined by swelling) or that the elastomer is less than about 3% extractable by cyclohexane at 23 ºC [8].

Several combinations of rubbers (butyl rubber (IIR), EPDM, natural rubber (NR), butadiene rubber (BR), styrene-butadiene-rubber (SBR), ethylene vinyl acetate (EVA), acrylate rubber (ACM), chlorinated polyethylene (CM), polychloroprene (CR) and nitrile rubber (NBR)) and thermoplastics (polypropylene (PP), polyethylene (PE), polystyrene (PS), acrylonitrile butadiene styrene (ABS), styrene acrylonitrile (SAN), polymethyl methacrylate (PMMA), polybutylene terephthalate (PBT), polyamide (PA) and polycarbonate (PC) underwent dynamic vulcanisation to achieve new TPVs [89]. However, only a few blends have industrial application because most of them are incompatible and require the use of compatibilisers [89]. Useful TPVs are obtained when the surface energies of the elastomer and thermoplastic match, the molecular weight between entanglements of the elastomer is low and the thermoplastic phase is crystalline [90]. Because EPDM/PP-based TPVs fulfil these requisites, it is the most successful commercial TPV.

Sulfur/accelerator combinations, peroxides/coagent, activated resole-resins and grafted silanes have been employed as cross-linking agents to cross-link the EPDM phase. The properties of

the EPDM/PP-based TPVs are largely influenced by the cross-linking agents. It has been shown that EPDM suffers from thermal degradation in the sulfur cure due to the instability of S-S and C-S bonds, which results in TPVs with poor compression set properties [91]. Significant improvements in the compression set, oil resistance and heat resistance of the EPDM vulcanisate (due to the relatively stable C-C bonds) were obtained by Abdout-Sabet and Fath [92]. They used the resole, phenolic resin, activated by stannous chloride dihydrate and zinc oxide as the vulcanised agent. Peroxide/coagent as the vulcanised agent has also been employed. Even though, C-C bonds are formed in the rubber the free radicals generated by peroxide decomposition also remove the hydrogen atoms from the tertiary carbon sites of PP, which leads to β-scission [93-99]. Consequently, PP molecular weight changes during EPDM cross-linking . Some advances have been made using coagents that prevent the degradation of the PP [100-102].

Other agents, such as organosilanes [103] and benzene-1,3-bis(sufonyl)azide [104], have also been investigated. However, resole phenolic resin is most commonly applied to cross-link the EPDM/PP blends, which can be explained by the optimum balance of properties/cost obtained.

3.2. Cross-linking Chemistry

Resoles provide TPVs with good mechanical properties and processing characteristics and yield thermally stable cross-links [105]. They are polycondensation products of alkylphenol and formaldehyde with a dimethylene ether bridge connecting the phenolic units. The chemistry of resole cross-linking has been studied using low-molecular-weight models for EPDM rubber first by Lattimer [106] and later by van Duin et al. [107, 108]. Usually, hydrated stannous chloride and zinc oxide are used as activators. The acidic stannous chloride creates mono-phenolic units with benzylic cations due to the activation of the scission of the dimethylol ether linkage of the resole. The benzylic cations connect two EPDM chains via methylene and/or chroman cross-links. A ^{13}C NMR study showed that only methylene/chroman cross-links are formed in the case of EPDM with ethylidene norbornene (ENB) as diene [109]. It has also been demonstrated that ENB is more reactive to resole cross-linking than dicyclopentadiene (DCPD), 1,4-hexadiene (HD) or vinylidene norbornene (VNB), which can be explained by the high degree of substitution of the residual ENB unsaturation and, consequently, the rather high stability of the cationic intermediate [105]. Resole seems not to react with PP due to the absence of unsaturation [105]. The Fig. 1.7

depicts the simplified mechanism for vulcanisation of ENB-EPDM with $SnCl_2$-activated resole as the cross-linking agent.

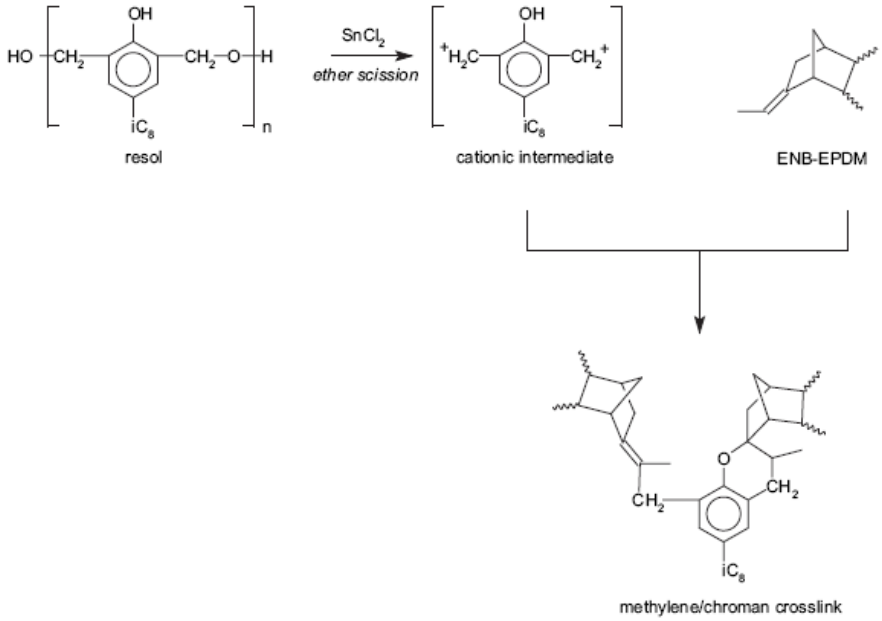

Fig. 1.7. Mechanism for vulcanisation of the ENB-EPDM cross-linked via activated resole $SnCl_2.H_2O$[9].

3.3. TPVs Morphology

To exhibit excellent elastic-mechanical properties and processability in typical thermoplastic technologies, TPV morphology has been claimed to consist of finely dispersed highly cross-linked rubber particles in a thermoplastic matrix [8, 91, 110-112]. In addition, appropriate adhesion between the phases is also required to achieve good stress transfer between the phases. Experimental studies have suggested that EPDM is the dispersed phase even at 75/25 [110] and 80/20 EPDM/PP compositions [91]. TPVs morphologies have been analyzed by SEM, SEM in back-scattering mode (BSE) and SEM with energy dispersive microanalysis techniques. In the latter technique, inorganic trace elements such as aluminum or potassium are added, which are concentrated in the rubber phase. More recently, transmission electron microscopy (TEM) has became the most common technique to study TPV morphology because it provides high-resolution images that make details of the microstructure evident that cannot be seen by other conventional techniques, like SEM, LVSEM and AFM. A typical SEM-BSE and TEM micrograph of TPV morphology is depicted in Fig. 1.8.

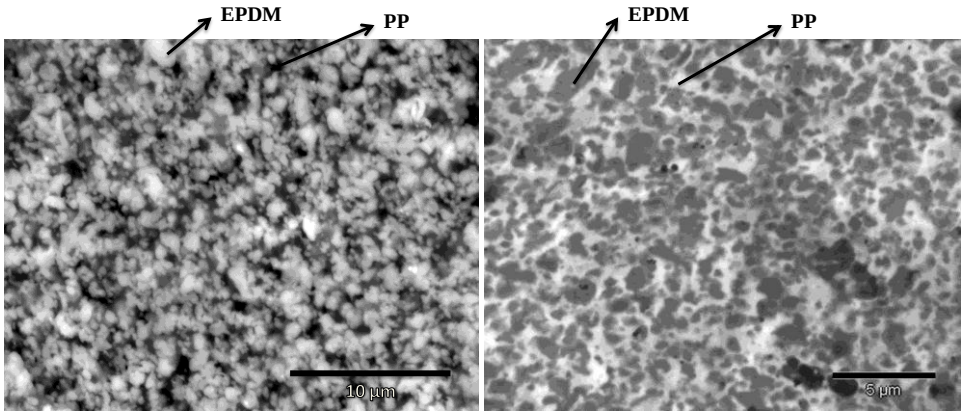

Fig. 1.8. Typical EPDM/PP-based TPV morphology.

As in the blends, TPVs morphology depends on the composition, individual characteristics of the components, viscosity and elasticity ratio, interfacial tension between the components and processing conditions. A good dispersion of the rubber particles is achieved by matching the viscosity of the blend components and by near equivalence energies of their surface [113]. Sengupta [114] showed that if the same energy is input during processing no changes are found between TPVs processed in the batch mixer and twin-screw extruder. Additionally, the TPV morphology also depends on the curing system and cross-linking degree of the EPDM phase. A typical cross-linked EPDM particle size in the range 0.5-5 µm has been obtained for EPDM/PP-based TPVs using resole as the cross-linking agent [111].

The presence of additives also influences the TPVs morphology: for example, Katbab et al. [115] showed that the addition of carbon black results in large EPDM particles after dynamic vulcanisation. Because TPV products usually contain large EPDM/PP ratios, oil and additives, a large distribution of rubber particles with irregular shapes is obtained, making the interpretation of electron micrographs not straightforward [9]. Some discussion on whether the morphology of thermoplastic vulcanisates is dispersed or co-continuous exists in the literature. It has been suggested that the rubber particles interact by forming a network of vulcanised rubbers particles that give the appearance of a co-continuous TPV morphology [3,85,116]. However, processing TPVs can be easy if the cross-linked rubber is dispersed in the thermoplastic phase.

Recently, tomography has been applied to TPVs, and it has shown that most rubber particles are separated in 3D space, whereas traditional 2D images show co-continuous morphologies [114]. The three-dimensional image is acquired from a series of TEM images that were

obtained by varying the angle of view and subsequently converted into 3D images using image analysis software.

3.4. Structure-property Relationship

Morphology is one of the major parameters that govern the solid state properties. Thus, EPDM/PP (w/w) composition has a significant effect on TPV properties. Modulus, hardness, tension set and tensile strength increase as the PP amount increases as a result of the increasingly thermoplastic behaviour [2]. In spite of TPV composition, melt viscosity and elasticity of the components, TPV properties have been found [84] to correlate with wetting surface tension difference ($\Delta\gamma$) between the elastomer and thermoplastic phase, the fraction of thermoplastic crystallinity (ϕ_c) and the critical entanglement spacing (N_c) of the rubber chains. It has been observed [83] that the tensile strength and ultimate elongation increase as ϕ_c increases and $\Delta\gamma$ and N_c decrease.

A critical dependence of the solid-state properties of the type of cross-link, cross-linking density and rubber particle size has also been reported [113]. Typical curves that describe the effect of the particle size and degree of cross-linking on the stress-strain properties are depicted in Fig. 1.9 a) and b), respectively [85,117].

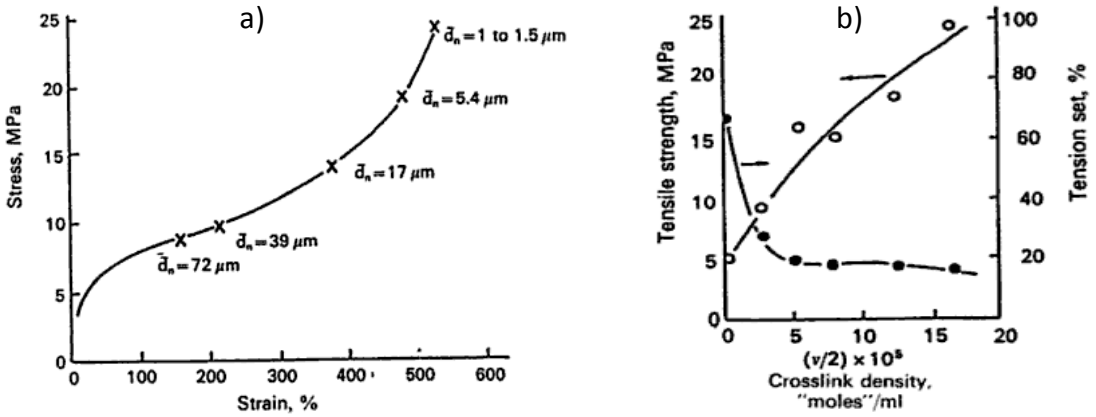

Fig. 1.9. a) Effect of rubber particle size on stress-strain properties and b) Effect of cross-linking density on mechanical properties of TPV [118].

The deformation behaviour of EPDM/PP-based TPVs has been widely studied [119-127]. In fact, explaining the rubberlike properties of conventional TPV morphology, where the rigid phase (thermoplastic) is the matrix and the soft phase (cross-linked rubber) is the dispersed phase, has been a difficult task. It has been suggested that the cross-linked rubber particles physically interact through the finer thermoplastic inter-layers and appear as a "network"

structure [113]. Kikuchi et al. [119] found that the yielding starts at the equatorial direction (perpendicular to the load) of the rubber inclusions using finite element modelling. According to them, when the TPV is stretched at least 70%, the PP phase is deformed beyond its yielding point. The unyielding PP phase seems to act as glue between the rubber particles and allows for elastic recovery of TPVs. However, this model is not able to explain how it is possible to pull the plastic deformed matrix back using elastic forces. Contrary to the statement made by Kikuchi et al., more recent studies provided by Boyce et al. [121] have shown that most of the PP phase does not yield but has rigid body motion. Yang et al. [122] have investigated the stretching and relaxation of oil-extended TPVs using WAXD. They concluded that only the thin PP layer between EPDM particles yields and a pseudo-continuous EPDM phase is created around the undeformed PP regions. Further improvements were provided by Soliman et al. [123], who measured the orientation of the different phases in situ using infrared spectroscopy in combination with tensile stress-strain measurements. They noted that the EPDM rubber phase stretched during deformation, while only the PP at the frontier between the cross-linked rubber particles suffered from plastic deformation.

Recently, Oderkerk et al. [126,127] have shown that during elongation of a nylon-6/EPDM-g-MA-based TPV, the thermoplastic matrix deforms progressively but inhomogeneously: deformation occurs in the thinnest layer matrix at equator of the rubber particles. The non-deformed matrix layers work as adhesion points that keep the rubber particles together [127]. Upon TPV relaxation, the elastic forces of the elongated rubber draw back the highly deformed matrix layer by either buckling or bending [127]. The schematic representation of the TPV deformation is given in Fig. 1.10.

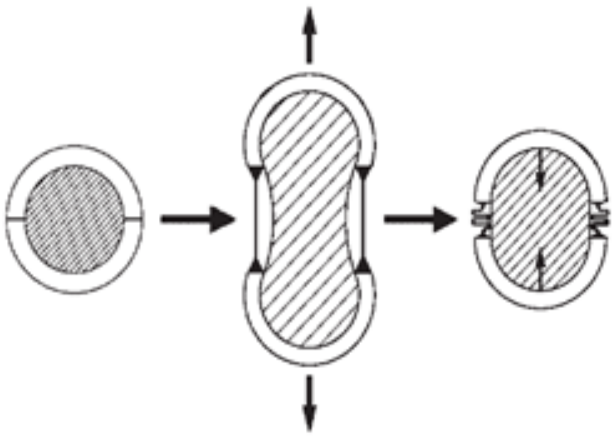

Fig. 1.10. Schematic representation of TPV deformation, showing yielding of PP layers upon deformation and buckling upon relaxation [126,127].

3.5. Rheology and Processing

The processability of a TPV is determined by its rheological behaviour, processing equipment and processing conditions. Since the thermoplastic phase is the matrix, it generally characterizes the rheological behaviour of a TPV. TPVs melt at the thermoplastic phase melting temperature and can be processed using thermoplastic techniques. It has been shown [7,115,128,129] that TPVs have higher viscosity when compared with their respective unvulcanised blend. TPVs exhibit higher shear thinning behaviour and a Newtonian plateau is not observed at low shear rates. Han et al. [130] showed experimentally that TPVs exhibit a critical stress or yield stress of flow that is related to the presence of an interacting network of cross-linked rubber particles. According to Steeman et al. [131], the rheological behaviour of TPV-melts is primarily determined by yield stress and is determined from plots of the viscosity as a function of shear stress. At low stress, the system behaves mostly elastically, which is attributed to the existence of an interacting network of particles. During the yield stress, the network is broken, and the TPV flow behaviour follows a power law model. At this intermediate stress, TPVs behave like a PP melt filled with stiff rubber particles, and the viscosity is largely dependent on the rubber content. Under high stress, the rheological properties of the thermoplastic matrix become dominant. In this regime, the viscosity of TPVs increases as the PP content increases. Consequently, during processing, deformation only occurs in the regions where the local shear stress is higher than the critical stress of flow. Below the yield stress, at low shear rates, the very poor flow enables high retention of melt integrity and maintains the shapes of parts during cooling.

The presence of fillers, such as carbon black, silica and oil, obviously affect TPV rheological behaviour. Large amounts of oil are normally used to obtain low hardness TPVs and improve processing. It has been shown that in the solid state, the oil is mainly in the EPDM phase and also in the PP amorphous phase [99]. However, experiments made in the molten state using solid state ^{13}C-NMR [132] indicate that upon melting, the oil diffuses out of the EPDM phase and forms a separate phase. Therefore, the TPV melt viscosity decreases, which improves processability.

3.6. Morphology Development

The morphological changes during dynamic vulcanisation of EPDM/PP blends has been claimed to develop very quickly as a consequence of cross-linking [91, 92, 100, 106, 107, 112-115]. A comparative study of the morphology development of TPVs in the internal mixer and twin-screw extruder were made by Sengupta [114]. Despite the differences in the mixing conditions in the melt flow mechanism and melt temperature, the final TPV morphology was found to be similar on both sets of equipment. In the internal mixer, the morphology development was found to occur within 1 minute after the addition of cross-linking agents, while in the twin-extruder, it occurs at the first kneading block [114]. Dynamic vulcanisation of TPVs in twin-screw extruders is much more complex than in batch kneaders [133]. In twin-screw extruders, the various processes (melting, mixing and dispersion of PP, EPDM, cross-linking agents, and stabilizers) occur and interact simultaneously while in the batch mixer; usually, EPDM and PP are blended before the cross-linking agents are added.

Several efforts have been made to follow the morphology development during dynamic vulcanisation in a batch mixer [111,112,133-137]. It has been shown that co-continuous blend morphology forms before the addition of cross-linking agents as a result of the higher rubber content and the matched viscosities in both phases. As soon as cross-linking starts, the viscosity and elasticity of the rubber phase increase, and, the continuous rubber phase becomes more elongated and then breaks up into micro-gel particles. Therefore, phase inversion takes place; the rubber phase becomes finely dispersed in the thermoplastic matrix.

Accordingly to Taylor [58,59] and Grace [60], deformation and breakup of the droplets with higher viscosity ($\lambda > 4$) is only possible under shear-elongation flows. However, this problem is overlapped in batch mixers (and extruders) because both shear and elongation flows co-exist; understanding how the high viscous rubber could be finely dispersed in the low-viscous thermoplastic phase is not straightforward. A detailed explanation based on the action of shear and elongation stress has been suggested by Radusch [135]. As cross-linking starts, the melt viscosity of the continuous rubber phase and the viscosity of the whole system increase. Consequently, the shear and elongation stresses acting in the system increase according to the follow equations (11 and 12)[135]:

$$\tau(t) = \eta^r(t) \times \dot{\gamma} \tag{11}$$

$$\sigma(t) = {\eta_e}^r(t) \times \dot{\varepsilon} \tag{12}$$

where $\tau(t)$ is the shear stress, $\eta^r(t)$ is the shear viscosity of the reactive system and $\dot{\gamma}$ is the shear rate. In equation (12), $\sigma(t)$, ${\eta_e}^r(t)$ and $\dot{\varepsilon}$ are the elongational stress, viscosity and

strain, respectively. The viscosity and stresses increase simultaneously, which causes the rubber phase to be continuously stretched. The rubber phase breaks up into small particles when a critical stress is reached.

An overview of morphology development during dynamic vulcanisation is provided in more detail in chapter 6 of this thesis.

References

[1] De SK, Bhowmick AK. Thermoplastic elastomers from rubber–plastic blends. New York: Ellis Horwood, 1990.

[2] Coran AY, Patel RP, Thermoplastic elastomers based on dynamically vulcanised elastomer/thermoplastic blends. In: Thermoplastic Elastomers, Holden G, Hans RK, Quirk RP, editors, 2nd ed., 1996, Munich: Hanser Publishers. p. 143-181.

[3] Karger-Kocsis J. Thermoplastic rubbers via dynamic vulcanization. In: Polymer blends and alloys, Shonaike GO, Simon GP, editors. New York: Marcel Dekker, 1999. p. 125-153.

[4] Holden G. Understanding Thermoplastic elastomers. Munich: Hanser Publishers, 2000. p. 9-25.

[5] Glesser AM, Haslett Jr, William H. Process for preparing a vulcanized blend of crystalline polypropylene and chlorinated butyl rubber. US Patent 3037954, 1962.

[6] Fischer WK. Thermoplastic blend of partially cured monoolefin copolymer rubber and polyolefin plastic. US patent 3758643, 1973; Thermoplastic blend of copolymer rubber and polyolefin plastic. US patent 3835201, 1974; Thermoplastic blend of partially cured monoolefin copolymer rubber and polyolefin plastic. US patent 3862106, 1975.

[7] Coran AY, Das B, Patel RP. Thermoplastic vulcanizates of olefin rubber and polyolefin resin. US Patent 4130535, 1978.

[8] Coran AY, Patel RP. Rubber-thermoplastic compositions - 2. NBR-nylon thermoplastic elastomeric compositions. Rubber Chem and Thecnol 1980;53(4):781-794.

[9] van Duin M. Recent developments for EPDM-based thermoplastic vulcanisates. Macromol Symp 2006;233(1):11-16.

[10] Utracki LA. Polymer Alloys and Blends: Thermodynamics and Rheology. Munich: Hanser Publishers, 1989.

[11] Olabisi O, Robeson LM, Shaw M T. Polymer-Polymer Miscibility. New York: Academy Press, 1979.

[12] Liu NC, Huang H. Types of Reactive polymers used in blending. In: Reactive Polymer blending, Baker W, Scott C, Hu G-H, editors. Munich: Hanser Publishers, 2001.p. 13-42.

[13] Favis BD. Factores influencing the morphology of immiscible polymer blends in melt processing. In: Polymer Blends, Volume 1: formulation, Paul DR, Bucknall CB, editors. New York:John Wiley & Sons, Inc., 2000. p.501-537.

[14] Utracki LA. On the viscosity-concentration dependence of immiscible polymer blends. J Rheol 1991;35(8):1615–1637.

[15] Lyngaae-Jorgensen J, Utracki LA. Dual phase continuity in polymer blends. Makromol Chem, Macromol. Symp 1991;48/49:189-209.

[16] Lyngaae – Jorgensen J, Lunde Rasmussen K, Chtcherbakova EA, Utracki LA. Flow induced formation of dual – phase continuity in polymer blends and alloys. Polym Eng Sci 1999;39(6):1060–1071.

[17] Paul DR, Barlow JW. Polymer blends (or alloys). J Macrom Sci, Rev Macromol Chem 1980;C18(1):109-168.

[18] Verhoogt H, van Dam J, Posthuma de Boer A. Morphology-processing relationship in interpenetrating polymer blends. In: Interpenetrating polymer networks, Klempner D, Sperling LH, Utracki LA, editors. Washington: Advances in chemistry series volume 239, 1994. p. 333-351.

[19] Willemse RC, Posthuma de Boer A, van Dam J, Gotsis AD. Co-continuous morphologies in polymer blends: a new model. Polymer 1998;39(24):5879-5887.

[20] Willemse RC, Speijer A, Langeraar AE, Posthuma de Boer A. Tensile moduli of co-continuous polymer blends. Polymer 1999;40(24):6645-6650.

[21] Veenstra H, van Dam J, Posthuma de Boer A. Formation and stability of co-continuous blends with a poly(ether-ester) block copolymer around its order-dosorder temperature. Polymer 1999;40(5):1119-1130.

[22] Veenstra H, van Lent BJJ, van Dam J, Posthuma de Boer A. Co-continuous morphologies in polymer blends with SEBS block coplolmers. Polymer 1999;40(24):6661-6672.

[23] Chaput S, Carrot C, Castro M, Prochazka F. Co-continuity interval in immiscible polymer blends by dynamic mechanical spectroscopy in the molten and solid state. Rheol Acta 2004;43(5):417-426.

[24] Castro M, Carrot C, Prochazka F. Experimental and theoretical description of low frequency viscoelastic behaviour in immiscible polymer blends. Polymer 2004;45(12):4095-4104.

[25] Li J, Favis BD. Characterizing co-continuous high density polyethylene/polystyrene blends. Polymer 2001;42(11):5047-5053.

[26] Dedecker K, Groeninckx G. Reactive compatibilisation of A/(B/C) polymer blends. Part 2. Analysis of the phase inversion region and the co-continuous phase morphology. Polymer 1998;39(21):4993-5000.

[27] Harrats C, Mekhilef N. Co-continuous phase morphologies: predictions, generation and practical applications. In: Micro- and nanostructured multiphase polymer blend systems: phase morphology and interfaces, Harrats C, Thomas S, Groeninckx G, editors. FL, USA: CRC Press Taylor & Francis Group, 2006. p. 91-132.

[28] Harrats C, Omonov TS, Groeninckx G, Moldenaers P. Phase morphology development and stabilization in polycyclohexylmethacrylate/polypropylene blends:

uncompatibilized and reactively compatibilized blends using two reactive precursors. Polymer 2004; 45(24):8115-8126.

[29] Omonov TS, Harrats C, Groeninckx G, Moldenaers P. Anisotropy and instability of the co-continuous phase morphology in uncompatibilized and reactively compatibilized polypropylene/polystyrene blends. Polymer 2007;48(18):5298-5302.

[30] Avgeropoulos GN, Weissert FC, Biddison PH, Böehm GGA. Heterogeneous blends of polymers. Rheology and morphology. Rubber Chem Techn 1976;49(1):93-104.

[31] Jordhamo GM, Manson JA, Sperling LH. Phase continuity and inversion in polymer blends and simultaneous interpenetrating networks. Polym Eng Sci 1986;26(8):517-524.

[32] Miles IS, Zurek A. Preparation, structure, and properties of two-phase co-continuous polymers blends. Polym Eng Sci 1988;28(12):796–805.

[33] Everaert V, Aerts L, Groeninckx G. Phase morphology development in immiscible PP/(PS/PPE) blends influence of the melt-viscosity ratio and blend composition. Polymer 1999;40(24):6627–6644.

[34] Ho RM, Wu CH, Su AC. Morphology of plastic/rubber blends. Polym Eng Sci 1990;30(9):511–518.

[35] Kitayama N, Keskkula H, Paul DR. Reactive compatibilization of nylon 6/styrene-acrylonitrile copolymer blends: part 1. Phase inversion behaviour. Polymer 2000;41(22):8041–8052.

[36] Omonov TS, Harrats C, Moldenaers P, Groeninckx G. Phase continuity detection and phase inversion phenomena in immiscible polypropylene/polystyrene blends with different viscosity ratios. Polymer 2007;48(28);5917-5927

[37] Metelkin VI, Blekht VP. Formation of a continuous phase in heterogeneous polymer mixtures. Coll J USSR 1984;6(3):425-429.

[38] Luciani A, Jarrin J. Morphology development in immiscible polymer blends. Polym Eng Sci 1996;36(12):1619-1626.

[39] Steinmann S, Gronski W, Friedrich C. Quantitative rheological evaluation of phase inversion in two-phase polymer blends with cocontinuous morphology. Rheol Acta 2002;41:77–86.

[40] Bourry D, Favis BD. Cocontinuity and phase inversion in HDPE/PS blends: influence of interfacial modification and elasticity. J Polym Sci, Part B: Polym Phys 1998;36(11):1889–1899.

[41] Sundararaj U, Dori Y, Macosko CW. Sheet formation in immiscible polymer blends: model experiments on initial blend morphology. Polymer 1995;36(10):1957–1968.

[42] Scott CE, Macosko CW. Model experiments concerning morphology development during the initial stages of polymer blending. Polymer Bulletin 1991;26(3):341–348.

[43] Shih CK, Tynan DG, Denelsbeck DA. Rheological properties of multicomponent polymer systems undergoing melting or softening during compounding. Polym Eng Sci 1991;31(23):1670-1673.

[44] Sundararaj U, Macosko CW, Nakayama A, Inoue T. Milligrams to kilograms: An evaluation of mixers for reactive polymer blending. Polym Eng Sci 1995;35(1):100-114.

[45] Sundararaj U, Macosko CW, Rolando RJ, Chan CT. Morphology development in polymer blends**.** Polym Eng Sci 1992;32(24):1814–1823.

[46] Lindt J T, Gosh AK. Fluid mechanics of the formation of polymer blends. Part I: Formation of lamellar structures. Polym Eng Sci 1992; 32(24):1802-1813.

[47] Walheim S, Böltau M, Mlynek J, Krausch G, Steiner U. Structure Formation via Polymer Demixing in Spin-Cast Films. Macromolecules 1997;30(17):4995– 5003.

[48] Shih CK. Polyarylate/ Rubber blend. SPE ANTEC Tech. Papers 1991;37:99.

[49] Shih CK. Fundamentals of polymer compounding: The phase-inversion mechanism during mixing of polymer blends**.** Adv Polym Thecnol 1992;11(3): 223-226.

[50] Shih C K. Mixing and morphological transformations in the compounding process for polymer blends: The phase inversion mechanism. Polym Eng Sci 1995;35(21):1688-1694

[51] Sundararaj U, Macosko CW, Shih CK**.** Evidence for inversion of phase continuity during morphology development in polymer blending**.** Polym Eng Sci 1996;36(13):1769-1781.

[52] Scott CE, Macosko CW. Morphology development during the initial stages of polymer-polymer blending. Polymer 1995;36(3):461–470.

[53] Hu G-H, Kadri I. Modeling reactive blending: An experimental approach. J Polym Sci, part B: Polym Phys 1998;36(12):2153-2163.

[54] Scott CE, Macosko CW. Morphology development during reactive and non-reactive blending of an ethylene-propylene rubber with two thermoplastic matrices. Polymer 1994;35(25):5422-5433.

[55] Machado AV, Covas JA, van Duin M. Chemical and morphological evolution of PA-6/EPM/EPM-g-MA blends in a twin screw extruder. J Polym Sci, part A: Polym Chem 1999;37(9):1311-1320.

[56] Favis BD. Effect of processing parameters on the morphology of an immiscible binary blend. J Appl Polym Sci 1990;39(2):285-300.

[57] Schreiber HP, Olguin A. Aspects of dispersion and flow in thermoplastic-elastomer blends. Polym Eng Sci 1983;23(3):129-134.

[58] Taylor GI. The viscosity of a fluid containing small drops of another fluid. Proc R Soc London 1932;A138:41-48.

[59] Taylor GI. The formation of emulsions in definable fields of flow. Proc R Soc London 1934; A146:501-523.

[60] Grace HP. Dispersion phenomena in high viscosity immiscible fluid systems and application of static mixers as dispersion devices in such systems. Chem Eng Comun 1982;14:225-227.

[61] Cox R G. The deformation of a drop in a general time-dependent fluid flow. J Fluid Mech 1969;37(3): 601-623.

[62] Karam H J, Bellinger JC. Deformation and breakup of liquid droplets in a simple shear field. Ind Eng Chem Fundam1968;7:576.

[63] Rumscheidt FD, Mason SG. Particle motions in sheared suspensions XII. Deformation and burst of fluid drops in shear and hyperbolic flow. J Colloid Sci 1961;16(3):238-261.

[64] Tomotika S. On the instability of a cylindrical thread of a viscous liquid surrounded by another viscous fluid. Proc R Soc Lond A 1935;150(870):322-337.

[65] Elmendorp JJ**.** A study on polymer blending microrheology. Polym Eng Sci 1986;26(6):418-426.

[66] Hagedorn J G, Martys NS, Douglas JF. Breakup of a fluid thread in a confined geometry: droplet-plug transition, perturbation sensitivity, and kinetic stabilization with confinement. Phys Rev E 2004; 69(5): 056312.1-056312.18.

[67] Utracki LA, Shi ZH. Development of polymer blend morphology during compounding in a twin-screw extruder. Part I: Droplet dispersion and coalescence - a review**.** Polym Eng Sci 1992;32(24):1824-1833.

[68] Van Oene H. Rheology of polymer blends and dispersions. In: Polymer Blends, Paul DR, Newman S, editors. San Diego CA: Academic Press, 1978. p.295-352.

[69] Van Oene H. Modes of dispersion of viscoelastic fluids in flow. J Colloid Interface Sci. 1972, 40(3),448–467.

[70] De Bruijn R A. Deformation and breakup of drops in simple shear flows. PhD thesis, University of Thecnology, Eindhoven, the Netherlands, 1989.

[71] Han CD, Funatsu, K. An experimental study on droplet deformation and breakup in pressure-driven flows through converging and uniform channels. J Rheol 1978;22(2):113-133.

[72] Sundararaj U, Macosko CW. Drop Breakup and Coalescence in Polymer Blends: The Effects of Concentration and Compatibilization. Macromol 1995;28(8):2647-2657.

[73] Ghodgaonkar PG, Sundararaj U. Prediction of dispersed phase drop diameter in polymer blends: The effect of elasticity. Polym Eng Sci 1996;36(12):1656-1665.

[74] Wu S. Formation of dispersed phase in incompatible polymer blends: Interfacial and rheological effects. Polym Eng Sci 1987;27(5):335-343.

[75] Favis BD, Chalifoux JP**.** The effect of viscosity ratio on the morphology of polypropylene/polycarbonate blends during processing. Polym Eng Sci 1987;27(21):1591-1600.

[76] Favis BD, Chalifoux JP. Influence of composition on the morphology of polypropylene/polycarbonate blends. Polymer 1988; 29(10): 1761–1767.

[77] Serpe G, Jarrin J, Dawans F**.** Morphology-processing relationships in polyethylene-polyamide blends. Polym Eng Sci 1990:30(9):553-565.

[78] Fortelný I, Kovár J. Theory of coalescence in immiscible polymer blends. Polym Compos 1988;9(2):119-124.

[79] Fortelný I, Cerná Z, Binko J, Kovár J. Anomalous dependence of the size of droplets of disperse phase on intensity of mixing. J Appl Polym Sci 1993;48(10):1731-1737.

[80] Fortelný I, Kovár J. Droplet size of the minor component in the mixing of melts of immiscible polymers. Eur Polym J 1989;25(3):317-319.

[81] Coran AY, Patel RP. Rubber-Thermoplastic Compositions. Part III. Predicting Elastic Moduli of Melt-Mixed Rubber-Plastic Blends. Rubber Chem Technol 1981;54(1):91-100.

[82] Coran AY, Patel RP. Rubber-thermoplastic compositions. Part II. NBR-nylon thermoplastic elastomeric compositions. Rubber Chem Technol 1981;53(4),781-794.

[83] Coran AY, Patel RP., Rubber-Thermoplastic Compositions Part V. Selecting Polymers for Thermoplastic Vulcanizates Rubber Chem. Technol. 55(1), 116-136 (1982)

[84] Coran AY, Patel RP. Elastoplastic compositions of butyl rubber and polyolefin resin. US Patent 4355139, 1982.

[85] Coran AY, Patel RP. Rubber-thermoplastic compositions. Part I. EPDM-polypropylene thermoplastic vulcanizates. Rubber Chem Technol, 1980;53(1):141-151.

[86] Coran AY, Patel RP. Rubber-thermoplastic compositions. Part VII. Chlorinated polyethylene rubber-nylon compositions. Rubber Chem Technol 1983;56(1):210-225.

[87] Coran AY, Patel RP. Rubber-thermoplastic compositions. Part VIII. Nitrile rubber polyolefin blends with technological compatibilization. Rubber Chem Technol 1983;56(5):1045-1060.

[88] Coran AY, Patel RP, Williams-Headd D. Rubber-thermoplastic compositions. Part IX, blends of dissimilar rubbers and plastics with technological compatibilization. Rubber Chem. Technol. 58(5), 1014-1023 (1985)

[89] Naskar K, Noordermeer JWM. Thermoplastic elastomers by dynamic vulcanization. Progress in Rubber, Plastics and Recycling Technology 2005;21(1):1-25.

[90] Abdou-Sabet S, Datta S. Thermplastics Vulcanizates. In: Polymer Blends – Volume 2: Performace, , Paul DR, Bucknall CB, editors. Wiley Interscience, 2000. p.517-554.

[91] Abdou-Sabet S, Patel RP. Morphology of elastomeric alloys. Rubber Chem Technol 1991;64(5):769-779.

[92] Abdou-Sabet S, Fath MA. Thermoplastic elastomeric blends of olefin rubber and polyolefin resin.US Patent 4311628, 1982.

[93] Tzoganakis C, Vlachopoulos J, Hamielec AE. Production of controlled-rheology polypropylene resins by peroxide promoted degradation during extrusion. Polym Eng Sci, 1988;28(3):170-180.

[94] Pabedinskas A, Cluett W, Balke S. Modeling of polypropylene degradation during reactive extrusion with implications for process control**.** Polym Eng Sci, 1994;34(7):598-612.

[95] Lachtermacher MG, Rudin A. Reactive processing of LLDPEs in corotating intermeshing twin-screw extruder. I. Effect of peroxide treatment on polymer molecular structure**.** J Appl Polym Sci, 1995;58(11):2077-2094.

[96] Lachtermacher MG, Rudin A. Reactive processing of LLDPES in corotating intermeshing twin-screw extruder. II. Effect of peroxide treatment on processability. J Appl Polym Sci, 1995;58(13):2433-2449.

[97] Kolbert AC, Didier JG, Xu L. Mechanochemical Degradation of Ethylene−Propylene Copolymers: Characterization of Olefin Chain Ends. Macromolecules, 1996;29(27):8591-8598.

[98] Lachtermacher MG, Rudin A. Reactive processing of LLDPEs with peroxides in counter-rotating nonintermeshing twin-screw extruder. IV. Effects of molecular structure of LLDPEs. J Appl Polym Sci, 1996;59(8):1212-1221.

[99] Machado AV, Covas JA, van Duin M. Monitoring polyolefin modification along the axis of a twin screw extruder. I. Effect of peroxide concentration. J App Polym Sci 2001;81(1);58-68

[100] Naskar K, Noordermeer JWM. Dynamically Vulcanized PP/EPDM Blends: Effects of Different Types of Peroxides on the Properties Rubber Chem. Technol. 76(4), 100-1018 (2003)

[101] Dluzneski PR. Peroxide vulcanization of elastomers. Rubber Chem Technol 2001;74(3):451-492.

[102] Class J. A review of the fundamentals of crosslinking with peroxides. Rubber World 1999;220(5):35-39.

[103] Fritz HG, Anderlik R. Elastic properties of thermoplastic elastomers on the basis of dynamic vulcanized PP/EPDM-blends. Kautsch Gummi Kunstst 1993;46(5):374-379.

[104] Manchado MAL, Kenny JM. Use of benzene-1,3-bis(sulfonyl)azide as crosslinking agent of TPVs based on EPDM rubber-polyolefin blends. Rubber Chem Technol, 2001;74(2):198-210.

[105] van Duin M, Machado AV. EPDM-based thermoplastic vulcanisates: Crosslinking chemistry and dynamic vulcanisation along the extruder axis. Polym Deg Stab, 2005;90(2):340-345.

[106] Lattimer RP, Kinsey RA, Layer RW, Rhee CK. The mechanism of phenolic resin vulcanization of unsaturated elastomers. Rubber Chem Technol, 1989;62(1):107-123.

[107] van Duin M, Souphantong A. The chemistry of phenol-formaldehyde resin vulcanization of EPDM: part I. Evidence for methylene crosslinks. Rubber Chem Technol, 1995;68(5):717-727.

[108] van Duin M. The chemistry of phenol-formaldehyde resin crosslinking of EPDM as studied with low-molecular-weight models: part II. Formation of inert species, crosslink precursors and crosslinks. Rubber Chem Technol, 2000;73(4):706-719.

[109] Winters R. Mechanism of resole and sulfur vulcanisation of EPDM. PhD thesis, Rijksuniversiteit Leiden, the Netherlands, 2000.

[110] Romani D, Garagnani E, Marchetti E. Reactive blending: structure and properties of crosslinking olefinic thermoplastic elastomer. Int Symp New Polym Mater. Naples, Italy, 1986. p.56-87.

[111] Kresge EN. Rubbery Thermoplastics blends. In: Polymer Blends, Paul DR, Newman S, editors. New York: Academic Press, Vol.II, 1978.

[112] Radusch HJ, Pham T. Morphology formation in dynamic vulcanized PP/EPDM blends. Kautsch Gummi Kunstst 1996;49(4):249-257.

[113] Rader CP, Abdou-Sabet S. Two-phase elastomeric alloys. In: Thermoplastic elastomers from rubber–plastic blends, De SK, Bhowmick AK, editors. New York: Ellis Horwood, 1990. p.159-197

[114] Sengupta P. Morphology of olefinic thermoplastic elastomer blends: A comparative study into the structure – property relationship of EPDM/PP/oil and SEBS/PP/oil blend. PhD thesis University of Twente, The Netherlands, 2004.

[115] Katbab AA, Nazockdast H, Bazgir S. Carbon black-reinforced dynamically cured EPDM/PP thermoplastic elastomers. I. Morphology, rheology, and dynamic mechanical properties. J Appl Polym Sci, 2000;75(9):1127-1137.

[116] Legge NR. Thermoplastic elastomers: three decades of progress. Rubber Chem Technol, 1989;62(3):529-547.

[117] Abdou-Sabet S, Puydak RC, Rader CP. Dynamically vulcanized thermoplastic elastomers. Rubber Chem Technol 1996;69(3):476-494.

[118] Coran AY, Patel RP. Thermoplastic elastomers by blending and dynamic vulcanization. In: Polypropylene: Structure, blends and composites, volume 2, Copolymers and Blends. Karger-kocsis J, editor. Chapman & Hall, 1995.

[119] Kikuchi Y, Fukui T, Okada T, Inoue T. Elastic-plastic analysis of the deformation mechanism of PP-EPDM thermoplastic elastomer: Origin of rubber elasticity. Polym Eng Sci, 1991;31(14):1029-1032.

[120] Boyce M, Kear K, Socrate S, Shaw K. Deformation of thermoplastic vulcanizates. J Mech Phys Sol, 2001,49(5):1073-1098

[121] Boyce M, Kear K, Socrate S, Yeh O, Shaw K. Micromechanisms of deformation and recovery in thermoplastic vulcanizates. J Mech Phys Sol, 2001;49(6):1323-1342.

[122] Yang Y, Chiba T, Saito H, Inoue T. Physical characterization of a polyolefinic thermoplastic elastomer. Polymer 1998;39(15):3365-3372

[123] Soliman M, Dijk van M, Es van M, Shulmeister V. Deformation mechanism of thermoplastics vulcanisates investigated by combined FTIR and stress strain measurements. ANTEC 1999. p.1947-1948.

[124] Huy TA, Luepke T, Radusch H J. Characterization of the deformation behavior of dynamic vulcanizates by FTIR spectroscopy. J Appl Polym Sci 2001;80(2):148-158

[125] Wright KJ, Indukuri K, Lesser AJ. Microcellular model evaluation for the deformation of dynamically vulcanized EPDM/iPP blends. Polym Eng Sci 2003;43(3):531-542.

[126] Oderkerk J, Groeninckx G, Soliman M. Investigation of the deformation and recovery behavior of nylon-6/rubber thermoplastic vulcanizates on the molecular level by infrared-strain recovery measurements. Macromolecules 2002;35(10):3946-3954.

[127] Oderkerk J, De Schaetzen G, Goderis B, Hellemans L, Groeninckx G. Micromechanical deformation and recovery processes of nylon-6/ rubber thermoplastic vulcanizates as studied by atomic force microscopy and transmission electron microscopy. Macromolecules 2002;35(17):6623-6629.

[128] Goettler LA, Richwine JR, Wille FJ. The rheology and processing of olefin-based thermoplastic vulcanizates. Rubber Chem Thecnol 1982:55(5);1448-1463.

[129] Kuriakose B, De SK. Studies on the melt flow behavior of thermoplastic elastomers from polypropylene - Natural rubber blends. Polym Eng Sci 1985;25(10):630-634.

[130] Han PK, White JL. Rheological studies of dynamically vulcanized and mechanical blends of polypropylene and ethylene-propylene rubber. Rubber Chem Thecnol 1995;68(5):728-738

[131] Steeman P, Zoetelief W. Rheology of TPVs. In: ANTEC conference proceeding, 2000. p.3297-3301

[132] Winters R, Lugtenburg J, Litvinov VM, van Duin M, de Groot HJM. Solid state ^{13}C NMR spectroscopy on EPDM/PP/oil based thermoplastic vulcanizates in the melt. Polymer 2001;42(24):9745-9752

[133] Machado AV, Duin M van. Dynamic vulcanisation of EPDM/PE-based thermoplastic vulcanisates studied along the extruder axis. Polymer 2005;46(17):6575-6586.

[134] Goharpey F, Katbab AA, Nazockdast H. Formation of rubber particle agglomerates during morphology development in dynamically crosslinked EPDM/PP thermoplastic elastomers. Part 1: Effects of processing and polymer structural parameters. Rubber Chem and Thecnol 2003;76(1):239-252.

[135] Radush HJ. Phase morphology of dynamically vulcanized thermoplastic vulcanizates. In: Micro-and nanostructured multiphase polymer blend system: Phase Morphology and Interfaces, Harrats C, Thomas S, Groeninckx G, editors. Taylor & Francis, 2006.

[136] Bhadane PA, Virgilio N, Favis BD, Champagne MF, Huneault MA, Tofan F. Effect of dynamic vulcanization on Co-continuous morphology. AIChE J 2006;52(10): 3411-3420.

[137] Nicolini A, de Campos Rocha TLÁ, Jacobi MAM. Dynamically vulcanized PP/EPDM blends: Influence of curing agents on the morphology evolution. J Appl Polym Sci 2008;109(5):3093-3100.

Chapter 2: Processing Equipment and Materials

This chapter is divided in three parts: *Processing Equipment*, *Modification of Commercial Materials* and *Materials*. *Processing Equipment* gives information that is relevant about the equipment used to produce the materials that were investigated in this study. *Modification of commercial materials* deals with an experimental study on degradation of commercial grades of EPDM and PP using two peroxides under different processing conditions. The main goal was to obtain EPDM and PP with low viscosities, which were not available in the market but were essential for this research. *Materials* presents all the polymers used in this work along with the relevant properties.

Part of this chapter was published in: Novel Trends in Rheology III, Zatloukal M, editors, 2009

1. Processing Equipment

1.1 Internal Mixer

Even though polymer blends are industrially processed in extruders, internal mixers have been widely used to investigate the chemical and physical behaviour of blends like mixing quality, viability of polymer-polymer inter-reaction, cross-linking, degradation, etc. The advantages of these equipments are the small amount of materials used and the possibility of monitoring the torque and melt temperature during the experiment. Torque date is quite useful since it is a qualitative measurement of the system viscosity.

The blends and TPVs studied in the present work were compounded in a Haake Rheomix 600 OS batch mixer using roller rotors running in a counter-rotating way, shown in Fig. 2.1. The degree of fill used was 78 % to provide good intermixing between the two halves of the mixing chamber. The internal mixer is characterized by high-stress zones, which are in the region between the rotors tips and the mixing chamber – narrow-gap regions - where dispersive mixing takes place [1]. The low-stress zones correspond to the large gap regions. Different regions of the high-stress zones and different flow field in the large gap regions between the two rotors can be achieved by change the blades designs [1].

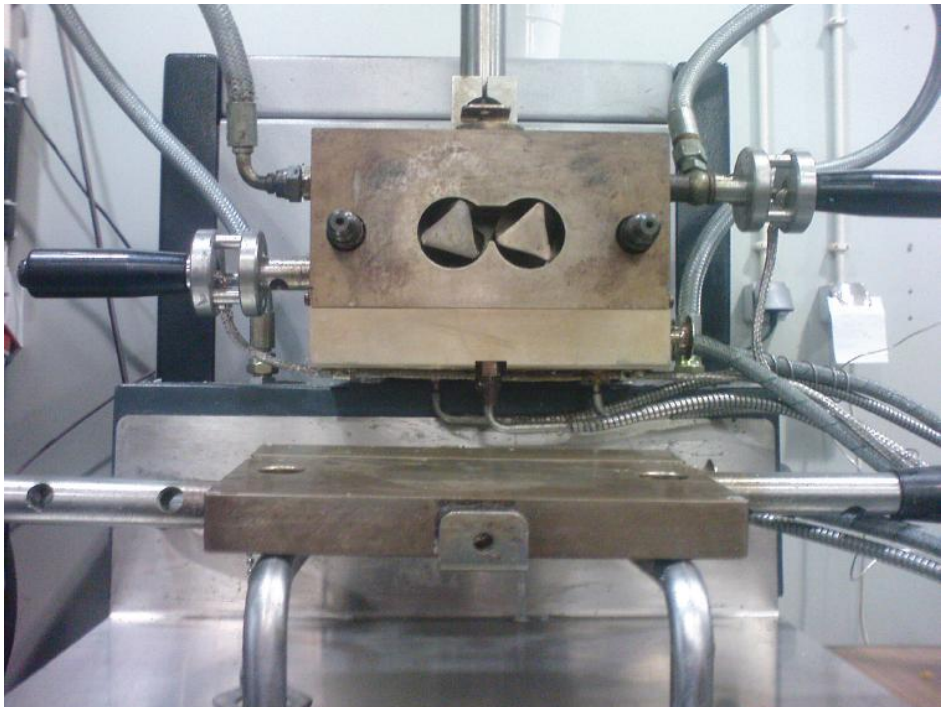

Fig. 2.1. Haake Rheomix 600 OS batch mixer.

1.2 Shear Rate

Several efforts have been made [2-5] to estimate the materials viscosity and shear rate inside of the internal mixer from the torque measurements and rotors speed. Bousmina et al. [5] developed a general model and experimental procedure to estimate the shear rate and viscosity from the rotor speed and torque data, which will be followed in this work. By using a dual-Couette analogy (shown in Fig. 2.2) to represent the rotor blades and mixing chamber, an effective hydrodynamic radius (Ri) was determined.

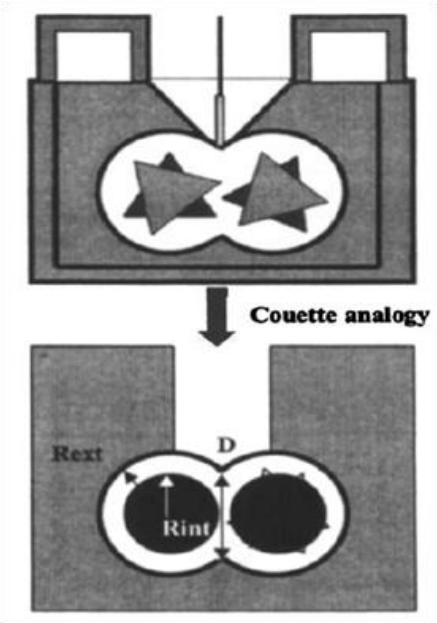

Fig. 2.2. Couette analogy of batch mixer [6].

Ri was found to be dependent of the geometrical dimensions of the mixer and the gear ratio but independent of the fluid under mixing and mixing conditions, as can be seen in equation (1):

$$Ri = \frac{\mathrm{Re}}{\left[1+\frac{4\pi N}{n}\left(2\pi ML\,\mathrm{Re}^2\frac{1+g^{n+1}}{\Gamma}\right)^{1/n}\right]^{n/2}} \qquad (1)$$

where Re is the chamber external radius of the internal mixer, N is the rotor speed, L is the length of the cylinder, g is the gear ratio, Γ, M and n are the torque, consistency and the power law index of polymer used (it can be Newtonian or non-Newtonian), respectively.

Once Ri is determined, the viscosity of any fluid (Newtonian or non-Newtonian) and shear rate can be determined. The shear rate can be determined by equation (2):

$$\dot{\gamma} = \frac{16 \times \pi \times N \times \beta^2}{(1+\beta)^2(\beta^2 - 1)} \qquad (2)$$

with

$$\beta = \frac{\mathrm{Re}}{Ri}$$

The dimensions of the internal mixer used are: Re = 19.5 mm, L = 46.5 mm and g = 2/3. The Γ, M and n were determined for some of the polymers used in this work. The Ri average value obtained was 17.15 mm, corresponding a β of 1.137. Thus, the shear rate inside of the chamber can be calculated by equation (3) where N is in rpm.

$$\dot{\gamma} = 0.81 \times N \qquad (3)$$

Since in the present work the rotor speed used is 80 rpm the shear rate is close to 65 s^{-1}.

2. Modification of EPDM and PP

2.1. Introduction

Polymer modification has been widely used to prepare polymers with specific properties. The use of controlled chain degradation became an important industrial application for the production of PP with controlled rheology [7]. As a result, a reduction of molecular weight is obtained, which corresponds to lower melt viscosity and improved processability. It is generally accepted that degradation of PP follows a series of free radical reactions, i.e., peroxide decomposition, hydrogen abstraction, chain scission and termination [7-13] (Fig. 2.3). Some kinetic models for PP degradation have been developed and combined with a simplified model of the melting mechanism in the extruder, in order to predict the molecular weight average [9].

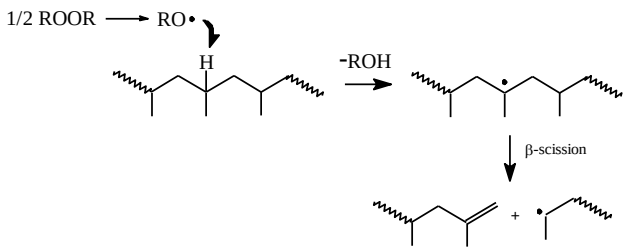

Fig. 2.3. Mechanism of peroxide induced degradation of PP.

Long side chains can be formed when the macroradicals, formed by hydrogen abstraction experience bimolecular termination by combination (Fig. 2.4). If this long chain branching continues, a three-dimensional network will form with high levels of insoluble gel (cross-linking). The formation of high molecular weight chains due to branching increases the melt strength and the die swell and improve the strain hardening properties [14-18].

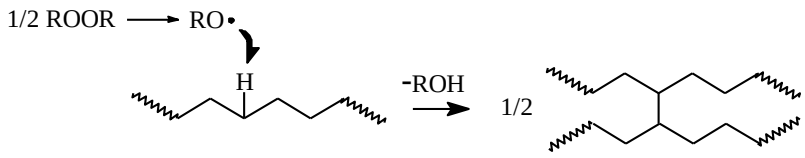

Fig. 2.4. Mechanism of branching/cross-linking reaction of polyolefins.

Often, cross-linking is considered undesirable because of reduced processability. However, it may also brings some property enhancement to the polymer, such as increased service temperature, solvent resistance, flexural modulus and dimensional stability.

The occurrence of degradation or/and cross-linking reactions depends on the polyolefin structure. In case of EPM and EPDM it is believed that cross-linking and chain scission are competing mechanisms and their relative effects depend on the copolymer composition, i.e., the relative amount of ethylene and propylene sequences [19-22]. Loan [23] found out that using only peroxide result in poor cross-linking of EPDM and EPM. Machado et al. [19] studied the rheological behaviour of PP, PE and EPM in a twin extruded monitored along the barrel, they observed that the degree of cross-linking/branching and/or degradation in EPM depends essential of ethene/propene ratio, on the original molecular weight of polymer and on the amount of peroxide used.

The present study aims to prepare EPDM and two PPs with very low viscosity throughout modification of commercial EPDM and PP grades. Another objective of this study is to make a comparative study on degradation/cross-linking of EPM and EPDM processed in a batch mixer with and without peroxide. The effect of rotor speed, temperature and peroxide amount was investigated. Rheological measurements and EPDM gel content, in case of EPDM and EPM, were used to monitor the chemical changes (cross-linking/branching or degradation).

2.2. Experimental

EPDM rubber (K2340A: 53 wt.% ethylene and 6 wt.% ENB; Mw = 150 kg/mol; Mooney viscosity (1+4) at 125 ºC: 25) and the EPM rubber (K3200A: 49 wt.% ethylene; Mw = 150 kg/mol; Mooney viscosity (1+4) at 100 °C: 51) were supplied by DSM Elastomers BV. The isotatic PP homopolymer (579S: with melt flow indices of 47 g/10 min at 230 ºC/2.16 kg), was supplied by Sabic Europe. The cumyl hydroperoxide (80 %; M= 84,16 g/mol) were supplied by Acros and used as received to modify the EPDM and EPM. The half time of this peroxide at 200 and 300 ºC are 260 and 0.73 s. The 2,5-bis(*tert*-butylperoxy)-2,5-dimethylhexane (DHBP; Trigonox T101) was supplied by Akzo Nobel and was used to obtain two PPs with low viscosity. The half time of this peroxide at 200 ºC is 6.1 s.

No special precautions against the presence of oxygen were taken, during processing. The polymers (EPDM, EPM and PP) with and without peroxides were processed in a batch mixer (Haake Rheomix 600 OS; 69 ml). The recipes and the operating conditions used in the experiment with EPDM and EPM are given in Table 2.1. After 25 minutes the rotors were stopped and the all material was collected. For PP a set temperature of 200 ºC, a rotor speed of 80 rpm and a mixing time of 5 minutes (after PP melting) were used. The amounts of peroxide used were 0.01 and 0.1 phr of Trigonox T101.

All polymers were pre-mixed with the peroxide and introduced in batch mixer.

Table 2.1. Recipes and Operation Conditions of EPDM and EPM polymers.

Polymer	Temperature (ºC)	Screw speed (rpm)	Peroxide (phr)
EPDM	200; 300	80	0; 0.05; 0.1
EPDM	200; 300	150	0; 0.05; 0,1
EPDM	350	20	0
EPDM	350	150	0; 0.05
EPM	200; 300	80	0; 0.05; 0.1
EPM	200; 300	150	0; 0.05; 0.1

The modified material were characterised by oscillatory rheological measurements using a Rheological Stress Tech HR, rotational rheometer using parallel-plate geometry. The gap and diameter of the plates were 1 mm and 25 mm, respectively. Isothermal frequency sweeps from 0,01 and 100 Hz at 200 ºC were performed. For each material, a stress sweep was carried out from 0.5 to 5000 Pa at frequencies of 1 and 10 Hz to determine the linear viscoelastic regime. The discs were prepared by compression molding at 200 ºC under a press of 30 ton. In case of very low viscous samples which are liquid at room temperature it was not possible to do discs and samples were place directly in the rheometer. Rheological measurements were not performed on samples presenting high cross-linking degree since they do not soften. EPDM and EPM gel content determinations were performed using approximately 300 mg of the collected samples, which were placed in 80 µm mesh stainless cages and immersed in cyclohexane under gentle stirring during 48 h at room temperature. The solvent was refreshed once after about 24 h. After removal of the cyclohexane, samples were dried in a vacuum oven for 12 h at 100 °C with nitrogen purging and weighed again.

2.3. Results and discussion

EPDM vs EPM

The torque behaviour recorded during processing of EPDM and EPM in the absence of peroxide at different temperatures is shown in Fig. 2.5. As it was expected, for both, EPDM and EPM, an increase of temperature results in a decrease of the torque, suggesting a decrease in viscosity. For EPDM it can be observed that mixing does not allow significant changes in the torque, with the exception of EPDM processed at 200 ºC were an increase is observed. This increase of the torque value suggests that cross-linking/branching occurred. In case of

EPM, while at 200 ºC the torque decreases along the processing time, at 300 ºC a pronounced decrease can be seen before 5 min. These results suggested that thermo-mechanical degradation took place during mixing and it was faster at 300 ºC.

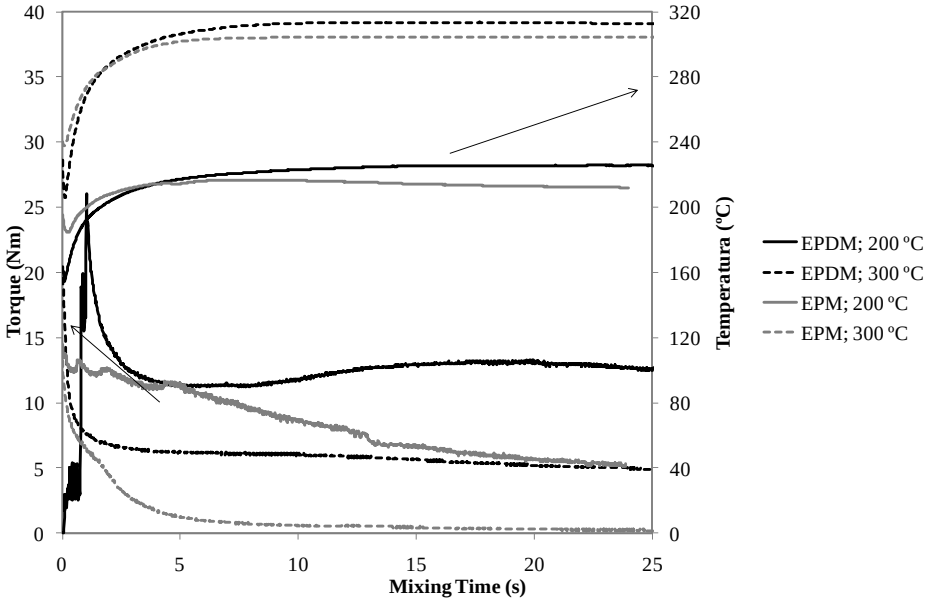

Fig. 2.5. Effect of the temperature on torque behaviour as a function of mixing time of EPDM and EPM in the absence of peroxide at a rotor speed of 80 rpm.

Fig. 2.6 depicts the torque measurements at the end of mixing as a function of peroxide concentration at 200 and 300 ºC and at a rotor speed of 150 rpm. At 200 ºC for both EPDM and EPM, peroxide amount does not have a significant influence on the torque. However, a slightly decrease of torque value is observed for EPM at 200 ºC when the concentration of peroxide increases from 0.05 to 0.1 phr. For the same variation of peroxide amount, EPDM at 300ºC shows a slightly increase of torque.

Fig. 2.7 shows the EPDM gel content at various processing conditions and peroxide amounts. Gel content measurements confirm if cross-linking/branching reactions took place during processing. An absolute error around 5 % was estimated to be in these experiments.

The EPM gel content samples (processed with different amount of peroxides and processing conditions) was measured and it was below 2 % for all samples. This suggests that cross-linking/branching does not occur during EPM modification. EPDM has a different behaviour, at 200 ºC and 80 rpm, the gel content was already quite higher (~ 65 %) even in the absence of peroxide and it remained basically the same when 0.05 phr of peroxide was added. An increase of peroxide concentration to 0.1 phr resulted in a small increase of gel content (~10 %). Different profile was obtained when the processing conditions were

changed. An increase of the rotor speed to 150 rpm (at 200 ºC), increased significantly the gel content (95 %) in the absence of peroxide. The addition of peroxide results in a decrease of gel content, which has a constant value (70 %) independently of the amount of peroxide used. Moreover, the gel content values were higher than those obtained at 80 rpm for the same conditions (temperature and amount of peroxide). Since the peroxide half-life time is 4.3 min at 200 ºC, the mixing time is enough to achieved complete decomposition. Therefore the increase of temperature due to the increase of rotor speed (around 10 %) does not affect peroxide decomposition. Thus, a possible explanation can be the higher energy input in the system, which increases the radical formation due to mechanical forces.

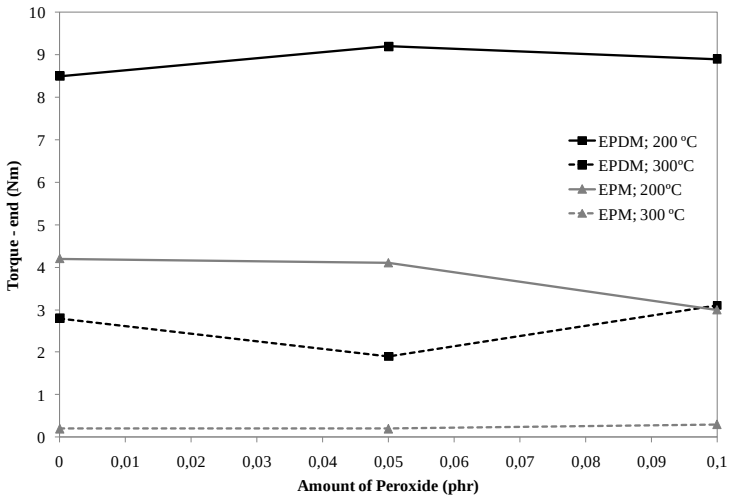

Fig. 2.6. Effect of peroxide concentration on the final torque for EPDM and EPM at a rotor speed of 150 rpm.

Similar profile was observed at 300 ºC and 80 rpm, in the absence of peroxide the EPDM gel content was high and changed to 35 and 40 % as the peroxide added was 0.05 and 0.1 phr, respectively. An increasing of rotor speed to 150 rpm at the same temperature (300 ºC) resulted in the same gel content profile. However, the gel content values were lower without peroxide and with 0.05 phrThe values of gel content were close to 0 % at 350 ºC using a rotor speed of 20 rpm. Suggesting that cross-linking reaction almost did not occur.

These results suggest that, at 200 and 300 ºC without and with peroxide, there is a competition between cross-linking/branching and degradation reactions. The main reaction depends on the interrelationship among temperature, rotor speed and amount of peroxide. In general the levels of cross-linking/branching are high in the absence of peroxide, suggesting that at these temperatures the radicals generation have to be taken into account. In fact, with the exception of the experiment at 200 ºC and 80 rpm, the addition of peroxide resulted in a

significant decrease of gel content, suggesting that degradation and cross-linking are competing and the addition of peroxide enhances degradation. An increase of temperature from 200 to 300 ºC had higher effect on the cross-linking/degradation reactions than an increase of peroxide amount (from 0.05 to 0.1 phr) or rotor speed. This can be explained by the fact that high temperature enhances the scission of polymer chains yielding the formation of macro-radicals that could easily recombined [24-28].

Since EPDM and EPM have a similar ethene/propene ratio (47 and 51 % of propene, respectively) and their molecular weights are the same, the cross-linking/branching reaction that was dominant in case of the EPDM should be related with presence of the reactive diene group.

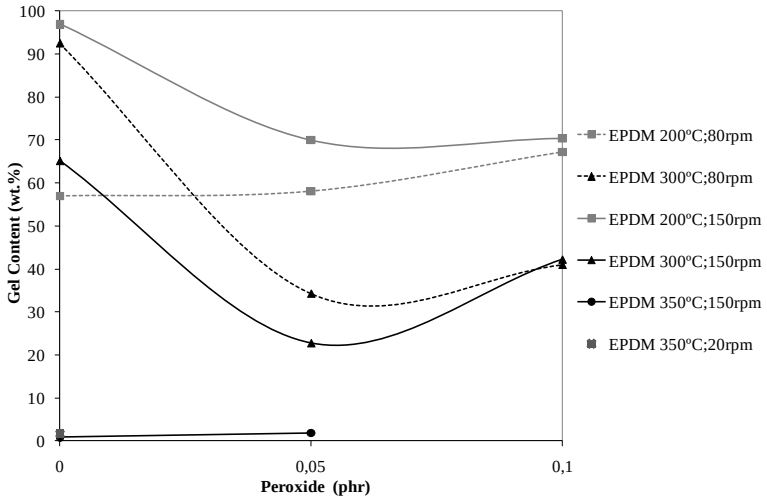

Fig. 2.7. EPDM gel content as a function of peroxide concentration at different processing conditions.

Rheological measurements were performed for the various samples produced under different processing conditions and different amount of peroxide. Samples with high cross-linking levels could not be analysed. The rheological behaviour of raw materials, EPDM and EPM were also performed under the same conditions and the results were added as reference in all the Figs. 2.8 and 2.9. As it can be seen, EPDM exhibit shear-thinning behaviour over the complete range of frequencies measured while the EPM show a normal pseudoplastic behaviour, with a Newtonian plateau at low frequencies and shear thinning behaviour at higher frequencies.

Fig. 2.8(a,b) shows the effect of the processing temperature on rheological behaviour of EPM and EPDM using a rotor speed of 80 rpm in the absence of peroxide. EPDM processed at 200 ºC presents higher viscosity and elasticity at low frequencies, increasing shear thinning, which suggests that cross-linking/branching took place during mixing. These results are in

agreement with the gel content value, which was close to 60 % at 200 ºC. EPDM sample processed at 300 ºC present a gel content value of 95 %, consequently rheological measurements could not be performed. Nevertheless, the results obtained by both techniques show that under these processing conditions cross-linking/branching of EPDM increases with temperature. A different behaviour can be observed for EPM, which shows a decrease of the viscosity and elasticity as the temperature increases. At 300 ºC the EPM viscosity becomes too low, the Newtonian plateau enlarges to high frequencies and the elasticity presents values below 1 at low frequencies. Thus, under these processing conditions and in the absence of peroxide, an increase of temperature decrease the viscosity and elasticity of the EPM, this can be associated with higher chain scission.

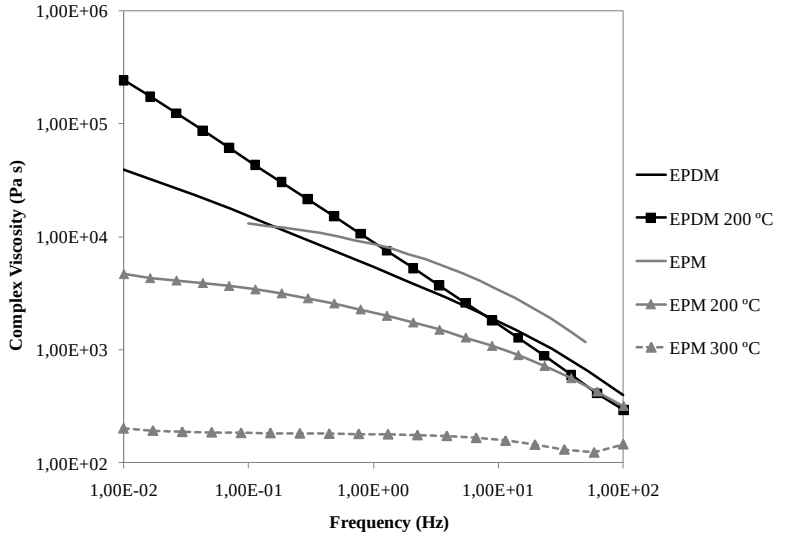

a)

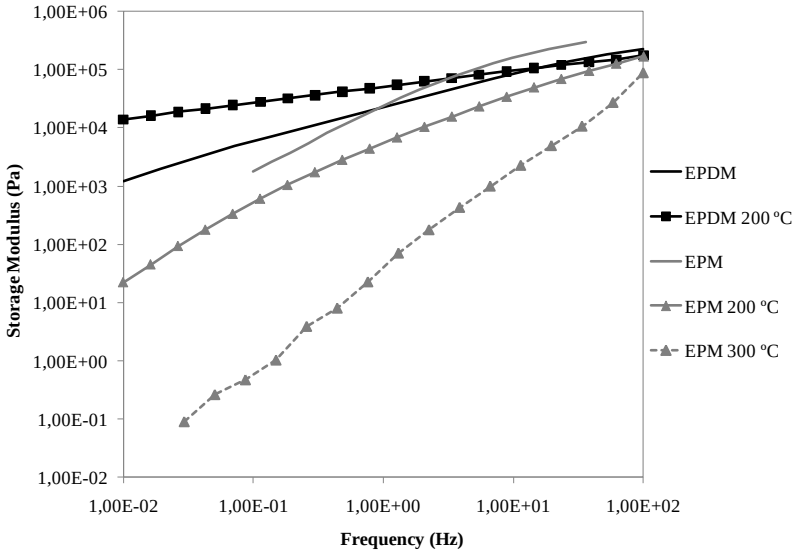

b)

Fig. 2.8. Effect of processing temperature on rheological behaviour of EPDM and EPM (80 rpm without peroxide): a) complex viscosity and b) storage modulus.

The rheological behaviour of EPDM samples prepared with different amounts of peroxide at different temperatures and rotor speed of 80 rpm is shown in Fig. 2.9. An increase of complex viscosity and elasticity at low frequencies can be observed in all cases, suggesting that cross-linking/branching were the main reaction occurring under the conditions used. However, due to the shear thinning behaviour, the slope of complex viscosity curves increases and at medium and high frequencies, the viscosity becomes smaller than the original EPDM. In general, cross-linking occurs and the viscosity of the modified EPDM is quite similar and independent of the temperature and the amount of peroxide used.

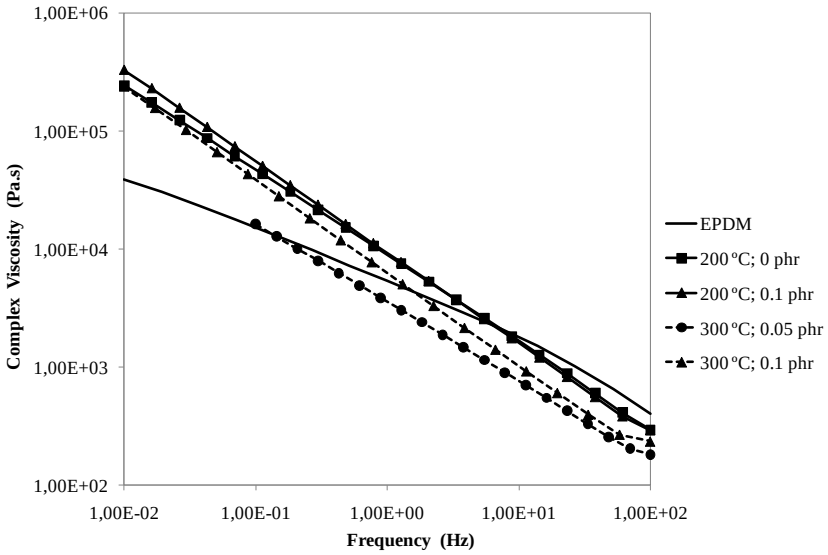

a)

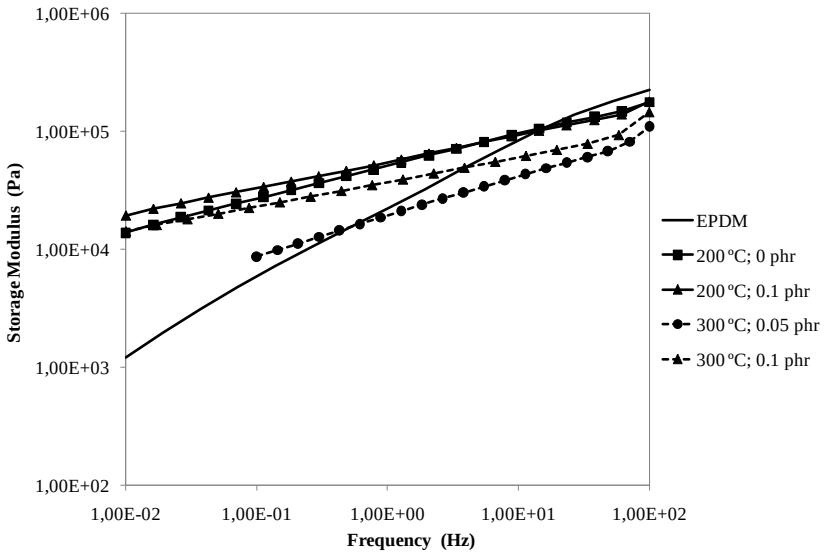

b)

Fig. 2.9. Effect of peroxide concentration on the rheological behaviour of EPDM at 80 rpm: a) complex viscosity and b) storage modulus.

The effect of peroxide amount at different temperatures under the same rotor speed (150 rpm) on the complex viscosity of EPDM is depicted in Fig. 2.10. The complex viscosity of EPDM modified with 0.05 phr of peroxide at 300 ºC is lower than the pure EPDM indicating that degradation occurred. Nevertheless the shear thinning behaviour was enhanced indicating that cross-linking also took place, as it can be confirmed by gel content which was 23 wt.% (Fig. 2.8). At 350 ºC, independently of the peroxide amount used the complex viscosity is very low and exhibits a Newtonian plateau over the range of frequencies measured. Under these conditions degradation occurred in a large extend. These results are in accordance with the gel content value, which was close to 0 % and it is a consequence of the very high temperature used. Probably both degradation and cross-linking occurred simultaneously but chain scission was the main reaction and lower EPDM gel content was obtained [29].

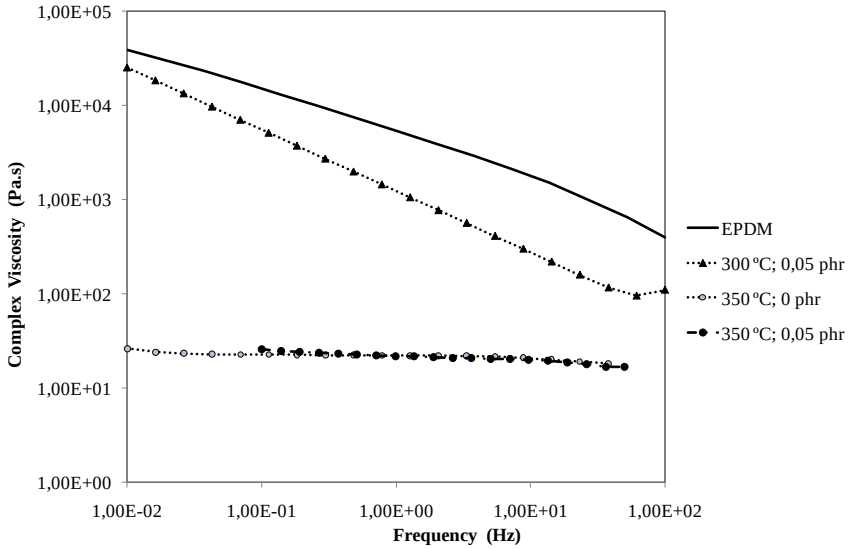

Fig. 2.10. Effect of peroxide on complex viscosity of the EPDM as a function of frequency.

Fig. 2.11 shows the results of rheological measurements of EPM samples prepared with a rotor speed of 80 rpm at different temperatures and with different amounts of peroxide. At 200 ºC complex viscosity and elasticity decreases and the lowest values were obtained when 0.05 phr of peroxide was added. Thus, increasing the amount of peroxide to 0.1 phr results in an increase of viscosity and elasticity, suggesting that cross-linking/branching also occur for EPM under certain conditions. Degradation is significantly improved by increasing the temperature to 300 ºC and it is almost independent of peroxide amount, in fact at this temperature the same level of degradation is achieved with and without peroxide. These

results are in agreement with the gel content measurements, since gel content values below to 2 % were obtained for all EPM samples.

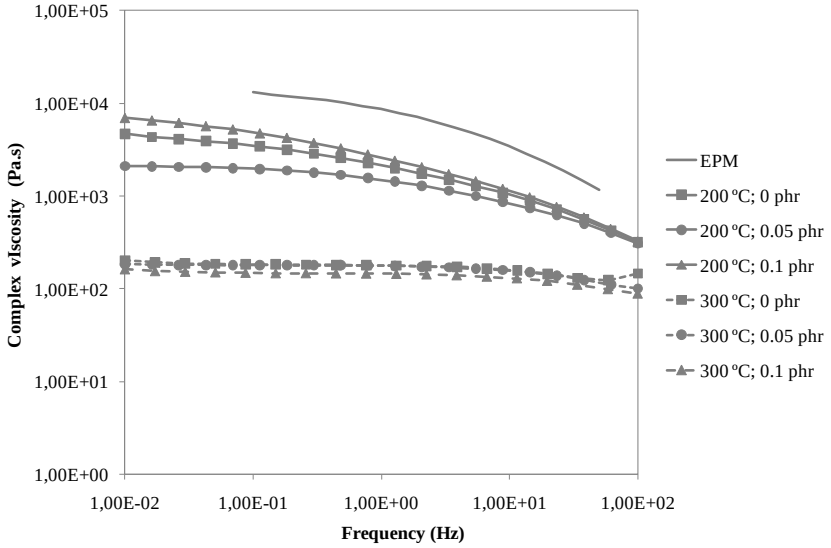

a)

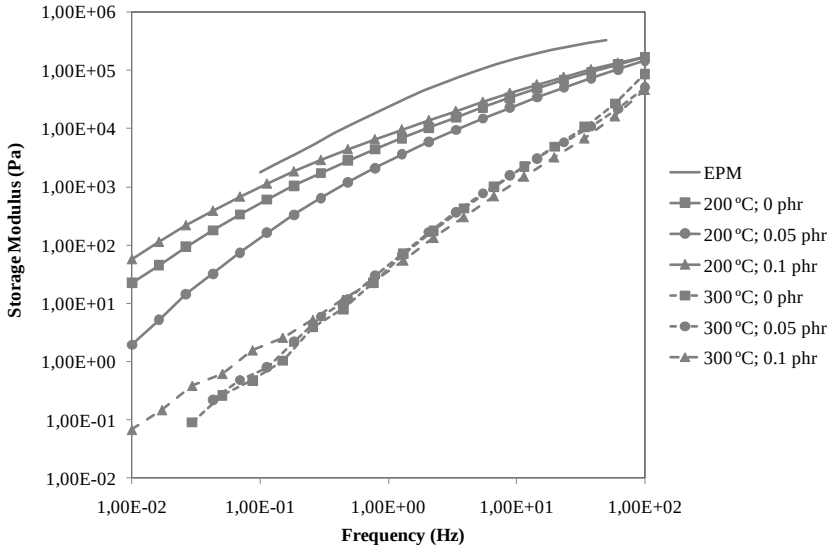

b)

Fig. 2.11. Effect of peroxide concentration on the rheological behaviour of EDM (rotor speed at 80 rpm): a) complex viscosity and b) storage modulus.

PP

The complex viscosities as a function of frequency measured for commercial PP and PP modified with 0.1 and 1 phr of peroxide (Trigonox T101) at 200 ºC is depicted in Fig 2.12. As expected, degradation occurs and the complex viscosity decreased as the peroxide amount increased.

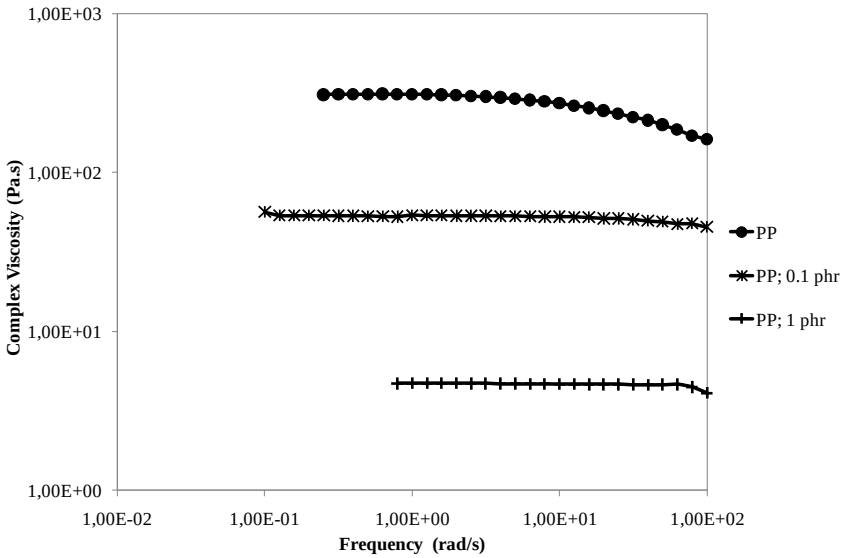

Fig. 2.12. Effect of peroxide on complex viscosity of the PP as a function of frequency.

2.4. Conclusions

EPDM processed at 200 and 300 ºC shows an increase of viscosity and elasticity at low frequencies and an increase of the shear thinning behaviour, which evidence that cross-linking/branching prevails over degradation. However, the balance between cross-linking/branching and degradation is a result of a complex interrelationship between peroxide amount, processing temperature and rotor speed. Degradation is only the main reaction at high temperature (350 ºC).

Degradation always occurs for EPM and it is mainly enhanced by increasing the temperature. Although the rheological measurements suggest that cross-linking/branching also occurs, degradation is the main reaction, as a consequence gel content is close to 0 % for all EPM samples obtained at different processing conditions and using different amounts of peroxide.

The above results for EPDM and EPM suggest that cross-linking/branching occurs in the diene group of EPDM, since the ethene/propene ratio is quite similar (47 and 51 % of propene for EPDM and EPM, respectively) and the molecular weight of the elastomers is the same.

Two low viscosity PPs were successful obtained from PP degradation using peroxide (Trigonox T101).

3. Materials

3.1. Commercial Polymers

Table 2.2 gives the characteristic properties (MFI - Melt flow index; Mw - Molecular weight; ENB - Ethylidene norbornene) of the raw polymers used in this work. Most of the (EPDM and PP) products used are commercially available. The EPDM elastomers, K5531A and K2340A, are commercial Keltan grades polymers, supplied by DSM Elastomers, B.V. Trilene®67 is a liquid EPDM kindly supplied by Chemtura. The EPDM K5531A product contains 50% by weight of oil, which was removed using acetone under reflux for several days. The PP homopolymers (531P, 524P, 575P and 579S) are commercial grade products supplied by Sabic Europe.

Table 2.2. Properties of the commercial polymers.

Polymer	Grade	MFI[a] (g/10 min)	Mw (kg/mol)	Ethylene content (%)	ENB content (%)
EPDM	K5531A		510	63	4.4
EPDM	K2340A		150	53	5.7
EPDM	Trilene®67		7.2	46	9.5
PP	531P	0.3			
PP	524P	2.0			
PP	575P	10.5			
PP	579S	47			

[a] at 230 ºC and 2.16 kg.

3.2. Modified Polymers

As shown in the second part of this chapter, two low-viscosity PPs were prepared by controlled degradation of PP MFI 47.

An EPDM with a viscosity between the two commercial elastomers, K2340A and Trilene®67, was prepared by controlled degradation of EPDM K2340A, which was performed in a Leistritz LSM 30.34 intermeshing co-rotating twin-screw extruder using a throughput of 0.33 kg/h, a screw speed of 10 rpm and a barrel set temperature of 380 ºC. EPDM was pre-mixed with 0.05 phr of cumyl hydroperoxide. The experimental conditions were chosen in accordance with the knowledge obtain from the study on EPDM degradation described in the part 2 of this chapter. The properties of the modified EPDM are summarized

in Table 2.3. The ENB content, Mw and the money viscosity were determined in accordance with internal procedure of DSM Research.

Table 2.3. Properties of Modified EPDM.

Material	Mw (kg/mol)	Ethylene (%)	ENB (%)	Gel (wt.%)
EPDM	47	56	4	6

3.3. Rheological Characterisation

The rheological behaviour of all polymers was characterised by dynamic rheological measurements in a stress-controlled AR-G2 rotational rheometer (TA Instruments) using a parallel-plate geometry (diameter = 25 mm; gap = 1 mm). EPDM53 and EPDM3.4 (see codes table 2.4) are viscous liquids at room temperature and were place in the rheometer. The other materials were compression-molded into discs of 25 mm diameter and 1 mm thickness at 200 ºC using a 30 ton press. Frequency sweep experiments were performed at 200 ºC across a range of 0.1 – 100 rad/s. For each material, a stress sweep was carried out from 0.5 to 5000 Pa at frequencies of 1 and 10 Hz to determine the linear viscoelastic domain. Fig. 2.13 represents the complex viscosity (η^*) of various EPDM and PP at 200 ºC, as a function of frequency. The polymers are coding in accordance with complex viscosity (η*) at 65 rad/s (which is the average shear rate estimated for the batch mixer at 80 rpm using the model developed by Bousmina et al.[5]) as shown in Table 2.4. This coding will be used in the chapter 4, 5 and 6 due to the several polymers used in those investigations.

As observed in Fig. 2.13, the high molecular weight rubbers (EPDM6414 and EPDM1648) show shear thinning behaviour over the complete range of frequencies. However, low molecular weight rubbers (EPDM53 and EPDM3.4) and low molecular weight PPs (PP48 and PP4.6) display a Newtonian plateau over most whole frequency ranges. Shear thinning behaviour is observed only at high frequencies. Other polymers show pseudo-plastic behaviour with a Newtonian plateau at lower frequencies and shear thinning behaviour at higher frequencies.

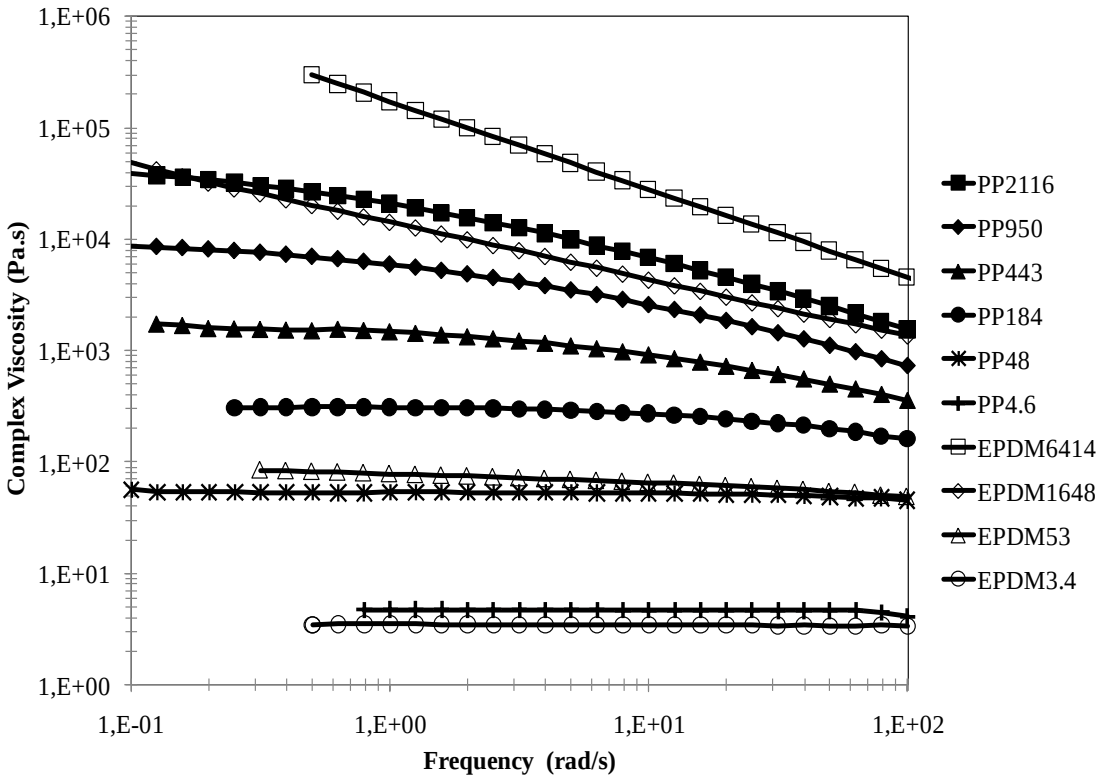

Fig. 2.13. Complex viscosity (η^*) of various PP and EPDM polymers at 200 ºC as a function of frequency.

Table 2.4. Polymers codes.

Material code	**Grade**	**η^{*b} (Pa·s)**
EPDM6414	K5531A	6414
EPDM1648	K2340A	1648
EPDM53		53
EPDM3.4	Trilene®67	3.4
PP2116	531P	2116
PP950	524P	950
PP443	575P	443
PP184	579S	184
PP48		48
PP4.6		4.6

References

[1] Ratnagiri R, Scott CE. Visualization and microscopic modeling of phase inversion during compounding**.** Polym Eng Sci 2001;41(8):1310-1321.

[2] Goodrich J E, Porter RS. A rheological interpretation of torque-rheometer data. Polym Eng Sci 1967;7(1):45-51.

[3] Yang, L-Y., Bigio D., Smith T. G.; J. Appl. Polym. Sci. 58, 129 (1995)

[4] Marquez A, Quijano J, Gaulin M. A calibration technique to evaluate the power-law parameters of polymer melts using a torque-rheometer. Polym Eng Sci 1996;36(20):2556-2563.

[5] Bousmina M, Ait-Kadi A, Faisant JB. Determination of shear rate and viscosity from batch mixer data. J Rheo 1999;43(2)**:** 415-433.

[6] Joubert C, Cassagnau P, Michel A. Influence of the processing conditions on a two-phase reactive blend system: EVA/PP thermoplastic vulcanizate. Polym Eng Sci 2002;42(11):2222-2233.

[7] Xanthos M, editor. Reactive Extrusion. New York: Hanser Publishers, 1992.

[8] Al-Malaika S, editor. Reactive Modifiers for Polymers. London: Blackie Academic & Professional, 1997.

[9] Pabedinskas A, Cluett WR, Balke S. Modeling of polypropylene degradation during reactive extrusion with implications for process control. Polym Eng Sci 1994;34(7):598-612.

[10] Ebner K, White JL. Peroxide induced and thermal degradation of polypropylene. In: Intern Polym Processing IX, 1994. p.233-239.

[11] Kolbert C, Didier JG, Xu L. Mechanochemical Degradation of Ethylene−Propylene Copolymers: Characterization of Olefin Chain Ends. Macromolecules 1996;29(27):8591-8598.

[12] Lachtermacher MG, Rudin A. Reactive processing of LLDPEs in counterrotating nonintermeshing twin-screw extruder. III. Methods of peroxide addition. J Appl Polym Sci 1996;59(11):1775-1785.

[13] Lachtermacher MG, Rudin A. Reactive processing of LLDPEs with peroxides in counter-rotating nonintermeshing twin-screw extruder. IV. Effects of molecular structure of LLDPEs. J Appl Polym Sci 1996;59(8):1213-1221.

[14] Suwanda D, Balke ST. The reactive modification of polyethylene. I: The effect of low initiator concentrations on molecular properties. Polym Eng Sci 1993;33(24):1585-1591.

[15] Suyama S, Ishigaki H, Watanabe Y, Nakamura T. Crosslinking of Polyethylene by Dicumyl Peroxide in the Presence of 2,4-Diphenyl-4-methyl-1-pentene. Polym J 1995;27(4):371-375.

[16] Suyama S, Ishigaki H, Watanabe Y, Nakamura T. Mechanism for the Peroxide-Initiated Crosslinking of Polyethylene in the Presence of 2,4-Diphenyl-4-methyl-1-pentene. Polym J 1995;27(5):503-507.

[17] Harlin A, Heino E-L. Comparison of rheological properties of cross-linked and thermal-mechanically degraded HDPE. J Polym Sci, Part B: Polym Phys 1995;33(3): 479-486.

[18] Smedberg A, Hjertberg T, Gustafsson B. Crosslinking reactions in an unsaturated low density polyethylene. Polymer 1997;38(16):4127-4138.

[19] Machado AV, Covas JA, van Duin M. Monitoring polyolefin modification along the axis of a twin screw extruder. I. Effect of peroxide concentration. J Appl Polym Sci 2001;81(1):58-68.

[20] Baldwin FP, Ver Strate G. Polyolefin elastomers based on ethylene and propylene. Rubber Chem Technol 1972;45(3):709-881.

[21] Dikland HG. Kauts Gum Kunst 1996;49(6):413-417.

[22] Camara S, Gilbert BC, Meier RJ, Duin M, Whitwood AC. EPR studies of peroxide decomposition, radical formation and reactions relevant to cross-linking and grafting in polyolefins. Polymer 2006:47(13);4683-4693.

[23] Loan LD. Peroxide crosslinking of ethylene-propylene rubber**.** J Polym Sci, Part A: Polym Chem 1964;2(7):3053-3066.

[24] Gugumus F. Re-examination of the role of hydroperoxides in polyethylene and polypropylene: chemical and physical aspects of hydroperoxides in polyethylene. Polym Degrad Sta 1995;49(1):29-50.

[25] Gugumus F. Physico-chemical aspects of polyethylene processing in an open mixer 3. Experimental kinetics of functional group formation. Polym Degrad Sta 2000;68(1):21-33.

[26] Gugumus F. Physico-chemical aspects of polyethylene processing in an open mixer 4. Comparison of PE-LLD and PE-HD with PE-LD. Polym Degrad Sta 2000;68(2):219-229.

[27] Gugumus F. Physico-chemical aspects of polyethylene processing in an open mixer 5. Kinetics of hydroperoxide formation. Polym Degrad Sta 2000;68(3):327-36.

[28] Pinheiro LA, Chinelatto MA, Canevarolo, SV. The role of chain scission and chain branching in high density polyethylene during thermo-mechanical degradation. Polym Degrad Sta 2004;86(3):445-453.

[29] Kampouris EM, Andreopoulos AG. Benzoyl peroxide as a crosslinking agent for polyethylene. J Appl Polym Sci 1987;34(3):1209-1216.

Chapter 3: Degradation of the Rubber Network during Dynamic Vulcanisation of EPDM/PP Blends using Phenolic Resole.

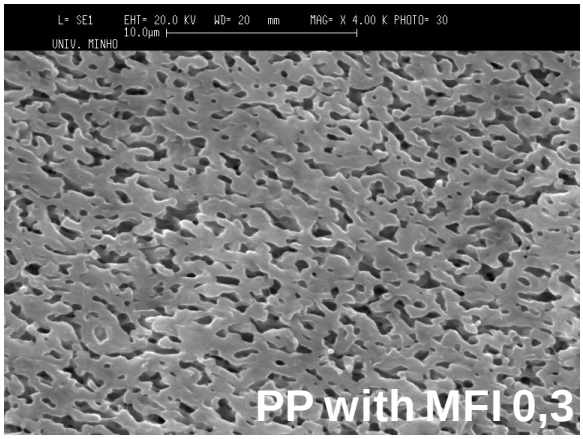

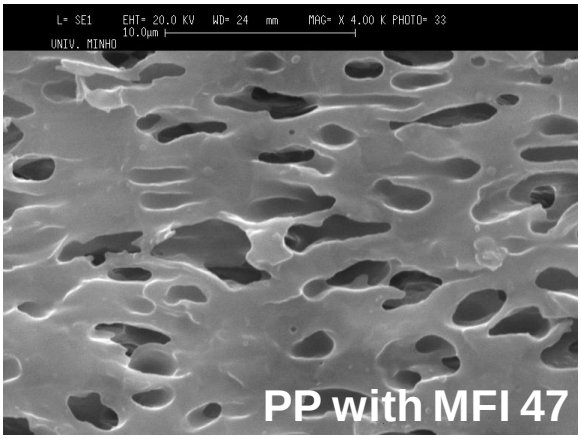

This chapter was published in Rubber Chem and Thecnol 2009;82(5):492-505

1. Introduction

Thermoplastics vulcanisates (TPVs) belong to the family of thermoplastic elastomers (TPEs), and, like other TPEs, combine the melt processability and recyclability of thermoplastics with the elasticity and the mechanical properties of thermoset rubbers [1-3]. TPV products can be melt processed by conventional techniques, such as extrusion, blow moulding, injection moulding, vacuum forming and calendaring. Most commercial TPVs are based on heterogeneous blends of isotactic polypropylene homopolymer (PP) and ethylene-propylene-diene (EPDM) rubber, because of the relatively high melting point of the former and the excellent oxygen, ozone and heat resistance of the latter [4]. TPVs usually contain large amounts of extender oil to improve processablility and to lower hardness.

TPVs are produced via dynamic vulcanisation, where the rubber is selectively cross-linked during its melt mixing with the thermoplastic. The final TPV morphology consists ideally of finely divided cross-linked rubber particles dispersed in a thermoplastic matrix. If large amounts of rubber are used to produce low-hardness TPVs, the initial blend morphology usually consists of a dispersion of PP particles in a rubber matrix or a co-continuous morphology. Several studies have demonstrated that cross-linking provokes drastic changes of the viscosity and the elasticity of the rubber phase [5-7]. Upon the high-shear dynamic vulcanisation of low-hardness TPVs, the morphology changes from a (co-) continuous EPDM phase to cross-linked particles of EPDM dispersed in the PP matrix, i.e. cross-linking is the driving force for the occurrence of phase inversion. According to Coran et al. [8] the typical elastomeric properties of TPVs are only obtained if the rubber is highly vulcanized and if the size of the cross-linked rubber particles is small (approximately 1 μm). According to Bhadane et al. [9], the interfacial tension of EPDM/PP blends is very low. It is estimated to be around 0,3 mN/m at a melt blending temperature of 190 ºC and, consequently, EPDM/PP blends are partially miscible in the melt. This explains the very fine morphologies of EPDM/PP–based TPVs even in the absence of a compatibiliser. The TPV morphology can be modified by changing the initial EPDM/PP viscosity ratio. According to Wu [10] an increase of the EPDM/PP viscosity ratio of the blend results in larger particles; a minimum particle size is obtained when the viscosity ratio is close to unity. It was shown by Sengputa et al. [11] that hardness, Young's modulus and tensile strength of TPVs decrease with a decrease of the PP viscosity, which is related to an increase of the EPDM particle size.

TPV properties can be adjusted by varying the EPDM structure, the blend composition and the cross-linking degree. It has been demonstrated by Datta [12] that low-molecular-weight

EPDM with low ethylene and diene contents results in TPVs with better compression set properties. Nevertheless, high-molecular-weight EPDM with high ethylene and diene content results in TPVs with better tensile and tear properties. Coran et al. [8] were the first to show that improved properties, such as tensile strength, modulus and compression set, are obtained if the rubber phase is highly cross-linked. Sabet et al. [13] have shown that high-molecular-weight EPDM results in a higher cross-linking degree.

Resoles are the most commonly used cross-linking systems for EPDM in TPVs, despite the inconvenience of discoloration and black speck formation. They provide TPVs with good mechanical properties and processing characteristics, and yield thermally stable cross-links [14]. The chemistry of resole cross-linking has been studied using low-molecular-weight models for EPDM rubber first by Lattimer [15] and later by van Duin et al. [16, 17]. Stannous chloride is usually used as activator; the acidic stannous chloride activates the degradation of resole into mono-phenolic units with benzylic cations, which eventually will connect two EPDM chains via methylene and/or chroman cross-links.

Although TPVs have been already commercially available from the 1970's and a large number of scientific studies have been published, they are still produced in a somewhat empirical fashion. The relationships between the production process, the structure and the final properties are still not fully understood [18]. The general goal of our studies aims at understanding the physical and chemical phenomena, which take place during dynamic vulcanisation of TPVs. In this particular study emphasis will be on the occurrence of network degradation during cross-linking. Further papers will be published on the relationship between cross-linking and morphology development, including phase inversion.

2. Experimental

2.1. Materials

The EPDM rubber (K2340A) and the three PPs, with different melt flow indices (531P: MFI = 0.3; 524P: MFI = 2; and 579S: MFI = 47 g/10 min at 230 ºC/2.16 kg) were used. The characteristics properties of the polymer used in this work are given in part 3.1 of Chapter 2 (Table 2.2).

Octylphenol–formaldehyde resin (SP1045, Schenectady International, USA) called resole in this work, stannous chloride and zinc oxide (Aldrich) were used as a crosslinking system. Irganox 1076 from Aldrich was used as a satibilizer. Physical blends without cross-linking and cross-linked TPVs were prepared for each PP grade using EPDM/PP ratios of 70/30, 50/50 and 30/70 (w/w). The amount of cross-linking agents was kept constant relative to the amount of EPDM and is expressed in parts per hundred rubber (phr). The cross-linking system was composed of resole cross-linker (5 phr) and a combination of $SnCl_2.2H_2O$ (1.5 phr) and ZnO (1.8 phr) as activators. Irganox 1076 was used at 0.25 wt. % relative to the total amount of polymers (EPDM and PP).

The rheological behaviour of raw materials (PP and EPDM) was characterised by dynamic rheological measurements as described in Chapter 2, part 3.3. The complex viscosities of EPDM and PP at a shear rate of 65 s^{-1} are given in Table 3.1.

Table 3.1. Dynamic Viscosities of the EPDM and PP at 200 ºC (shear rate of 65 s^{-1})

Material	**MFI (g/10 min at 230 ºC/2.16 kg)**	**Dynamic viscosity, (Pa.s)**
EPDM	---	1648
PP	0.3	2116
PP	2.0	950
PP	47	184

2.2 Preparation of Blends and TPVs

Physical blends and TPVs were prepared in a Haake batch mixer (HAAKE Rheomix 600 OS; volume 69 ml) equipped with two counter-rotating rotors. The rotor speed was 80 rpm and the set temperature was 200 ºC. The following mixing sequence was used. First, PP pellets were introduced into the hot mixer, after melting the stabilizer was added, and then the EPDM

rubber. When the torque reached a constant value, which took about 3 minutes, and indicated the formation of a homogenous melt, ZnO, resole and $SnCl_2$ were added in this order (which took about 5 s). The instant when $SnCl_2$ was added is defined as time zero. At 45 s and 120 s the rotors were stopped and samples, weighing approximately 1.5 g, were taken from the mixer using a spatula, which took about 5 s, and then the mixing was continued. At 300 s the total sample was removed. In case of physical blends (without cross-linking) samples were only collected at 300 s, after the torque reached a constant value.

Dynamic vulcanisation of EPDM rubber in the absence of PP was performed in the same way as for the TPVs at different temperatures (170, 200 and 220 ºC). In order to prepare vulcanized EPDM via static vulcanisation, EPDM rubber, ZnO, resole and $SnCl_2$ were pre-blended in the internal mixer at 80 ºC during approximately three minutes at a rotor speed of 80 rpm. The cross-linking reaction does not occur at this low temperature. Then the EPDM mixture was vulcanized in a hot press at different temperatures (170, 200 and 220 ºC). All the samples collected from the mixer and the hot-press (at 45, 120 and 300 s) were cooled between two metal plates in order to stop the cross-linking reaction and to avoid morphological changes.

2.3. Sample Characterisation

The EPDM gel content was determined as a measure of the cross-linking degree by extraction in cyclohexane at room temperature and in boiling xylene. For extractions in cyclohexane, approximately 200 mg of TPV sample was weighed and then immersed in cyclohexane for 48 h under gentle stirring; the cyclohexane was refreshed after 24 h. After drying the sample in a vacuum oven at 100 °C for 12 h with nitrogen purging, the weight was determined. The EPDM gel content was calculated assuming that the residue consists of insoluble PP, ZnO, resole, $SnCl_2$ and cross-linked EPDM. For extractions in xylene, approximately 500 mg of TPV sample was weighed and placed in a 80 μm mesh stainless-steel cage, the cage was also weighed, and then immersed in boiling xylene for 48 h. The samples were dried using the same conditions as used for the cyclohexane extractions. The EPDM gel content was calculated assuming that the residue consists of insoluble cross-linked EPDM and resole and corrected for the presence of ZnO. The degree of equilibrium swelling was also measured to confirm the trends of cross-linking determined with extractions. The procedure was the same as described previously for the determination of EPDM gel content via cyclohexane extraction. However, in this case before drying the swollen sample, it was weighed in a sealed

glass bottle after carefully removing the surplus cyclohexane with a tissue. The swelling degree was calculated as the ratio of the weights of the swollen and dried samples.

The morphology was studied by scanning electron microscopy (SEM) in the back-scattering mode using a Leica Scanning Electron Microscope. Samples were fractured in liquid nitrogen and vapour-stained with ruthenium tetroxide for 120 minutes.

3. Results and Discussion

3.1. Torque and Temperature

Fig. 3.1 shows the torque and temperature curves upon dynamic vulcanisation of a 50/50 (w/w) EPDM/PP (MFI 0.3) blend in the batch mixer. The first and second peaks in the torque curve correspond to the introduction of PP and EPDM into the mixer, respectively. The torque reaches more or less a constant value, indicating complete melting of PP and full homogenisation of the EPDM/PP blend. The addition of the cross-linking system produces an immediate decrease of the torque, which is attributed to lubrication of the blend system by the molten resole and $SnCl_2$. Then, the torque increases steeply and reaches a maximum at approximately 85 s after adding the cross-link system, which is related to drastic changes in the viscosity and elasticity of the EPDM phase due to cross-linking. The next two interruptions in the torque curve are the result from stopping the rotors in order to take samples at 45 and 120 s after adding the cross-linking system. Upon prolonged mixing the torque shows a moderate but continuous decrease. In the temperature curve a decrease from 198 to 181 ºC is observed when the polymers are fed due to the introduction of a cold mass in the mixer and the melting of PP. Upon addition of the high-molecular-weight EPDM a continuous temperature increase up to 220 ºC is observed, due to viscous dissipation, which is enhanced as a result of cross-linking. Both the torque and temperature curves are similar to the ones reported in other studies for dynamic vulcanisation of EPDM/PP blends [11,19,20].

Since the mixing torque represents the overall viscosity of the blend and the melt temperature is influenced by viscous dissipation, it is expected that both torque and temperature could be correlated. Table 3.2 shows the values of the mixing torque and melt temperature at different mixing times for all studied compositions. The torque value corresponding to a reaction time of 0 s was registered just before adding the cross-linking system. The torque values at 45, 120 and 300 s were taken just before stopping the rotors to collect the samples. Independently of the blend composition and the reaction time, it is observed that the mixing torque and the melt temperature increase when the PP molecular weight increases, which contributes to an

increase of the viscous dissipation. An increase of the EPDM content also results in an increase of both torque and temperature; the largest relative increase in torque is noted for PP MFI 47 at high reaction times. The mixing torque increases up to a certain level at 45 – 120 s and then it decreases. This could be explained by the occurrence of phase inversion. Since after phase inversion the viscosity of the molten TPV will be determined by the PP matrix where cross-linked rubber particles are dispersed. Temperature increases approximately 5 ºC with an increase of the EPDM content from 30 to 70 %. The increase in torque and temperature is explained by the fact that the EPDM melt viscosity is higher than those of PP MFI 47 and 2, and is further increased by cross-linking. In the case of PP MFI 0.3 at low reaction times, an increase in the EPDM content actually results in a decrease of the torque and temperature because the EPDM viscosity is somewhat lower than that of PP MFI 0.3. At high reaction times cross-linking of the EPDM phase will be completed and the viscosity of EPDM phase will be higher than that of all PPs. Finally, for all TPVs, the melt temperature shows increases from 17 to 27 ºC upon prolonged mixing time up to 300 s, due to viscous dissipation.

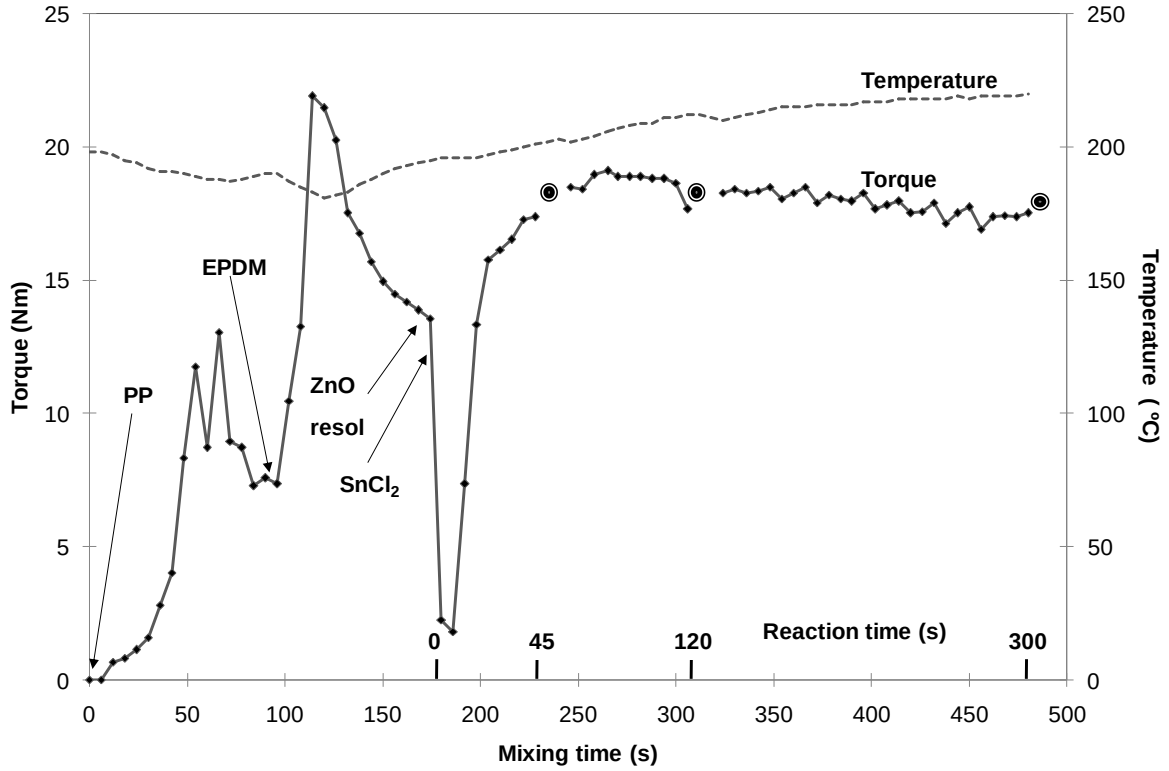

Fig. 3.1. Evolution of torque and temperature as a function of mixing time for 50/50 (w/w) EPDM/PP, MFI 0.3 TPV. The arrows indicate the instants of addition of the various ingredients. The filled circles indicate the time of sampling.

The decrease in torque, after going through a maximum, once the cross-linking system was added, has been explained in terms of morphological changes [5,21]. However, for the 30/70 (w/w) EPDM/PP compositions with PP MFI 0.3 and 2, where phase inversion is rather improbable because the initial morphology already consists of a continuous PP phase (see below), the torque still goes through a maximum. Thus, a more probable explanation for the final decrease of the torque might be the degradation of PP and/or the EPDM network.

Table 3.2. Mixing torque (Γ) and melt temperature (T) recorded during dynamic vulcanisation of EPDM/PP blends.

Sample		**Reaction time (s)**							
EPDM/PP	**PP**	**0**		**45**		**120**		**300**	
w/w	**MFI**	**Γ, Nm**	**T,ºC**	**Γ, Nm**	**T, ºC**	**Γ, Nm**	**T, ºC**	**Γ, Nm**	**T, ºC**
70/30	0.3	12.5	194	18.0	202	18.6	214	18.4	221
70/30	2	10.0	191	13.0	196	15.9	207	14.8	216
70/30	47	6.3	190	9.8	194	10.9	203	9.8	209
50/50	0.3	13.6	196	17.4	201	18.6	212	16.5	220
50/50	2	10.0	188	13.4	195	13.3	204	11.1	212
50/50	47	4.9	186	6.2	192	7.2	200	6.6	206
30/70	0.3	13.4	201	18.7	206	17.0	213	15.4	218
30/70	2	9.3	188	11.3	196	10.5	203	9.3	210
30/70	47	3.4	186	3.3	192	3.3	197	3.6	203

3.2. Effect of PP MFI and Blend Composition on Dynamic Vulcanisation

Resole/$SnCl_2$ is the most common system used for dynamic vulcanisation of PP/EPDM blends [18]. The resole reacts only with unsaturation, i.e. only the EPDM phase will be affected (cross-linking). Reaction of the resole with PP, such as graft EPDM/PP copolymer formation, as suggested by Sabet et al. [21] is highly improbable.

The cross-linking degree of the EPDM phase was measured by determination of the EPDM gel content in cyclohexane and xylene and by the degree of equilibrium swelling in cyclohexane. The EPDM gel content, determined by extraction in boiling xylene, is not affected by the EPDM/PP ratio, since PP dissolves in refluxing xylene and the residue consists only in cross-linked EPDM, resole, and ZnO. Thus, it will allow a fair comparison of the cross-linking degree of the EPDM phase in different TPV compositions. Since at early

stages of mixing, cross-linking may proceed during extraction due to the high boiling temperature of xylene and unreacted resole is still present, xylene extractions were only performed for physical blends and for TPV samples collected after 5 min. In the case of the EPDM gel content determined by extraction in cyclohexane, the PP phase does not dissolve. Thus, in TPVs with PP-rich compositions, where PP might be the matrix and EPDM the dispersed phase, the solvent should not be able to remove all the uncross-linked EPDM efficiently. Still, the cyclohexane gel content was measured in order to follow the evolution of the cross-linking as a function of time at least in a qualitative way. Since the presence of rigid PP limits the swelling of the (cross-linked) EPDM phase, the degree of swelling in cyclohexane is not only determined by the cross-linking degree, but also by the composition and the morphology of the TPVs. In addition, at high EPDM levels micro-gel rubber particles were observed in the solvent. Although, the degree of swelling was measured for all samples and it decreases for all compositions as a function of time, suggesting an increase of the cross-linking degree, these data will not be discussed in detail, because the interpretation is not straightforward.

Fig. 3.2 shows the gel content in cyclohexane as a function of the reaction time for the various TPVs with different EPDM/PP compositions and PP MFIs. The values at 0 s were measured for the physical blends. The PP-rich compositions, 30/70 (w/w) EPDM/PP, show gel content values between 40 – 50 % at 0 s, significantly different from zero. Since no cross-linking system was presented, this can be related to the inefficiency of the solvent to remove all EPDM, as explained above. The absolute error in the values of the EPDM gel content for TPVs samples at 120 and 300 s is less than ± 2 %, while at 45 s it is close to ± 5 %. The larger error for data at 45 s can be explained by the heterogeneous distribution of the cross-linking system in the early stages of mixing, resulting in cross-linking heterogeneity.

In general, the rubber gel content increases with time, indicating an increase in cross-linking degree. The curves of the gel content versus time for each EPDM/PP composition are more or less similar and independent of the PP MFI. For 70/30 (w/w) EPDM/PP TPVs compositions the rate of cross-linking is slow: gel content at 0 s is close to 0 %, at 45 s it is below 30 % and even after 300 s of mixing the values are only around 65 %, i.e. far below to the theoretical maximum of 100 %. For 50/50 (w/w) EPDM/PP compositions, cross-linking proceeds somewhat faster. Gel content at 0 s is again close to 0 %, then it varies between 40 - 75 % at 45 s and at 300 s it is between 85 – 95 %. Mainly in case of the two high-molecular-weight PPs (PP MFI 0.3 and 2), gel content values are significantly less than 100 %. A decrease of the PP molecular weight yields higher gel content at higher reaction time. For 30/70 (w/w)

EPDM/PP compositions, the evolution of cross-linking is similar for all PPs. The gel content is around 50 % at 0 s, above 80 % at 45 s and close to 100 % at 300 s. Although, these values may be overestimates, it is reasonable to presume that for this PP-rich composition the cross-linking degree reaches higher levels than for others compositions.

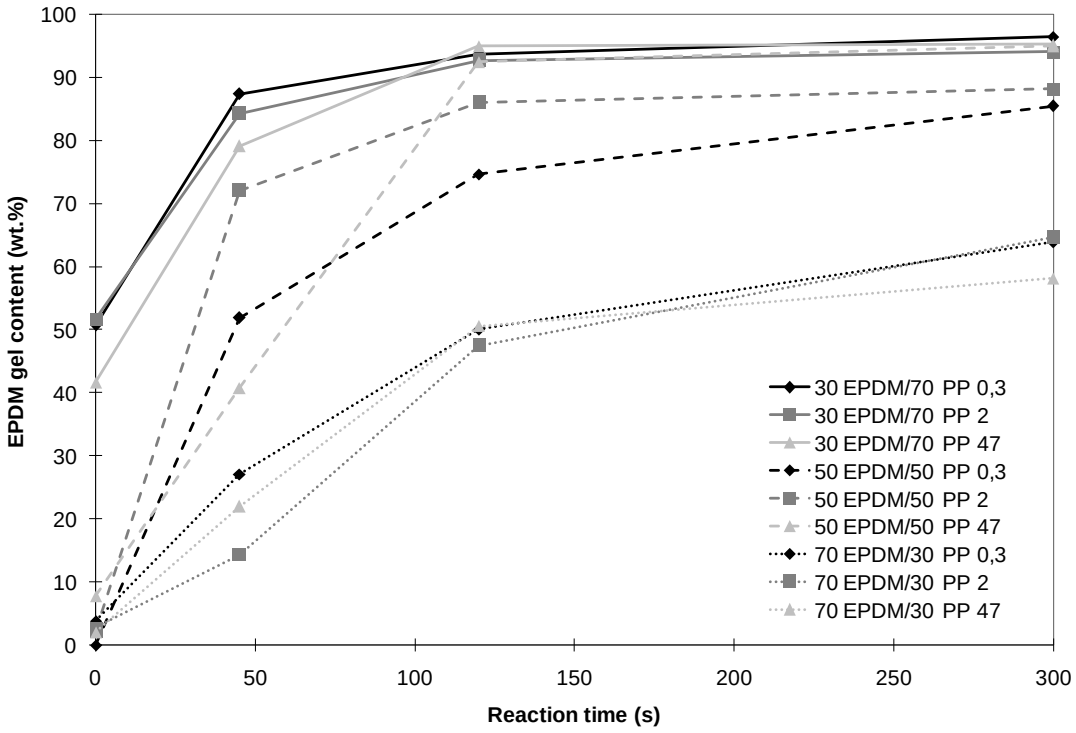

Fig. 3.2. EPDM gel content of the various EPDM/PP compositions (different lines) and PP MFI (different symbols) as a function of reaction time, determined via cyclohexane extraction.

In summary these results indicate that PP molecular weight does not have a major influence on the cross-linking of the EPDM phase. Since the amount of cross-linking chemicals was kept constant relatively to the amount of EPDM, more or less similar trends of gel content for all three EPDM/PP compositions were expected. However, comparing the actual gel content data for the different TPV compositions indicates that gel content decreases as the EPDM content increases; the lowest values are obtained for the 70/30 (w/w) EPDM/PP compositions. Due to the limitations of cyclohexane extractions as discussed above, some extractions in refluxing xylene were performed. The gel content values determined by xylene extraction of TPVs collected at 5 min are shown in Table 3.3. The gel content was also determined for physical blends and the values obtained were 0 % for all compositions, as expected. EPDM-rich 70/30 (w/w) EPDM/PP compositions show similar gel content values, remaining below 50 % for all PPs. For 50/50 (w/w) EPDM/PP compositions, gel content increases from 51 to

92 % as the PP MFI increases. For PP-rich 30/70 (w/w) EPDM/PP compositions, it is also observed that gel content increases from 63 % to 84 % as the PP MFI increases.

Table 3.3. EPDM gel content by xylene extraction for TPVs collected at 300 s

Composition EPDM/PP	**PP MFI (g/10 min at 230 ºC/2.16 kg)**	**EPDM gel content (wt. %)**
70/30	0.3	42
50/50		51
30/70		63
70/30	2.0	44
50/50		68
30/70		73
70/30	47	42
50/50		92
30/70		84

Comparing these xylene extraction results with those obtained by cyclohexane, it can be noticed that the general trends are the same, although the gel content data obtained by xylene extraction are smaller. The latter can be explained, as discussed before, by the fact that in case of cyclohexane extraction the PP is not dissolved and, consequently, the solvent is not able to remove all the non-cross-linked EPDM, especially when PP is the matrix. During xylene extractions, PP is also dissolved and, thus, removal of the non-cross-linked EPDM by the solvent is more efficient. Most probably these trends in gel content, determined via both cyclohexane and xylene extractions, are related to differences in morphology of the EPDM/PP blends. To investigate this in more detail, scanning electron microscopy (SEM) in the back-scattering mode was performed on non-cross-linked blends. The micrographs of the various compositions are depicted in Fig. 3.3. White regions in the micrographs are assigned to the EPDM phase and black regions to the PP phase. The morphology of the corresponding TPVs were also studied, but it will be discussed separately in a detailed study on morphology development during dynamic vulcanisation with emphasis on phase inversion [22]. The morphology of the EPDM/PP blends can be explained in terms of the viscosity ratio and the blend composition, as it has been shown previously by several authors [13,19,20,24]. The morphologies, obtained for blends with the highest amount of EPDM (70 wt. %) and PPs with

different MFIs, consist mainly of an EPDM matrix with a dispersed PP phase (Fig. 3.3). An increased tendency towards co-continuity of the PP phase is observed as the PP MFI increases, because the phase with the lowest viscosity in general has a preference to become the matrix. Morphologies obtained for 50/50 (w/w) compositions indicate some sort of co-continuity for all 3 PP MFIs. For the blend with high molecular weight, PP MFI 0.3, the EPDM phase seems to be more continuous than in the blend with PP MFI 2. For the blend with the low molecular weight, PP MFI 47, the EPDM phase seems to be dispersed in the PP matrix, although some EPDM particles seem to be connected. These differences are again related to the increase of EPDM/PP viscosity ratio. For the blends with the lowest amount of EPDM (30 wt.%), PP is always the matrix. Nevertheless, with the two high molecular weight PPs (MFI 0.3 and 2) the dispersed EPDM particles are elongated and sometimes seem to be connected. For all blend compositions, it is noticed that the size of the EPDM particles increases as the EPDM/PP viscosity ratio increases, i.e. becomes larger than 1, which is in accordance with the study by Wu et al. [10].

For EPDM-rich 70/30 (w/w) EPDM/PP compositions, it is shown that PP is mainly the dispersed phase and, thus, the cross-linking system will end up initially in the EPDM phase and it is able to react immediately with the rubber. For PP-rich, 30/70 (w/w) EPDM/PP compositions, it is shown that the morphology consists mainly of EPDM domains dispersed in the PP phase and, thus, the cross-linking agents have first to migrate through the PP matrix, before reaching and cross-linking the EPDM phase. Surprisingly, for the latter TPVs, the highest values of the gel content are obtained. This shows that the decrease of the cross-linking degree upon increasing the rubber content in the TPV formulation is not related to the localisation or migration of the cross-linking agents, but may be related to the fact whether EPDM is the matrix or the dispersed phase. The increase in the gel content values, both in cyclohexane and xylene, upon increasing the PP amount (with the exception of TPVs based on PP 47 as will be explained below), may be explained by the occurrence of degradation of the EPDM network during dynamic vulcanisation, mainly when EPDM is the continuous phase and is more sensitive to high shear and elongation stresses. In addition, it seems that EPDM degradation is not only an outcome of shear and elongation stresses applied directly to the EPDM phase, but may also occur when shear and elongation stresses are transferred via PP matrix to the dispersed EPDM phase. Since shear and elongation stresses increase as the viscosity of the matrix increases, this explains the decrease of the rubber gel content as the PP molecular weight increases, i.e. as PP MFI decreases, in the cases of 50/50 and 30/70 (w/w) EPDM/PP compositions. For PP MFI 47 a decrease of the cross-linking degree, determined

by xylene extraction, is observed when the PP amount increases from 50 to 70 wt.% (see Table 3.3). This suggests that shear and elongation stresses, transferred by this low viscous PP, are not strong enough to cause degradation of the EPDM network.

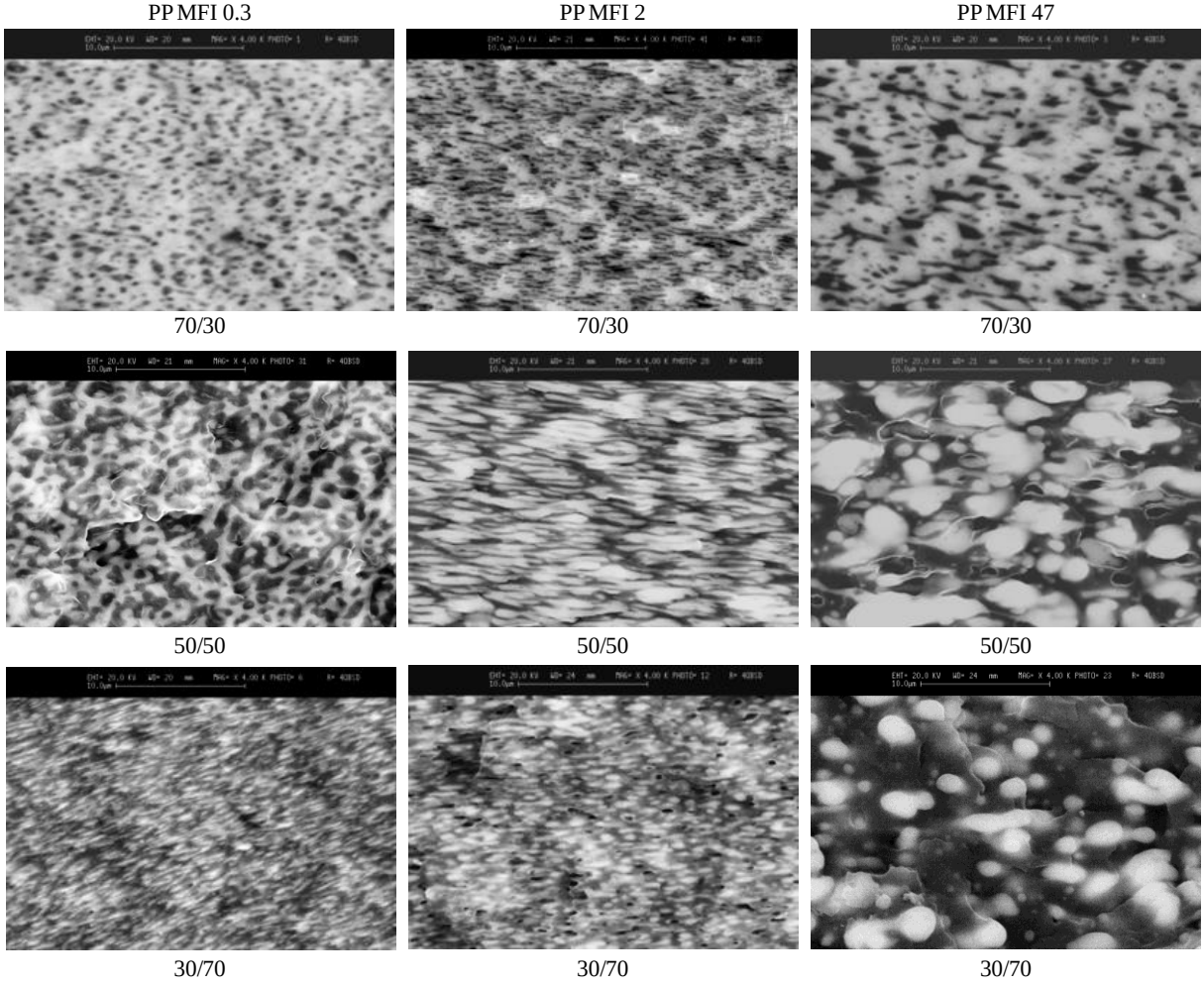

Fig. 3.3. SEM images of non-cross-linked EPDM/PP blends. (EPDM is the light phase and PP is the dark phase)

To validate if degradation of the EPDM network occurs during dynamic vulcanisation of EPDM/PP blends, static vulcanisation of EPDM/PP blends was performed in the batch mixer by stopping the rotors after adding the cross-linking system. However, due to the high melt temperature the cross-linking reaction has already proceeded significantly before the cross-linking chemicals were well dispersed. Therefore, both static and dynamic vulcanisation of EPDM in the absence of PP was investigated.

3.3. Static and Dynamic Vulcanisation of EPDM in the absence of PP

Fig. 3.4 shows the EPDM gel content and the degree of equilibrium swelling upon cross-linking EPDM in the absence of PP in a hot press as a function of the curing time and temperature (static vulcanisation). The gel content increases both with time and temperature. The rate of the cross-linking reaction is low at 170 ºC, the gel content at 45 s is below 30 % and at 300 s it is only 80 %. At 200 ºC the gel content is close to 80 % at 45 s and then increases to 95 % at 300 s. Finally, at 220 ºC the gel content at 45 s is already 93 % and is 97 % at longer times. It should be noticed that the levelling off of the gel content at approximately 100 % does not mean that cross-linking stops at prolonged reaction times at 200 and 220 ºC. At 100 % gel all rubber chains are coupled to the 3D network by at least one link. Cross-linking probably continues, resulting in higher cross-linking densities, the rubber gel content has already reached its upper limit and cannot increase above 100 %. However, at higher degrees of cross-linking the changes in cross-linking density can be studied by determining the degree of equilibrium swelling, which indeed decreases indicating that the cross-linking degree increases at longer times (Fig. 3.4). The degree of swelling at low cross-linking degree (at 45 s and 170 ºC) cannot be determined accurately due to the presence of micro-gel rubber particles in the solvent. Generally, the equilibrium swelling data confirm the trends observed for the gel content. In summary, resole cure of just EPDM under static conditions proceeds as expected according to a normal Arrhenius behaviour, i.e, the cross-linking reaction increases as the temperature increases.

The torque curves obtained during dynamic vulcanisation of EPDM in the absence of PP in the batch mixer at different temperatures (Fig. 3.5) are in a way quite similar to those of the TPVs shown in Fig. 3.1. In all cases, the first torque peak corresponds to the introduction of the cold EPDM rubber, which is homogenised after approximately 75 s. The corresponding torque level decreases as the set temperature of the batch mixer increases, which is due to the decrease of melt viscosity. Adding the cross-linking agents, first results in a torque decrease, due to lubrication, but then in a strong increase as a result of cross-linking. A maximum torque level is reached at approximately 225 s. For EPDM dynamically vulcanised at 170 ºC, the maximum value in torque is followed by a rapid decrease, due to crumbling of the cross-linked rubber. The powdery rubber crumb is simply turned around in the mixing chamber and does not apply any mechanical force on the rotors. A different behaviour was observed for EPDM samples dynamically vulcanized at 200 and 220 ºC. The torque remains practically constant when the maximum was reached, and at both temperatures the rubber mass remained

a viscous melt. Again a lower torque level were obtained for high temperature. These results indicated that the cross-linking degree of the EPDM dynamically vulcanized at 170 ºC is larger than at 200 and 220 ºC, which is confirmed by the EPDM gel content measurements (Fig. 3.6). EPDM gel content increases with time and temperature in a rather unexpected sequence: 170 ºC > 220 ºC > 200 ºC. Due to the low level of cross-linking at 45 s and 120 s, the degrees of equilibrium swelling could only be measured at the end of the dynamic cross-linking of EPDM at 200 and 220 ºC, being 22 and 18, respectively. This corroborates the trend obtained for the EPDM gel content. For samples cross-linked at 170 ºC it was not possible to determine the degree of swelling, due to the crumb form of the product.

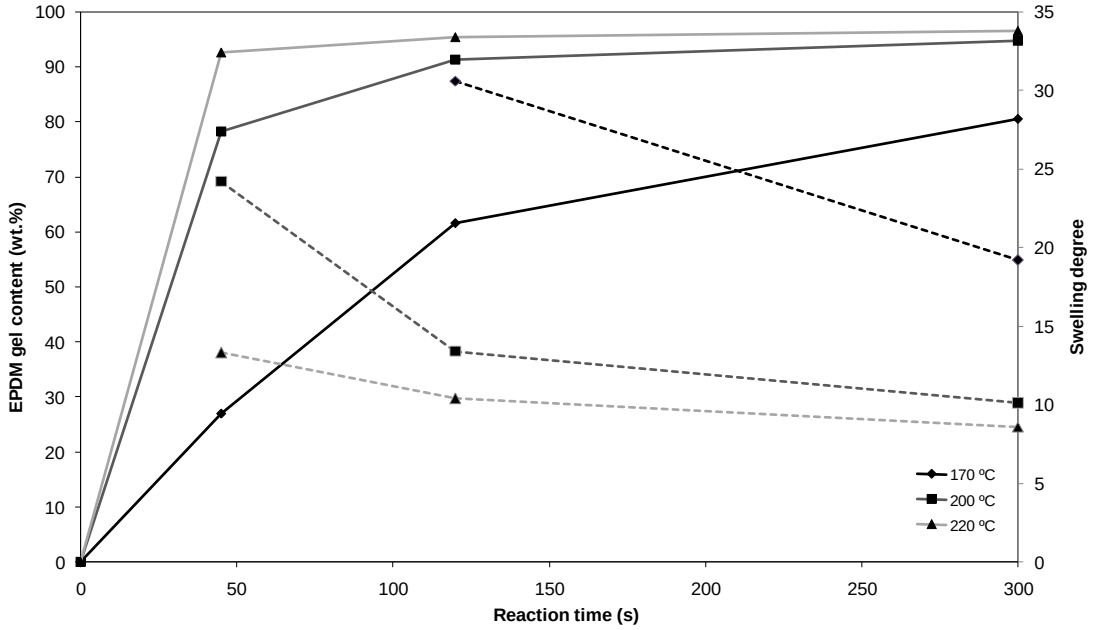

Fig. 3.4. EPDM gel content (solid lines) and degree of equilibrium swelling (dashed lines), using cyclohexane, of EPDM statically vulcanized in the absence of PP at different temperatures in a hot press.

The comparison of Fig. 3.4 and 3.6 show that the cross-linking degree at 170 ºC for dynamic vulcanisation is similar to that of static vulcanisation. Cross-linking at this temperature is relatively slow, and no degradation as a result of shear seems to occur. At 200 and 220 ºC the cross-linking degree under dynamic conditions are significantly smaller when compared to those obtained under static conditions. It can be concluded that degradation of the EPDM network is indeed induced by high shear stress at elevated temperatures. The higher cross-linking degree achieved at a set temperature of 220 ºC compared to that at 200 ºC is explained by the faster cross-linking reaction and the lower viscosity at 220 ºC, the latter probably

resulting in less shear degradation. Since the gel content of the EPDM melt at 220 ºC is 57 % and that of the crumb obtained at 170 ºC and 120 s is 64 %, it seems that the point where the transition from viscous melt to elastic solid occurs is around 60 % gel.

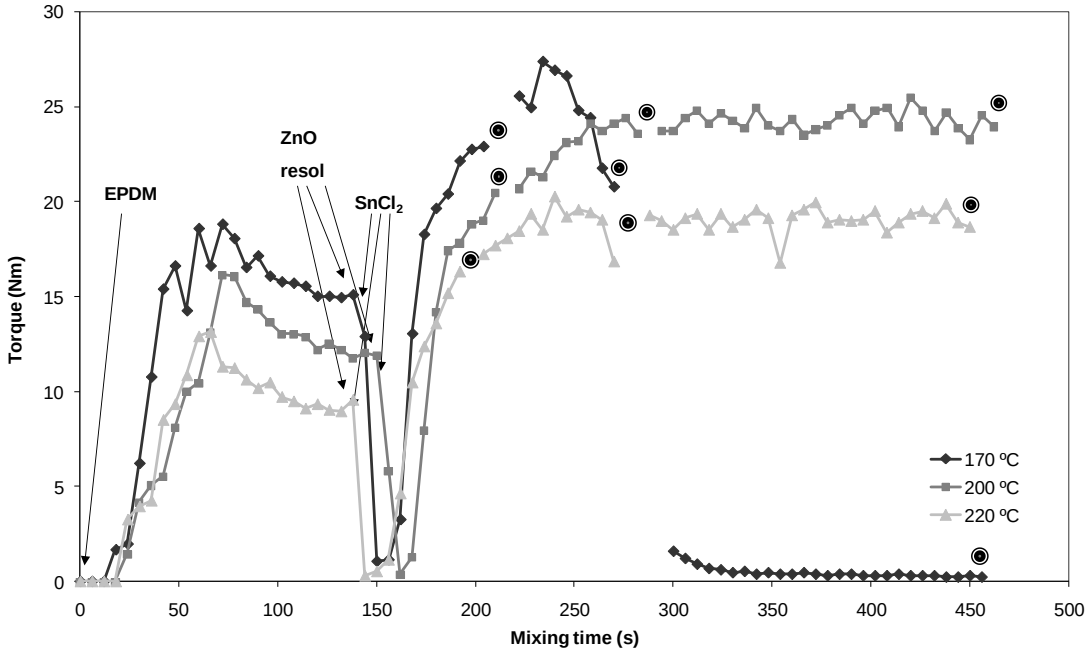

Fig. 3.5. Evolution of torque as a function of mixing time for EPDM, dynamically vulcanized in the absence of PP at different temperatures in the batch mixer.

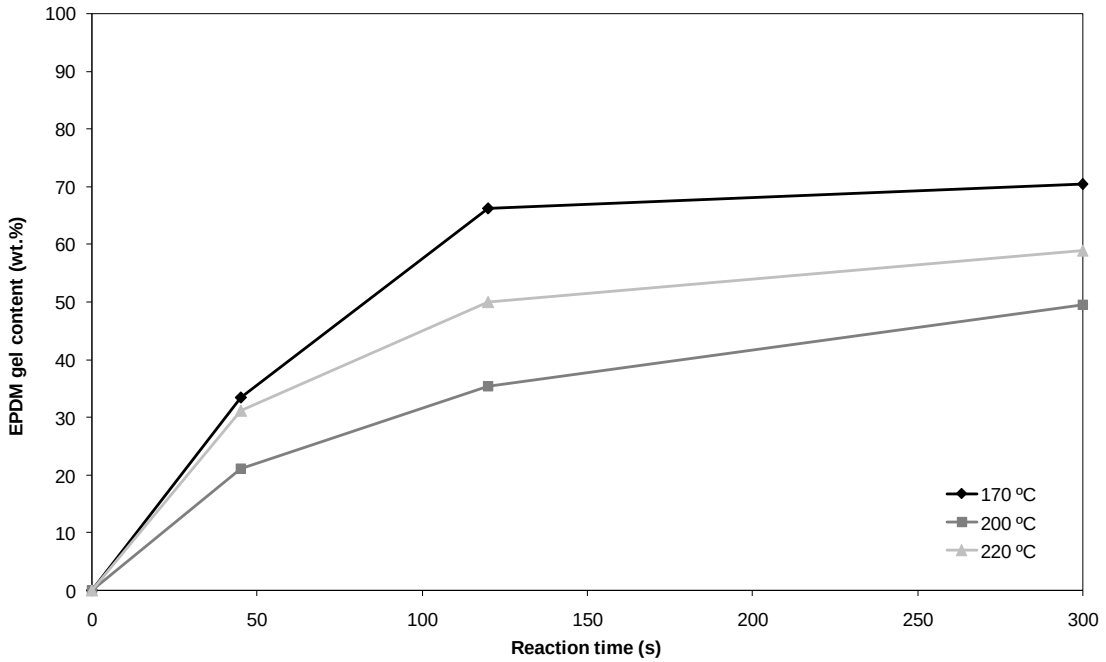

Fig. 3.6. EPDM gel content as a function of time for EPDM in the absence of PP, dynamically vulcanized at different temperatures in the batch mixer.

The results of dynamic vulcanisation of EPDM in the absence of PP at 200 ºC (Fig. 3.6) are rather similar to those of dynamic vulcanisation of 70/30 (w/w) EPDM/PP TPVs (Fig. 3.2). Obviously, EPDM is the matrix in these EPDM-rich TPV and suffers significantly from degradation, similar to what occurs to EPDM in the absence PP. In case of PP-rich TPVs compositions and also for the 50/50 (w/w) EPDM/PP MFI 47 TPV composition, the gel content trend is similar to those obtained for the static vulcanisation of EPDM. This supports the hypothesis that degradation of the EPDM (network) occurs during dynamic vulcanisation, especially if EPDM is the matrix.

Actually, cross-linking and degradation are competing processes during dynamic vulcanisation, while during static vulcanisation only cross-linking occurs. Degradation is probably related to thermo-mechanical effects (high temperature and high shear). Oxidation due to the presence of oxygen can also occur. This phenomenon has not been reported in the literature on dynamic vulcanisation of TPVs, although devulcanisation under high shear flow of EPDM rubber, cured with sulphur or with peroxide, as a way of recycling has been reported [26-28].

3.4. Dynamic Vulcanisation of TPVs at different Temperatures

Finally, in order to evaluate the effect of set temperature of the batch mixer on the extent of cross-linking during dynamic vulcanisation of a full TPV formulation, experiments were performed at 170, 200 and 220 ºC. The 30/70 (w/w) EPDM/PP composition with the PP MFI 47 was used, in order to have EPDM as the dispersed phase and to keep degradation of the EPDM (network) to a minimum. EPDM gel content in cyclohexane as a function of time and in xylene at 300 s as a function of temperature is presented in Fig. 3.7. EPDM gel content determined with cyclohexane is hardly affected by the increase of temperature. At 45 s a slight increase of the cross-linking degree with increasing temperature is observed, which is probably related to the faster cross-linking at higher temperatures (see Fig. 3.6). A comparison between dynamic vulcanisation of EPDM in the presence of PP at 170 ºC with static vulcanisation of only EPDM (Fig. 3.6) shows that the former results in faster cross-linking and achieves higher gel content. This is probably related to the more efficient heat transfer in the latter case due to mixing. These results are confirmed by xylene extraction on the 300 s samples. The EPDM gel content is similar at 170 and 200 ºC. At 220 ºC a slight decrease of gel content is observed. These data demonstrate that if EPDM is mainly dispersed

in the low viscous PP matrix, degradation of the EPDM network does not occur to a significant extent.

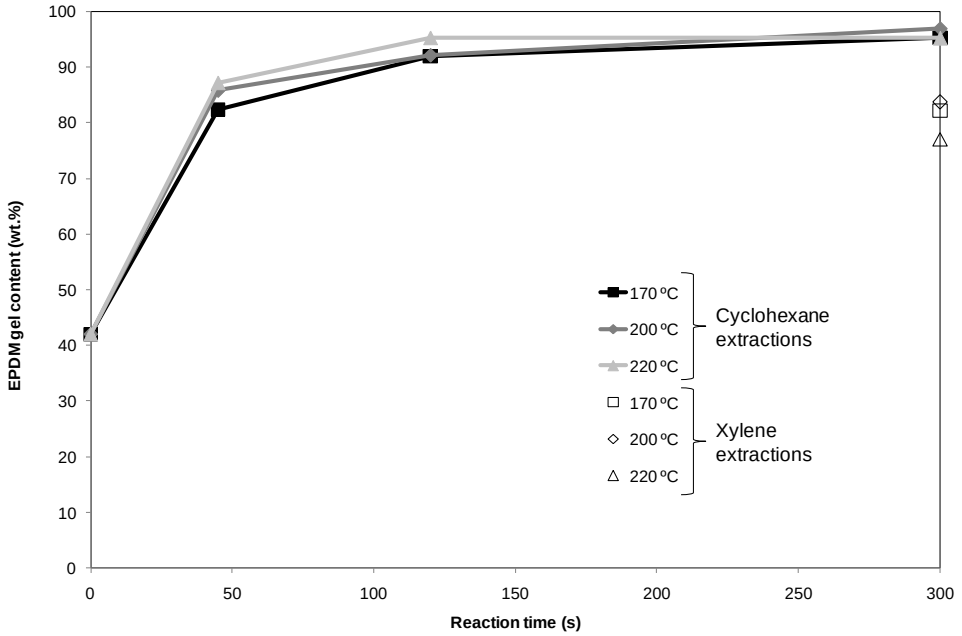

Fig. 3.7. EPDM gel content of EPDM/PP (30/70; w/w) TPVs with PP MFI 47 as a function of reaction time at different temperatures (closed symbols - data from cyclohexane and open symbols - data from xylene only at 300 s).

4. Conclusions

EPDM/PP – based TPVs were prepared via dynamic vulcanisation using resole/$SnCl_2$ as the cross-linking system. Although the amount of the cross-linking agents was kept constant relative to EPDM amount, it was noticed that the evolution of cross-linking as a function of time decreases as the EPDM amount increases. In case of static vulcanisation of only EPDM in the absence of PP the cross-linking reaction proceeds according to normal Arrhenius behaviour and high degrees of cross-linking are obtained at higher temperatures. Dynamic vulcanisation of EPDM in the absence of PP results in relatively low levels of cross-linking. It could be concluded that degradation of the EPDM network occurs during dynamic vulcanisation, due to the action of both high shear and elongation stresses and high temperature. Combining the gel content data for TPVs with the corresponding blend morphologies, it was shown that degradation of the EPDM network in a TPV formulation is minimized if EPDM is the dispersed phase and/or if the PP matrix has low viscosity.

References

[1] De SK, Bhowmick AK. Thermoplastic elastomers from rubber–plastic blends. New York: Ellis Horwood, 1990.

[2] Coran AY, Patel RP. Thermoplastic elastomers based on dynamically vulcanized elastomer/thermoplastic blends. In: Thermoplastic Elastomers, Holden G, Hans RK, Quirk RP, editors, 2nd ed., 1996, Munich: Hanser Publishers. p. 143-181.

[3] Karger-Kocsis J. Thermoplastic rubbers via dynamic vulcanization. In: Polymer blends and alloys, Shonaike GO, Simon GP, editors. New York: Marcel Dekker, 1999. p. 125-153.

[4] Machado AV, Duin M van. Dynamic vulcanisation of EPDM/PE-based thermoplastic vulcanisates studied along the extruder axis. Polymer 2005;46(17):6575-6586.

[5] Verbois A, Cassagnau P, Michel A, Guillet J, Raveyre C. New thermoplastic vulcanizate, composed of polypropylene and ethylene-vinyl acetate copolymer cross-linked by tetrapropoxysilane: Evolution of the blend morphology with respect to the cross-linking reaction conversion. Polym Int 2004;53(5):523-535.

[6] Martin P, Devaux J, Legras R, Leemans L, van Gurp M, van Duin M. Reactive compatibilization of blends of polybutyleneterephthalate with epoxide-containing rubber. The effect of the concentrations in reactive functions. Polymer 2003;44(18):5251-5262.

[7] L. D'Orazio, C. Mancarella, E. Martuscelli and R. Ghisellini, J. Appl. Polym. Sci. **53**, 387 (1994).

[8] Coran AY, Patel RP. Rubber-thermoplastic compositions - 2. NBR-nylon thermoplastic elastomeric compositions. Rubber Chem and Thecnol 1980;53(4):781-794.

[9] Bhadane PA, Champagne MF, Huneault MA, Tofan F, Favis BD. Continuity development in polymer blends of very low interfacial tension. Polymer 2006;47(8):2760-2771

[10] Wu S. Formation of dispersed phase in incompatible polymer blends: Interfacial and rheological effects. Polym Eng Sci 1987;27(5):335-343.

[11] Sengupta P. Morphology of olefinic thermoplastic elastomer blends: A comparative study into the structure – property relationship of EPDM/PP/oil and SEBS/PP/oil blend. PhD thesis University of Twente, The Netherlands, 2004.

[12] Datta S. 157th Spring Technical Meeting of the American Chemical Society, Rubber Division, Dallas, Texas, 2000.

[13] Abdou-Sabet S, Patel RP. Morphology of elastomeric alloys. Rubber Chem Technol 1991;64(5):769-779.

[14] van Duin M, Machado AV. EPDM-based thermoplastic vulcanisates: Cross-linking chemistry and dynamic vulcanisation along the extruder axis. Polym Deg Stab, 2005;90(2):340-345.

[15] Lattimer RP, Kinsey RA, Layer RW, Rhee CK. The mechanism of phenolic resin vulcanization of unsaturated elastomers. Rubber Chem Technol, 1989;62(1):107-123.

[16] van Duin M, Souphantong A. The chemistry of phenol-formaldehyde resin vulcanization of EPDM: part I. Evidence for methylene cross-links. Rubber Chem Technol, 1995;68(5):717-727.

[17] van Duin M. The chemistry of phenol-formaldehyde resin cross-linking of EPDM as studied with low-molecular-weight models: part II. Formation of inert species, cross-link precursors and cross-links. Rubber Chem Technol, 2000;73(4):706-719.

[18] van Duin M. Recent developments for EPDM-based thermoplastic vulcanisates. Macromol Symp 2006;233(1):11-16.

[19] Radusch HJ, Pham T. Morphology formation in dynamic vulcanized PP/EPDM blends. Kautsch Gummi Kunstst 1996;49(4):249-257.

[20] Goharpey F, Katbab AA, Nazockdast H. Mechanism of morphology development in dynamically cured EPDM/PP TPEs. I. Effects of state of cure. J Appl Polym Sci 2001;81(10):2531-2544.

[21] Abdou-Sabet S, Fath MA. Thermoplastic elastomeric blends of olefin rubber and polyolefin resin.US Patent 4311628, 1982.

[22] Antunes CF, Machado AV, van Duin M. Morphology development and phase inversion during dynamic vulcanisation of EPDM/PP blends, *submitted to Polymer*.

[23] Avgeropoulos GN, Weissert FC, Biddison PH, Böehm GGA. Heterogeneous blends of polymers. Rheology and morphology. Rubber Chem Techn 1976;49(1):93-104.

[24] Romani D, Garagnani E, Marchetti E. Reactive blending: structure and properties of cross-linking olefinic thermoplastic elastomer. Int Symp New Polym Mater. Naples, Italy, 1986. p.56-87.

[25] Gergen WP, Lutz R, Davison S. Thermoplastic elastomers: A comprehensive review. In: Legge NR, Hodeln, G, Davison *S*, editors. Munich: Carl Hanser, 1987.

[26] Mouri M, Sato N, Okomoto H, Matsushita M, Honda H, Nakashima K, Takeushi K, Suzuki Y, Owaki M. Int Polym Sci Technol 2000:27(T/17 – T/22).

[27] Fukumori K, Matsushlta M, Mouri M, Okamoto H, Sato N, Takeuchi K, Suzuki Y. KGK Kautsch Gummi Kunstst 2006;59**(**7-8):405.

[28] Sutanto P, Laksmana FL, Picchioni F, Janssen LPBM. Modeling on the kinetics of an EPDM devulcanization in an internal batch mixer using an amine as the devulcanizing agent. Chemical Eng Sci 2006;61(19):6442-6453.

Chapter 4: Effect of Viscosity and Elasticity Ratios on the Morphology and Phase Inversion of EPDM/PP Blends

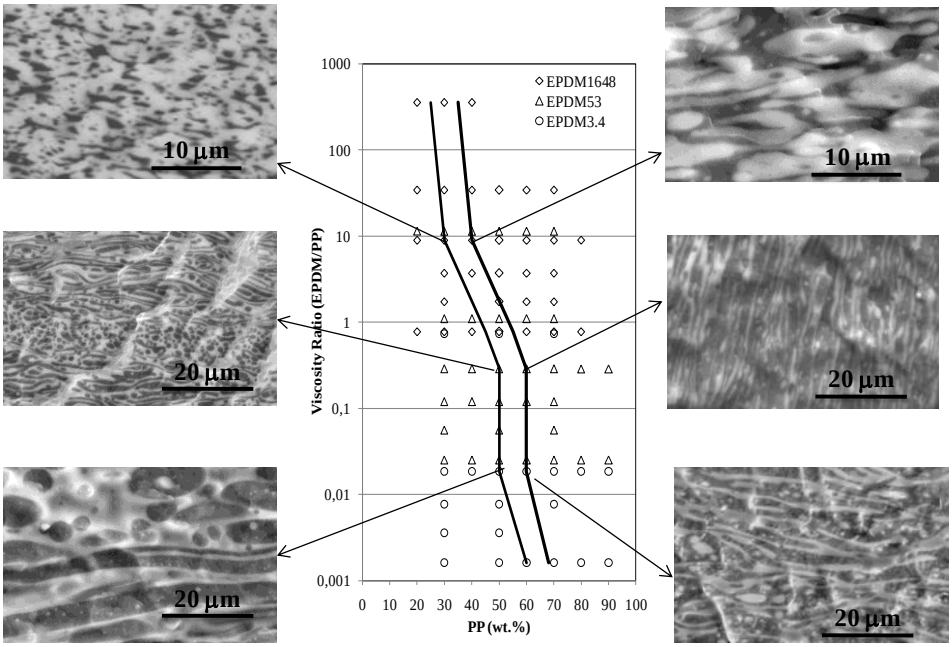

This chapter was submitted to J Polym Sci Part B: Polym Phys.

1. Introduction

Polymer blending is an efficient and economical way to develop and produce new polymeric materials with specific properties unachievable from their individual components [1-2]. As an example, thermoplastic vulcanisates (TPVs) are designed to combine rubber-like properties and thermoplastic processability in a single product [2]. Most commercial TPVs are based on a cross-linked ethylene propylene diene monomer (EPDM) phase that is dispersed in a polypropylene (PP) matrix. These materials are produced by selective cross-linking of EPDM upon melt-mixing with PP.

Blend properties are determined by the characteristics of each component and by the morphology and phase dimensions that develop during the melt mixing process. The final blend morphology depends on the volume composition, rheological properties of individual blend components, interfacial tension and processing conditions [1].

Heterogeneous morphologies are achieved because most polymer blends are immiscible. Thus, polymer blends can be categorized into the following four types: matrix-dispersed particle; matrix-fiber; lamellar structures; and co-continuous structures [3]. Co-continuous structures are particularly interesting because both components can fully contribute to blend properties. The term "co-continuous" is applied usually when a completely continuous structure is achieved for both polymers. The composition range to achieve co-continuity can be narrow or wide depending on blend system characteristics and processing conditions, and the phase inversion composition or phase inversion point is located at it center. Phase inversion is defined as the point where blend components exchange their discontinuity. The dispersed phase becomes the matrix and vice versa. Several authors [4-7] have found that phase inversion depends on the blend composition and viscosity ratio. Thus, a theoretical prediction of the phase inversion has been proposed:

$$\frac{\phi_{1,PI}}{\phi_{2,PI}} = \frac{\eta_1}{\eta_2} \qquad (1)$$

where $\phi_{1,PI}$ is the volume fraction of component *i* at the phase inversion point and η_i is the corresponding melt viscosity. However, substantial deviations from Eq. (1) have been noted, especially for viscosity ratios that depart from unity [8-12]. Thus, several authors [11, 13, 14] have modified the general relationship by introducing an exponent and/or a prefactor to obtain better fits with experimental results. A different approach based on Tomotika's theory of filament instability concept [15] was derived by Metelkin and Blekht [16] to predict the critical volume fraction for phase inversion:

$$\phi_{2,PI} = [1 + F(\lambda) \times \lambda]^{-1} \quad (2)$$

where F(λ) = 1+ 2.25 log (λ) + 1.81 [log (λ)]^2 and λ is the viscosity ratio [1]. Luciani and Jarrin [17] also proposed a model based on Tomokita's theory that effectively predicted the phase inversion composition for the following three blended systems: ethylene propylene rubber (EPR)/polyvinylidene fluoride (PVDF); EPR/polyamide 6 (PA6); and EPR/polyamide 11 (PA11). However, this model could only be applied to viscosity ratios ranging between 0.25 – 4.

Utracki [8] suggested another approach based on the emulsion theory that could be applied to viscosity ratios departing from unity. Therefore, using the relation given by Krieger and Dougherty [18] for monodisperse hard spheres in a fluid assuming that the blend viscosities will result from the addition of polymer B to polymer A and vice versa, have to be the same at phase inversion composition. The viscosity ratio is as follows:

$$\lambda = \left[\frac{\phi_m - \phi_{2,PI}}{\phi_m - \phi_{1,PI}}\right]^{[\eta]\phi_m} \quad (3)$$

where the intrinsic viscosity [η] was assumed to be 1.9 and the maximum packing volume fraction [ϕ_m] was assumed to be 0.84 for spherical domains.

Because the models described above do not always fit with experimental results, Bourry and Favis [19] suggested a model based on Van Oene's theory [20, 21], which considers the elasticity contribution. This model predicts the phase inversion composition in terms of elasticity using the storage modulus $G'_i(\omega)$ and the loss angle $\tan\delta_i$ as shown in Eq. 4 and 5, respectively.

$$\frac{\phi_{1,PI}}{\phi_{2,PI}} = \frac{G'_2(\omega)}{G'_1(\omega)} \quad (4)$$

$$\frac{\phi_{1,PI}}{\phi_{2,PI}} = \frac{\tan\delta_2}{\tan\delta_1} \quad (5)$$

Furthermore, this model estimates that the more elastic phase tends to encapsulate the less elastic phase at sufficiently high concentrations during mixing.

Steinmann [22] investigated the rheological properties of blends in the phase inversion region and found that the storage modulus was the most robust and suitable predictor of phase inversion. Thus, the following expression was developed to predict the phase inversion composition:

$$\phi_{2,PI} = \frac{1}{(\lambda^{1/z} + 1)} \quad (6)$$

where Z characterizes the specific interfacial area and the relaxation rate of the structure and is dependent on the blend system.

Although numerous studies have been performed on co-continuous blends and phase inversion, only limited research [12, 23-29] provides detailed information on these phenomena for EPDM/polypropylene (PP) blends with and without cross-linking. Usually, morphological characteristics of non-cross-linked EPDM/PP blends have been compared to that of corresponding dynamic vulcanisates [28-31]. Romani [23], using electron microscopy, proposed a diagram for the co-continuity region of ethylene propylene rubber (EPM) and PP as a function of the viscosity ratio and composition. Specifically, EPM/PP blends can exhibit co-continuity over a wide range of compositions depending on the viscosity ratio. Recently, Bhadane [25] studied the co-continuity of EPDM/PP blends with viscosity ratios between 0.7 – 5 and shear stress values between 12 – 231 kPa. The co-continuity region, based on solvent extractions, for the EPDM/PP blend was symmetrical relative to the 50/50 composition, but the region was not affected by changes in the viscosity ratio. However, in another study [26], these same authors found an asymmetrical behaviour for EPDM/PP (50/50) blends at high viscosity ratios (11 and 17).

Although the main goal of our research was to study the effects of cross-linking on morphological development and phase inversion during the production of TPVs, it was necessary to characterize the morphology of EPDM/PP blends without cross-linking. Thus, aims of the present work involved investigating the phase morphology of non-cross-linked EPDM/PP blends with a wide range of viscosity ratios (10^{-3} to 10^{2}) and studying the influence of the viscosity and elasticity of the blend components on the phase inversion composition.

2. Experimental

2.1. Materials

The characteristic properties of the raw polymers used in this work (Tables 2.2 and 2.3) and the polymers codes (Table 2.4) are given in part 3 of the Chapter 2. All the polymers (EPDM6414, EPDM1648, EPDM53, EPDM3.4, PP2116, PP950, PP443, PP184, PP48 and PP4.6) were used in this chapter. Irganox 1076 (purchased from Ciba) was used as a stabilizer. The rheological characterisation of polymers is described in Chapter 2, part 3.3.

2.2. Blend Preparation

A series of blends with varying viscosity ratios and EPDM/PP compositions between 10/90 to 80/20 (w/w) were prepared in the internal mixer (Haake Rheomix 600 OS) by combining the EPDM and PP polymers presented in Table 1. The rotor speed was 80 rpm and the set temperature was 200 ºC. The mixing sequence involved introducing PP pellets into the hot mixer. After melting the PP, the stabilizer (Irganox 1076) was added (0.25 wt.% relative to the total polymer mass), and finally the EPDM rubber was incorporated. The torque reached a constant value after about 3 minutes, indicating that a homogenous melt had formed. Samples were collected after an additional five minutes of mixing. Samples were cooled between two metal plates to avoid morphological changes.

2.3. Solvent Extraction

Solvent extractions were performed to determine the composition range where the EPDM/PP blends exhibited a droplet-in-matrix or co-continuous phase morphology. Samples were weighted and immersed in cyclohexane at room temperature for 48 h under gentle stirring. The cyclohexane was refreshed after 24 h. Samples were weighted again after drying them in a vacuum oven at 100 °C for 12 h with nitrogen purging. Because cyclohexane selectively extracts the EPDM phase, the co-continuity index of the EPDM phase was calculated with the following equation as the percentage of the EPDM phase that was extracted:

$$cc_{EPDM} = \frac{w_i - w_f}{w_i} \times 100 \quad (7)$$

where w_i is the weight of the EPDM phase present in the original EPDM/PP blend and w_f is the weight of the EPDM phase in the sample after solvent extraction. Sample thickness was sustained between 2 - 3 mm (approximately 200 mg) because the co-continuity index depends on the sample thickness [32]. The PP continuity was qualitatively classified by the visual aspect of the final solution. PP was considered fully continuous if the sample preserved its shape and did not disintegrate. The PP phase was considered to be partially dispersed if samples disintegrated into small fragments in the cyclohexane solution. The PP phase was considered fully dispersed if a milky solution was observed.

2.4. Scanning Electron Microscopy (SEM)

The morphology of the EPDM/PP blends was analyzed by SEM using a Leica Scanning Electron Microscope following two different approaches. First, samples were fractured in liquid nitrogen. SEM was performed on gold-coated surfaces after removal of the EPDM phase using cyclohexane to confirm PP continuity of the EPDM/PP blends. Under the second approach, samples were fractured in liquid nitrogen and then vapor-stained with ruthenium tetroxide for 120 minutes. SEM in the back-scattering mode (BSE) was performed on samples coated with a thin layer of gold. The average areas and aspect ratios of the dispersed phase were quantified using image analysis software (Image-Pro Plus). To obtain representative results, at least 100 particles were examined with each SEM micrograph.

3. Results and Discussion

Before discussing the blend morphologies in detail, the rheological behaviour of pure polymers and experimental limitations related to the characteristics of samples and techniques used in this study will be pointed out. Regarding the blend morphology first the extraction experiments yielding the EPDM co-continuity index will be presented, followed by SEM images obtained in BSE mode. Then, the co-continuous region as a function of the viscosity ratio and composition among both techniques will be compared. Finally, experimental results obtained for the phase inversion composition will be compared with theoretical predictions and discussed in terms of viscosity and elasticity ratios.

3.1. Rheological Behaviour of Blend Components

Dynamic rheological measurements were performed to characterize EPDM/PP blends in terms of melt viscosity and elasticity ratios of EPDM and PP polymers at applied processing conditions (i.e., set temperature and shear rate). The complex viscosity (η^*) of various EPDM and PP at 200 ºC, as a function of frequency was presented in Chapter 2, Fig. 2.13.

Because PP and EPDM are known to follow the Cox-Merz rule [33], it is assumed that the shear rate dependence of the steady shear viscosity is equal to the frequency (rad/s) dependence of the complex viscosity [34]. Table 4.1 provides the melt viscosity (p_η), storage modulus ($p_{G'}$), loss modulus ($p_{G''}$) and tan δ ($p_{tan\delta}$) ratios of the EPDM and PP polymers at 200 ºC and at an average shear rate of 65 s^{-1}. Thus, viscosity ratios varied five orders of

magnitude from 10^{-3} to 10^{2}, and elasticity ratios varied eight orders of magnitude from 10^{-4} to 10^{4}. Viscosity and elasticity ratios increased for each series of blends (i.e, blends made with the same EPDM but different PPs). This makes it difficult to independently evaluate the effects of each parameter on co-continuity and phase inversion. However, as can be seen in Table 4.1 blends with similar viscosity ratios but different elasticity ratios were obtained by varying both EPDM and PP polymers. Therefore, the effects of viscosity and elasticity ratios on co-continuity and phase inversion can be distinguished.

Table 4.1. Melt viscosity (p_η), storage modulus ($p_{G'}$), loss modulus ($p_{G''}$) and tan δ ($p_{tan\delta}$) ratios of EPDM and PP polymers at a shear rate of 65 s^{-1} and temperature of 200 ºC.

Blend		$p_\eta = \frac{\eta_{EPDM}}{\eta_{PP}}$	$p_{G'} = \frac{G'_{EPDM}}{G'_{PP}}$	$p_{G''} = \frac{G''_{EPDM}}{G''_{PP}}$	$p_{tan\delta} = \frac{tan\delta_{EPDM}}{tan\,\delta_{PP}}$
EPDM	**PP**				
6414	2116	3.0	3.3	2.2	6.5×10^{-1}
	184	3.5×10^{1}	7.5×10^{1}	1.2×10^{1}	1.6×10^{-1}
1648	2116	7.8×10^{-1}	6.6×10^{-1}	1.2	1.9
	950	1.7	1.6	2.0	1.2
	443	3.7	4.2	3.3	7.9×10^{-1}
	184	9.0	1.5×10^{1}	6.7	4.5×10^{-1}
	48	3.4×10^{1}	1.4×10^{2}	2.3×10^{1}	1.6×10^{-1}
	4.6	3.6×10^{2}	2.2×10^{4}	2.4×10^{2}	1.1×10^{-2}
53	2116	2.5×10^{-2}	7.3×10^{-3}	5.5×10^{-2}	7.5
	950	5.6×10^{-2}	1.8×10^{-2}	9.1×10^{-2}	5.0
	443	1.2×10^{-1}	4.6×10^{-2}	1.5×10^{-1}	3.3
	184	2.9×10^{-1}	1.6×10^{-1}	3.1×10^{-1}	1.9
	48	1.1	1.5	1.0	6.9×10^{-1}
	4.6	1.1×10^{1}	2.4×10^{2}	1.1×10^{1}	4.6×10^{-2}
3.4	2116	1.6×10^{-3}	1.1×10^{-4}	3.6×10^{-3}	34
	950	3.6×10^{-3}	2.6×10^{-4}	5.6×10^{-3}	23
	443	7.7×10^{-3}	6.8×10^{-4}	1.0×10^{-2}	15
	184	1.9×10^{-2}	2.4×10^{-3}	2.0×10^{-2}	8.4
	4.6	7.3×10^{-1}	3.6	7.4×10^{-1}	2.1×10^{-1}

3.2. Experimental Limitations of Characterising EPDM/PP Blends

The main objective of this work was to investigate the morphology of EPDM/PP blends as a function of composition and viscosity ratio with emphasis on co-continuity and phase inversion. Therefore, EPDM and PP polymers with different viscosities were used to accommodate a broad range of viscosity ratios. Low viscosity EPDMs (EPDM53 and EPDM3.4) are very difficult to handle because they are very sticky at room temperatures. Blend morphologies of these two liquid EPDMs could not be studied by SEM because these blends are gluey and easily deformed. Thus, only extraction results are presented. Conversely, blends of EPDM6414 could only be studied by SEM as these high viscous rubbers do not dissolve in cyclohexane at room temperature. As a consequence, the co-continuity of EPDM6414/PP blends could not be determined by extraction.

The morphology of the EPDM/PP blends was investigated by SEM on samples after EPDM extraction (i.e., denoted “SEM”) and by SEM in the BSE mode after sample staining with ruthenium tetroxide (i.e., denoted “SEM-BSE”). Fig. 4.1 shows SEM-BSE micrographs (a, b, c) and SEM micrographs (d, e, f) of 30/70, 50/50 and 70/30 EPDM1648/PP184 blends, respectively. The white phase is EPDM and the dark phase is PP due to staining with ruthenium tetroxide. Resulting holes and pores indicate the original location of the EPDM phase when EPDM is extracted with cyclohexane. Similar morphologies can be observed in Fig. 4.1a and 4.1b micrographs and in Fig. 4.1d and 4.1e micrographs, which were obtained post-extraction using SEM and SEM-BSE, respectively. Both SEM techniques showed that PP is the matrix and EPDM is the dispersed phase for blends of 30 and 50 wt.% of EPDM. However, notable differences are observed in micrographs 4.1c and 4.1f that correspond to blends with 70 wt.% EPDM. In micrograph 4.1c, obtained by SEM-BSE, PP seems to be the dispersed phase. However, PP and EPDM seem to be continuous in micrograph 4.1f acquired after EPDM extraction. This discrepancy is an example of the errors that can arise from the interpretation of 2-dimensional SEM images. Despite this limitation, SEM-BSE was selected to study the morphology because it provides detailed information on the microstructure of both EPDM and PP phases. However, SEM was also performed on the extracted samples, especially when the morphology observed by SEM-BSE was not in agreement with the extraction.

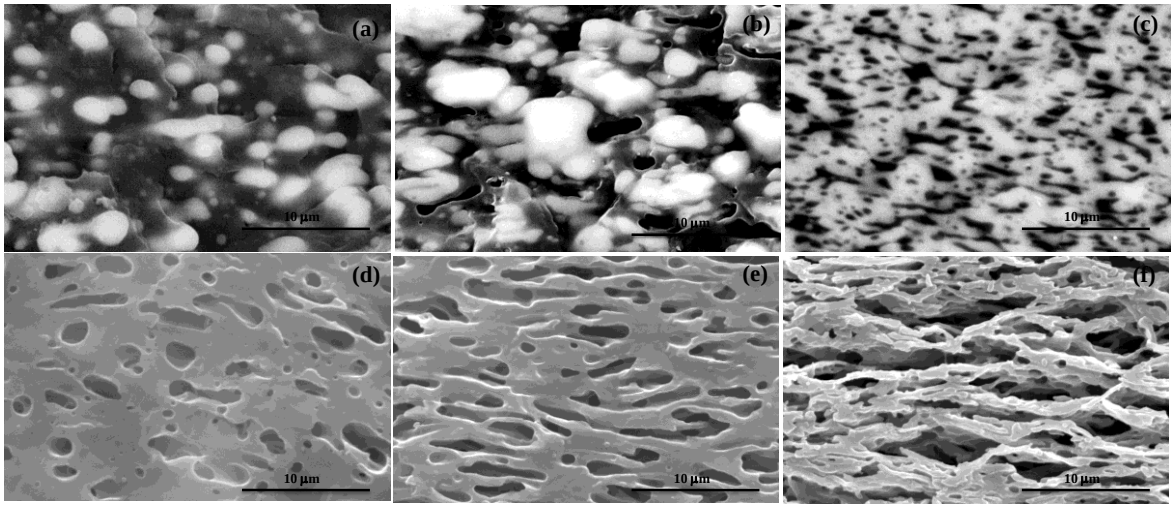

Fig. 4.1. SEM micrographs of EPDM1648/PP184 blends at 30/70, 50/50 and 70/30 (EPDM/PP; w/w) in the BSE mode after staining (a, b, c) and after EPDM extraction (d, e, f).

3.3. Extraction of EPDM/PP Blends

Results of extraction experiments in cyclohexane that yielded the EPDM co-continuity index (%) for the EPDM/PP blends are shown in Fig. 4.2. No quantitative data on PP co-continuity were collected because is not available any solvents that can dissolve PP exclusively. It was considered the structure to be co-continuous if the co-continuity index of the extracted component was 100 % and the sample remained intact after extraction. The structure was fully dispersed if the co-continuity index was 0 %. In most cases, values of 100 % and 0 % were not reached experimentally, and a relative error of ± 5 % in the EPDM co-continuity index was determined. The EPDM was considered to be fully continuous in the blend if the corresponding co-continuity index was higher than 90 %.

Fig. 4.2a presents the co-continuity index of blends prepared with EPDM1648. The threshold of co-continuity is nearly independent of the PP viscosity. Although all blends with 20 wt.% PP disintegrated, a milky solution was obtained only for the EPDM1648/PP4.6 blend, indicating that PP is fully dispersed in this case alone. For other blends of this composition, fragmentation of samples into small pieces in a milky solution was observed, suggesting that the PP is partially dispersed and partially continuous. Full co-continuity was found in the composition range from 30 to 50 wt.% PP. At 60 wt.% of PP, the EPDM co-continuity index remains high (close to 90 %) for most blends, suggesting that the EPDM remains continuous. The percolation point was found at 80 wt.% of PP, indicating that EPDM is fully dispersed in the PP matrix.

Results of EPDM co-continuity of EPDM53/PP blends are shown in Fig. 4.2b. Disintegration was observed at 30 wt.% of PP for all blends. However, fragmentation into small and large pieces in a milky solution was noticed for all samples, suggesting that PP was not yet fully dispersed. The lower limit of co-continuity was at 40 wt.% of PP and was independent of the PP used. The higher limit of co-continuity depended slightly on the PP viscosity, which was 60 wt.% of PP for EPDM/PP blends prepared from higher viscosity PPs (PP2116, PP950 and PP443) and 50 wt.% of PP for blends prepared with lower viscosity PPs (PP184, PP48 and PP4.6). This shift of 10 wt.% of PP in the upper limit of co-continuity of EPDM53 blends can be explained by an increase in the EPDM/PP viscosity ratio, which enhances the tendency of EPDM to be the dispersed phase. EPDM53 is only fully dispersed at 90 wt.% of PP.

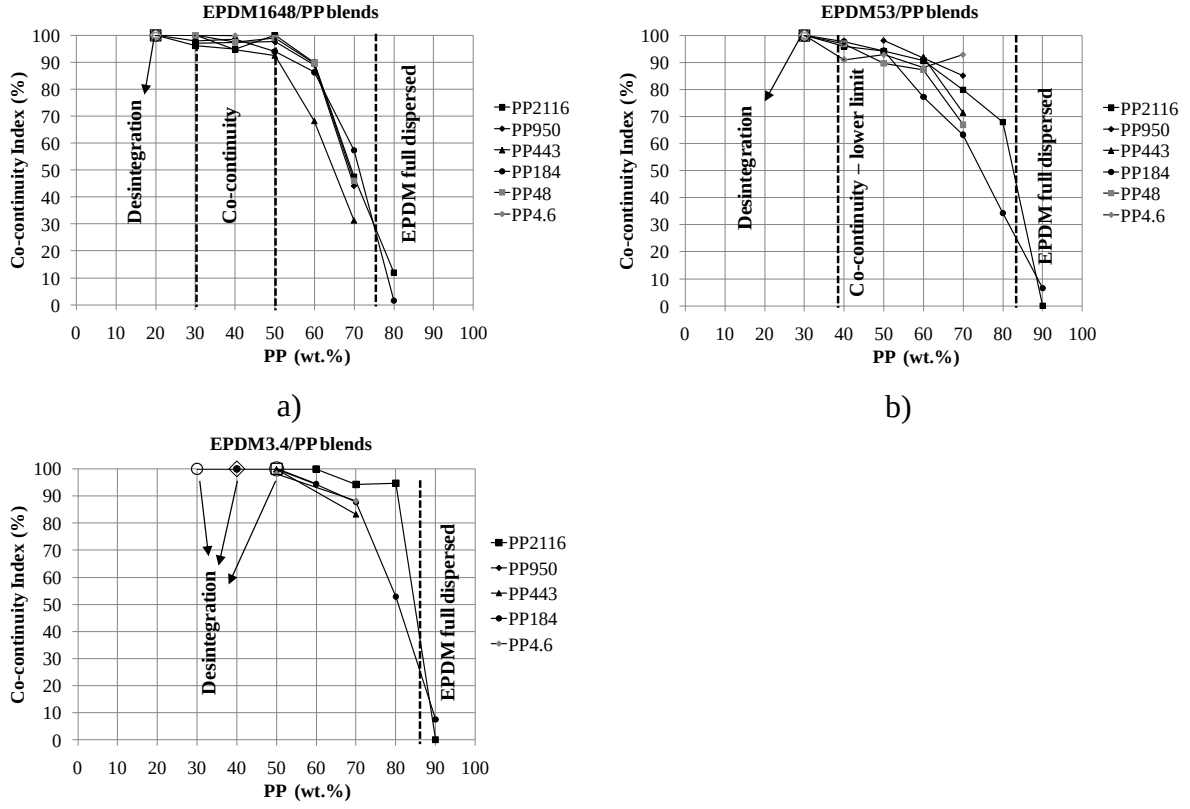

Fig. 4.2. EPDM co-continuity index of EPDM/PP blends as a function of the PP content (open symbols indicate disintegration of samples).

Fig. 4.2c shows that the co-continuity interval of EPDM3.4/PP blends depends on the PP used. The EPDM3.4/PP2116 blend disintegrated at up to 50 wt.% of PP, and its co-continuity region was between 60 – 80 wt.% of PP. The percolation point was observed at 90 wt.% of PP. For EPDM3.4/PP950 blends, fragmentation was observed at 40 wt.% of PP, whereas for EPDM3.4/PP184 blends, fragmentation was only observed at 30 wt.% of PP.

EPDM3.4/PP184 blends display co-continuity in compositions consisting of 40 – 60 wt.% of PP. The co-continuity index proximate to the upper limit (70 wt.% of PP) is higher, suggesting that the EPDM domains still have high levels of continuity. The shift in the lower and upper limits of the co-continuity index of EPDM3.4/PP2116 blends, when compared to EPDM3.4/PP184 blends, was related to a decrease in the EPDM/PP viscosity ratio. EPDM3.4 blends become the matrix for PP2116 blends more readily at low PP amounts because PP2116 has a much higher viscosity than PP184. At higher PP amounts, the low viscosity EPDM can be substantially deformed, including the formation of elongated fibrils, which allows EPDM continuity with relatively low EPDM amounts.

Extraction results provide evidence that the threshold of EPDM phase co-continuity depends on the viscosity of both EPDM and PP phases. For EPDM1648 blends, the EPDM co-continuity index is nearly independent of the PP type used, thereby independent of the viscosity ratio. For low viscosity EPDMs, the EPDM co-continuity index depends on the PP viscosity, mainly for EPDM3.4 blends. A remarkable observation was that blends prepared with EPDM53 and EPDM3.4 and with high viscosity ratios (EPDM53/PP48, EPDM53/PP4.6 and EPDM3.4/PP4.6) did not have the same behaviour as blends prepared with EPDM1648 and similarly high viscosity ratios. This finding suggests that the viscosity ratio is not the only parameter that determines co-continuity, and both viscosity and elasticity ratios probably play a role in phase morphology. This will be discussed in more detail.

3.4. Morphology of EPDM/PP Blends

SEM-BSE micrographs of blends made with EPDM1648, EPDM53, EPDM3.4 and EPDM6414 will be discussed separately and are depicted in Fig. 4.3, 4.4, 4.5 and 4.6, respectively. For each figure, micrographs are organized as polymer arrays, PPs used and blend compositions. The PP viscosity decreases from the bottom of the figure to the top, and the EPDM/PP viscosity ratio increases as a consequence (Table 4.1). Only compositions that evolved from PP dispersed in the EPDM matrix to EPDM dispersed in the PP matrix will be addressed. Therefore, SEM-BSE micrographs are shown for different composition ranges for a given EPDM. For well defined dispersed-matrix morphologies, domain size and shape were evaluated by quantification of average domains area and aspect ratio, respectively. As the shape of the dispersed phase changes significantly among the various blends, the area of the dispersed domains seemed to be the most suitable parameter to quantify domain size.

EPDM1648/PP blends

SEM-BSE micrographs of EPDM1648/PP blends with 20 to 60 wt.% of PP are shown in Fig. 4.3. For these blends, the lowest viscosity ratio is 7.8×10^{-1} (with PP2116) and the highest viscosity ratio is 3.6×10^{2} (with PP4.6). The domain size and the heterogeneity of the domain size distribution generally decreased as the EPDM/PP viscosity ratio decreases. This decrease was independent of the dispersed phase (PP or EPDM) and was also observed for the co-continuous morphologies. For EPDM-rich compositions (20 wt.% of PP), PP particles from the EPDM1648/PP2116 blend had an average area of 4.5×10^{-1} μm^2 with an area range of 5.0×10^{-2} - 1.2 μm^2. These area values were higher for EPDM1648/PP4.6 blend at 2.7 μm^2 and 1.5×10^{-1} – 6.2×10^{1} μm^2. As expected, PP domains became more elongated as the viscosity ratio increased. Low viscosity PP was easily deformed by the highly viscous EPDM1648 blend and elongated fibrils were formed. The same trend was observed for the aspect ratio, which increased from 1.7 to 5.4 when the PP changed from PP2116 to PP48. One notable exception to this observation was PP4.3, for which the aspect ratio decreased to 3.4. This decrease could be explained by the large domain size of the dispersed PP particles. For PP-rich compositions (60 wt.% of PP), the opposite trend was observed, and the aspect ratio decreased from 3.4 to 1.7 as the PP changed from PP2116 to PP48. As the EPDM/PP viscosity ratio increased, the shear and elongation stresses that were generated by the low viscosity PP matrix could not deform the highly viscous dispersed EPDM phase. Thus, we observed an increase in the domain area and a broadening of the EPDM area distribution. The EPDM1648/PP2116 blend had an average area of 0.4 μm^2 and an area range of 4.0×10^{-2} – 1.8 μm^2, which increased to 25 μm^2 and 7.0×10^{-1} – 9.2×10^{2} μm^2, respectively, for the EPDM1648/PP48 blend.

Morphological development as a function of composition was quite similar among all EPDM1648/PP blends. Changes in morphology are smaller at viscosity ratios close to unity. For the EPDM1648/PP2116 blend (30 wt.% of PP), PPs seem to be mainly dispersed with some domains already interconnected. PPs were dispersed and continuous at 40 wt.% of PP and were fully continuous at 50 wt.% PP. The PP phase surrounds the EPDM phase and becomes the matrix at 60 wt.% of PP, but the EPDM domains continue to be somewhat interconnected. Thus, for this EPDM/PP blend, co-continuous structures were formed at around 50 wt.% of PP.

For EPDM1648/PP184 blends, PP domains with some degree of continuity were observed at 20 wt.% of PP. At 30 wt.%, PP is becoming continuous although EPDM remains the

dominant matrix. PP seems to be the dominant matrix at 40 wt.% of PP, although EPDM domains remain large and interconnected. At 50 wt.% of PP, EPDM domains are almost completely dispersed and more spherical albeit still interconnected. Thus, for EPDM1648/PP184 blends, phase inversion occurs between 30 – 40 wt.% of PP.

Coarse morphologies were obtained for blends prepared with PP48 and PP4.6. Therefore, SEM-BSE micrographs at low magnification are shown in Fig. 4 to enhance visualization of the phase morphology. The morphology of the EPDM1648/PP4.6 blend at 20 wt.% of PP consisted of an EPDM matrix with a PP phase that was partially dispersed and continuous. PP is the dominant matrix at 40 wt.% of PP, although the EPDM phase still has interconnected domains. Thus, phase inversion seems to occur at around 30 wt.% of PP when both PP and EPDM are mostly co-continuous.

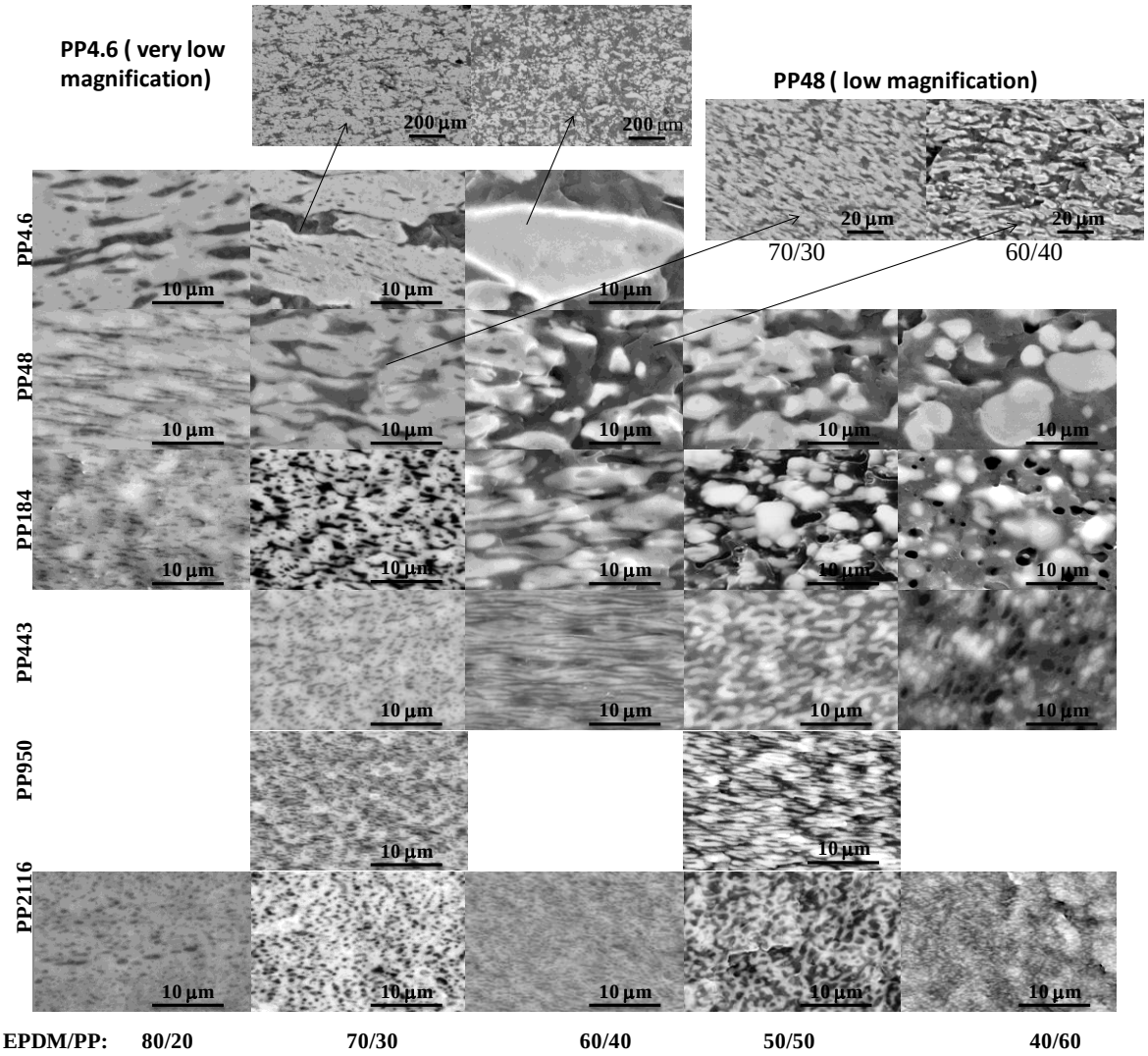

Fig. 4.3. SEM-BSE micrographs of the EPDM1648/PP blend with compositions between 20 – 60 wt.% of PP.

These results indicate that as the PP viscosity increases, the phase inversion composition shifts to lower PP contents. Nonetheless, the EPDM1648 dispersion remained somewhat interconnected at relatively high amounts of PP, even under scenarios of high viscosity ratios.

EPDM53/PP blends

Morphologies of EPDM53/PP blends with compositions between 30 – 70 wt.% of PP are depicted in Fig. 4.4. Viscosity ratios of these blends vary between 2.5×10^{-2} (PP2116) and 1.2×10^{1} (PP4.6). These ratios were less than one for PP2116, PP950, PP443 and PP184 and approximately one for PP48 (Table 4.1). Only SEM-BSE micrographs of the EPDM53/PP950 and EPDM53/PP184 blends with 30 wt.% of PP were obtainable because the other samples were too sticky for microscopy due to the very low EPDM viscosity.

PPs seemed to be in the dispersed phase for all 30 and 40 wt.% PP blends with the exception of the blend containing PP4.6. PP domains of the EPDM53/PP2116 blend, which has a lower viscosity ratio, had an average area of 1.3×10^{1} μm^2 with an area range of 4.9×10^{-1} – 2.9×10^{2} μm^2. The average area decreased to 1.0×10^{1} μm^2 (area range of 2.4×10^{-1} – 1.8×10^{2} μm^2) as the viscosity ratio increased below unity for the EPDM53/PP184 blend. An increase in the average area to 1.7×10^{1} μm^2 (area range of 4.2×10^{-1} – 4.4×10^{2} μm^2) was observed for the EPDM53/PP48 blend, which was not expected because the viscosity ratio is 1.3. The latter results can be explained by the extraction results. The EPDM co-continuity index was around 95 % and the remaining sample did not disintegrate, indicating that PP was a continuous phase. Thus, the PP phase became the matrix as the PP viscosity decreased to levels less than the EPDM viscosity. Likewise, for blends containing PP2116 and PP184, PP domain aspect ratios were consistent with one another at about 1.5, but increased to 3 for PP48. For the EPDM53/PP4.6 blend, which had the lowest PP viscosity, the PP phase seemed to encapsulate the EPDM phase at 40 wt.% of PP. EPDM co-existed as a dispersed phase and elongated structures (Fig. 4.4; low magnification images). The area range of the dispersed EPDM phase varied between 5.4 – 5.5×10^{2} μm^2 with an average area of 1.2×10^{2} μm^2.

For PP-rich compositions at 70 wt.% of PP where most of the EPDM was dispersed, morphologies were significantly more refined than blends containing less PP at 30 wt.% where PP was dispersed. The EPDM53/PP4.6 blend was an exception. EPDM domains have a relatively large area of 3.0×10^{2} μm^2 (range of 4.0×10^{-1} – 3.8×10^{3} μm^2) because the low viscosity PP4.6 matrix cannot break up the EPDM phase. For blends with low EPDM/PP viscosity ratios, the area of the dispersed EPDM phase increased as the viscosity ratio

increased. Specifically, the following average areas and area ranges were determined: 4.5 × 10^{-1} μm^2 (range of 2.0 × 10^{-2} - 2.9 μm^2) for the EPDM53/PP2116 blend; 9.6 × 10^{-1} μm^2 (range of 1.0 × 10^{-1} – 4.7 μm^2) for the EPDM53/PP184 blend; and 1.0 μm^2 (range of 1.6 × 10^{-1} – 3.2 μm^2) for the EPDM53/PP48 blend. The increase in the EPDM domain size can be explained by the decrease in the PP viscosity and elasticity. Consequently, the EPDM phase was less deformed and larger particles were obtained. The decrease in the PP viscosity can also explain the decrease in aspect ratios, which were 2.3 for the PP2116 blend and 1.3 for PP184 and PP49.

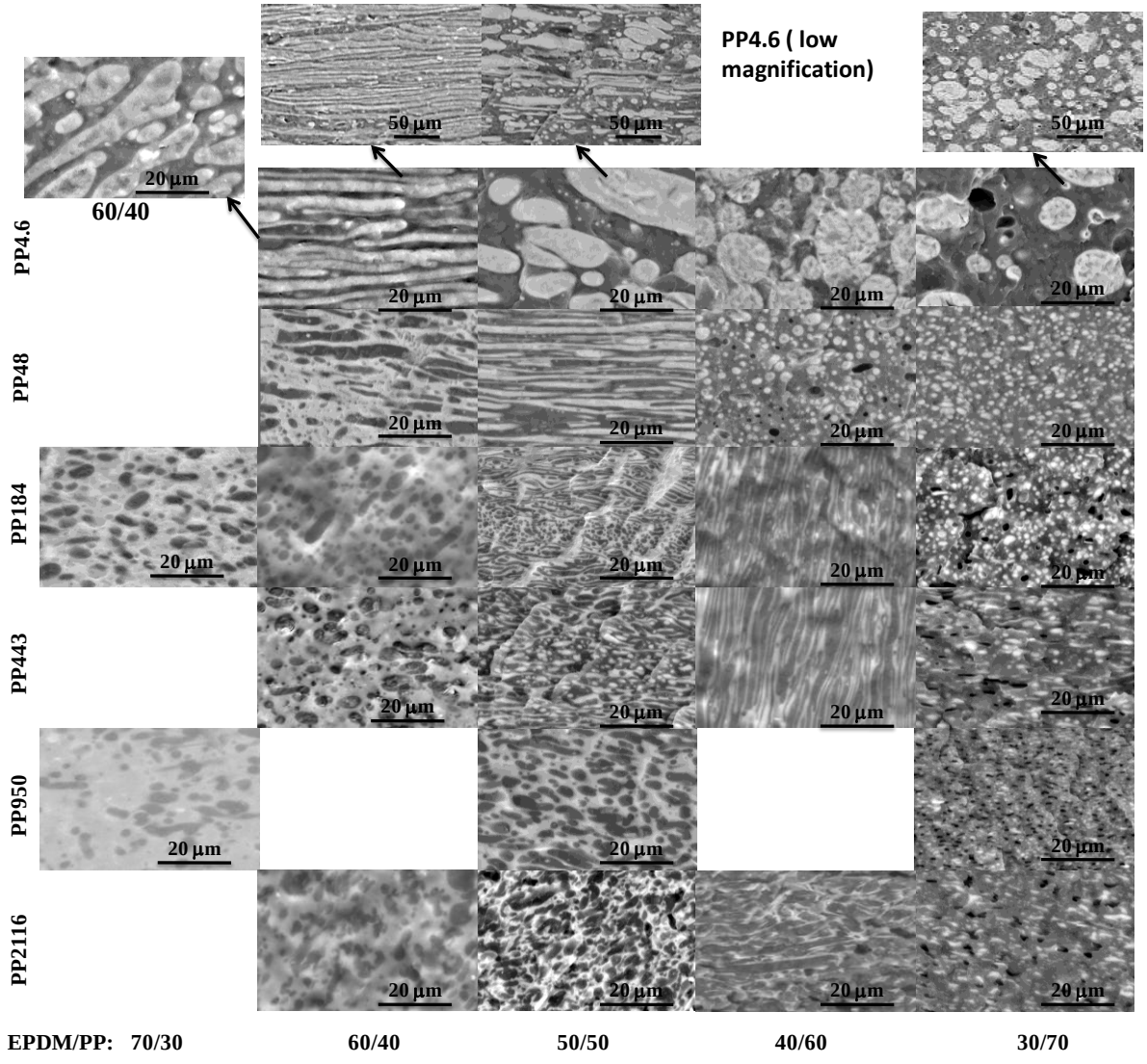

Fig. 4.4. SEM micrographs of EPDM53/PP blends with compositions ranging between 30 – 70 wt.% of PP.

The phase inversion from dispersed PP phase to dispersed EPDM phase with increasing PP content seemed to occur at higher PP levels for EPDM53 blends containing PP2116. The

EPDM phase is the matrix and PP is presented both as the dispersed and continuous phase at 40 and 50 wt.% of PP. At 60 wt.% of PP, both PP and EPDM phases seemed to be continuous, although EPDM was partly dispersed. At 70 wt.% of PP, the PP phase was the matrix and the EPDM phase was fully dispersed. Thus, the phase inversion occurred at approximately 60 wt.% of PP. PP seemed to be the dispersed phase at up to 40 wt.% of PP for the EPDM53/PP184 blends. At 50 wt.% of PP, both the EPDM and PP phases seemed to be continuous, although the PP phase sometimes appeared dispersed in the EPDM phase. The PP phase is the matrix and contains elongated and somewhat interconnected EPDM particles at 60 wt.% of PP. EPDM particles were dispersed in the PP matrix at 70 wt.% of PP. Thus, phase inversion occurred between 50 – 60 wt.% of PP. For the EPDM53/PP48 blends, PP became the matrix at around 50 wt.% of PP. For the EPDM53/PP4.6 blends, PP matrix formation occurred at approximately 40 wt.% of PP. This shift in the phase inversion composition was related to the increased viscosity ratio. These results show that the morphology becomes coarser when low viscous materials are used as a consequence of the low shear and elongation stresses generated by these low viscosity materials. It is also notable that the size of the dispersed phase is smaller if a high viscosity matrix is used.

EPDM3.4/PP blends

Fig. 4.5 presents morphologies of EPDM3.4/PP blends with compositions between 40 – 80 wt.% of PP. Viscosity ratios of these blends increased as follows (Table 4.1): 1.6×10^{-3} for PP2116; 1.9×10^{-2} for PP184; and 7.3×10^{-1} for PP4.6. As mentioned, EPDM3.4 is a very soft and sticky liquid. Thus, in most cases, SEM images of continuous or co-continuous morphologies were not obtainable.

PP seems to be dispersed with large domains at 40 and 50 wt.% of PP. Therefore, lower magnifications were used to gather more information on these blend morphologies. For EPDM3.4/PP184 at 40 wt.% of PP, the average area was 4.9×10^{2} μm^2 (range of $1.0 – 1.1 \times 10^{4}$ μm^2). For PP-rich blends, relatively small EPDM particles were obtained when a high viscosity PP was used as the matrix, as was observed for EPDM53. For 70 wt.% of PP, the average area of the EPDM particles in EPDM3.4/PP2116 blends was 2.6 μm^2 (range of $2.0 \times 10^{-3} – 3.7 \times 10^{1}$ μm^2). This average area increased to 6.4 μm^2 (range of $7.0 \times 10^{-3} – 5.4 \times 10^{1}$ μm^2) as the viscosity ratio increased (EPDM3.4/PP184 blend). The EPDM3.4/PP4.6 blend has a viscosity ratio close to one, but the domain size of the PP dispersion is quite large (9.7 μm^2; range of $1.5 – 2.1 \times 10^{1}$ μm^2) relative to blends with low viscosity ratios. This

observation can be explained by the high viscosity and elasticity of the PP matrix relative to the dispersed EPDM phase.

The phase inversion for EPDM3.4/PP2116 blends occurs at higher PP levels than that of other blends. At 60 wt.% of PP, the EPDM phase seemed to be the matrix and the PP phase was dispersed. However, low magnifications suggest PP continuity probably because the sample did not disintegrate. PP was the matrix with EPDM domains partially dispersed and continuous for blends of 70 wt.% of PP. EPDM seemed to be fully dispersed in the PP matrix with 80 wt.% of PP. The transition from a dispersed PP phase to a dispersed EPDM phase seemed to occur between 60 – 70 wt.% of PP. EPDM is fully dispersed in the PP matrix of EPDM3.4/PP184 blends at 70 wt.% of PP. In this case, the phase inversion appeared to take place between 50 – 60 wt.% of PP. For EPDM3.4/PP4.6 blends, large elongated EPDM structures and EPDM particles were dispersed in the PP matrix at 50 wt.% of PP, indicating that phase inversion begins to occur before this composition. At higher PP levels, EPDM was the dispersed phase and PP was the matrix.

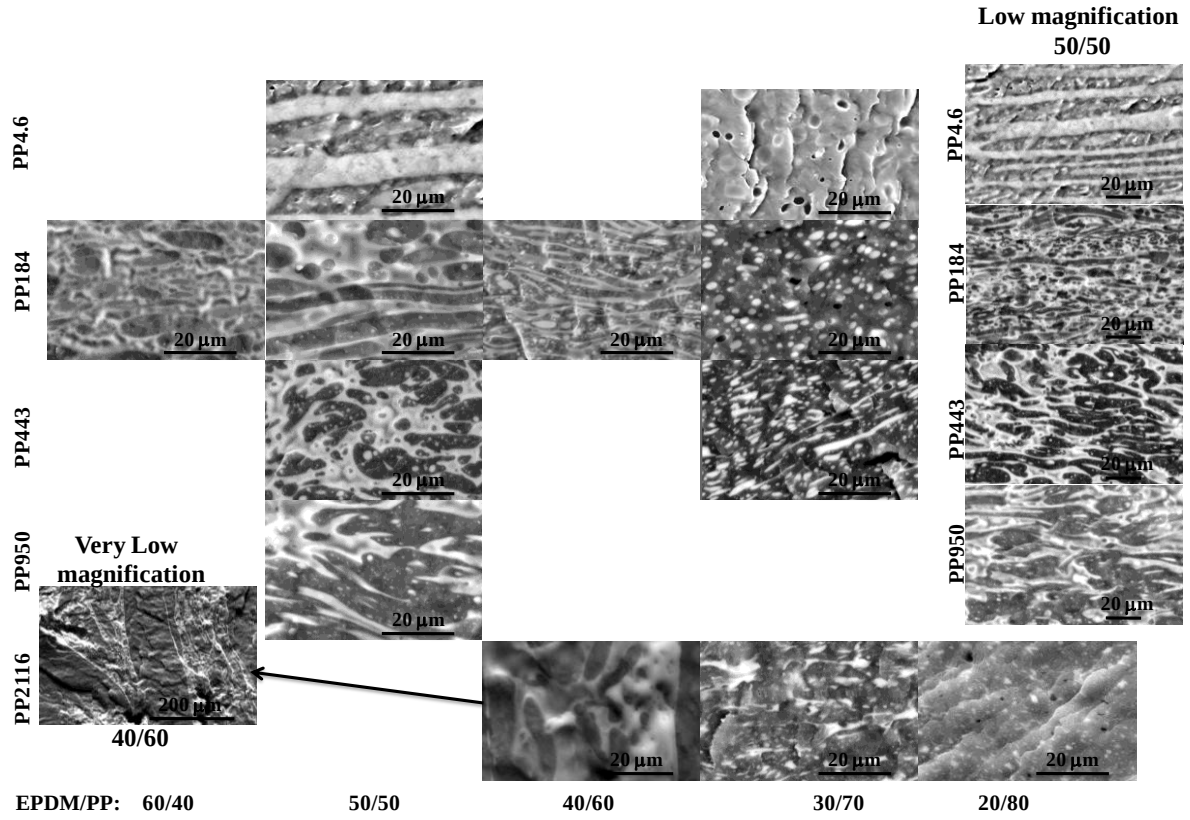

Fig. 4.5. SEM micrographs of EPDM3.4/PP blends with compositions ranging between 40 – 80 wt.% of PP.

EPDM6414/PP blends

Morphologies of blends prepared with the highest viscous rubber, EPDM6414, are shown in Fig. 4.6. Only two blends (EPDM6414/PP2116 and EPDM6414/PP184) with viscosity ratios of 3.0 and 3.5×10^{1} were prepared (Table 4.1). EPDM6414/PP2116 blend at 30 wt.% PP exhibits a co-continuous morphology. Even though at 50 wt.% of PP, EPDM is already the dispersed phase, poor dispersion is observed at low magnification. A large heterogeneity of domain size can be observed with particle areas between $5.0 \times 10^{-2} – 9.2 \times 10^{4}$ μm^2. In the case of the EPDM6414/PP184 blend, the morphology was already co-continuous at 20 wt.% of PP and the EPDM phase was fully dispersed at 30 % of PP. EPDM particles had an area in the range of $6.0 \times 10^{-1} – 1.2 \times 10^{5}$ μm^2. Particle dispersion was very poor at $4.0 – 1.7 \times 10^{5}$ μm^2 for blends containing 50 wt.% of PP. A possible explanation is that the relatively low viscosity PP matrix is not able to break up the highly viscous EPDM phase. EPDM1647/PP443 and EPDM1647/PP48 blends exhibit better EPDM dispersion than EPDM6414/PP2116 and EPDM6414/PP180 blends, respectively, although the blends had similar viscosity ratios. This finding may be related to the increase in the interfacial tension resulting from the relatively high ethylene content (63 wt.%) when compared with that of EPDM1648 (53 wt.%). Alternatively, this high viscosity EPDM was not able to be well-dispersed by the shear and elongation stress generated by the mixing conditions.

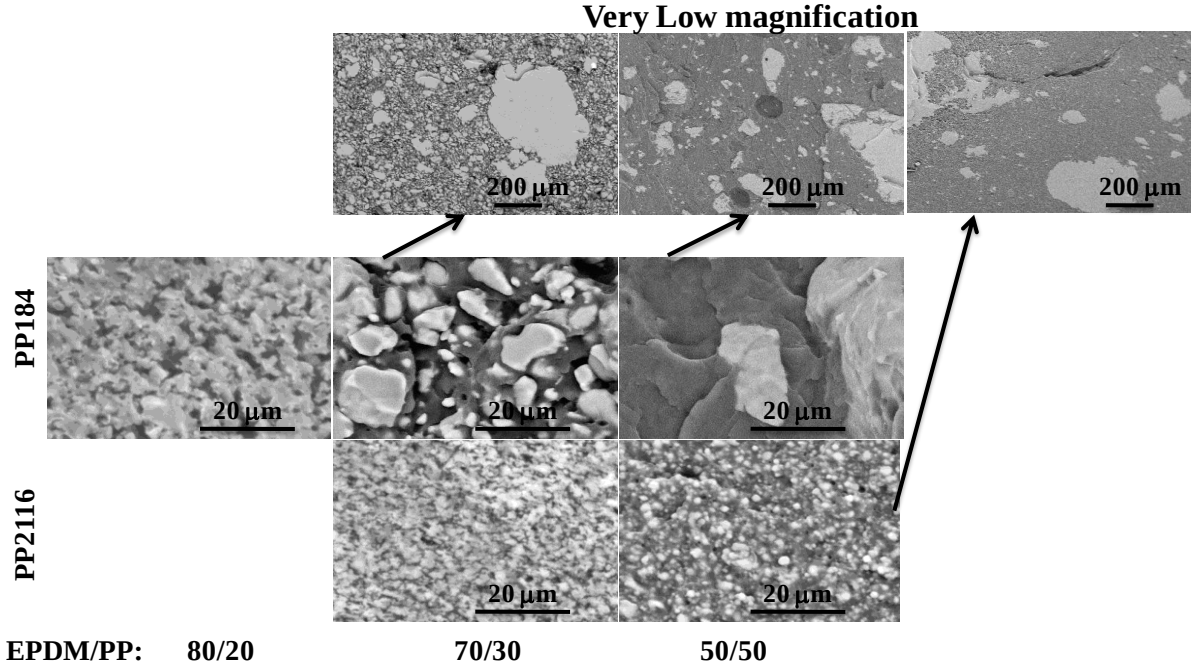

Fig. 4.6. SEM micrographs of EPDM6414/PP blends with compositions ranging between 20 – 50 wt.% of PP.

3.5. Co-Continuity Region

Using data obtained from extractions and SEM-BSE, phase morphology diagrams of viscosity ratios as a function of PP content are presented in Fig. 4.7. Specifically, diagram (a) represents the co-continuity region obtained from the EPDM co-continuity index. Under diagram (b), lines were drawn for blends where EPDM and PP phases were visualized as continuous by SEM-BSE. Each diagram will be discussed separately and compared in more detail below. Fig. 4.7a shows that the co-continuous region was influenced primarily by the EPDM. At higher PP levels and for low viscosity EPDMs, the EPDM co-continuity index depended on the viscosity ratio. For blends made with EPDM1648, the co-continuous region depended on the EPDM/PP (w/w) composition alone. For EPDM53/PP blends, the upper limit of co-continuity was slightly dependent on the viscosity ratio, which was attributable to PP being the matrix. As the viscosity and elasticity of the PP phase increased, the formation of elongated EPDM structures were enhanced, promoting the continuity of the EPDM phase. For EPDM3.4/PP blends, the co-continuous region changed with viscosity ratio, which is probably related to the large difference between the viscosity and elasticity of the EPDM and PP phases.

The EPDM53/PP48 and EPDM53/PP4.6 blends with viscosity ratios of 1.3 and 1.1×10^{1}, respectively, showed different behaviours from blends made with EPDM1648 but similar viscosity ratios. The lower limit of the co-continuity region was shifted to higher PP levels (about 10 wt.%) as is shown in Fig. 4.7a. Because the viscosity ratio of the blends was nearly the same, the viscosity of EPDM1648/PP, EPDM53/PP and EPDM3.4/PP blends with 30 wt.% of PP were investigated. The blend torque recorded at the end of mixing time was used as a qualitative measure of the blend viscosity. Fig. 4.8 shows the blend torque as a function of the viscosity ratio. For the blend made with EPDM1648, the torque decreased as the viscosity ratio increased, which can be correlated to a decrease in the PP viscosity. EPDM53/PP blends exhibited a slight torque that decreased as the viscosity ratio increased. The torque of EPDM3.4/PP blends was close to zero. The viscosity of EPDM1648/PP blends was quite different from those blends made with EPDM53 and EPDM3.4. This observation suggests that the co-continuity region seems to also be an outcome of the final blend viscosity, which is driven here by the EPDM phase. The elasticity ratio measured by the storage modulus ratio was also evaluated. The elasticity ratios of EPDM53/PP4.6 and EPDM1648/PP180 blends (viscosity ratios close to 1.0×10^{1}) were 2.4×10^{2} and 1.5×10^{1}, respectively (Table 4.1). Thus, to be the matrix, the EPDM53 constituent will have more of a

tendency to encapsulate the PP4.3 than the EPDM1648 relative to the PP180. This behaviour could explain why the EPDM53/PP4.6 blend disintegrated until 30 wt.% of PP, whereas the EPDM1648/PP180 blend disintegration ceased after PP levels of 20 wt.%. However, the same co-continuity region would be expected but was not observed for EPDM53/PP48 and EPDM1648/PP950 blends with viscosity ratios of 1.1 and 1.7, respectively, and elasticity ratios of 1.5 and 1.6, respectively. Thus, elasticity ratios, measured by storage modulus, were not the main rheological parameter controlling lower limits of co-continuity regions at high EPDM levels. These results suggest that the co-continuity region is mainly governed by EPDM/PP composition and EPDM characteristics. Another feature of these EPDM/PP blends seems to be an asymmetrical region of co-continuity at 50 wt.% of PP. According to the morphology diagram suggested by Romani et al. [23], EPR/PP blends showed a relatively symmetrical region of co-continuity at 50/50 compositions and viscosity ratios of one. Moreover, a broad range of viscosity ratios around unity was noted, which becomes increasingly narrow as the viscosity ratios depart from unity. These results cannot be compared directly to the Romani diagram because their morphologies were obtained using SEM and Energy Dispersive X-ray Spectroscopy (EDS). Bhadane et al. [25, 26] studied co-continuity based on extraction experiments (viscosity ratios ranging from $1.1 \times 10^{1} – 1.7 \times 10^{1}$). They observed asymmetrical behaviour in EPDM/PP blends and a broad co-continuity range between 35 - 70 wt.% of PP [26]. In another study [25], the same authors found that EPDM/PP blends (viscosity ratio between $7.0 \times 10^{-1} – 5.0$) exhibited co-continuity ranges between 40 – 60 wt.% of PP. For high EPDM viscosity phases, a conceptual model of a collision-coalescence-separation type of erosion mechanism was proposed to explain the broadening of the co-continuity region at high viscosity ratios [26]. In the present study, although a relatively large co-continuity region was found at high and very high viscosity ratios, a widening of the co-continuity range at high viscosity ratios (1.1×10^{1} and 1.7×10^{1}) was not observed. Differences in our results may be attributable to differences in experimental conditions (i.e., blend preparation and extraction methodology); therefore, co-continuity ranges cannot be compared. However, it is confirmed that EPDM/PP blends with high viscosity ratios exhibited a broad range of co-continuities. Moreover, it seems that rheological features of individual blend components (EPDM and PP) and processing conditions play a major role in phase morphologies.

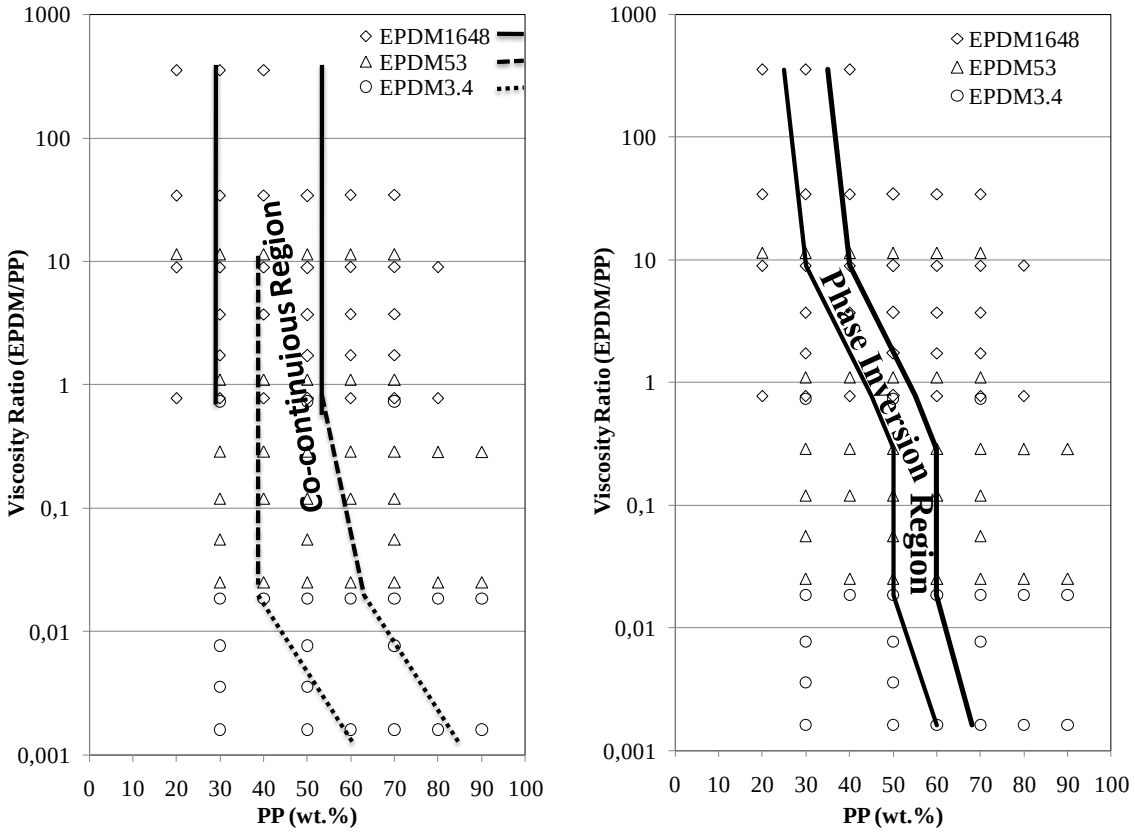

a) b)

Fig. 4.7. Phase morphology diagram of viscosity ratios as a function of PP wt.%: a) co-continuity region and b) phase inversion region.

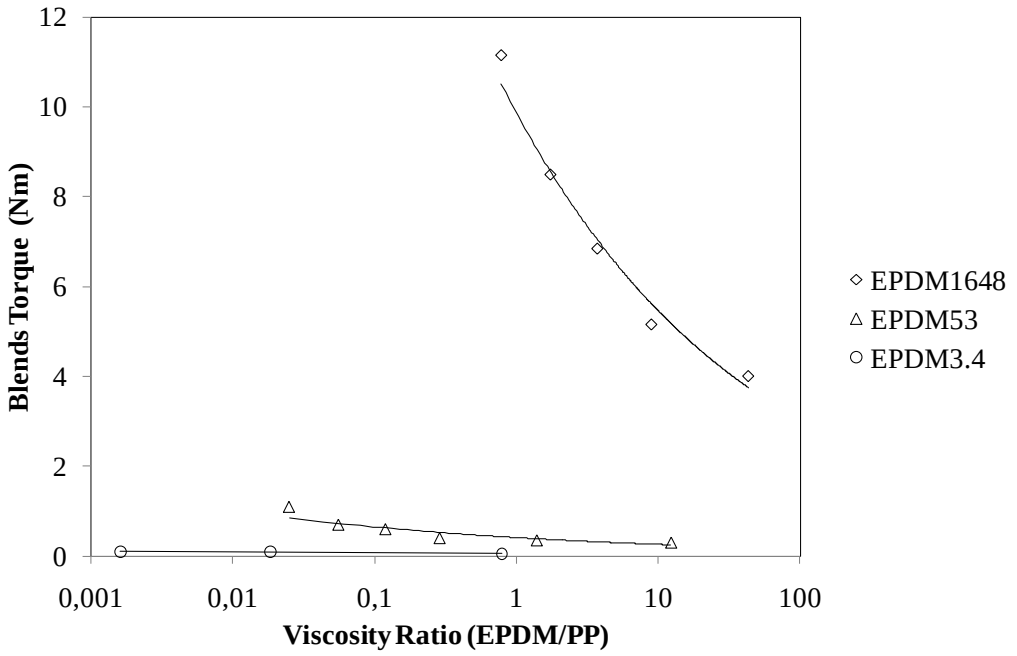

Fig. 4.8. End torque of 70/30 EPDM/PP blends as a function of the viscosity ratio.

The co-continuity region obtained from SEM-BSE microscopy (Fig. 4.7b) is quite narrow when compared to that obtained by extraction (Fig. 4.7a). This may be attributable to continuous structures appearing as a dispersed phase in SEM-BSE micrographs, as discussed previously (Fig. 4.1). Although extractions provide more accurate information on phase continuity, SEM-BSE microscopy was used to estimate the location of the phase inversion point because it narrows the co-continuity region.

As can be seen in Fig. 4.7b, the phase inversion region shifted to higher PP levels as the viscosity ratio decreased. The phase inversion region of EPDM53/PP blends, with viscosity ratios greater than 1, was similar to that of EPDM1648/PP blends with similar viscosity ratios. The phase inversion region obtained by SEM-BSE was more sensitive to viscosity ratio in contrast to the co-continuous region obtained from extraction. At high viscosity ratios, an increase in the viscosity ratio from 1.0×10^{1} to 3.6×10^{2} caused a decrease of PP by 5 wt.% at phase inversion. However, when the viscosity ratio decreased from 1.0×10^{1} to 7.0×10^{-1}, an increase of 15 wt. % of PP was observed. Thus, phase inversion becomes less dependent on the EPDM/PP composition at higher viscosity ratios. At lower viscosity ratios, phase inversion composition was nearly unchanged for EPDM53/PP blends when the viscosity ratio varied from 3.0×10^{-1} to 2.5×10^{-2}. This observation was related to the increase in PP elasticity relative to EPDM53 elasticity as the viscosity ratio decreased. Consequently, the PP phase tends to encapsulate the EPDM phase, shifting the phase inversion region to lower PP amounts and creating an asymmetry relative to blends of 50/50 composition and viscosity ratios of one.

EPDM3.4/PP blends with viscosity ratio declines from 1.8×10^{-2} to 1.6×10^{-3} showed increased PP levels of 10 wt.% at the phase inversion region. This decline was probably related to the low viscosity of the EPDM3.4 constituent, which tends to be matrix even at relatively high PP amounts.

3.6. Phase Inversion

EPDM6614/PP blends were not included in our studies of co-continuity due to difficulties in extracting the high molecular weight EPDM rubber in cyclohexane at room temperatures. However, SEM-BSE data for these blends will be included in this section.

3.6.1. Influence of the viscosity ratio

To study the influence of the viscosity ratio on phase inversions, experimental results will be compared to theoretical predictions using phase inversion models presented in the introduction. The phase inversion composition was estimated from morphological studies with an error of ± 5 wt.% because blends were prepared in 10 wt.% intervals and weight fractions were converted to volume fractions (vol.%). The experimental data describing phase inversion compositions were fitted using theoretical models of phase inversion. Results are shown in Fig. 4.9 as a plot of the viscosity ratio as a function of vol.% of PP. Because deviations were noticed using existing models, a new expression, equation (8), was developed after modification of equation (1) by adding an exponent and a pre-factor.

$$\frac{\phi_{EPDM}}{\phi_{PP}} = 1.30 \left(\frac{\eta_{EPDM}}{\eta_{PP}} \right)^{0.13} \quad (8)$$

The fitting results are also shown in Fig. 4.9. Thus, at viscosity ratios of one, this outcome provides evidence that the PP amount is 43.4 vol. % (or 45 wt.%) (ϕ_{EPDM}/ϕ_{PP}=1.30) at the phase inversion composition, depending only slightly on the viscosity ratio. When our experimental data were compared with models predicted by Miles and Zurek [7] and Metelkin and Blekht [16], it was found that they overestimated the phase inversion composition at viscosity ratios departing from unity. Using standard values of 1.9 ([η]) and 0.84 (ϕ_m), Utracki's model fits well with our experimental data at viscosity ratios near and higher than one. For viscosity ratios less than one, this model overestimates the phase inversion composition. A best fit of our experimental data was obtained by changing the values of [η] and ϕ_m to 2.5 and 0.7, respectively. Although changing the ϕ_m, to 0.7 means that the percolation threshold is around 30 vol.% of PP, which does not agree with data obtained from our extractions. The percolation threshold was close to 19 vol.% of PP (20 wt.%) for EPDM1648 and 9.4 vol.% of PP (10 wt.%) for EPDM53 and EPDM4.3. Using the ϕ_m experimental values, an improved fit was determined for viscosity ratios higher than one. However, the phase inversion composition was overestimated for viscosity ratios less than one. Steinman's model fits our experimental results well in viscosity ratio ranges between $1.0 \times 10^{-1} - 5.0 \times 10^{1}$.

The above discussion demonstrates that phase inversion is not a straightforward topic. Nonetheless, most studies show that a simple relationship between composition and viscosity ratio can describe the phase inversion composition under some systems and processing conditions.

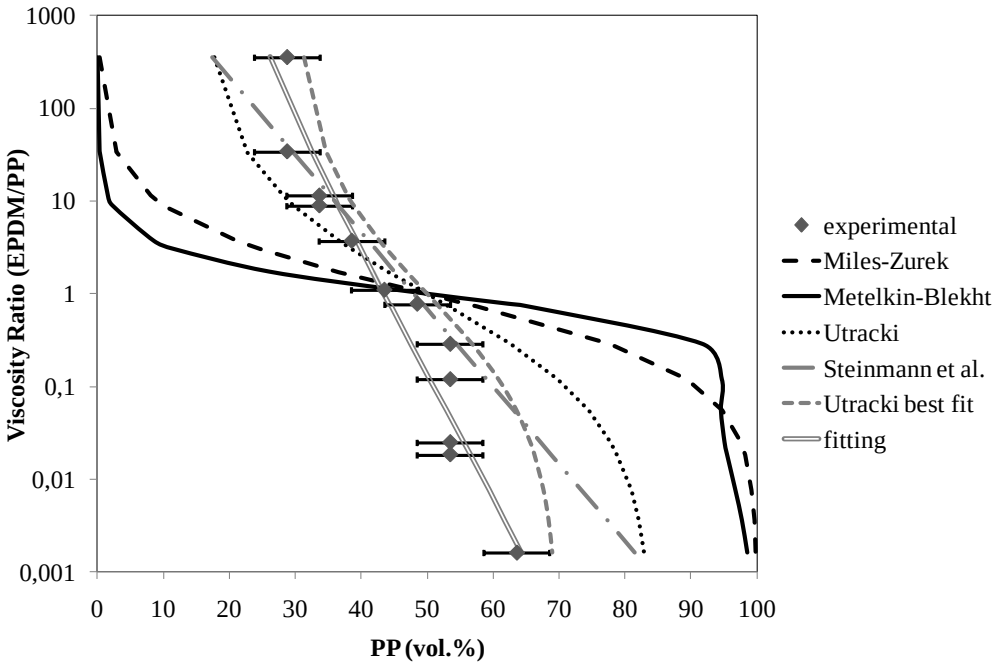

Fig. 4.9. Viscosity ratios of EPDM/PP as a function of vol.% PP based on theoretical predictions and experimental data.

3.6.2. Influence of the elasticity ratio

Experimental data obtained for phase inversion composition were not well described by models based on (mainly low) viscosity ratios.

For each EPDM/PP blend series, the melt elasticity increases with increasing viscosity ratio. Therefore, the effects of the melt elasticity ratio could not be pried apart from the melt viscosity ratio. Consequently, an empirical equation similar to equation (8) can also be achieved using the elasticity ratio. The approach proposed by Bourry and Favis [19] was based on the assumption that the more elastic phase has a propensity to be the matrix. It was apparent that an opposite behaviour would be found by applying this model to the phase inversion composition. The same behaviour was also reported for polystyrene (*PS*)/polymethylmethacrylate (*PMMA*) blends and poly(styrene-co-acrylonitrile (PSAN)/PMMA blends by Steinmann et al. [35].

In the present study, different EPDMs were used to obtain blends of different series at similar viscosity ratios but different elasticity ratios. For example, EPDM6414/PP184 and EPDM1648/PP48 blends have viscosity ratios around 3.5×10^1, but the elasticity ratio is 7.5×10^1 and 1.4×10^2 (Table 4.1), respectively, and the phase inversion composition was estimated to be around 20 and 30 wt.% of PP, respectively. The shift may be attributable to the elasticity ratio because EPDM1647 relative to PP48 is more elastic than EPDM6414

relative to PP184. However, we did not expect a shift of 10 wt.% of PP with EPDM6414 as was observed when comparing EPDM6414/PP2116 and EPDM1648/PP443 blends, which have similar viscosity ratios (3.0 and 3.7, respectively) and elasticity ratios (3.3 and 4.2, respectively). Other examples are shown by the EPDM1647/PP184 and EPDM53/PP4.6 blends with viscosity ratios of 9.0 and 1.1×10^1, respectively, and elasticity ratios of 1.5×10^1 and 2.4×10^2, respectively. Although viscosity ratios for these blends are dissimilar, the variation in elasticity ratios is quite large. Thus, it would be expected a shift in the phase inversion composition to higher PP amounts for the EPDM53/PP4.6 blend. Nevertheless, no variation in the phase inversion composition was found (Fig. 4.9). These results suggest that the elasticity ratio seems to not be an effective indicator to study the influence of elasticity on the phase inversion composition. This agrees with results by Astruc et al. [36]. They studied an immiscible polymer blend of polydimethylsiloxane (PDMS)/hydroxypropylcellulose (HPC) (50/50) and found that phase morphology was not influenced by elasticity ratio variations.

These results suggest that the absolute viscosity and elasticity of blend components play an important role in the phase inversion composition mainly when high viscosity materials are used. Blends made with EPDM53 and EPDM1648, which have similar viscosity ratios, exhibit different morphological development and domain size but have the same composition at phase inversion composition. However, when the highly viscous EPDM6414 was used, the phase inversion composition shifts 10 wt.% when compared to blends with similar viscosity ratios. The most probable explanation seems to be that the high viscosity and elasticity of this EPDM cannot be substantially altered under shear and elongation stresses imposed during processing.

4. Conclusions

EPDM/PP blends with different viscosity ratios and compositions were prepared in a Haake batch mixer under constant processing conditions.

Results obtained by solvent extraction and electron microscopy showed that a large composition range of co-continuity morphologies for EPDM/PP blends exists under a wide range of viscosity ratios. The data suggest that the melt viscosity and elasticity of the major phases are the main parameters that drive the co-continuity region. Different co-continuity ranges were obtained when different EPDMs and PPs with similar viscosities ratios were

used. The co-continuity region was mainly dependent on the EPDM used with the exception of blends made with low molecular weight EPDMs. Using only SEM-BSE micrographs, a narrow co-continuity region was obtained that was used to estimate the phase inversion composition and was therefore determined to be the phase inversion region. The phase inversion region depended both on viscosity ratio and composition.

The experimental results for phase inversion compositions were compared with several empirical models used to predict the phase inversion point using dynamic viscoelastic properties of blend components. By introducing an exponent and a prefactor to modify the general relationship of the composition as a function of the viscosity ratio, the phase inversion composition of the EPDM/PP blends was accurately predicted for a wide range of viscosity ratios.

References

[1] Utracki LA. Polymer Alloys and Blends: Thermodynamics and Rheology. Munich: Hanser Publishers, 1989.

[2] Paul DR. Polymer Blends. Paul DR and Newman S, editors. New York: Academic Press 1978. vol. 2.

[3] Pötschke P, Paul DR. Formation of co-continuous structures in melt-mixed immiscible polymer blends. J Macromol Sci, Part C Polym Rev 2003; 43 (1):87-141.

[4] Avgeropoulos GN, Weissert FC, Biddison PH, Böehm GGA. Heterogeneous blends of polymers. Rheology and morphology. Rubber Chem Techn 1976;49(1):93-104.

[5] Paul DR, Barlow JW. Polymer blends (or alloys). J Macrom Sci, Rev Macromol Chem 1980;C18(1):109-168.

[6] Jordhamo GM, Manson JA, Sperling LH. Phase continuity and inversion in polymer blends and simultaneous interpenetrating networks. Polym Eng Sci 1986;26(8):517-524.

[7] Miles IS, Zurek A. Preparation, structure, and properties of two-phase co-continuous polymers blends. Polym Eng Sci 1988;28(12):796–805.

[8] Utracki LA. On the viscosity-concentration dependence of immiscible polymer blends. J Rheol 1991;35(8):1615–1637.

[9] Favis BD, Chalifoux JP. Influence of composition on the morphology of polypropylene/polycarbonate blends. Polymer 1988; 29(10): 1761–1767.

[10] Steinmann S, Gronski W, Friedrich C. Cocontinuous polymer blends: influence of viscosity and elasticity ratios of the constituent polymers on phase inversion. Polymer 2001;42 (15):6619–6629.

[11] Everaert V, Aerts L, Groeninckx G. Phase morphology development in immiscible PP/(PS/PPE) blends influence of the melt-viscosity ratio and blend composition. Polymer 1999;40(24):6627–6644.

[12] Valenza A, Demma GB, Acierno D. Phase inversion and viscosity-composition dependence in PC/LLDPE blends. Polym Networks Blends 1993;3(1):15–19.

[13] Ho RM, Wu CH, Su AC. Morphology of plastic/rubber blends. Polym Eng Sci 1990;30(9):511–518.

[14] Kitayama N, Keskkula H, Paul DR. Reactive compatibilization of nylon 6/styrene-acrylonitrile copolymer blends: part 1. Phase inversion behaviour. Polymer 2000;41(22):8041–8052.

[15] Tomotika S. On the instability of a cylindrical thread of a viscous liquid surrounded by another viscous fluid. Proc R Soc Lond A 1935;150(870):322-337.

[16] Metelkin VI, Blekht VP. Formation of a continuous phase in heterogeneous polymer mixtures. Coll J USSR 1984;6(3):425-429.

[17] Luciani A, Jarrin J. Morphology development in immiscible polymer blends. Polym Eng Sci 1996;36(12):1619-1626.

[18] Krieger IM, Dougherty TJ. A mechanism for non-newtonian flow in suspensions of rigid spheres. J Rheol 1959;3(1):137-152.

[19] Bourry D, Favis BD. Cocontinuity and phase inversion in hdpe/ps blends: influence of interfacial modification and elasticity. J Polym Sci, Part B: Polym Phys 1998;36(11):1889–1899.

[20] Van Oene H. Rheology of polymer blends and dispersions. In: Polymer Blends, Paul DR, Newman S, editors. San Diego CA: Academic Press, 1978. p.295-352.

[21] Van Oene H. Modes of dispersion of viscoelastic fluids in flow. J Colloid Interface Sci. 1972, 40(3),448–467.

[22] Steinmann S, Gronski W, Friedrich C. Quantitative rheological evaluation of phase inversion in two-phase polymer blends with cocontinuous morphology. Rheol Acta 2002;41:77–86.

[23] Romanini D, Garagnani E, Marchetti E. Reactive blending: structure and properties of crosslinked olefinic thermoplastic elastomers. Int Symp New Polym Mater 1987:56-87.

[24] Abdou-Sabet S, Patel RP. Morphology of elastomeric alloys. Rubber Chem Technol 1991;64(5):769-779.

[25] Bhadane PA, Champagne MF, Huneault MA, Tofan F, Favis BD. Continuity development in polymer blends of very low interfacial tension. Polymer 2006;47(8):2760-2771.

[26] Bhadane PA, Champagne MF, Huneault MA, Tofan F, Favis BD. Erosion-dependant continuity development in high viscosity ratio blends of very low interfacial tension. J Polym Sci Part B: Polym Phys 2006;44(14):1919-1929.

[27] Mighri F, Huneault M. Drop deformation and breakup mechanisms in viscoelastic model fluid systems and polymer blends. Can J Chem Eng 2002;80(6):1028–1035.

[28] De SK, Bhowmick AK. Thermoplastic elastomers from rubber–plastic blends. New York: Ellis Horwood, 1990.

[29] Coran AY, Patel RP. Thermoplastic elastomers based on dynamically vulcanised elastomer/thermoplastic blends. In: Thermoplastic Elastomers, Holden G, Hans RK, Quirk RP, editors, 2nd ed., 1996, Munich: Hanser Publishers. p. 143-181.

[30] Karger-Kocsis J. Thermoplastic rubbers via dynamic vulcanization. In: Polymer blends and alloys, Shonaike GO, Simon GP, editors. New York: Marcel Dekker, 1999. p. 125-153.

[31] Abdou-Sabet S, Puydak RC, Rader CP. Dynamically vulcanized thermoplastic elastomers. Rubber Chem Technol 1996;69(3):476-494.

[32] Galloway JA, Koester KJ, Paasch BJ, Macosko CW. Effect of sample size on solvent extraction for detecting cocontinuity in polymer blends. Polymer 2004;45(2):423-428.

[33] Chung O, Coran AY. The morphology of rubber/plastic blends. Rubber Chem Technol 1997;70(5):781-797.

[34] Cox WP, Merz EH. Correlation of dynamic and steady flow viscosities. J Polym Sci 1958;28(118):619-622

[35] Steinmann S, Gronski W, Friedrich C. Cocontinuous polymer blends: influence of viscosity and elasticity ratios of the constituent polymers on phase inversion. Polymer 2001;42(15):6619–6629.

[36] Astruc M, Navard P. Influence of the elasticity ratio on the point of phase inversion in an immiscible polymer blend. Macromol Symp 2000;149(1):81-86.

Chapter 5: Effect of the Viscosity Ratio on Morphology and Phase Inversion of EPDM/PP TPVs

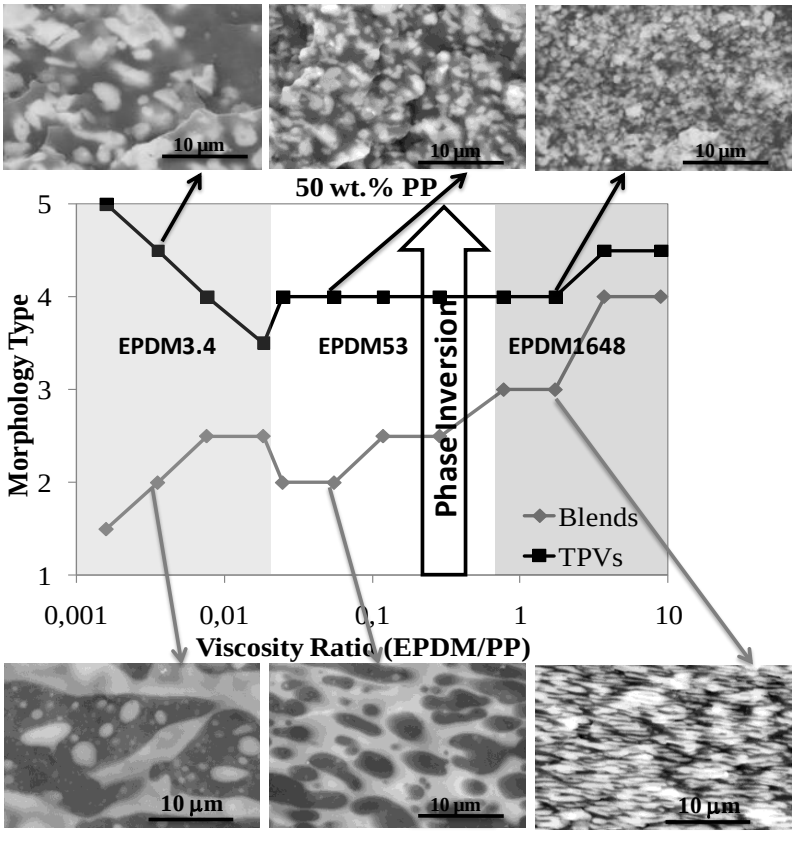

This chapter was submitted to J Polym Sci Part B: Polym Phys.

1. Introduction

It is well-known that dynamic vulcanisation can be used to achieve fine morphologies consisting of high amounts of micro-size cross-linked rubber particles dispersed in a thermoplastic matrix. Generally, the thermoplastic is blended with rubber, and when a homogeneous blend is formed, the rubber is selectively cross-linked under intensive mixing. As a result of cross-linking, the viscosity and elasticity of the rubber phase increases and phase inversion occurs, i.e., the initial morphology consisting of thermoplastic domains dispersed in a rubber matrix change to cross-linked rubber particles dispersed in a thermoplastic phase. The produced material is called thermoplastic vulcanisate (TPV), which is a particular family of thermoplastic elastomers (TPE) with commercial relevance nowadays [1]. These materials are attractive because they combine the melt processability of the thermoplastics and the elastic and mechanical properties of the thermoset cross-linked rubbers [2-4]. This disperse-matrix morphology explains the melt processability of the TPVs. However, the rubberlike properties have been quite difficult to explain with this morphology. It seems that the cross-linked rubber particles physically interact through the finer thermoplastic inter-layers, which appear as a "network" structure [5]. Several studies [6-9] have been performed to understand the deformation behaviour of TPVs. Oderkerk et al. [9] have shown that during elongation of a nylon-6/EPDM-g-MA-based TPV, the thermoplastic matrix deforms progressively but in an inhomogeneous way. This occurs in the thinnest matrix layers at the equatorial region of the rubber particles. The non-deformed matrix layers work as adhesion points keeping the rubber particles together. Upon TPV relaxation, the elastic forces of the elongated rubber draw back the highly deformed matrix layer either by buckling or bending.

The TPVs performance has also been attributed to its fine morphology. TPVs with good properties are only obtained if the rubber is fully vulcanised and the particle size is around 1 μm [10]. Therefore, controlling the final morphology becomes crucial to achieving mechanical performance.

The morphology of non-cross-linked polymer blends has been studied by several authors [11-17]. In the case of ethylene-propylene-diene monomer (EPDM)/polypropylene (PP) blends, which are the most successful systems for TPVs production, it has been demonstrated that EPDM and PP can exhibit co-continuous morphologies in a wide range of compositions and viscosity ratios. D. Romani et al. [13] studied the morphology of EPR/PP blends as a function of composition and melt viscosity ratio. It was shown that at viscosity ratios close to 1, co-

continuity of EPDM/PP blends exists in a broad range of compositions. As the viscosity ratios move away from unity, the composition range of co-continuity becomes narrow and moves to high EPR or PP content, depending on whether the viscosity ratio is higher or lower than 1. In a previous study [18], the morphology of EPDM/PP blends was investigated in detail by solvent extraction and scanning electron microscopy. The results showed that co-continuity exists in a wide range of compositions and viscosity ratios. Moreover, the composition range of co-continuity was practically independent of the viscosity ratio and appears to be more dependent on individual viscosities and elasticities of the EPDM and PP phases.

Since the cross-linking degree also affects the morphology, TPV's morphology is more complex than its corresponding physical blends. It has been suggested that cross-linking undergoes phase inversion during processing independently of the initial blend morphology, i.e., the EPDM phase is dispersed or continuous even at very low PP content [13]. Phase inversion at 80/20 EPDM/PP composition has been reported for the rubber phase with a high degree of cross-linking [19]. However, for EPDM/PE based TPVs with 80/20 composition, Machado et al. [20], found the EPDM cross-linked phase to be a matrix, suggesting that the increase of the viscosity and elasticity of the rubber phase due to dynamic cross-linking was not enough to result in phase inversion. Bouilloux et al. [21] observed that starting from a dispersion of the PE in an EMA matrix and increasing the viscosity of EMA by cross-linking, the morphology became co-continuous. However, EMA dispersed in the PE continuous phase were not achieved. Other studies suggest that the initial morphology of the blend, before cross-linking, plays an important role in the development of the TPV morphology. Radusch et al [22] suggested, for EPDM/PP blends, that obtaining an initial co-continuous morphology is crucial to achieving the desired fine dispersed particle morphology. The initial co-continuous morphology allows for effective shear and elongational stresses in both phases, which is essential to break up the elastomeric phase during dynamic vulcanisation [22]. Oderkerk et al [23], for a nylon6/EPDM based TPV, found that the viscosity of the nylon phase should be low enough to shift phase inversion toward higher rubber content, but at the same time it should not be too low to avoid obtaining a coarse morphology. Joubert et al. [24] showed that the initial viscosity ratio of EVA/PP blends governs the morphological development of the corresponding TPV. According to their results, the viscosity ratio should be close to the value determined by Utracki's model at phase inversion for the corresponding volume fraction. Martin et al. [25] found that cross-linking of PBT/modified E-MA-GMA blends induces an important shift in the phase inversion composition to higher rubber content. The same effect

was observed by Ma et al. [26]. Ma found a shift of the phase inversion composition from 30 – 40 to 70 – 80 wt.% of the elastomer content for PET/E-EA-MA blends.

Despite the large number of studies that have been published concerning the production, morphology, and rheological and mechanical properties of EPDM/PP based TPVs, a systematic study of the influence of the viscosity ratio and composition on the morphology and phase inversion behaviour of the EPDM/PP TPVs is lacking in the literature. The effect of dynamic vulcanisation on the phase inversion location of the EPDM/PP blends is also missing in the literature. Moreover, it remains unknown whether only the increase of the viscosity and elasticity of the elastomeric phase is due to the cross-linking that drives phase inversion and if phase inversion can occur at very low EPDM/PP viscosity ratios. Thus, this study aims to get a better understanding of the phase inversion phenomena of EPDM/PP based TPVs as a function of the viscosity ratio and blend composition. TPV morphological behaviour will be compared with the respective blends that was investigated in a previous paper [18] to comprehend the effect of dynamic vulcanisation on phase inversion of the EPDM/PP blends. Therefore, EPDM/PP blends with different ratios were dynamically vulcanised using a resole cross-linker that was activated by stannous chloride and zinc oxide in a Haake batch mixer. Different viscosity ratios of the EPDM/PP blends were achieved using different rubbers and PPs. Because some of the used materials were not commercially available, it was necessary to prepare them in our laboratory.

2. Experimental

2.1. Materials

In this investigation the EPDM1648, EPDM53, EPDM3.4, PP2116, PP950, PP443, PP184 and PP48 polymers are used. Some characteristic properties of the polymers used (Tables 2.2 and 2.3) and their codes (Table 2.4) are given in part 3 of the Chapter 2.

The cross-linking system was composed by octylphenol–formaldehyde resin (SP1045, Schenectady International, USA) called resole (5 phr), and a combination of stannous chloride ($SnCl_2.2H_2O$) (1.5 phr) and zinc oxide (ZnO) (1.8 phr) as activators (both from Aldrich). Irganox 1076 from Aldrich was used as a stabilizer (0.25 wt.% relative to the total amount of polymer (EPDM and PP)).

The rheological characterisation of the PP and EPDM polymers was carried out on a stress-controlled rotational rheometer as described in the Chapter 2, part 3.3. The ratios of the viscosity and storage modulus of the EPDM/PP blends are provided in Table 5.1.

Table 5.1. Viscosity and storage modulus ratios of EPDM/PP blends (65 s^{-1} and 200ºC).

Blend name EPDM/PP	**Viscosity ratio**	**Storage modulus Ratio**
1648/2116	7.8×10^{-1}	6.6×10^{-1}
1648/950	1.7	1.6
1648/443	3.7	4.2
1648/184	9.0	1.5×10^{1}
1648/48	3.4×10^{1}	1.4×10^{2}
53/2116	2.5×10^{-2}	7.3×10^{-3}
53/950	5.6×10^{-2}	1.8×10^{-2}
53/443	1.2×10^{-1}	4.6×10^{-2}
53/184	2.9×10^{-1}	1.6×10^{-1}
3.4/2116	1.6×10^{-3}	1.1×10^{-4}
3.4/950	3.6×10^{-3}	2.6×10^{-4}
3.4/443	7.7×10^{-3}	6.8×10^{-4}
3.4/184	1.9×10^{-2}	2.4×10^{-3}

2.2. Compositions

EPDM/PP - TPVs were prepared using different EPDM and PP grades and at different EPDM/PP weight ratios, which are shown in a general scheme in Fig. 5.1. TPVs of EPDM1648/PP48 and EPDM53/PP184 with 30 and 40 wt.% of PP, respectively were also prepared. In total, 38 EPDM/PP blends were dynamically vulcanised. The amount of cross-linked chemicals was kept constant relative to the amount of EPDM. The amount of stabilizer was kept constant relative to the total quantity of polymers (EPDM plus PP). The compositions, in weight percentage of the components, are presented in Table 5.2.

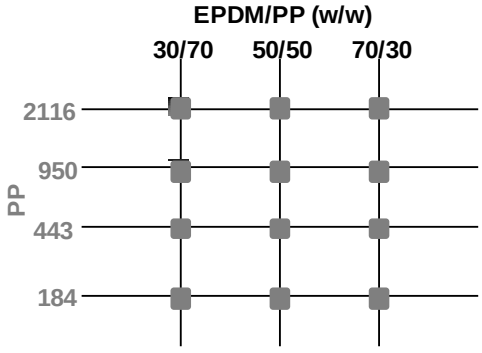

Fig. 5.1. Scheme of the experimental plan.

Table 5.2. Composition of the EPDM/PP-based TPVs.

Coding (wt. % PP)	EPDM	PP	Irganox	ZnO	Resole	$SnCl_2$
70	29.20	68.13	0.24	0.53	1.46	0.44
50	47.89	47.89	0.24	0.86	2.39	0.72
40	57.02	38.01	0.24	1.03	2.85	0.86
30	66.00	28.29	0.24	1.19	3.30	0.99

2.3. TPV Preparation

TPVs were prepared in an internal mixer under the same conditions, 80 rpm rotor speed and a set temperature of 200 ºC. The following mixing sequence was used. First, PP pellets were introduced into the hot mixer. After melting of the PP phase, the stabilizer, Irganox 1076, was added and then the EPDM rubber was mixed in. The torque reached a constant value, after about 3 minutes, indicating the formation of a homogenous melt. Next, the ZnO, resole and $SnCl_2.2H_2O$ were added in this order (which took about 5 s with time zero being the instant $SnCl_2.2H_2O$ was added). After an additional 300 s of mixing, the sample was removed and cooled down between two metal plates to stop the cross-linking reaction and to avoid further morphological changes.

2.4. Sample Characterisation

Extractions using boiling xylene were used to determine the EPDM gel content as a measure for the cross-link density of the EPDM phase. Approximately 500 mg of TPV was weighted and placed in an 80-mesh stainless steel pouch. The cage was also weighted and then immersed in boiling xylene for 48 h. After drying the sample in a vacuum oven at 100 °C for 12 h with nitrogen purging, the weight was determined. The EPDM gel content was calculated assuming that the residue consisted of insoluble cross-linked EPDM and resole and corrected for the presence of ZnO.

The morphology was studied by scanning electron microscopy in the back-scattering mode (SEM-BSE) using a Leica Scanning Electron Microscope. Previously, the samples were fractured in liquid nitrogen and vapor-stained with ruthenium tetroxide for 120 minutes. In the case of TPVs made with the highly viscous EPDM (EPDM1648), morphology was also characterised by TEM using a Philips CM120 Transmission Electron Microscope (TEM). Samples were cryomicrotomed to 100 nm thin sections at -130 ºC and were then vapor-stained with ruthenium tetroxide for 20 minutes.

3. Results and Discussion

In regard to the phase morphology, the location and width of the phase inversion of the EPDM/PP blends were previously studied in Chapter 4. Thus, in the present Chapter, the results of the EPDM/PP blends morphologies will be used to better understand the effect of dynamic vulcanisation on morphology and on phase inversion of TPVs.

3.1. Torque and Temperature

Fig. 5.2 shows the torque and temperature behaviour as a function of the mixing time of an EPDM53/PP443 blend and respective TPV with 50 wt.% PP. The first and second peaks observed in each torque curve are related to the loading of PP and EPDM, respectively. After that, the torque reaches a more or less constant value, indicating complete melting of PP and full homogenization of the EPDM/PP blend. Then, the torque of the physical blend decreases slowly until the end of mixing. Meanwhile, the torque of the TPV decreases after the addition of the phenolic resin, due to its lubricating effect after melting, and then it increases abruptly. This is related to drastic changes in the viscosity and elasticity of the EPDM phase due to cross-linking. After going through to a maximum, the torque of EPDM53/PP443 TPV reaches a plateau much higher than that of the EPDM53/PP443 blend and it remains more or less constant until the end of mixing.

Both temperature curves exhibit a decrease when the polymers were fed in due to the introduction of a cold mass in the hot mixer and the melting of PP. Upon addition of EPDM, a continuous increase over the set temperature, 6 ºC for the blend and 12 ºC for the TPV, was observed. The temperature increase is due to viscous dissipation, which is enhanced in the case of the TPV due to cross-linking of the EPDM phase. Both torque and temperature curves are similar to those reported in other studies for dynamic vulcanisation of EPDM/PP blends [1, 22, 27-29].

Even though the torque and temperature curves of the others, EPDM/PP blends and TPVs prepared in this study have shown similar behaviour, the torque level is quite dependent on the EPDM and PP used and, of course, on the dynamic vulcanisation occurrence. As an example, the mixing torque at end of the EPDM1648/PP443 and EPDM3.4/PP443 blends and TPVs is depicted in Fig. 5.3, at different EPDM/PP weight ratios. As expected, the EPDM1648/PP443 blend torque increases and EPDM3.4/PP443 blend torque decreases as the EPDM content increases, because PP443 is less viscous than EPDM1648 and more viscous than EPDM3.4. For both EPDMs, the torque of their respective TPVs is always higher than

those of the respective blends, as is predictable due to cross-linking of the EPDM phase. The differences are less significant between the EPDM3.4/PP443 blend and its respective TPV.

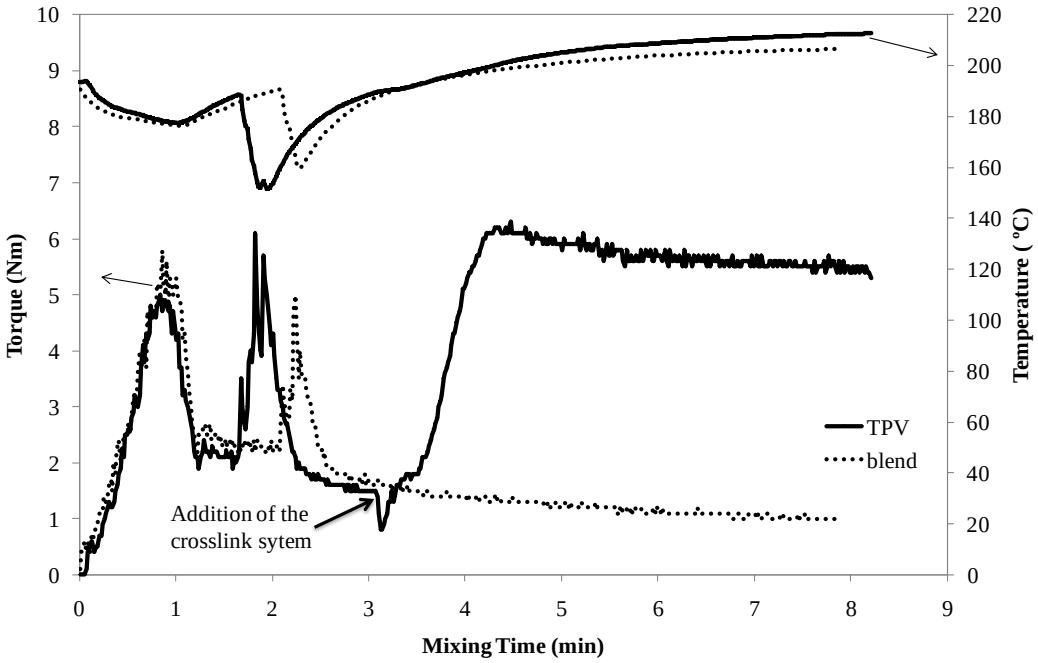

Fig. 5.2. Torque and temperature curves of the EPDM53/PP443 with 50 wt. % PP as a function of mixing time.

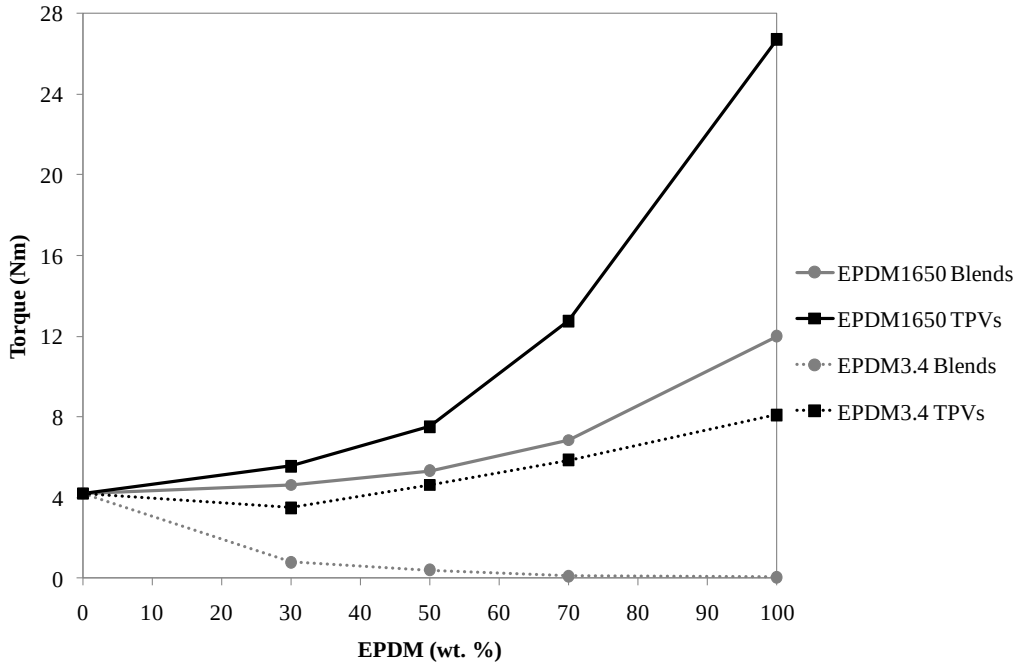

Fig. 5.3. End torque as a function of EPDM (wt. %) for blends and TPVs of EPDM1648/ PP443 and EPDM3.4/PP443.

3.2. EPDM Gel Content

Fig. 5.4 depicts the EPDM gel content of the prepared EPDM/PP TPVs as a function of the EPDM wt.%. The EPDM gel content of the EPDM/PP blends was also measured, being 0 % for all blends. This would be expected, once no cross-linking agents were added, both EPDM and PP completely dissolved in boiling xylene. In case of the EPDM/PP TPVs, the residue consisted of cross-linked EPDM, resole and ZnO. Thus, the determined EPDM gel content will allow for a fair comparison of the cross-link degree of the TPVs with different compositions.

The gel content of EPDM1648/PP TPVs decreases as the amount of EPDM increases (Fig. 5.4a). An exception is noted for EPDM1648/PP184 TPV with 50 wt.% of EPDM. Moreover, for the TPVs with 30 and 50 wt.% EPDM, the gel content increases as the PP viscosity decreases. The decrease of EPDM gel content was shown in a recent study [29] to be related with EPDM (network) degradation, which occurs during the preparation of TPVs made with EPDM1648. The degradation of the EPDM (network) was related to the action of shear and elongation stresses under high temperature, being cross-linking and degradation competing processes. It was also shown that degradation is enhanced if the EPDM phase is the matrix before cross-linking takes place. Therefore, the level of cross-linking obtained is also an outcome of the blend morphology, which varies with composition and PP viscosity [29].

For TPVs made with the low viscosity EPDMs (EPDM53 and EPDM4.3), the EPDM gel content tends to increase as the EPDM amount increases (Fig. 5.4b and 5.4c), suggesting that EPDM (network) degradation during dynamic vulcanisation does not occur. Since the amount of cross-linking chemicals was kept constant relatively to the EPDM amount, similar cross-linking levels would be expected independently of the TPV composition. The slightly higher values obtained for EPDM-rich compositions can be related to the location of the cross-linking system. For these compositions the cross-linking system will be initially in the EPDM phase and does not have to migrate through the PP matrix. Consequently, it is able to react immediately with the rubber resulting in higher of cross-linking degrees.

Comparing the cross-linking levels of the TPVs with EPDM1648 with those made with the low viscosity EPDMs (EPDM53 and EPDM3.4) at 30 wt.% of EPDM, lower levels were obtained for the low molecular weight EPDMs. This is in accordance with the results obtained by Sabet et al.[15], low cross-linking levels were achieved with the low Mw EPDM.

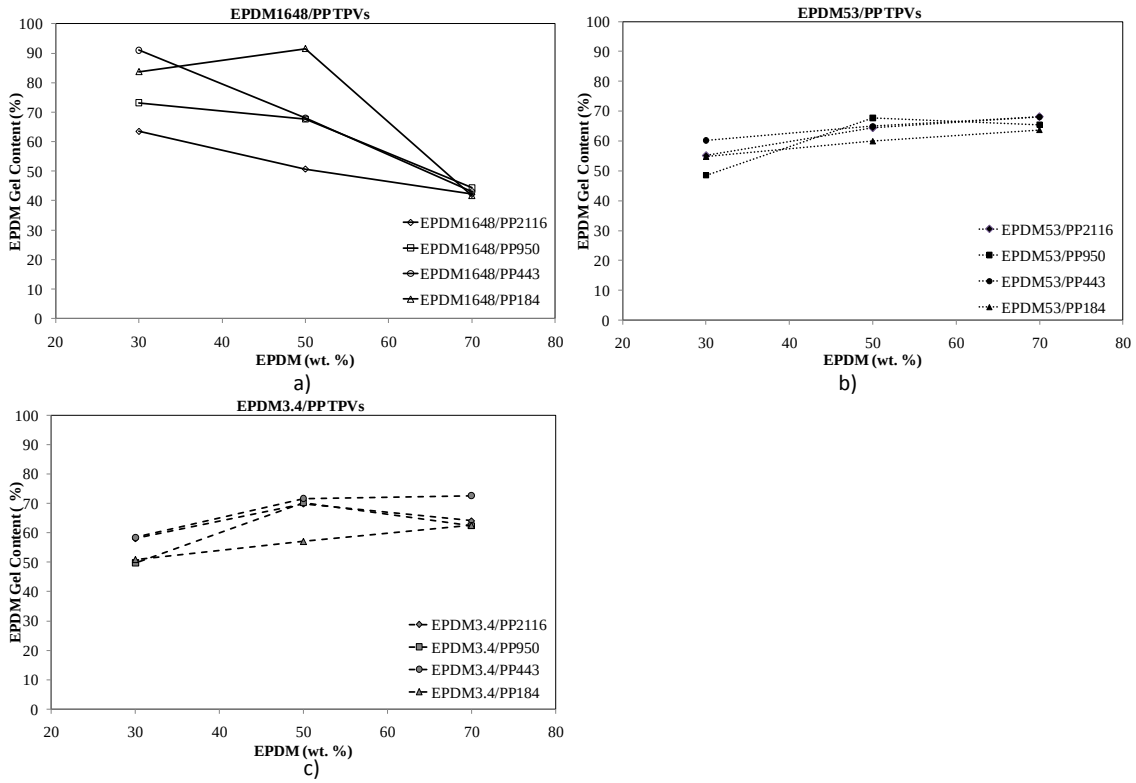

Fig. 5.4. EPDM gel content as a function of composition for various TPVs: a) EPDM1648/PP; b) EPDM53/PP c) EPDM4.3/PP.

3.3. Morphology

It is difficult to provide high-quality micrographs of EPDM/PP based TPV due to their similar chemical nature and the very low interfacial tension between both polymers. Moreover, the TPVs morphology consists of irregular shaped rubber particles, which can hardly be distinguished from each other due to the low interfacial tension and/or microscopy artefacts [20]. Usually, a TPV's morphology is studied by transmission electron microscopy (TEM) because it provides high-resolution images that allow details of the microstructure to be obtained, which cannot be given by other techniques like SEM, LVSEM and AFM [27]. However, SEM-BSE allows one to distinguish the EPDM and PP phases of a TPV when the samples are previously stained with ruthenium tetroxide. This technique has been successfully applied to TPVs, mainly in case of the TPVs made with low Mw EPDMs.

The morphology of the binary blends can consist of matrix-dispersed particles and co-continuous structures. Nevertheless, blends morphologies have been observed in an intermediate state between being fully dispersed and co-continuous [30-33]. To distinguish the morphologies obtained and make a fair comparison between the morphologies of the blends and correspondent TPVs, the morphologies were classified into different types

according to the description in Table 5.3. Often, values in the middle were also used to better distinguish the different morphologies obtained. As an example, Fig. 5.5 shows the micrographs of the EPDM/PP blends classified according to their morphology type as described in Table 5.3.

Table 5.3. Morphology type.

Type	Designation	Description
1	Matrix	PP is clearly dispersed in the EPDM matrix
2	Partially continuous	PP is dispersed with continuous domains in the EPDM matrix
3	Fully co-continuous	PP and EPDM are both continuous
4	Partially dispersed	EPDM is dispersed with continuous domains in the PP matrix
5	Dispersed particles	EPDM is clearly dispersed in the PP matrix

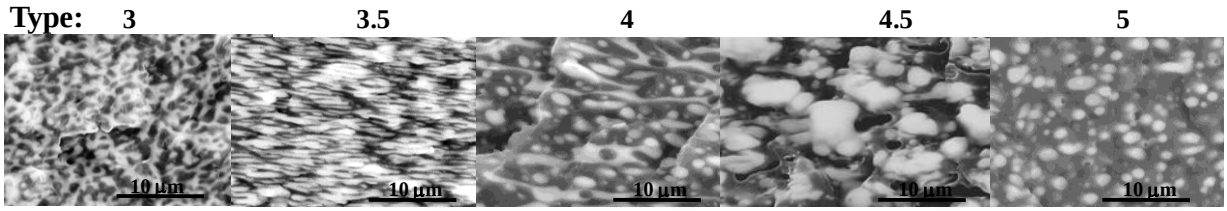

Fig. 5.5. SEM-BSE micrographs of the EPDM/PP blends and the corresponding morphology type.

3.3.1. TPV morphology

Figs. 5.6, 5.7 and 5.8 show the BSE-SEM micrographs of the TPVs with 30, 50 and 70 wt.% PP, respectively. Due to the large distribution of the EPDM domain size obtained for TPVs with the lowest viscosity EPDM, low magnification SEM-BSE micrographs are also depicted. Also, TEM micrographs of the EPDM1648/PP2116 and EPDM1648/PP184 TPVs are shown, due to the micro-size of the cross-linked EPDM particles of the TPVs made with the high viscosity EPDM, EPDM1648. In the SEM-BSE micrographs, EPDM is noted as light domains and PP as dark domains, in TEM micrographs is the opposite. The viscosity ratios of the EPDM/PP-blends given in Table 2 will be used to discuss the TPVs morphologies. The average diameter of the cross-linked EPDM particles as a function of their viscosity ratio is shown in Fig. 5.9 for TPVs with 30 and 50 wt. % of PP. Because the cross-linked EPDM particles sometimes appear overlaid, it became difficult to find the particle's limit. Therefore, the average diameter of cross-linked EPDM particles was calculated from the mean diameter

of 50 “isolated” particles at least. In case of the TPVs with 30 wt.% PP, the complex morphologies obtained did not allow us to measure the domain size.

EPDM1648/PP TPVs morphologies with 30 wt.% PP (Fig. 5.6) seem to be co-continuous, which is confirmed by the TEM micrographs acquired for TPVs made with PP2116 and PP184. However, the cross-linked EPDM phase seems to become more dispersed as the PP viscosity decreases, i.e., EPDM/PP viscosity ratio increases (Table 5.2). This can be ascribed to the propensity of the low viscosity PP to become a continuous phase. Opposite behaviour is observed for TPVs made with EPDM53 and EPDM3.4. The rubber becomes less dispersed as the PP viscosity decreases. Even so, the EPDM domain size distribution became rather heterogeneous as shown in the low magnification micrographs of the EPDM3.4/PP184 and EPDM3.4/PP2116 TPVs (Fig. 5.6). Because the gel content is similar (Fig. 5.4) around 67 ± 5 wt. % for all TPVs with low viscosity EPDMs at 30 wt.% of PP, this parameter is not relevant to the discussion. Thus, for the TPVs made with low viscosity EPDMs, the viscosity and elasticity of the PP phase seems to have a larger effect on TPV morphology than the viscosity ratio of the EPDM/PP blend. For the PPs and EPDMs used, the more viscous polymer is also the more elastic one, because the storage modulus increases as the complex viscosity increases (Table 2). Thus, for the EPDM53 and EPDM3.4 TPVs series, as the elasticity of the PP phase increases, the tendency of the PP phase to encapsulate the less elastic EPDM phase also increases, which could explain why the cross-linked EPDM phase becomes more dispersed as the PP viscosity increases. Therefore, phase inversion seems to be driven by cross-linking and PP elasticity when a large difference in the melt elasticity between PP and EPDM exists.

Comparing the TPVs made with the same PP but different EPDM, a refinement of the morphology was noticed as the viscosity of the EPDM phase increased. For the EPDM-rich composition, blend viscosity is governed by the EPDM phase. Consequently, in the high viscosity systems, the shear and elongational stresses acting in the system are higher. As a result, smaller particles are obtained. However, the EPDM phase seems to become more dispersed as the viscosity difference between the EPDM and PP phase increases.

It has been reported [19] that even at 20 wt.% PP, by dynamic vulcanisation of EPDM/PP blends, the rubber can be dispersed in the continuous PP phase. However, this was not observed in the present work. EPDM/PP TPVs with 30 wt.% PP exhibit co-continuous morphologies, the exception is the EPDM3.4/PP2116 – TPV with a very low viscosity ratio. A reasonable explanation might be the low EPDM gel content obtained, which does not allow

for a complete phase inversion process to occur and co-continuous morphologies are achieved instead.

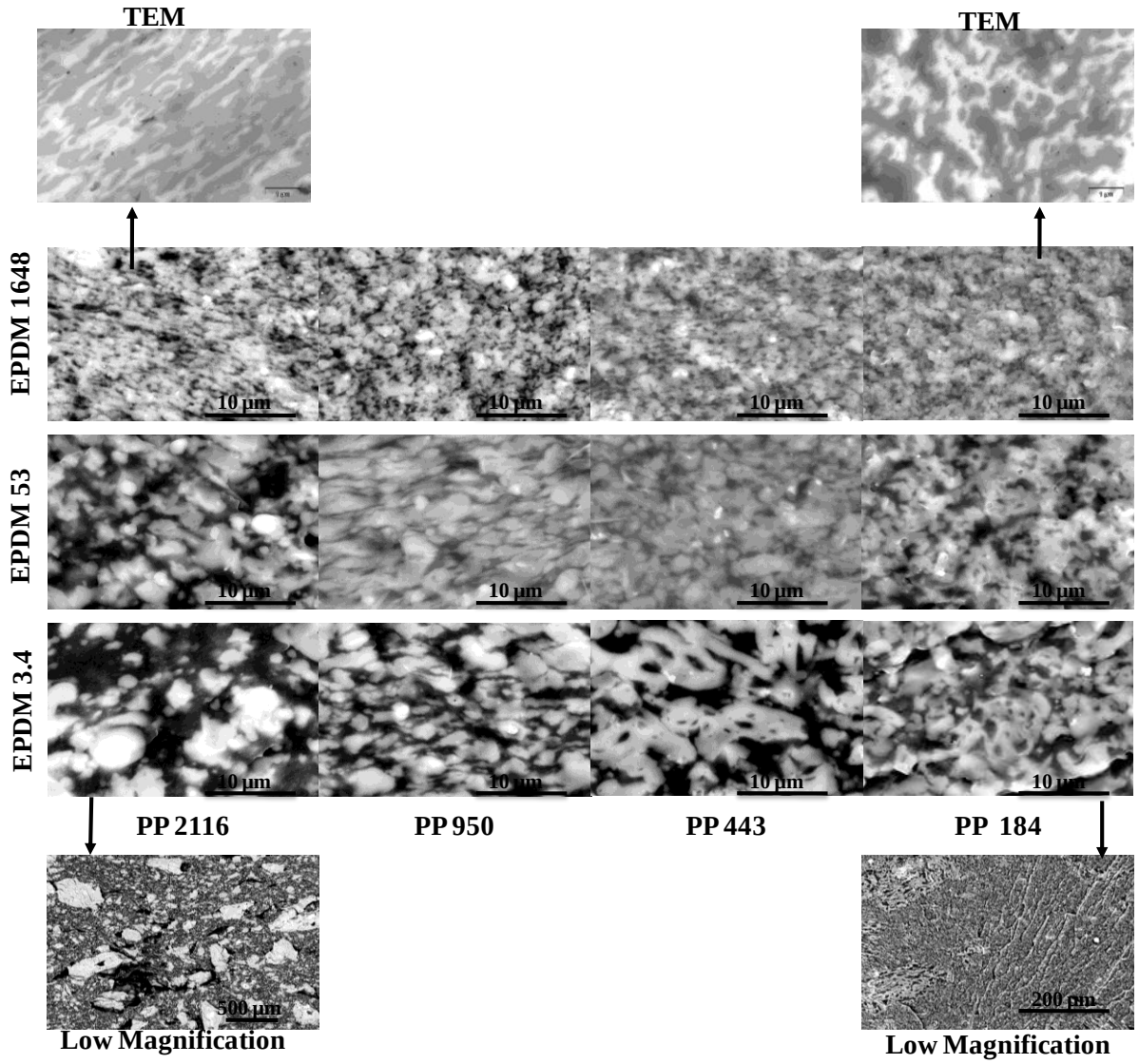

Fig. 5.6. Micrographs of TPVs prepared with 30 wt.% PP.

TEM and SEM-BSE micrographs of the TPVs with 50 wt.% PP are depicted in Fig. 5.7. For the EPDM1648/PP TPVs, the morphology consists of rubber particles dispersed in the PP continuous phase. By SEM-BSE, the EPDM particles seem to be linked, but TEM micrographs show that they are separated by a thin PP layer. The EPDM domains in EPDM1648/PP2116 - TPV are quite irregular and several EPDM particles are interconnected. Conversely, for the EPDM1648/PP184 -TPV the EPDM domains are more spherical and dispersed in the PP matrix. Nevertheless, the average diameters of the EPDM domains is approximately the same for all TPVs made with EPDM1648 (50 wt.% PP), as is shown in Fig. 5.9 (see the last four points in black), being 0.6 in the range of 0.3 – 1.4 µm for

EPDM1648/PP2116 - TPV and 0.7 raging from 0.3 - 1.6 μm for EPDM1648/PP184 -TPV. A major effect of the viscosity ratio, or the decrease in PP viscosity on the cross-linked EPDM domain size would be expected. However, the EPDM gel content values explain the observed results. The EPDM gel content increases as the PP viscosity decreases (Fig. 5.4), being around 50 and 90 % for EPDM1648/PP2116 and EPDM1648/PP184 TPVs, respectively, and around 68 % for the TPVs in the middle. This explains the more spherical particles obtained for EPDM1648/PP148-TPV, because higher cross-linking degrees result in less deformable particles.

Because the determined EPDM gel content was quite similar for TPVs prepared with the low viscosity EPDMs (EPDM53 and EPDM3.4), the cross-linking degree will not be taken into account when discussing the morphology. For both series EPDM53/PP and EPDM3.4/PP TPVs, the cross-linked EPDM domains are dispersed in the PP matrix. In the case of EPDM53/PP - TPVs, the EPDM domain size increases as the PP viscosity decreases. These results can be confirmed by average diameter measurements (Fig. 5.9). The EPDM53/PP2116 TPV has an average diameter of 1.2 in and a range of 0.3 - 2.7 μm Then, it increases slightly until the EPDM53/PP443 – TPV and the EPDM53/PP184 have the highest value of 2.8 μm in the range of 0.6 – 4.7 μm. This is quite unexpected because the viscosity ratio becomes closer to unity as the PP viscosity decreases. Probably, the high viscosity PP enhances the shear and elongation stresses applied to the EPDM phase during dynamic vulcanisation. As a result, a better dispersion is obtained. Opposite behaviour is noticed for the EPDM3.4/PP – TPVs series, where the domain size and the heterogeneity of the domain size distribution of the rubber particles increases as the PP viscosity increases. The average diameter of the EPDM3.4/PP2116 is 13 in a range of 0.3 – 120 μm. Then, it decreases significantly to 2.9 μm (0.7 – 10.5 μm) for the EPDM3.4/PP950 - TPV and decreases slightly to 2.1 μm (0.5 – 5.1 μm) for the EPDM3.4/PP184 -TPV. This can be explained by the large differences between the viscosities of the EPDM and PP phases.

As mentioned before, for the EPDM3.4/PP - TPV with 30 wt. % PP, because PP2116 is much more elastic than EPDM3.4, it tends to encapsulate the EPDM phase. Therefore, in this case, phase inversion is not only driven by cross-linking but also by the high elasticity of the PP phase. Another reason could be the initial blend morphology, which has an effect on the final TPV morphology. For the EPDM3.4/PP2116 blend, PP is dispersed in the EPDM matrix, whereas for the other EPDM3.4/ PP blends, a co-continuous morphology was achieved [18]. Therefore, in the initial stages of cross-linking, the viscosity of the EPDM3.4/PP2116 - TPVs is governed by the low viscosity EPDM3.4 matrix. The applied shear forces are smaller than

in the case of the other TPVs, which in the initial stages have co-continuous morphologies. This might also have contributed to the poor dispersion obtained for EPDM3.4/PP2116 – TPVs.

The shape of the cross-linked EPDM particles of the TPVs with the low viscosity rubbers are quite irregular, suggesting that the cross-linked EPDM particles are deformable, which is a consequence of the low cross-link degree achieved, which is in agreement with the results obtained by Deyrail et al [34].

Comparing the TPVs with the same PP but different EPDMs, a refinement of the morphology is achieved as the EPDM viscosity increases. Again, as for TPVs with 30 wt. % of PP, it can be related to the shear and elongational stresses applied, which decrease as the blend viscosity decreases.

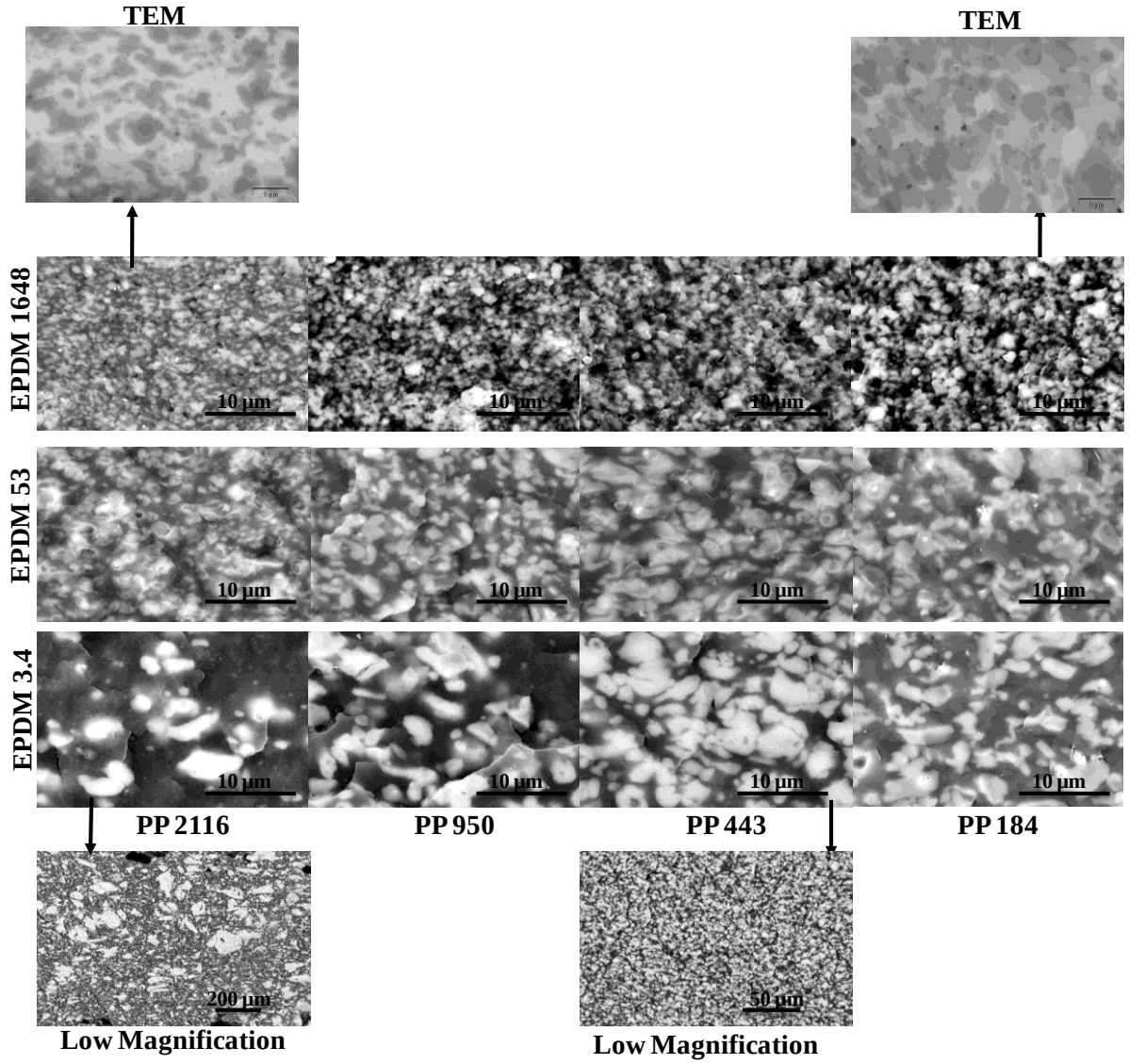

Fig. 5.7. Micrographs of the TPVs prepared with 50 wt. % PP.

For EPDM/PP - TPVs with 70 wt. % PP, the morphology consists of EPDM particles dispersed in the PP matrix, as can be observed in Fig. 5.8. In a general way, the cross-linked EPDM domain size increases as the PP viscosity decreases, with the exception of EPDM3.4/PP2116 - TPV. In case of the EPDM1648/PP – TPVs the cross-linking degree increased as the PP viscosity decreased (Fig. 5.4), being 63 and 84 wt. % for TPV with PP2116 and PP184, respectively. This suggests that the high viscous PP matrix has a major effect on the dispersed phase particle size, rather than the cross-linking degree. For TPVs prepared with EPDM53 and EPDM3.4, the cross-linking degree is more or less the same (gel content around 55 ± 5 %), which corroborates that the viscosity and elasticity of the PP phase are the major parameters that control the domain size of the cross-linked EPDM particles for each TPVs series (TPVs made with the same EPDM). The exception to this behaviour is the EPDM3.4/PP2116 - TPV, which presents the largest domain size (Fig. 5.10). A possible explanation could be the low shear applied in the initial stage of mixing (very low torque values were observed), suggesting that the EPDM phase was the matrix in the early stages of cross-linking, thus avoiding a good dispersion of the EPDM phase during cross-linking. Besides, the poor dispersion is consistent with the very low viscosity ratio of the blend. Again, the EPDM domains size of TPVs with the same PP decreased as the EPDM viscosity increased (Fig. 5.9) as observed for TPVs with 50 wt. % PP. However the cross-linked EPDM particles tended become agglomerated as the viscosity of the EPDM phase increased.

According to published studies [5, 15, 22], fine TPVs morphologies can be achieved at high EPDM/PP ratios if the viscosity ratio of the EPDM/PP blend is around 1 and both phases are co-continuous. Although complete phase inversion was not achieved for EPDM/PP TPVs with 30 wt. % PP, the results of TPVs with 50 wt. % PP show that the finest morphologies are obtained at viscosity ratios around 1. However, relatively fine morphologies were also achieved at low viscosity ratios (between 0.01 and 0.1) using high viscosity PP phases. Contrary to the suggestion made by Wright et al. [35], a slight increase in the particle size was observed as the PP viscosity decreased.

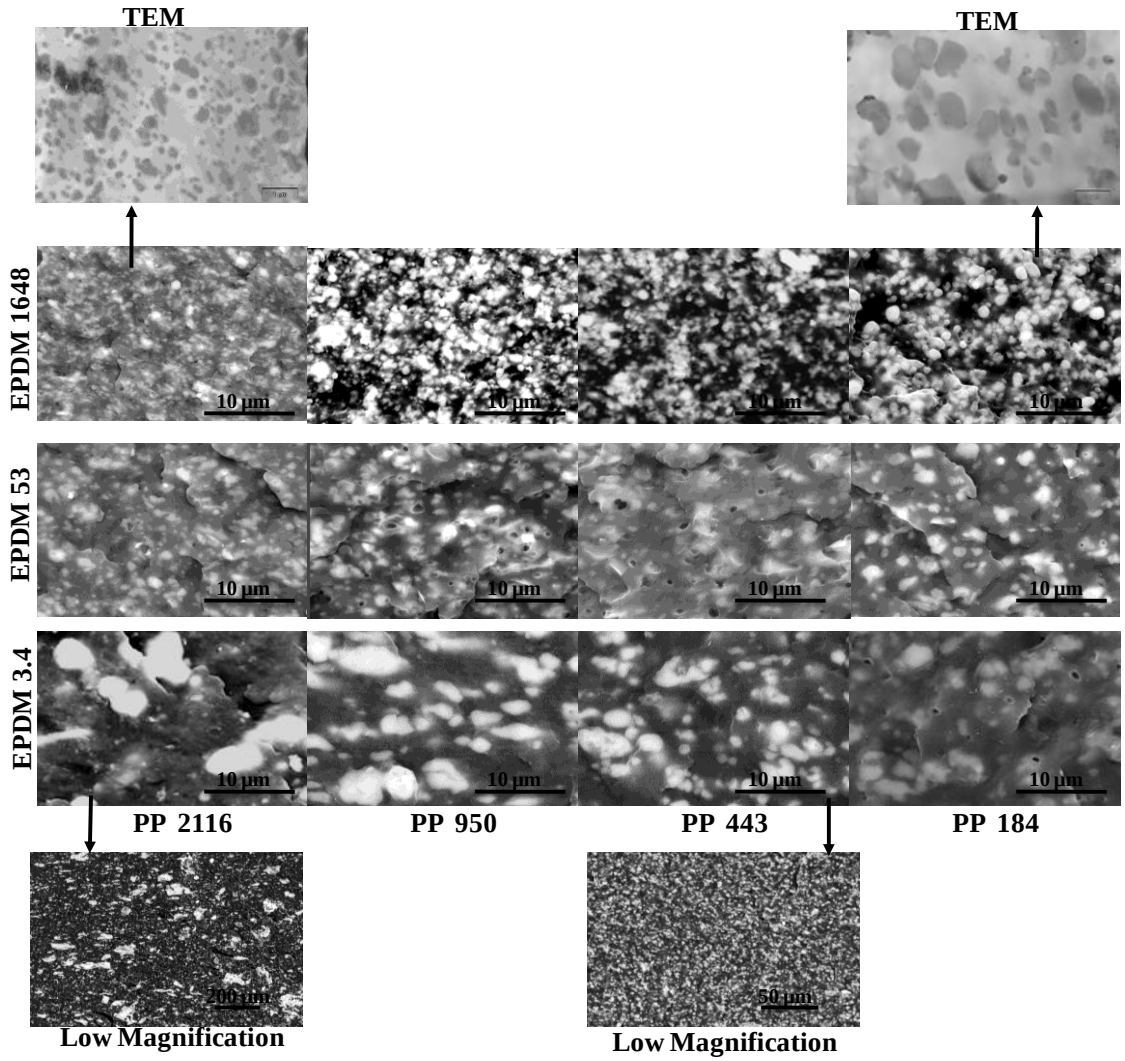

Fig. 5.8. Micrographs of TPVs prepared with 70 wt.% PP.

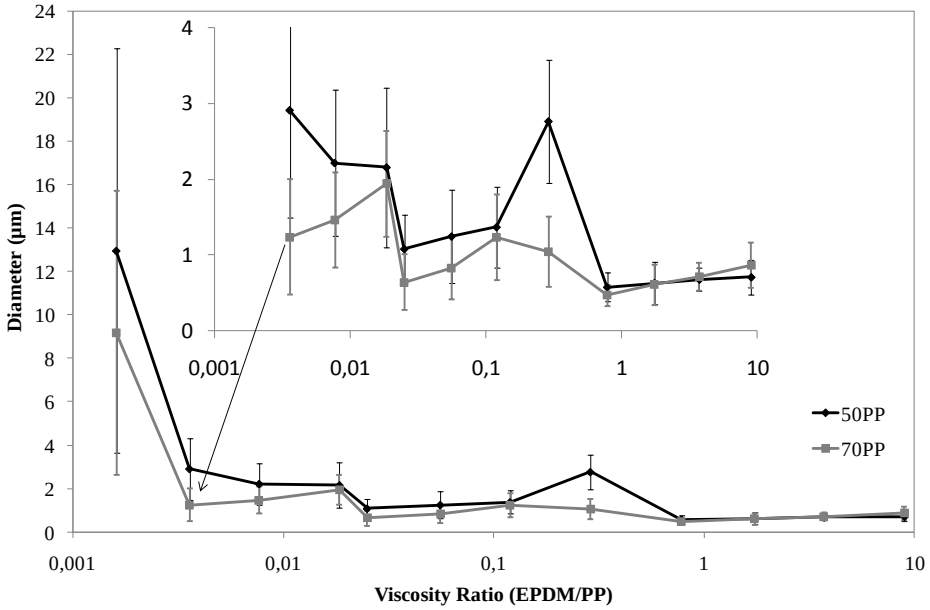

Fig. 5.9. Average diameter of the cross-linked EPDM particles in TPVs with 50 and 70 wt.% PP.

3.3.2. Effect of cross-linking on the domain size of the EPDM particles

The data obtained indicate that dynamic vulcanisation leads to a stable and homogeneous morphology with EPDM particles mainly dispersed in the PP matrix for EPDM/PP – TPVs with a PP amount higher than 30 wt.%. To evaluate the effect of dynamic vulcanisation on the shape and size of the EPDM phase, the blends and TPVs morphologies of EPDM/PP with 70 wt.% of PP will be compared. As an example, the morphologies of EPDM53/PP blends with 70 wt.% of PP are depicted in Fig. 5.10. The EPDM/PP blend morphologies are quite heterogeneous. A mixture of strongly elongated, elongated and more spherical domains are observed, with the exception of the EPDM53/PP184 blend, where the particles are more spherical. In a general way, EPDM particles become more spherical as the PP viscosity decreases. Comparing the micrographs of the blends with the respective TPVs (Fig. 5.8), it can be seen that the shape of the cross-linked EPDM particles are more regular and spherical, independent of the PP viscosity.

The average diameter as a function of the viscosity ratio is depicted in Fig. 5.11. The smaller error bars associated to the TPVs values might indicate that the morphology is more homogeneous than the respective blends. In a general way, TPVs have a smaller domain size, with the exception of the EPDM3.4/PP2116 system, where the particle size increases. It can also be observed that sometimes the average size of the EPDM particles are quite similar to the average size of the respective cross-linked EPDM particles, mainly at viscosity ratios lower than one with the high viscosity PPs. This can be related to the low viscosity of the EPDMs (EPDM53 and EPDM3.4) phase, which can be strongly deformed and break into very small particles (Fig. 5.11). For TPVs with EPDM1648, the domain size of TPVs is more independent of the viscosity ratio, contrary to the respective blends.

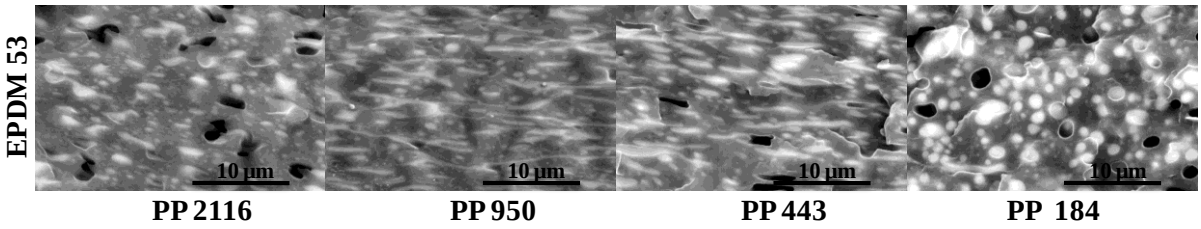

Fig. 5.10. SEM-BSE of EPDM53/PP blends with 70 wt. %.

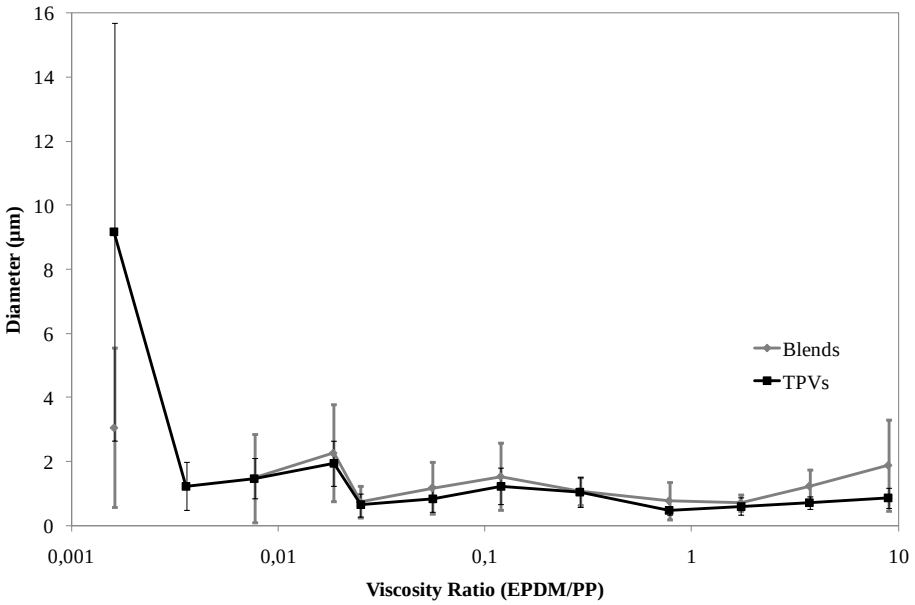

Fig. 5.11. Average diameter as a function of viscosity ratio, for EPDM/PP blends and TPVs with 70 wt. %.

3.3.3. Effect of cross-linking on phase inversion of EPDM/PP blends

EPDM/PP blends and TPVs were classified using the morphology type defined in Table 4.3. The diagrams of the morphology type as a function of viscosity ratio are depicted in Figs. 5.12a, 5.12b and 5.12c, which allows one to evaluate the effect of cross-linking on phase inversion of the EPDM/PP blends. The grey lines represent the blends and the black lines the TPVs. The morphology type, in general, increases with cross-linking and it becomes closer for blends and their respective TPVs as the viscosity ratio increases. Although a large range of viscosity ratios were used, EPDM/PP blends do not exhibit morphology type 1. Morphology type 5 is achieved for several EPDM/PP blends and TPVs with 70 wt.% of PP. For PP amounts lower than 70 wt.%, only the EPDM3.4/PP2116 TPV with 50 wt.% of PP achieved morphology type 5.

For EPDM-rich compositions with 30 wt.% PP, dynamic vulcanisation was not enough to turn the EPDM's continuous phase into the dispersed phase. Therefore, co-continuous morphologies (type 3) were mainly achieved.

For 50/50 composition, in most of the cases, PP is the continuous phase in the blend. After dynamic vulcanisation, the cross-linked EPDM was not full dispersed in the PP phase. Only the EPDM3.4/PP2116 system underwent practically complete phase inversion. The morphology changes from type 1.5 to 5.

For EPDM/PP blends with 70 wt. % PP, the morphologies type are between 4 and 5 and thus blends and TPVs have almost the same phase morphology.

The results demonstrate that, even though dynamic vulcanisation induces significant changes in morphology, a complete phase inversion process (i.e., change the morphology type from 1 to 5) is hardly achieved. Nevertheless, as morphology changes from type 2 to 4 it is considered that phase inversion as a result of cross-linking occurred.

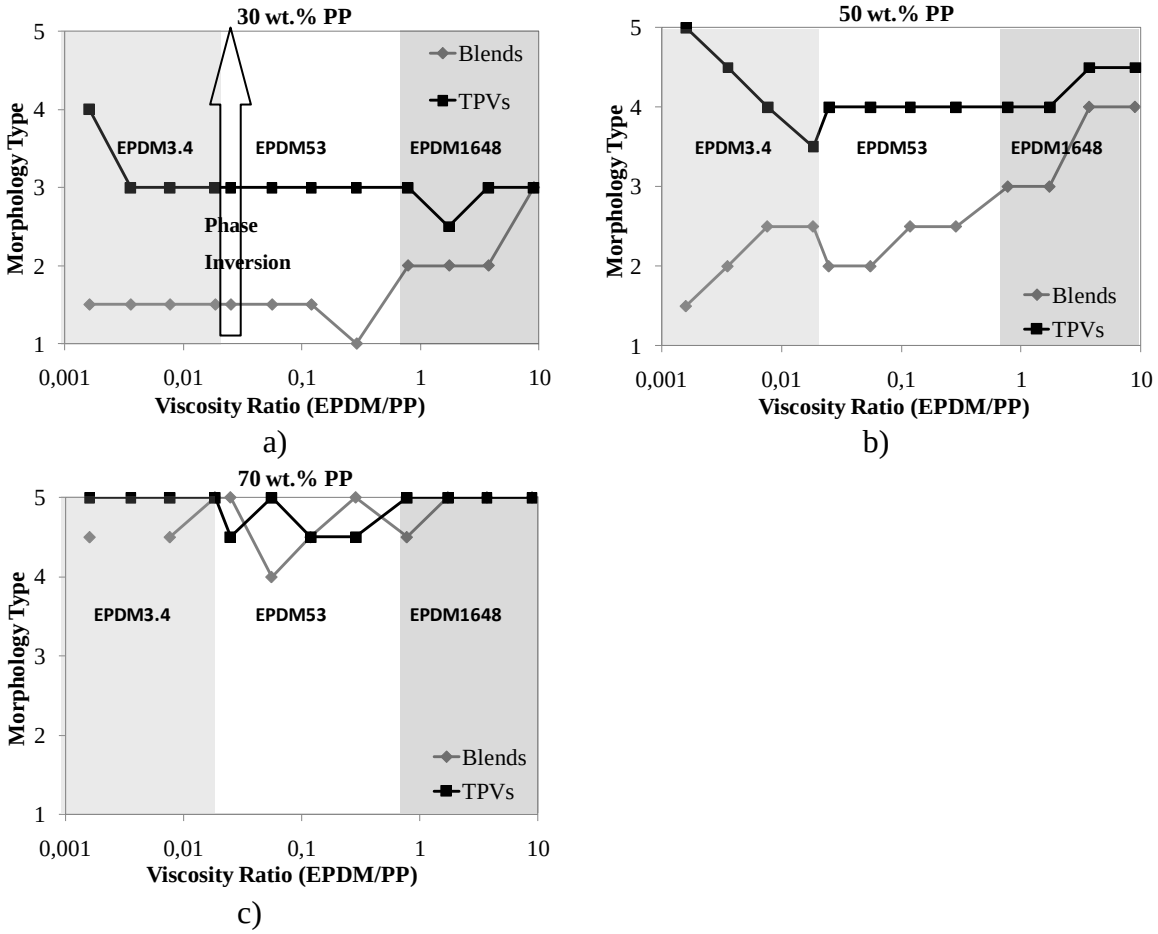

Fig. 5.12. Morphology type as a function of viscosity ratio of the EPDM/PP with: a) 30; b) 50; and c) 70 wt. % PP.

In a recent study [18], a diagram of phase morphology of the EPDM/PP blends was obtained by SEM–BSE. The phase inversion region was considered only when both EPDM and PP were visualized as continuous (the morphology type varies between 2.5 and 3.5). The same methodology was applied to TPVs and the diagram of Fig. 5.13 was obtained. For a better comparison between blends and TPVs, the region of phase inversion of the EPDM/PP blends (lines in grey) is also presented. The phase inversion region of the EPDM/PP blends is dependent on both composition and viscosity ratio, whereas the phase inversion region of TPVs is mainly governed by composition. The phase inversion region of the TPVs is around

30 wt.% PP in a wide range of viscosity ratios and it is independent of the phase morphology of the respective blend. At very high (~34) and very low viscosity ratios, the phase inversion region goes to compositions lower than 30 wt. % PP. This suggests that at very high viscosity ratios, the phase inversion process is driven by the (low) PP viscosity, and at very low viscosity ratios, phase inversion is driven by the (high) PP elasticity. It is observed that cross-linking shifts the region of phase inversion from 60 to 25 wt.% of PP for viscosity ratios lower than 0.01; from 55 to 30 wt.% PP for viscosity ratios around 0.1; from 50 to 30 wt.% PP around viscosity ratio of 1; and at viscosity ratio around 10, the region of phase inversion of the TPVs overlaps the phase inversion region of the respective blends.

The shift of the phase inversion region to high EPDM/PP ratios due to cross-linking is in agreement with observations made by other authors [23,25,26].

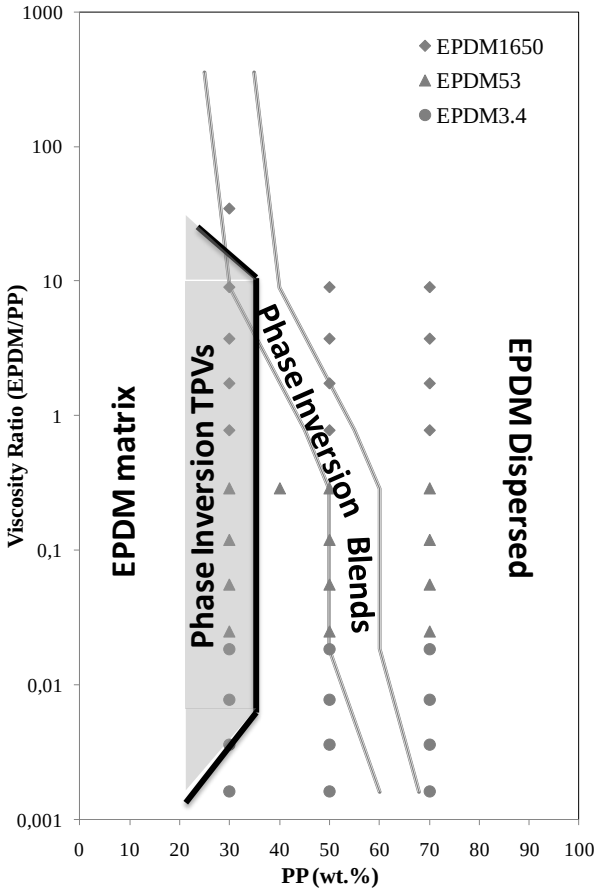

Fig. 5.13. Phase inversion region: diagram of the viscosity ratio as a function of composition.

Since during dynamic vulcanisation of the EPDM/PP blends only the rubber phase is cross-linked and the viscosity of the PP phase remains unchanged, the viscosity ratio of the respective TPV can be estimated from the viscosity of the cross-linked EPDM and initial PP viscosity. Therefore, this procedure was used to estimate the viscosity ratio of the TPVs with EPDM53. EPDM53 was premixed in the batch mixer with the cross-linking system for three

minutes at low temperature (80ºC). Under these conditions, cross-linking did not take place, as was confirmed by extractions. The mixed EPDM completely dissolves in cyclohexane. Then, the mixture was dynamically vulcanised in the rotational rheometer at an angular frequency of 65 rad/s (equivalent to the average shear rate in the batch mixer) and at 200 ºC. The evolution of complex viscosity, elasticity and loss modulus are depicted in Fig. 5.14. As expected, the rheological parameters increase as a function of time, which is more pronounced initially (until 200 s). After that, only a slight increase can be noticed. Once the rheometer started to collect the data, the cross-linking reaction was already quite advanced due to the equilibrium time that needs to be reached before starting the measurements. As suggested, the viscosity measurement at the beginning of the experiment was already 132.4 Pa.s, whereas the viscosity of pure EPDM53 was 53 Pa.s. Moreover, the crossover between storage and loss modulus seems to occur before the measurements start, meaning that the gel point was missed. The EPDM gel content of the sample at the end of the experiment was determined to be 66 wt. %. This value is in good agreement with the gel content obtained for the TPVs with EPDM53. Thus, the complex viscosity of the cross-linked rubber was used to calculate the viscosity ratio of the EPDM53/PP – TPV.

Figs. 5.15a and 5.15b compares the viscosity ratio (a) and storage modulus (b) of the blend and TPVs as a function of composition. The region of phase inversion of the EPDM/PP blends is also drawn in the diagrams. As can be observed in the diagrams, both the viscosity and the storage modulus ratios of the TPVs are higher than the corresponding blends. However, the viscosity ratio of TPVs with 50 wt.% PP remains in the co-continuous region and not in the upper part of the diagram, which would not be expected because in TPV the cross-linked EPDM is the dispersed phase. For the TPVs with 30 wt.% PP the TPVs viscosity ratio remains well below the co-continuous morphology region. The same trend is observed for the storage modulus ratio (Fig. 5.15b). These results show that phase inversion, in the case of TPVs, seems not to follow the same rules as the EPDM/PP blends. Phase inversion occurs before a certain viscosity ratio is achieved. A possible explanation can be a decrease in the flow deformability of the rubber phase as cross-linking advances. When the 3D network is formed, the EPDM particles become more rigid and have to breakup to react to the shear forces applied from dynamic conditions, which leads to phase inversion.

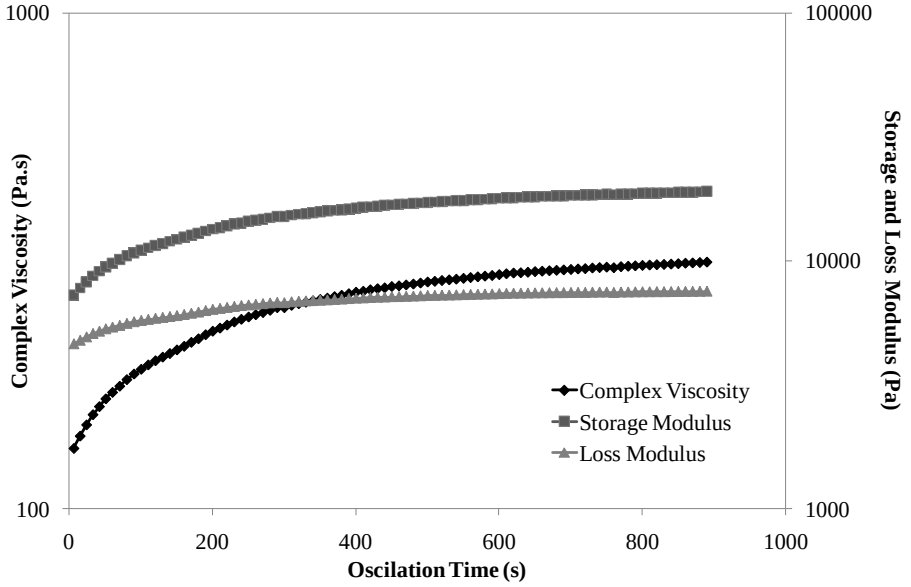

Fig. 5.14. Complex viscosity, storage and loss modulus as a function of time for a mixture of EPDM and cross-linking agents at 200 ºC and 65 s^{-1}.

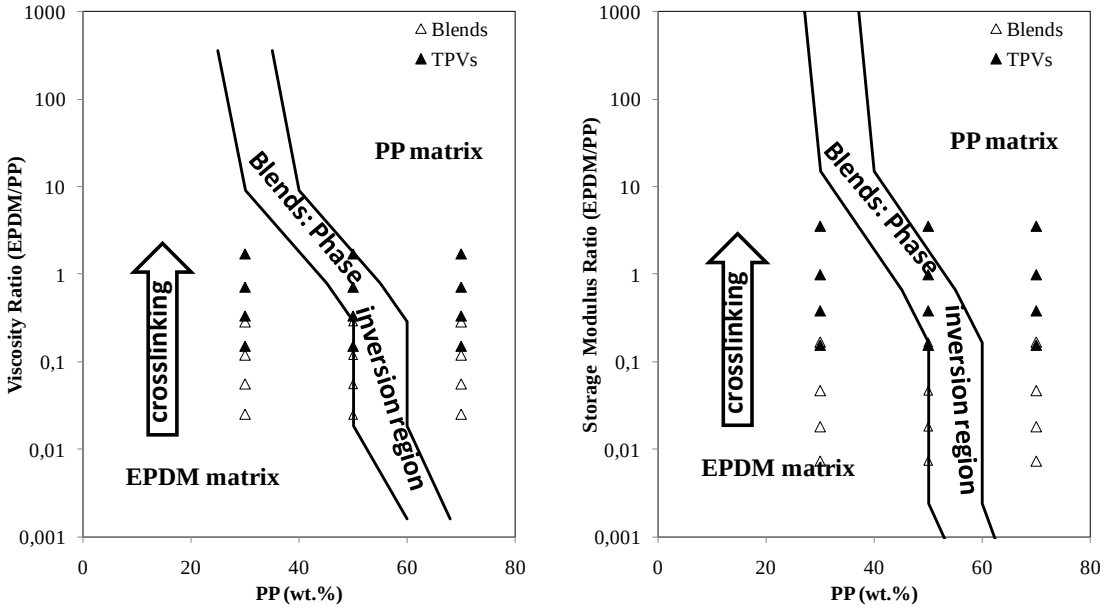

a) b)

Fig. 5.15. Blends and TPVs morphology diagram: viscosity a) and storage b) ratio as a function of PP amount (wt. %).

4. Conclusions

Aiming to get a better understanding of the phase inversion phenomena of the EPDM/PP TPVs as a function of viscosity ratio and composition, TPVs with different viscosity ratios

and compositions were prepared and characterised in terms of gel content, swelling and morphology.

The morphologies of EPDM/PP TPVs with 30 wt.% of PP are in general co-continuous, suggesting that cross-linking was insufficient to drive phase inversion. In the case of the EPDM/PP TPVs with 50 and 70 wt.% PP, the morphologies obtained consisted of cross-linked EPDM particles dispersed in a PP matrix, in the whole range of viscosity ratios. However, mainly for 50/50 compositions, some of the cross-linked EPDM particles dispersed in the PP matrix still connected. For viscosity ratios higher than 1 (TPVs made with EPDM1648), the cross-linked EPDM particles size increased as the EPDM/PP viscosity ratio increased. For viscosity ratios lower than one, in the EPDM53/PP TPVs, the EPDM particle size exhibited the opposite behaviour, i.e., the size of the cross-linked EPDM particles decreased as the viscosity ratio departed from unity. At very low viscosity ratios, for EPDM3.4/PP TPVs, the size of cross-linked particles was observed to start to increase as the viscosity ratio decreased.

A comparison between the TPVs made with the same PP but different EPDMs allows one to conclude that the morphology is refined as the EPDM viscosity increases, i.e., the EPDM/PP viscosity ratio increases. However, the cross-linking EPDM particles became more agglomerated.

While for blends, the phase inversion region was a function of the viscosity ratio and composition, for TPVs the phase inversion region is only a function of composition in a wide range of viscosity ratios. The phase inversion composition of the TPVs was located around 30 wt. % PP in a wide range of viscosity ratios, between 34 and 0.01. Thus, in all ranges of viscosity ratios used, dynamic vulcanisation shifted the phase inversion composition to lower PP content relative to the respective EPDM/PP blend.

A complete phase inversion process driven by cross-linking was hardly achieved. Low viscosity EPDMs facilitated the phase inversion process, suggesting that the elasticity of the PP matrix also plays an important role in the encapsulation of the EPDM phase at low viscosity ratios. Thus, it would be interesting to follow the morphological changes during dynamic vulcanisation in these systems to follow the phase inversion mechanism.

The comparison of the viscosity ratio estimated for the EPDM53/PP TPVs with those estimated for blends at phase inversion showed that phase inversion driven by cross-linking can occur at viscosity ratios above those estimated for the phase inversion of the blends.

References

[1] Coran AY, Patel RP. Rubber-thermoplastic compositions - 1. EPDM-polypropylene thermoplastic vulcanizates. Rubber Chem and Thecnol 1980;53(1):141-150.

[2] Karger-Kocsis J. Thermoplastic rubbers via dynamic vulcanization. In: Polymer blends and alloys, Shonaike GO, Simon GP, editors. New York: Marcel Dekker, 1999. p.125-153.

[3] De SK, Bhowmick AK. Thermoplastic elastomers from rubber–plastic blends. New York: Ellis Horwood, 1990.

[4] Coran AY, Patel RP. Thermoplastic elastomers based on dynamically vulcanised elastomer/thermoplastic blends. In: Thermoplastic Elastomers, Holden G, Hans RK, Quirk RP, editors. Munich: Hanser Publishers, 2nd ed, 1996. p. 143-181.

[5] Rader CP, Abdou-Sabet S. Two-phase elastomeric alloys. In: Thermoplastic elastomers from rubber–plastic blends, De SK, Bhowmick AK, editors. New York: Ellis Horwood, 1990. p.159-197

[6] Soliman M, Dijk van M, Es van M, Shulmeister V. Deformation mechanism of thermoplastics vulcanisates investigated by combined FTIR and stress strain measurements. ANTEC 1999. p.1947-1948.

[7] Boyce MC, Kear K, Socrate S, Shaw K. Deformation of thermoplastic vulcanizates. J Mech Phys Solids 2001;49(5):1073-1098.

[8] Oderkerk J, Groeninckx G, Soliman M. Investigation of the deformation and recovery behavior of nylon-6/rubber thermoplastic vulcanizates on the molecular level by infrared-strain recovery measurements. Macromolecules 2002;35(10):3946-3954.

[9] Oderkerk J, De Schaetzen G, Goderis B, Hellemans L, Groeninckx G. Micromechanical deformation and recovery processes of nylon-6/ rubber thermoplastic vulcanizates as studied by atomic force microscopy and transmission electron microscopy. Macromolecules 2002;35(17):6623-6629.

[10] Coran AY, Patel RP. Rubber-thermoplastic compositions - 2. NBR-nylon thermoplastic elastomeric compositions. Rubber Chem and Thecnol 1980;53(4):781-794.

[11] Bhadane PA, Champagne MF, Huneault MA, Tofan F, Favis BD. Continuity development in polymer blends of very low interfacial tension. Polymer 2006;47(8):2760-2771.

[12] Fortelný I, Kovár J, Sikora A, Hlavatá D, Kruslis Z, Nováková Z, Pelzbaeur Z, Cefelín P. The structure of blends of polyethylene and polypropylene with EPDM elastomer. Die Angewandte Makromolekulare Chemie 1985;132(1):111-122.

[13] Romani D, Garagnani E, Marchetti E. Reactive blending: structure and properties of crosslinking olefinic thermoplastic elastomer. Int Symp New Polym Mater. Naples, Italy, 1986. p.56-87.

[14] Valenza A, Demma GB, Acierno D. Phase inversion and viscosity-composition dependence in PC/LLDPE blends. Polym. Networks Blends 1993;3:15–19.

[15] Abdou-Sabet S, Patel RP. Morphology of elastomeric alloys. Rubber Chem Technol 1991;64(5):769-779.

[16] Mighri F, Huneault M. Drop deformation and breakup mechanisms in viscoelastic model fluid systems and polymer blends. Can J Chem Eng 2002;80(6):1028–1035

[17] Bhadane PA, Champagne MF, Huneault MA, Tofan F, Favis BD. Erosion-dependant continuity development in high viscosity ratio blends of very low interfacial tension. J Polym Sci Part B: Polym Phys 2006;44(14):1919-1929

[18] Antunes CF, Machado AV, van Duin M. Effect of viscosity and elasticity ratios on the morphology and phase inversion of EPDM/PP blends – *Part I. Submited to J Polym Sci Part B: Polym Phys.*

[19] Abdou-Sabet S, Puydak RC, Rader CP. Dynamically vulcanized thermoplastic elastomers. Rubber Chem Technol 1996;69(3):476-494.

[20] Machado AV, Duin M van. Dynamic vulcanisation of EPDM/PE-based thermoplastic vulcanisates studied along the extruder axis. Polymer 2005;46(17):6575-6586.

[21] Bouilloux A, Ernst B, Lobbrecht A, Muller R. Rheological and morphological study of the phase inversion in reactive polymer blends. Polymer 1997;38(19):4775-4783.

[22] Radusch HJ, Pham T. Morphology formation in dynamic vulcanized PP/EPDM blends. Kautsch Gummi Kunstst 1996;49(4):249-257.

[23] Oderkerk J, Groeninckx G, Morphology development by reactive compatibilisation and dynamic vulcanisation of nylon6/EPDM blends with a high rubber fraction. Polymer 2002;43(8):2219-2228.

[24] Joubert C, Cassagnau P, Michel A, Choplin L. Influence of the processing conditions on a two-phase reactive blend system: EVA/PP thermoplastic vulcanizate. Polym Eng Sci 2002;42(11):2222-2233.

[25] Martin P, Devaux J, Legras R, Leemans L, van Gurp M, van Duin M. Reactive compatibilization of blends of polybutyleneterephthalate with epoxide-containing rubber. The effect of the concentrations in reactive functions. Polymer 2003;44(18):5251-5262.

[26] Ma PL, Favis BD, Champagne MF, Huneault MA, Tofan F. Effect of dynamic vulcanization on the microstructure and performance of polyethylene terephthalate/elastomer blends. Polym Eng Sci 2002;42(10):1976-1989.

[27] Goharpey F, Katbab AA, Nazockdast H. Mechanism of morphology development in dynamically cured EPDM/PP TPEs. I. Effects of state of cure. J Appl Polym Sci 2001;81(10):2531-2544.

[28] Sengupta P. Morphology of olefinic thermoplastic elastomer blends: A comparative study into the structure – property relationship of EPDM/PP/oil and SEBS/PP/oil blend. PhD thesis University of Twente, The Netherlands, 2004.

[29] Antunes CF, Machado AV, van Duin M. Degradation of the rubber network during dynamic vulcanization of EPDM/PP blends using phenolic resol. Rubber Chem and Thecnol 2009;82(5):492-505.

[30] Utracki LA. On the viscosity-concentration dependence of immiscible polymer blends. J Rheol 1991;35(8):1615–1637.

[31] Lyngaae-Jorgensen J, Utracki LA. Dual phase continuity in polymer blends. Makromol Chem, Macromol. Symp 1991;48/49:189-209.

[32] Joseph S, Rutkowska M, Jastrzêbska M, Janik H, Haponiuk, JT, Thomas S. Polystyrene/polybutadiene blends: An analysis of the phase-inversion region and cophase continuity and a comparison with theoretical predictions. J Appl Polym Sci 2003;89(4):1007-1016.

[33] Omonov TS, Harrats C, Groeninckx G, Moldenaers P. Anisotropy and instability of the co-continuous phase morphology in uncompatibilized and reactively compatibilized polypropylene/polystyrene blends. Polymer 2007;48(18):5298-5302.

[34] Deyrail Y, Cassagnau P. Phase deformation under shear in an immiscible polymer blend: Influence of strong permanent elastic properties. J Rheol 2004;48(3):505-524.

[35] Wright KJ, Lesser AJ. Initial development of structure-property relationships for dynamically vulcanized EPDM/IPP elastomers. Rubber Chem and Thecnol 2001;74(4): 677-687.

Chapter 6: Morphology Development and Phase Inversion during Dynamic Vulcanisation of EPDM/PP Blends

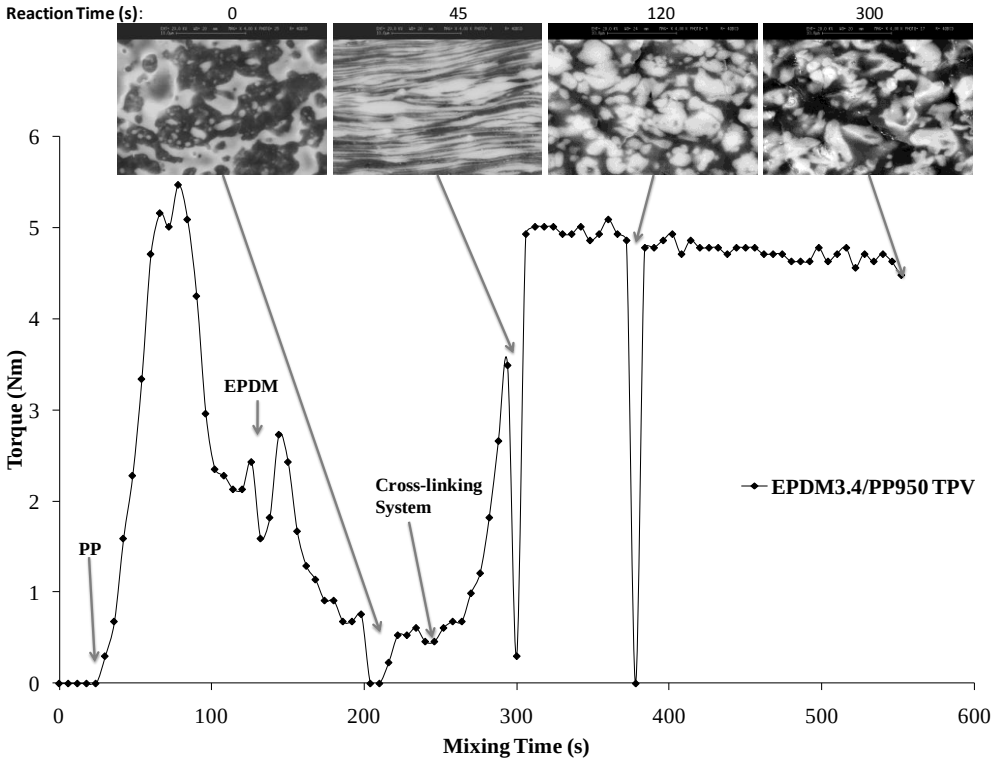

This chapter was submitted to Polymer.

1. Introduction

Thermoplastic vulcanisates (TPVs) are a particular group of thermoplastic elastomers (TPEs). These materials combine the melt processability of the thermoplastics and the elastic and mechanical properties of the thermoset cross-linked rubbers [1-3]. Thus, they can be processed by conventional techniques such as extrusion, blow moulding, injection moulding, vacuum forming and calendaring. The combination of their properties, recyclability and relatively low price explain the abundant and still growing application of these materials, especially in the automotive sector [4]. TPVs are produced via dynamic vulcanisation of immiscible blends of a thermoplastic and an elastomer. Dynamic vulcanisation consists of the selective cross-linking of the elastomer and its fine dispersion throughout the thermoplastic phase under intensive mixing [3]. Therefore, the final TPV morphology consists of cross-linked rubber particles finely dispersed in a thermoplastic matrix. Typical TPVs are formulated with high elastomer/thermoplastic ratios. Because the initial blend morphology consists of a thermoplastic phase dispersed in an elastomeric matrix or co-continuous phases, phase inversion must occur during TPVs production.

TPVs morphology results from complex interrelationship among composition, viscosity and elasticity ratios of individual components, processing conditions and cross-linking reaction. Several authors have previously investigated the morphology development during dynamic vulcanisation [5-11]. It has been shown that if the rubber is partially cross-linked a co-continuous morphology is established, even if the initial non-cross-linked blend consists of a thermoplastic phase dispersed in the rubber phase [6,11]. Abdou-Sabet [12] suggested that phase inversion during dynamic vulcanisation occurs through co-continuous morphology, i.e., a co-continuous structure is formed in the initial stages of cross-linking and as the cross-linking degree increases the continuous rubber phase becomes more elongated and then breaks up into microgel particles. According to Radush et al. [8], at high rubber contents, the formation of fine rubber particles dispersed in the thermoplastic phase is only achieved if an initial co-continuous blend morphology exists before the addition of the cross-linking system. A scheme for morphology development was suggested based on these observations [9]. According to this scheme, the co-continuous structure is deformed by shear and elongation stresses but it remains the same until the addition of the cross-linking system. As the cross-linking degree increases, shear and elongation stresses increase and the rubber phase is stretched out until it reaches a critical stress then breaks up into small particles. Machado et al. studied the morphology development of EPDM/HDPE/oil-based TPVs with different

compositions along the screw axis in a co-rotating twin-screw extruder [13]. They reported that the melt temperature increased very quickly in the first kneading zone (mainly for high EPDM levels) and that the rubber gel content was close to 100% before HDPE melting was completed. For a 33/33/33 (w/w/w) EPDM/HDPE/oil TPV, phase inversion of the EPDM was found to be driven by a combination of the completed melting of the HDPE phase and the continued cross-linking of the EPDM phase. Verbois et al. [14] showed that phase inversion in an EVA/PP system during dynamic vulcanisation occurred via a co-continuous morphology at an EVA gel content of approximately 60 wt.%.

Despite of the studies to date, following the morphological-development mechanism during EPDM(ethylene-propylene-diene monomer)/PP(polypropylene)-based TPVs production remains a difficult task, mainly due to the speed of the cross-linking reaction. Final TPV morphology can be achieved in less than one minute [7,8,13,15]. Therefore, the collection of samples to follow the morphological development and correlate it with the evolution of the physical and chemical phenomena taking place is rather complex. In the present work, a strategy was adopted to overcome these problems, namely, the use of two low-molecular-weight (low-Mw) EPDMs. This formulation was expected to retard the cross-linking of the EPDM phase, resulting in a slower morphological development during dynamic vulcanisation. Thus, this work aimed to obtain a better understanding of the mechanisms of morphology developed and phase inversion during the production of EPDM/PP TPVs. To achieve this goal, EPDM/PP blends with different weight ratios and EPDM and PP polymers with different Mws were dynamically vulcanised using resole/$SnCl_2 \cdot 2H_2O$ as the cross-linking agent. TPVs were prepared in a Haake Batch mixer and samples were collected over time for subsequent characterisation.

2. Experimental

2.1. Materials

In this chapter the EPDM1648, EPDM53 and EPDM3.4 as elastomers and PP2116, PP950, PP443 and PP184 as thermoplastic phase are used. The characteristic properties (Table 2.2 and 2.3) and codes (Table 2.4) of the polymers are summarized in part 3 of the Chapter 2.

The cross-linking system was composed of an octylphenol-formaldehyde resin (SP1045, Schenectady International, USA) called a "resole" (5 phr), and a combination of stannous chloride ($SnCl_2 \cdot 2H_2O$) (1.5 phr) and zinc oxide (ZnO) (1.8 phr) as activators (both from Aldrich). Irganox 1076 from Aldrich was used as a stabilizer (0.25 wt.% relative to the total amount of polymer (EPDM and PP)).

The rheological characterisation of the raw polymers are reported in part 3.3 of the Chapter 2. Thus, only the melt-complex viscosities and the storage modulus of the EPDMs and PPs at a shear rate of 65 s^{-1} are shown in Table 6.1.

Table 6.1. Melt-complex viscosities (η^*) and the storage modulus (G').

Material code	η^{*a} (Pa·s)	G'^{a} (Pa)
PP2116	2116	1.2×10^5
PP950	950	5.0×10^4
PP443	443	1.9×10^4
PP184	184	5.4×10^3
EPDM1648	1648	8.1×10^4
EPDM53	53	9.0×10^2
EPDM3.4	3.4	1.3×10^1

[a] at 200 ºC, 65 rad/s

2.2. Compositions

Blends and TPVs (without and with cross-linking, respectively) were prepared using different EPDM/PP weight ratios. Three EPDMs (EPDM1648, EPDM53 and EPDM3.4) were combined with each PP (PP) at 30/70, 50/50 and 70/30 (EPDM/PP, w/w) compositions. The compositions in terms of the weight percentage of components for blends and TPVs are presented in Table 6.2. The amount of stabilizer, Irganox 1076, was maintained constant relative to the total amount of polymers (EPDM plus PP). The weight percentage of cross-linking agents was varied for each composition to maintain a constant concentration relative to the amount of EPDM.

Table 6.2. Compositions of the EPDM/PP blends without (PBs) and with cross-linking (TPVs).

Coding	EPDM (wt%)	PP (wt%)	Irganox (wt%)	ZnO (wt%)	resole (wt%)	$SnCl_2$ (wt%)
PBs						
30/70	29.93	69.83	0.25	-	-	-
50/50	49.88	49.88	0.25	-	-	-
70/30	69.83	29.93	0.25	-	-	-
TPVs						
30/70	29.20	68.13	0.24	0.53	1.46	0.44
50/50	47.89	47.89	0.24	0.86	2.39	0.72
70/30	66.00	28.29	0.24	1.19	3.30	0.99

2.3. Blend and TPV Preparation

Blends and TPVs were prepared in a Haake batch mixer (HAAKE Rheomix 600 OS; volume 69 mL) at 200 ºC and a rotor speed of 80 rpm. The PP pellets were introduced into the hot mixer first; after the PP was melted, the stabilizer was added and then the EPDM rubber. After about three minutes the torque reached a constant value, indicating the formation of a homogenous melt; a sample was then collected (i.e., at time zero). Then the mixing was continued and ZnO, resole and $SnCl_2 \cdot 2H_2O$ were added in this order (which took about 5 s). Time zero (beginning of the reaction) was defined as the instant when $SnCl_2 \cdot 2H_2O$ was added. After that, samples were collected at different reaction times (45, 120 and 300 s and/or at 30, 60, 90, 120 and 300 s). For sampling, the rotors were stopped and samples weighing approximately 1.5 g were quickly taken from the mixer using a spatula, which took about 5 s. Then mixing was continued and this process was repeated several times up to 300 s. At this time (300 s), the total amount of material was removed.

The blends were prepared and collected using the same procedure as for the TPVs, with the exception of the addition of the cross-linking system. All of the samples collected from the mixer were cooled between two metal plates to stop the cross-linking reaction and to avoid morphological changes.

2.4. Sample Characterisation

The EPDM gel content was determined as a measure of the cross-linking density by extraction in cyclohexane at room temperature. For extractions, approximately 200 mg of TPV sample was weighed and then immersed for 48 h under gentle stirring; the solvent was refreshed after 24 h. The residual weight was determined after drying the sample in a vacuum oven at 100 °C for 12 h with nitrogen purging. The EPDM gel content was calculated

assuming that the residue consisted of insoluble PP, ZnO, resole, $SnCl_2 \cdot 2H_2O$ and cross-linked EPDM.

The degree of equilibrium swelling was measured because it can be used to confirm the trends in cross-linking and also gives a qualitative indication of the occurrence of phase inversion. The procedure was the same as described previously for the determination of EPDM gel content. However, in this case the swollen sample was weighed in a sealed glass bottle after carefully removing the excess cyclohexane with a tissue before drying. The swelling degree was calculated as the ratio of the weights of the swollen and dried sample.

The morphology was studied by scanning electron microscopy in back-scattering mode (SEM-BSE) using a Leica scanning electron microscope. Samples were fractured in liquid nitrogen and vapour stained with ruthenium tetroxide for 120 minutes. In the case of TPVs produced with the high-viscosity EPDM (EPDM1648), the morphology was also characterized by TEM using a Philips CM120 transmission electron microscope (TEM); samples were cryomicrotomed into 100-nm-thick sections at -130 ºC and then vapour stained with ruthenium tetroxide for 20 minutes. Disintegration tests were performed on samples collected before adding the cross-linking system (at time zero) to provide complementary information on phase morphology. Extractions in cyclohexane were carried out at room temperature and done according to a procedure described elsewhere [16].

3. Results and Discussion

Even though it has been reported in the literature that the morphology of blends is established quite rapidly and a (significant) reduction of domain size occurs during melting (or softening in case of an elastomer) [17-22], the morphology development of EPDM/PP blends during mixing was further investigated here. The blend morphologies corresponding to each TPV prepared in the present work were also analyzed after 300 s of mixing [16]. Comparing the morphologies of these samples with the samples collected at time 0 s (before the addition of the cross-linking system), no significant changes in morphology were generally observed. The exceptions to this behaviour were the blends made with the lowest-Mw EPDM. In the case of the EPDM3.4/PP2116 blend with 50 wt.% PP, it was verified that the initial blend morphology, consisting of PP dispersed in the EPDM matrix, became co-continuous after five minutes of mixing. Phase inversion during mixing occurred for the EPDM3.4/PP2116 blend with 70 wt.% EPDM; the initial blend morphology (0 s), consisting of PP dispersed in an EPDM matrix, changed to EPDM, partially dispersed and partially continuous, within a PP

matrix (at 300 s). Thus, to guarantee that these changes in TPV morphology were only induced by cross-linking, blend morphology development over time was first investigated.

3.1. Blend Morphology Development

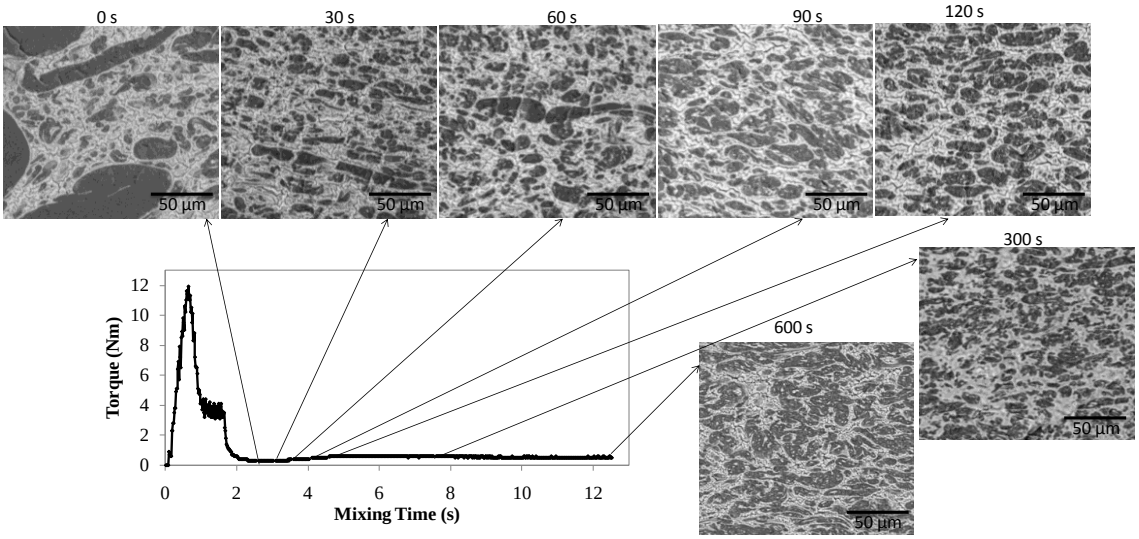

Fig. 6.1. Torque and SEM-BSE micrographs of EPDM3.4/PP950 blend with 50 wt.% PP versus mixing time.

Fig. 6.1 shows the morphology development during melt mixing of the EPDM3.4/PP950 blend with a 50/50 composition together with a plot of the torque as a function of mixing time. The first peak in the torque curve corresponds to the loading of PP; after PP melting, EPDM3.4 was added and a decrease of the torque, to close to 0 Nm, was observed. The torque then remained fairly stable until the end of mixing; however, a slight increase in the torque at around four minutes of mixing was noticed. The SEM-BSE micrograph of a sample collected at 0 s (the formation of a homogenous melt) shows a coarse dispersion of PP phase, very small and large PP domains co-exist in the EPDM matrix. After 30 s, a better dispersion of PP was achieved. Although the torque slightly increased just before a sample was collected at 60 s, no significant difference in morphology between the 30-s and 60-s samples was detected. At 90 and 120 s, the EPDM matrix seemed to become thinner at some locations and began to break up while PP became more continuous, this being more evident at 120 s. At longer mixing times, e.g., 600 s, it seems that the shear induced some phase coarsening. This behaviour was also reported by Thomas et al. [23] in the case of blends with a pronounced tendency to coalesce. These results show that the blend morphology changed slightly during

mixing and was most likely not stable up to 600 s; additionally, after 300 s a considerable degradation of the PP can occur, which also contributes to morphological changes.

Taking these results into consideration, the mechanism of morphology development during dynamic vulcanisation of this blend was investigated at two times (0 and 90 s) with the addition of the cross-linking system. Because no significant differences on either cross-linking degree or morphology development were observed, the cross-linking system was subsequently added at 0 s for all of the TPVs prepared.

3.2. Dynamic Vulcanisation

3.2.1. Torque and temperature

Fig. 6.2 shows the torque and temperature evolution as a function of time recorded during the dynamic vulcanisation of 50/50 (w/w) EPDMs/PP950 blends. The marked points correspond to sample collections (0, 45, 120 and 300 s). For all torque curves, the first peak corresponds to the introduction of PP into the mixer. The second peaks in the cases of EPDM1648 and EPDM53 correspond to EPDM loading. For the EPDM/PP TPV with EPDM3.4, a decrease of torque was observed when the EPDM was added, which is associated with the low viscosity of this rubber. Afterward, the torque reached a relatively constant value, indicating that PP melting was complete and the EPDM/PP mixture was fully homogenized. The addition of the phenolic resin caused a sudden decrease in the torque due to a lubricating effect. This effect was not noted in the case of EPDM3.4 due to the very low torque values before its addition. The torque then increased sharply, which is related to the drastic changes in the viscosity and elasticity of the EPDM phase due to cross-linking. As expected, at the end of mixing, the torque value was correlated with the molecular weight of the non-cross-linked EPDM, i.e., the final torque value increased as the EPDM Mw increased.

The temperature curves show a decrease when the polymers were fed due to the introduction of a cold mass into the hot mixer and the melting of PP. Upon EPDM addition, a continuous increase in the melt temperature was observed, surpassing the set temperature after the addition of the cross-linking system due to viscous energy dissipation enhanced by the cross-linking reaction. The melt temperature increased as the EPDM molecular weight increased, as expected. Both the torque and temperature curves are similar to those reported in other studies of the dynamic vulcanisation of EPDM/PP blends [15,24-26].

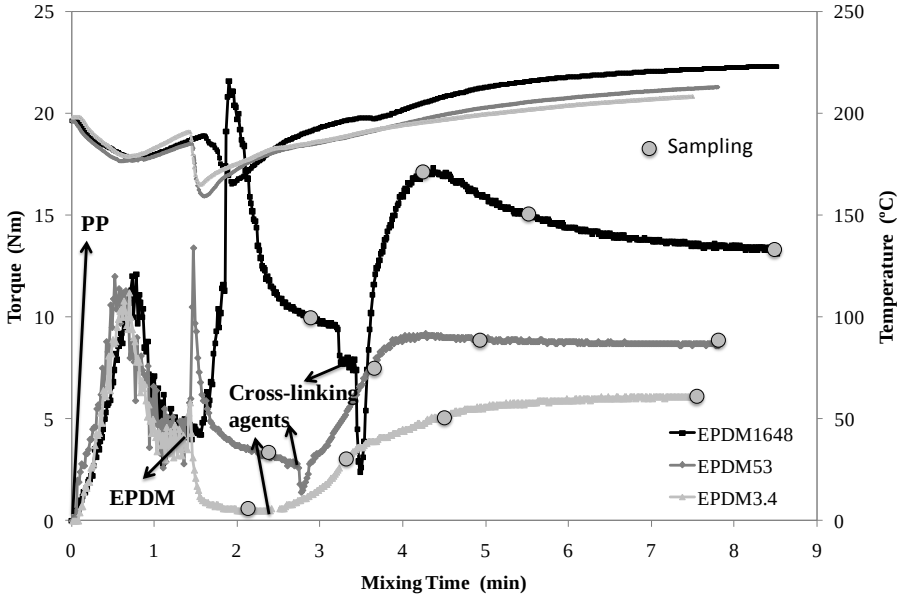

Fig. 6.2. Torque and temperature of EPDM/PP TPVs made with the various EPDMs and PP950 at 50 wt.% PP during mixing time.

3.2.2. Disintegration tests

The results of the disintegration tests performed in cyclohexane at room temperature on samples collected before adding the cross-linking system are shown in Table 6.3. Extractions give complementary information on phase morphology. As only EPDM dissolves in cyclohexane at room temperature, the following can be concluded from these tests: (i) if the sample disintegrates (D), it means that EPDM phase is the matrix; (ii) if the sample does not disintegrate (ND), it means that PP is the continuous phase.

Disintegration was not observed for blends made with EPDM1648, even in EPDM-rich compositions (30 wt.% PP), suggesting that PP was continuous for all of the blend compositions at time zero, as shown in Table 6.3. In the case of the EPDM53/PP blends, disintegration was observed for all EPDM-rich compositions (30 wt.% PP), indicating that the EPDM phase was the matrix. For EPDM/PP blends with 50 and 70 wt.% PP, the samples remained intact, suggesting that PP was already fully continuous. In the case of blends made with EPDM3.4, disintegration was observed for blends with 30 wt.% PP, with 50 wt.% PP with high viscosity (PP2116 and PP950) and with 70 wt.% PP2116. Blends prepared with EPDM53 and EPDM3.4 containing high EPDM amount were too sticky and soft and their samples could not be characterized by microscopy.

Table 6.3. Disintegration tests of the EPDM/PP blends.

Blend at 0 s	**EPDM/PP composition**		
EPDM/PP	70/30	50/50	30/70
1648/2116	ND	ND	ND
1648/950	ND	ND	ND
1648/443	ND	ND	ND
1648/184	ND	ND	ND
53/2116	D	ND	ND
53/950	D	ND	ND
53/443	D	ND	ND
53/184	D	ND	ND
3.4/2116	D	D	D
3.4/950	D	D	ND
3.4/443	D	ND	ND
3.4/184	D	ND	ND

3.2.3. Cross-linking degree

The EPDM gel content and the degree of equilibrium swelling were determined as a measure of the cross-linking degree of the EPDM phase. In a previous study [26], it was shown that the EPDM gel content determined by extraction in cyclohexane at room temperature is affected by the EPDM/PP weight ratio and morphology. Because the residue after extraction consists of PP, cross-linked EPDM and cross-linking agents, if the PP phase is the matrix and the EPDM phase is the dispersed phase, the solvent will not be able to efficiently remove all of the non-cross-linked EPDM. As PP dissolves in boiling xylene, extraction in boiling xylene would be more suitable for determining the cross-linking degree [26]. However, due to the high boiling temperature of xylene, samples collected at the early reaction times might contain unreacted resole and cross-linking might proceed during extraction. Consequently, to follow the evolution of the cross-linking degree as a function of time, EPDM gel content was determined by extractions in cyclohexane at room temperature instead.

Because the rigid PP becomes the matrix when phase inversion occurs, a significant decrease in the swelling degree is expected after the phase-inversion point. Thus, swelling degree was also used as a qualitative measure of phase inversion.

The values determined for the gel content and swelling degree will be presented later, during the morphology discussion, to make it easier to correlate the evolution of cross-linking degree and swelling with morphology development. Nevertheless, to compare the cross-linking kinetics of the different EPDMs used (i.e., of varying Mw), the EPDM gel content and the equilibrium swelling degree versus reaction time are shown in Fig. 6.3 for EPDM/PP950

TPVs with 50 wt.% PP as an example. The absolute error of the EPDM gel-content values for the TPV samples were approximately 5 %. Generally, the EPDM gel content increased and the swelling degree decreased with reaction time, indicating that the degree of cross-linking increases, as expected. A more detailed analysis shows that at 45 s after adding the cross-linking system, the EPDM gel contents were 68, 55 and 39 % for the EPDM1648, EPDM53 and EPDM3.4, respectively. Then at 120 s, the EPDM gel content increased to 87 % for EPDM1648 and to around 70 % for the others. After that, the EPDM gel content slightly increased, reaching 90 % for the high-Mw EPDM and close to 80 % for the low-Mw EPDMs. These results suggest that the cross-linking reaction slowed down as the Mw EPDM decreased, mainly in the early mixing stages (45 s). The final cross-linking degree of the TPVs was higher for the highest-Mw EPDM and no significant differences were found between the other two blends prepared with lower-Mw EPDMs.

The swelling degree of EPDM1648/PP950 TPV remained almost unchanged after 45 s, (3.1 at 45 s and 2.9 at 300 s) suggesting that PP was already the matrix at 45 s. TPVs made with low-Mw EPDMs exhibited a different behaviour; here, a significant decrease of the degree of equilibrium swelling was detected between 45 s and 120 s, from 3.7 to 2.8 and 3.5 to 2.8 for TPVs made with EPDM53 and EPDM3.4, respectively. This decrease suggests that phase inversion occurred or was fully completed during this time period.

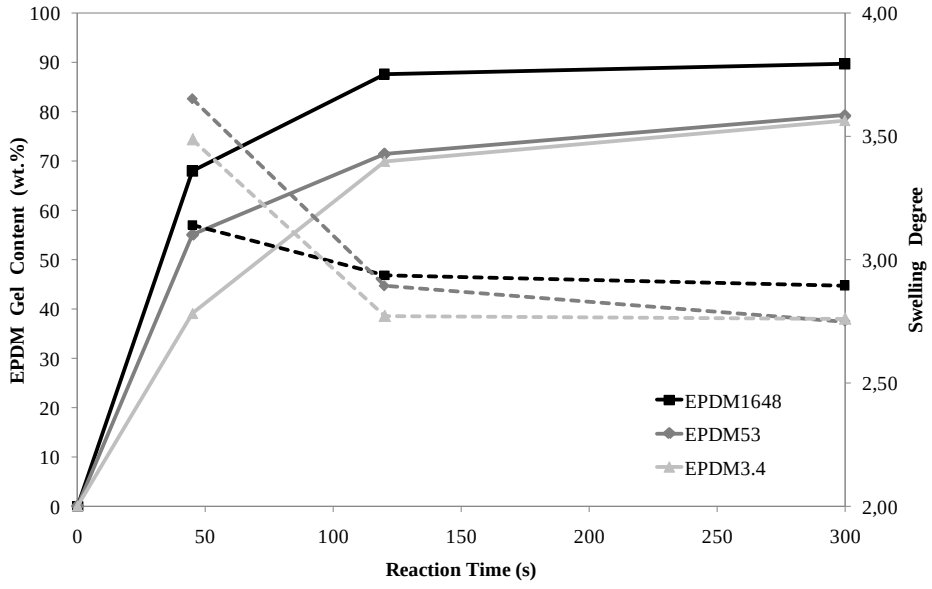

Fig. 6.3. Evolution of EPDM gel content and swelling degree of EPDM/PP950 TPVs with 50 wt.% PP with reaction time.

3.2.4. Influence of EPDM Mw on morphology development

Micrographs of the samples collected before (at 0 s) and after adding the cross-linking system (at 45, 120 and 300 s) are depicted in Fig. 6.4 for the EPDM/PP950 TPVs with 50 wt.% PP. Here EPDM appears as the darker phase and PP as the lighter one. On the contrary, in SEM-BSE micrographs EPDM is white and PP is the dark phase. Generally, the morphologies shown in the micrographs are representative of the whole sample. The exceptions are the samples collected at 45 s, which had rather heterogeneous morphologies.

The initial morphology of the EPDM1648/PP950 TPV before adding the cross-linking system (at 0 s) was co-continuous, i.e., both EPDM and PP were continuous. At 45 s, the EPDM (dark phase) appear to be dispersed, but several elongated EPDM domains, sometimes connected by a thin EPDM thread, were also observed. At 120 and 300 s, similar morphologies were obtained, consisting of EPDM domains dispersed within the PP matrix.

Even though the PP phase (dark phase) seems to be mainly dispersed in the EPDM matrix in the EPDM53/PP950 TPV at 0 s, the sample did not disintegrate in cyclohexane (Table 6.3), suggesting that PP is a continuous structure here. At 45 s, EPDM and PP were stretched, resulting in elongated structures. Although both phases appear continuous, PP seems to be more the matrix. Micrographs of the samples collected at 120 and 300 s exhibited EPDM dispersed in the PP the matrix without significant differences between the morphologies.

At 0 s in the EPDM3.4/PP950 TPV, PP was dispersed in the EPDM matrix before the addition of the cross-linking system. It can be seen that the PP domain size was rather heterogeneous, which was probably related to the large difference between the PP and EPDM viscosities. This morphology is in agreement with the disintegration tests (Table 6.3); the sample disintegrated, meaning that EPDM was the matrix. In the early stage of cross-linking, 45 s, both EPDM and PP were continuous and exhibited elongated structures. It seems that the EPDM phase was connected by thin layer that started to break up, leading to the formation of EPDM threads dispersed in the PP phase. At later reaction times (120 and 300 s), EPDM was already the dispersed phase and PP was the matrix.

Comparing the TPV morphologies at 45 s, the EPDM phase became less continuous as the EPDM Mw increased. This is related to the differences in the cross-linking degree and probably to the initial blend morphology. As stated above, the EPDM gel contents were 68, 55 and 39 % for EPDM1648, EPDM53 and EPDM3.4, respectively (Fig. 6.3). Thus, the cross-linking reaction was slower for the low-Mw EPDM and, consequently, the morphology development was also slower. At 120 s, the morphology of all TPVs was already established,

with EPDM dispersed in the PP matrix independently of the EPDM gel-content value, meaning that gel point and phase inversion both occurred before the formation of an EPDM gel content of 70 wt.%.

Comparing the morphological development with the data for the degree of equilibrium swelling, a pronounced decrease in swelling values for EPDM53 and EPDM3.4 between 45 and 120 s can be observed in Fig. 6.3. This change was not only related to the increase of cross-linking degree but also to the morphological changes (phase inversion). In the case of EPDM1648, at 45 s, PP was already the matrix and, thus, no pronounced decrease in the swelling degree was observed.

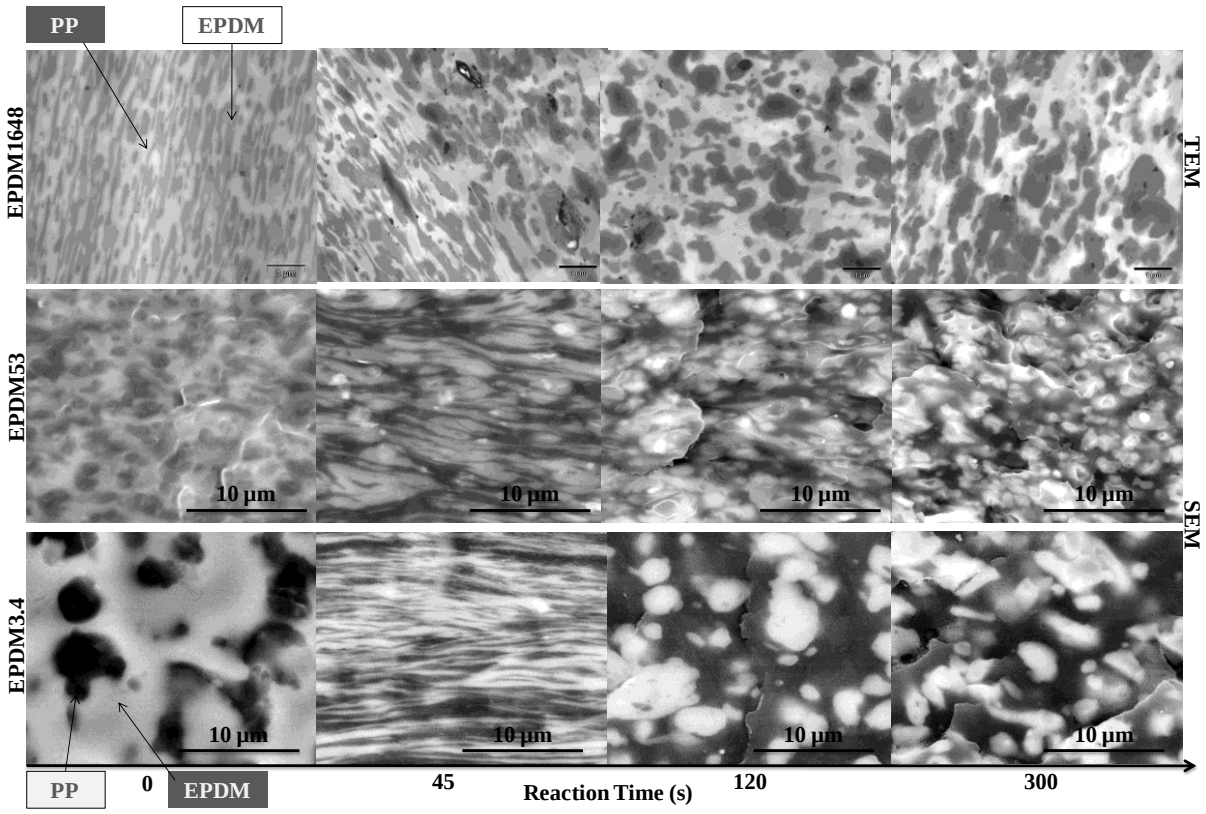

Fig. 6.4. Micrographs of samples of EPDM1648/PP950 (TEM) and EPDM53/PP950 and EPDM3.4/PP950 (SEM-BSE) TPVs with 50 wt.% of PP, collected at 0, 45, 120 and 300 s.

3.2.5. Influence of EPDM/PP weight ratio on morphology development

To investigate the effect of composition on morphology development during dynamic vulcanisation, SEM-BSE micrographs, EPDM gel contents and the degrees of equilibrium swelling for the EPDM53/PP950 TPVs with 30 and 70 wt.% PP were determined and are depicted in Fig 6.5.

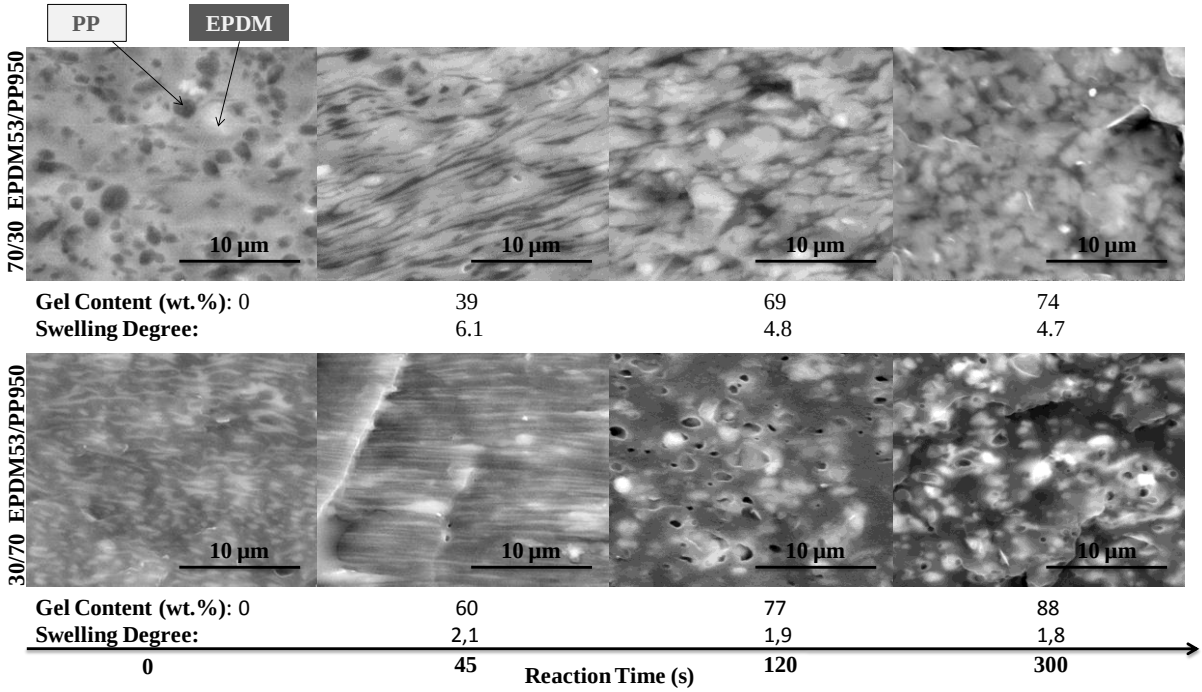

Fig. 6.5. SEM-BSE micrographs of samples of EPDM53/PP950 TPVs with 30 and 70 wt.% PP collected at 0, 45, 120 and 300 s. Below the micrographs are the corresponding EPDM gel contents and swelling degrees.

For the EPDM-rich TPV (30 wt.% PP), PP was dispersed in the EPDM matrix before the addition of the cross-linking system (0 s). This was also confirmed by the disintegration tests. At 45 s, the initial structure was strongly deformed and EPDM started to break up, leading to the formation of elongated EPDM domains and, simultaneously, the deformed PP phase started to coalesce. The morphologies obtained at 120 and 300 s were quite similar, suggesting that morphology was already stable at 120 s. It was observed that the EPDM phase had a greater tendency to be dispersed; however, it appears rather continuous here, suggesting that the cross-linking reaction was insufficient to achieve complete phase inversion in this case.

For the PP-rich compositions (70 wt.% PP) before cross-linking began, PP was the matrix and EPDM was dispersed with a heterogeneous domain size. After 45 s, thin EPDM threads were detected in the PP matrix, which broke up and led to the formation of homogeneous EPDM particles dispersed in the PP matrix at 120 s. As no significant differences were detected between the morphologies at 120 and 300 s here, it seems that the morphology was fully developed at 120 s, consisting of EPDM particles dispersed in a PP matrix.

Despite the composition difference (30 and 70 wt.%), the mechanisms of morphology development in the two blends seem to be quite similar and also similar to that observed with 50 wt.% (Fig. 6.4). Taking into account the EPDM gel contents, i.e., 39, 55 and 60% for

compositions of 30, 50 and 70 wt.% PP, respectively, the stage of morphological development seems to be more related to the cross-linking degree than to composition. Although composition influenced the final TPV morphology, the general stages of the morphology development mechanism seem to be independent of the composition. At early reaction stages, 45 s, the structure was highly deformed; here, it seems that the cross-linking reaction induces the formation of a lamellar/fibrillar structure which then breaks up, resulting in small particles. Then at 120 s, the morphology is fully developed and stabilized.

3.2.6. Influence of PP viscosity on morphology development

It is known that the viscosity ratio affects the initial blend morphology and the EPDM particle size of the TPV final morphology [9,15]. However, there have been no reports on the influence of the viscosity ratio on morphology development during dynamic vulcanisation. Fig. 6.6 depicts SEM-BSE micrographs of TPVs prepared with EPDM3.4 and PPs of different viscosities. The micrographs of the samples collected at different reaction times are displayed in relation to EPDM gel content. The morphology of the EPDM3.4/PP2116 at 0 s was not available, but extraction experiments confirmed that EPDM was the matrix and PP seemed to be dispersed. For the EPDM3.4/PP950, the morphology at 0 s consisted of PP dispersed in an EPDM matrix, whereas for the EPDM3.4/PP443 a co-continuous morphology was observed. As before, in TPVs made with PP950, cross-linking induced the formation of elongated EPDM structures at 45 s, appearing as lamellar structures. The elongated EPDM structures seen at 45 s were also observed for PP443, even when the initial morphology (at 0 s) was co-continuous rather than PP dispersed in the EPDM matrix. The formation of these elongated structures occurred in the range of EPDM gel contents between 20 and 60 %. In contrast, for EPDM gel contents around 20 % the morphology remained co-continuous; for EPDM gel contents around 60 %, dispersed and somewhat continuous elongated EPDM structures were observed. At 120 s, the EPDM was fully dispersed in the PP matrix. In Fig. 6.6, a plot of swelling degree versus reaction time is also shown. The TPVs made with PP950 and PP443 exhibited significant decreases in swelling degree between 45 and 120 s, corroborating the morphological changes from co-continuous to dispersed-matrix morphologies.

The EPDM3.4/PP2116 TPV presented a different behaviour. The initial blend morphology consisted of PP dispersed in an EPDM matrix and, 45 s after adding the cross-linking system, EPDM was already dispersed in the PP matrix. The swelling degree (Fig. 6.6) was practically unchanged, also suggesting no further changes in morphology after 45 s. In this case, phase

inversion occurred earlier than in the TPVs made with the other PPs. One possible explanation is the high gel content (65 wt.%) observed at 45 s; another is the large difference between the viscosities and elasticities of the EPDM and PP phases. As the EPDM viscosity began to increase due to the cross-linking reaction, the highly elastic PP was able to encapsulate the EPDM phase. Therefore, EPDM was encapsulated before being well stretched and a coarse morphology (as can be seen in the low-magnification micrograph of Fig. 6.6) resulted for these TPVs. These results provide evidence that the viscosity ratio affects morphology development during dynamic vulcanisation.

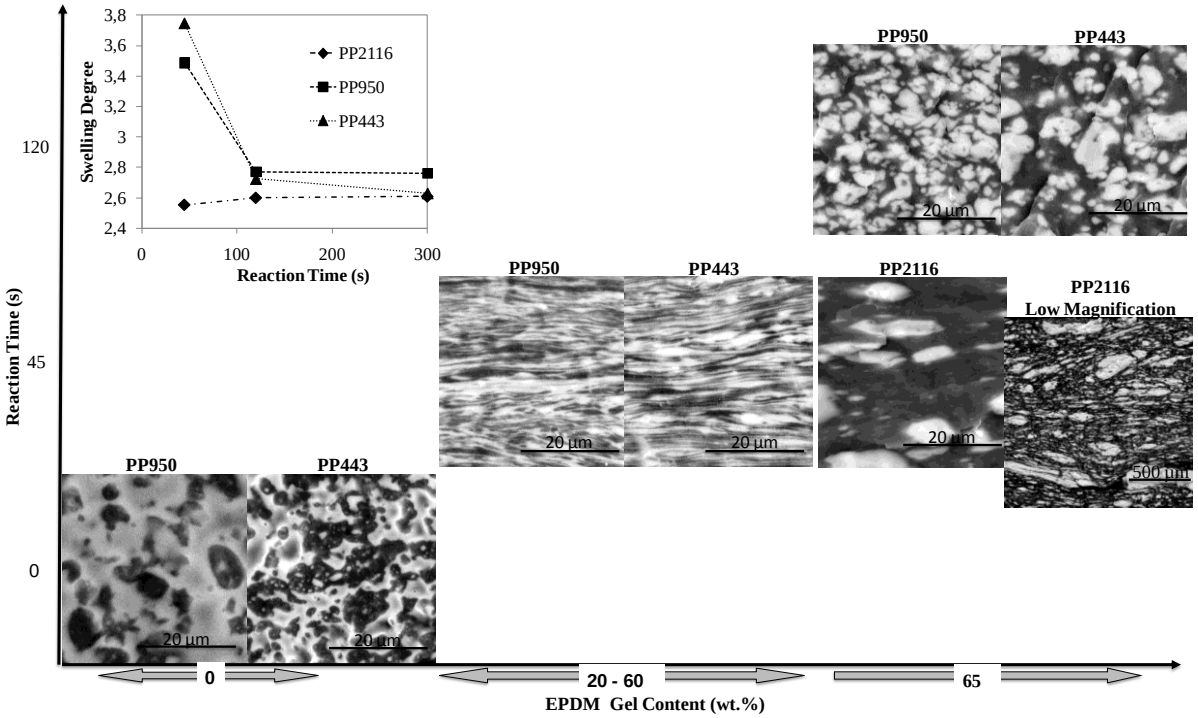

Fig. 6.6. EPDM3.4/PP TPVs with 50 wt.% PP: SEM-BSE micrographs at different reaction times in relation to EPDM gel content and swelling degree versus reaction time (inset plot).

3.3. Morphological-development Mechanism

The results presented above yielded information on the effects of the Mw of the EPDM, the blend composition, the viscosity ratio and the EPDM gel content on morphology development. However, for more detailed insight into the morphological-development mechanism during dynamic vulcanisation, samples were collected at smaller time intervals after adding the cross-linking system (30, 60, 90, 120 and 300 s). As the use of low-Mw EPDM allowed to slow down the cross-linking reaction, EPDM3.4/PP950 with 50 wt.% PP was chosen to investigate the mechanism of morphological development in more detail, including phase inversion driven by cross-linking. Moreover, the initial morphology of this

blend consisted of dispersed PP instead of a co-continuous structure and, thus, complete phase inversion could be observed. The same experiment was performed with a conventional rubber used in TPV production (EPDM1648/PP950 with 50 wt.% PP) to compare the results in both cases.

Fig. 6.7 shows the TEM micrographs of the EPDM1648/PP950 TPV collected before (0 s) and after adding the cross-linking agents (30, 60 and 90 s). General views of the morphologies are shown in the micrographs at the top (at low magnification), and more detail is provided in the micrographs below (at higher magnification); the EPDM gel contents and the equilibrium swelling degrees are also given below each micrograph. Initially (0 s), the morphology was co-continuous; 30 s after adding the cross-linking agents, EPDM is dispersed and continuous. Some elongated EPDM domains, sometimes connected by thin threads, were observed, similarly to the morphology obtained above at 45 s (Fig. 6.4). These kinds of structures can also be observed at 60 s. At 90 s, the cross-linked EPDM particles were mainly dispersed in the PP matrix, and, after that, no more changes in morphology were detected. The swelling degree remained practically unchanged after 30 s, confirming that, afterward, no significant morphological changes took place. The EPDM gel contents, 61 % at 30 s and 76 % at 60 s, indicate that the cross-linking reaction had proceeded to quite an extent even at 30 s. Most probably, the elongated structures observed (at 30 and 60 s) resulted from further deformation of the EPDM domains formed in the early stages of cross-linking by the breakdown of the co-continuous structure. Despite the results obtained, the cross-linking reaction with the high-Mw EPDM is quite fast and the morphological development in the initial stages of cross-linking could not be monitored.

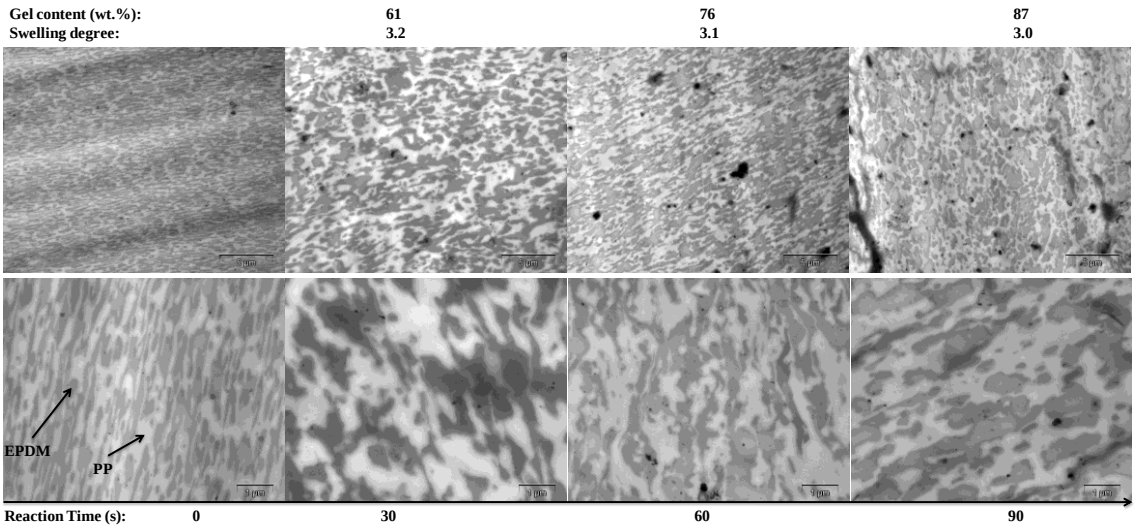

Fig. 6.7. Morphology development of EPDM1648/PP950 with 50 wt.% PP during dynamic vulcanisation.

The morphology of the samples collected during dynamic vulcanisation of the EPDM3.4/PP950 blend are shown in Fig. 6.8. At 0 s, the PP phase was dispersed in the EPDM matrix. After cross-linking began (30 s), the initial structure was strongly elongated; the EPDM matrix broke down and the PP coalesced, leading to the formation of elongated EPDM and PP domains, appearing as a lamellar structure. At 60 s, different types of morphologies, such as PP dispersed in the EPDM phase, lamellar structures, elongated EPDM particles and dispersed EPDM particles were observed. This heterogeneity of TPVs morphology remained until 90 s. At this time, the EPDM appeared more as the dispersed phase and PP more as the continuous phase. EPDM fully dispersed in the PP phase was obtained at 120 s. After this, no further changes in morphology were detected. Judging by the swelling degree, the main changes in the morphology (phase inversion) occurred between 30 and 60 s because a decrease from 6.2 to 3.7 was observed; after 60 s of reaction time, it remained approximately constant.

Comparing the morphology development of both TPVs, it can be observed that the morphology of EPDM1648/PP950 was stable at 90 s whereas for EPDM3.4/PP950 it only became stable at 120 s. This may be related to the faster cross-linking reaction of the EPDM1648 and the viscosity ratio of the blend components. Another difference between the TPVs was the EPDM gel contents at which the morphology stabilizes, which were 62 % (at 120 s) for TPV made with EPDM3.4 and 87 % (at 90 s) for TPV made with EPDM1648. In the latter, even though the PP phase was the matrix at 30 s, an evolution of the EPDM phase (from connected to dispersed EPDM domains) was observed up to 90 s, and the EPDM gel content varied from 61 to 87 %. In the case of the TPV made with EPDM3.4, at 120 s the EPDM gel content was 62 % and no morphology refinement (further deformation and breakup of the dispersed EPDM phase) was seen. It seems that as soon as the PP950 encapsulated the EPDM3.4, no refinement of the morphology occurs; this may be related to the high elasticity of the PP950 relative to the EPDM3.4 (while the elasticity of PP950 is smaller than that of EPDM1648). Although cross-linking enhances the melt viscosity and melt elasticity of the EPDM phase, it was shown in a previous study [27] that the melt-complex viscosity and storage modulus of the cross-linked low-molecular-weight EPDM (at a cross-linking degree around the gel point) remained smaller than the PP phase. This suggests that PP (with higher elasticity) encapsulates the EPDM phase and no further deformation and break-up occur. The same behaviour was also observed in the case of the EPDM3.4/PP2116 TPV, where phase inversion was observed to occur much earlier than in the other TPVs, after which no refinement of morphology was observed (Fig. 6.6). This can be explained by the

Van Oene theory [28,29], which states that the interfacial tension under dynamic conditions will be lower in a system where the highly elastic material is the matrix and the less elastic material is the dispersed phase.

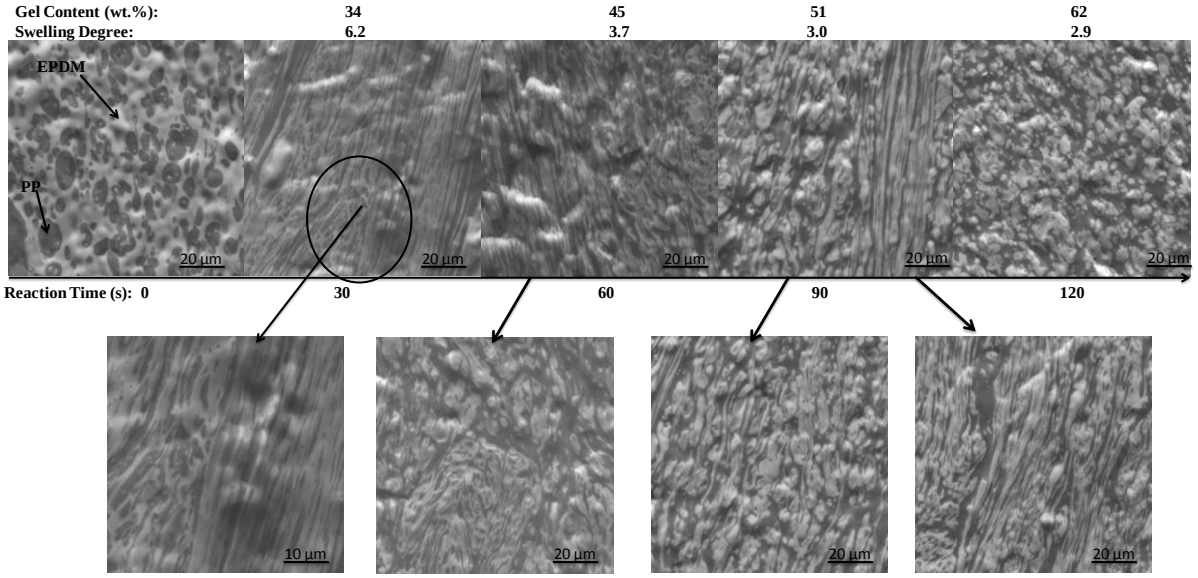

Fig. 6.8. SEM micrographs of EPDM3.4/PP950 samples with 50 wt.% PP collected during dynamic vulcanisation.

From the above results, it is clear that the phase-inversion process and morphology refinement during dynamic vulcanisation occurs through the formation of elongated EPDM structures. The formation of elongated EVA structures was also observed by Deyrail and Cassagnau [30] in EVA/PDMS TPVs using a hot optical-shear device. They observed that droplet deformation decreased when the cross-linking level increased and, even though major deviations of the droplet deformation near the gel point were not noticed, it was possible to observe deformation of the EVA phase for cross-linking levels higher than the gel point. Radusch [9] also proposed that deformation of the rubber phase would be possible in the initial stages of cross-linking through the stresses transferred by the viscous thermoplastic matrix. According to Radusch, the initial co-continuous morphology is stretched more and more after the addition of the cross-linking system by the shear and elongation stresses, which increase as the viscosity of the rubber phase increases due to cross-linking. Then when a critical stress is reached, the stretched rubber phase will break apart into small particles and, after that, only distribution of the cross-linked particles occurs [9]. In the present work, it was observed that the stretched continuous EPDM structure first broke into EPDM threads, which were further elongated by the thermoplastic matrix and then broke up into small particles. Even in the case of the EPDM1648/PP950, where it was not expected that the low-viscosity

PP matrix would be able to deform the already cross-linked EPDM phase, elongated EPDM domains were observed. Bhadane et al. [10] studied the effects of dynamic vulcanisation on the phase continuity and co-continuity of EPDM/PP blends using focused-ion-beam (FIB) etching of the sample surface followed by topological investigation of the sample surface using tapping-mode atomic-force microscopy (TMAFM). They reported the formation of a much finer and more extensive EPDM network (i.e., a continuous structure) upon dynamic vulcanisation of the coarse EPDM network in the initial uncross-linked EPDM/PP blend. They suggested that the cross-linking reaction starts at the outer envelope of the EPDM phase and works its way towards the centre. Consequently, due to the viscosity mismatch created between cross-linked and uncross-linked EPDM and in response to the dynamic mixing conditions, the microgel particles detached from the initial network pull entangled chains of non-cross-linked EPDM, resulting in a refined continuous structure [10].

According to the above discussion, it is expected that cross-linking enhances the deformation and breakup of the EPDM structures, not only due to the increase of the shear and elongation stresses but also because of the viscosity mismatch created between the cross-linked and non-cross-linked EPDM particles. Once EPDM threads are formed, they seem to break up according to a Raleigh mechanism applied to polymers by Tomotika [31], as can be observed in the micrographs of Fig. 6.9. According to Tomokita, a thread surrounded by another polymer will break up due to instabilities driven by the interfacial tension. He suggested that the breakup of threads is related to the distortion of the elongated thread that runs sinusoidally. The growth-rate parameter (q) of the sinusoidal distortion (α) is described by the following equations:

$$\alpha = \alpha_0 \exp(qt) \tag{1}$$

$$q = \left(\frac{\sigma}{2\eta_m R_0}\right) \Omega(l, \lambda) \tag{2}$$

where α is the distortion amplitude, α_0 is the amplitude of the initial distortion, t is time and q is the growth rate. The growth rate is dependent on the interfacial tension (σ), the matrix viscosity (η_m), the initial thread radius (R_0) and the Tomokita function (Ω *(l,λ)*), a dimensionless distortion growth rate depending on the distortion wavelength (l) and the viscosity ratio (λ). According to Tomokita, the breakup of threads occurs when a critical distortion amplitude is reached. Although these relations were developed under quiescent conditions and for a Newtonian system, Elmendorp [32] found a good agreement for viscoelastic polymers.

This present study also shows that phase inversion, mainly with the low-Mw EPDM, is a rather heterogeneous process, suggesting that EPDM domains in the same sample have different levels of cross-linking. Indeed, it is anticipated that upon addition of cross-linking agents to the EPDM/PP blend they are not instantaneously well distributed by the batch mixer, resulting in microscopically different levels of cross-linking. As the gel content measured is an average value of the macroscopic sample, it is not representative of the cross-linking degree at a microscopic scale. Deyrail et al. [33] showed that the dispersion of the reagents in the EVA phase obtained in the batch mixer was very heterogeneous from a microscopic point of view. They showed that even when the cross-linking extent in the bulk corresponds to an 85 % insoluble product (where deformation is not expected), some EVA droplets in a PDMS matrix were strongly deformed under shear flow, suggesting low levels of cross-linking. These results might also explain the elongated domains observed in the EPDM1648 TPVs product even at high degrees of cross-linking. Thus, the sort of structures observed in the micrographs at early reaction times are an effect of the different kinetic stages of the EPDM phase resulting from the heterogeneous distribution of the cross-linking agents in the melt.

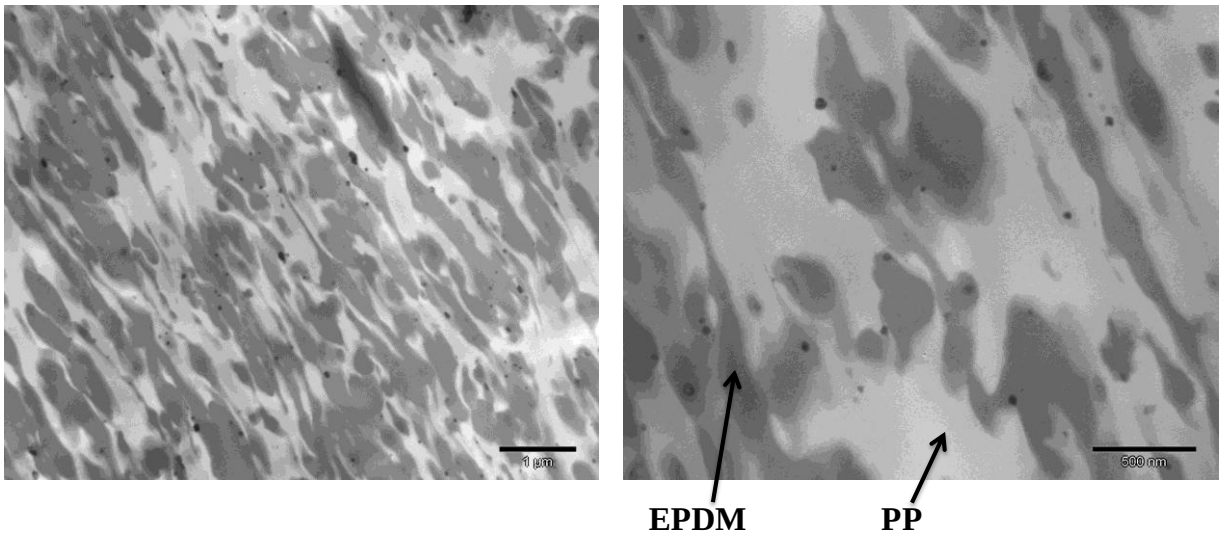

Fig. 6.9. TEM micrographs of a sample of the EPDM1648/PP950 TPV collected at 45 s.

According to the results and the discussion above, a mechanism for phase inversion driven by cross-linking is proposed and is shown schematically Fig. 6.10. The mechanism can be described by the following steps (which correspond to each micrograph of Fig. 6.10):

- Before adding the cross-linking system, PP is dispersed in the EPDM matrix (Fig. 6.10a).
- Upon addition of the cross-linking system, as soon as the cross-linking agent comes into contact with EPDM, the reaction starts immediately:
    - EPDM microgel particles formed start to effect the deformation of the EPDM matrix, which begins to break up, and PP starts to coalesce and become continuous (Fig. 6.10b).
    - PP becomes more continuous (a highly viscous material in this case) and cross-linking advances; the shear and elongation stresses increase, resulting in further elongation of both phases, leading to the formation of a lamellar/fibrillar structure (Fig. 6.10c).
    - As cross-linking proceeds, EPDM is further elongated and starts to break due to capillary instabilities (Fig. 6.10d).
    - Finally, PP becomes the matrix and the cross-linked EPDM the dispersed phase (Fig. 6.10e).

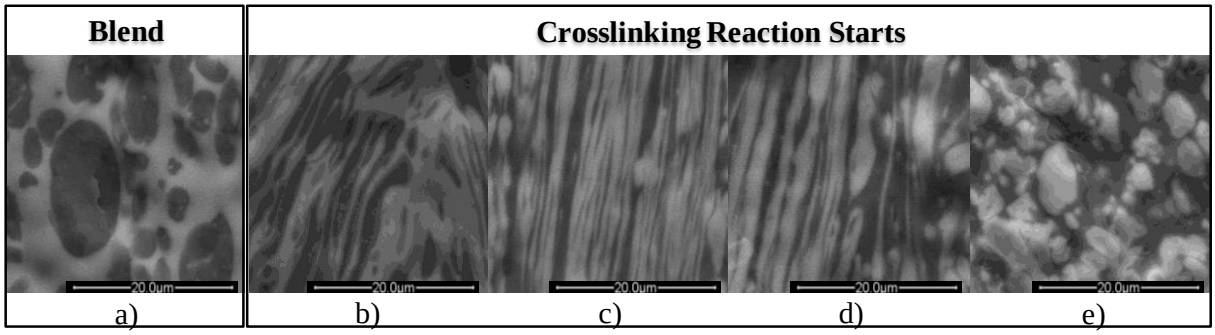

Fig. 6.10. Morphological-development mechanism proposed for phase inversion during dynamic vulcanisation.

4. Conclusions

The morphology development during dynamic vulcanisation was investigated using an experimental plan consisting of vulcanising combinations of three rubbers and four PPs with different viscosities. It was demonstrated that the Mw of the EPDM has a significant effect on the extent of the cross-linking reaction. At 45 s after adding the cross-linking system, the EPDM gel contents were 68, 55 and 39% for the EPDM1648, EPDM53 and EPDM3.4 TPVs, respectively. As the cross-linking reaction was delayed by the low-Mw EPDM, the morphology development was also slowed, and it was possible to monitor the morphology development during TPV production. A stable morphology was achieved earlier for TPVs made with high-Mw EPDM. PP viscosity also plays an important role in both morphological development and phase inversion. A correlation between EPDM gel content evolution and morphology development was established.

The results obtained allowed to establish a general mechanism for morphology development during TPV production, including phase inversion. Starting from PP dispersed in an EPDM matrix, at the early stages (30–45 s after cross-linking initiation) the EPDM matrix breaks down and the PP coalesces, leading to the formation of elongated EPDM and PP domains, appearing as a lamellar structure. Between 60–90 s, different types of morphology, such as PP dispersed in the EPDM phase, lamellar structures, elongated EPDM particles and dispersed EPDM particles were observed. Only at 120 s was EPDM fully dispersed in the PP matrix.

References

[1] De SK, Bhowmick AK. Thermoplastic elastomers from rubber–plastic blends. New York: Ellis Horwood, 1990.

[2] Coran AY, Patel RP. Thermoplastic elastomers based on dynamically vulcanised elastomer/thermoplastic blends. In: Thermoplastic Elastomers, Holden G, Hans RK, Quirk RP, editors. Munich: Hanser Publishers, 2nd ed, 1996. p. 143-181.

[3] Karger-Kocsis J. Thermoplastic rubbers via dynamic vulcanization. In: Polymer blends and alloys, Shonaike GO, Simon GP, editors. New York: Marcel Dekker, 1999. p.125-153.

[4] van Duin M. Recent developments for EPDM-based thermoplastic vulcanisates. Macromol Symp 2006;233(1):11-16.

[5] Kresge EN. Rubbery Thermoplastics blends. In: Polymer Blends, Paul DR, Newman S, editors. New York: Academic Press, Vol.II, 1978.

[6] Abdou-Sabet S, Patel RP. Morphology of elastomeric alloys. Rubber Chem Technol 1991;64(5):769-779.

[7] Goharpey F, Katbab AA, Nazockdast H. Formation of rubber particle agglomerates during morphology development in dynamically crosslinked EPDM/PP thermoplastic elastomers. Part 1: Effects of processing and polymer structural parameters. Rubber Chem and Thecnol 2003;76(1):239-252.

[8] Radusch HJ, Pham T. Morphology formation in dynamic vulcanized PP/EPDM blends. Kautsch Gummi Kunstst 1996;49(4):249-257.

[9] Radush HJ. Phase morphology of dynamically vulcanized thermoplastic vulcanizates. In: Micro-and nanostructured multiphase polymer blend system: Phase Morphology and Interfaces, Harrats C, Thomas S, Groeninckx G, editors. Taylor & Francis, 2006.

[10] Bhadane PA, Virgilio N, Favis BD, Champagne MF, Huneault MA, Tofan F. Effect of dynamic vulcanization on Co-continuous morphology. AIChE J 2006;52(10): 3411-3420.

[11] Nicolini A, de Campos Rocha TLÁ, Jacobi MAM. Dynamically vulcanized PP/EPDM blends: Influence of curing agents on the morphology evolution. J Appl Polym Sci 2008;109(5):3093-3100.

[12] Abdou-Sabet S, Datta S. Thermplastics Vulcanizates. In: Polymer Blends – Volume 2: Performace, , Paul DR, Bucknall CB, editors. Wiley Interscience, 2000. p.517-554.

[13] Machado AV, Duin M van. Dynamic vulcanisation of EPDM/PE-based thermoplastic vulcanisates studied along the extruder axis. Polymer 2005;46(17):6575-6586.

[14] Verbois A, Cassagnau P, Michel A, Guillet J, Raveyre C. New thermoplastic vulcanizate, composed of polypropylene and ethylene-vinyl acetate copolymer crosslinked by tetrapropoxysilane: Evolution of the blend morphology with respect to the crosslinking reaction conversion. Polym Int 2004;53(5):523-535.

[15] Sengupta P. Morphology of olefinic thermoplastic elastomer blends: A comparative study into the structure – property relationship of EPDM/PP/oil and SEBS/PP/oil blend. PhD thesis University of Twente, The Netherlands, 2004.

[16] Antunes CF, Machado AV, van Duin M. Effect of viscosity and elasticity ratios on the morphology and phase inversion of EPDM/PP blends – *Part I. Submited to J Polym Sci Part B: Polym Phys.*

[17] Favis BD. Effect of processing parameters on the morphology of an immiscible binary blend. J Appl Polym Sci 1990;39(2):285-300.

[18] Schreiber HP, Olguin A. Aspects of dispersion and flow in thermoplastic-elastomer blends. Polym Eng Sci 1983;23(3):129-134.

[19] Hu G-H, Kadri I. Modeling reactive blending: An experimental approach. J Polym Sci, part B: Polym Phys 1998;36(12):2153-2163.

[20] Scott CE, Macosko CW. Morphology development during reactive and non-reactive blending of an ethylene-propylene rubber with two thermoplastic matrices. Polymer 1994;35(25):5422-5433.

[21] Scott CE, Macosko CW. Morphology development during the initial stages of polymer-polymer blending. Polymer 1995;36(3):461-470.

[22] Machado AV, Covas JA, van Duin M. Chemical and morphological evolution of PA-6/EPM/EPM-g-MA blends in a twin screw extruder. J Polym Sci, part A: Polym Chem 1999;37(9):1311-1320.

[23] Thomas S, Groeninckx G. Nylon 6/ethylene propylene rubber (EPM) blends: Phase morphology development during processing and comparison with literature data. J Appl Polym Sci 1999;71(9):1405-1429.

[24] Coran AY, Patel RP. Rubber-thermoplastic compositions - 1. EPDM-polypropylene thermoplastic vulcanizates. Rubber Chem and Thecnol 1980;53(1):141-150.

[25] Goharpey F, Katbab AA, Nazockdast H. Mechanism of morphology development in dynamically cured EPDM/PP TPEs. I. Effects of state of cure. J Appl Polym Sci 2001;81(10):2531-2544.

[26] Antunes CF, Machado AV, van Duin M. Degradation of the rubber network during dynamic vulcanization of EPDM/PP blends using phenolic resol. Rubber Chem and Thecnol 2009;82(5):492-505.

[27] Antunes CF, Machado AV, van Duin M. Effect of viscosity ratio on the morphology and phase inversion of EPDM/PP TPVs – Part II. *Submited to J Polym Sci Part B: Polym Phys.*

[28] Van Oene H. Rheology of polymer blends and dispersions. In: Polymer Blends, Paul DR, Newman S, editors. San Diego CA: Academic Press, 1978. p.295-352.

[29] Van Oene H. Modes of dispersion of viscoelastic fluids in flow. J Colloid Interface Sci. 1972, 40(3),448–467.

[30] Deyrail Y, Cassagnau P. Phase deformation under shear in an immiscible polymer blend: Influence of strong permanent elastic properties. J Rheol 2004;48(3):505-524.

[31] Tomotika S. On the instability of a cylindrical thread of a viscous liquid surrounded by another viscous fluid. Proc R Soc Lond A 1935;150(870):322-337.

[32] Elmendorp J. Study on polymer blending microrheology. J Polym Eng Sci 1986;26(6):418-426.

[33] Deyrail Y, Michel A, Cassagnau P. Influence of the dispersion scale of reagents on the deformation of a reactive dispersed phase under shear flow. Polymer 2005;46(13):4686-4694

Chapter 7: General Conclusions

1. Conclusions

Dynamic vulcanisation of EPDM/PP blends was investigated to obtain better knowledge on the morphology development during production and to establish the relationship between the morphology, viscosity ratio, composition and cross-linking. EPDM/PP blends and TPVs with different viscosity ratios and compositions were prepared in a Haake batch mixer under constant processing conditions. The cross-linking system used was resole/$SnCl_2.H_2O$.

Dynamic vulcanisation of EPDM/PP using a commercial EPDM and different PPs was investigated in Chapter 3. It was shown that the cross-linking degree decreased as the EPDM amount increases, even though the amount of the cross-linking agents was kept constant relative to EPDM amount. The action of both high shear and elongation stresses and high temperature induces degradation of the EPDM network during dynamic vulcanisation. The results illustrated that degradation of the EPDM network in a TPV formulation is minimized if EPDM is the dispersed phase and/or if the PP matrix has low viscosity.

Co-continuity and phase inversion region of EPDM/PP blends with different viscosity and elasticity ratio was studied in Chapter 4. While co-continuity region was determined using selective solvent extraction combined with SEM, phase inversion region was identified by SEM-BSE. The results showed that a large composition range of co-continuity morphologies of EPDM/PP blends existed in a wide range of viscosity ratios. The co-continuity region was dependent on the EPDM rheological properties and also on the melt viscosity and elasticity of the major phase. Phase inversion region as a function of composition was located inside of the co-continuity region. The phase inversion region depends on both viscosity ratio and composition. The phase inversion composition was estimated and the following equation was proposed to predict the composition at phase inversion.

$$\frac{\phi_{EPDM}}{\phi_{PP}} = 1.30 \left(\frac{\eta_{EPDM}}{\eta_{PP}}\right)^{0.13}$$

Chapter 5 aimed to investigate the phase inversion phenomena of EPDM/PP-based TPVs as a function of viscosity ratio and composition. Phase inversion detection was determined by SEM-BSE. EPDM gel content and swelling were measured to understand how cross-linking affected EPDM/PP blends morphology. TPVs with 30 wt.% of PP exhibited co-continuous morphologies, suggesting that cross-linking was insufficient to drive phase inversion. The morphologies of TPVs with 50 and 70 wt.% PP, consisted of cross-linked EPDM particles dispersed in a PP matrix, in the whole range of viscosity ratios. However, mainly for 50/50 compositions, some of the cross-linked EPDM particles dispersed in the PP matrix were connected. TPVs morphology was refined (the size of the dispersed phase become smaller)

as the EPDM viscosity increased, i.e., the EPDM/PP viscosity ratio increased. For TPVs, the phase inversion region depends mainly on the composition in a wide range of viscosity ratios, being located around 30 wt. % PP in a wide range of viscosity ratios between 34 and 0.01. Thus, dynamic vulcanisation shifted the phase inversion composition to lower PP content when compared to the blends. The results showed that cross-linking affects phase inversion. Nevertheless, complete phase inversion process, from a complete PP dispersed in EPDM matrix to a complete EPDM dispersed in the PP matrix, driven by cross-linking was hardly achieved. Low viscosity EPDMs facilitated the phase inversion process, suggesting that the elasticity of the PP matrix also plays an important role in the encapsulation of the EPDM phase at low viscosity ratios.

The morphology development during dynamic vulcanisation, including phase inversion phenomena driven by cross-linking was studied in chapter 6. The results demonstrated that the molecular weight of the EPDM had a significant effect on the extent of the cross-linking reaction. By using a low molecular weight EPDM it was possible to delay the cross-linking reaction and to slow down the morphology development. Consequently, for high molecular weight EPDM a stable morphology was achieved earlier. The used of a low molecular EPDM allowed to monitor in detail the morphology development during TPV production (from PP dispersed in a EPDM matrix to EPDM dispersed in a PP matrix). Therefore, a general mechanism of morphology development during TPV production and its relationship with the cross-linking level was established. The morphological mechanism starts from PP dispersed in an EPDM matrix, at the early stages (30–45 s after cross-linking begins) the EPDM matrix breaks down and the PP coalesces, leading to the formation of elongated EPDM and PP domains, appearing as a lamellar/fibrillar structure (EPDM gel content between 20 and 60 %). Between 60–90 s, different types of morphology, such as PP dispersed in the EPDM phase, lamellar structures, elongated EPDM particles and dispersed EPDM particles co-exist. At 120 s a stable morphology, consisting of cross-linked EPDM particles dispersed in the PP matrix was achieved.

The methodology used in this work allowed to get important information on the phase morphology of the EPDM/PP blends and also on phase inversion behaviour of blends and TPVs in a wide range of viscosity ratios and compositions. Furthermore, the morphological mechanism developed during dynamic vulcanisation was monitored and was related with the evolution of the cross-linking reaction. Therefore, this study contributed to understand the chemical and physical phenomena occurring during TPVs production. This knowledge can be used for process optimisation and to guide the development of improved models.

2. Future Work

Although, TPVs are already commercially available since 1970's and a large number of studies have been published, many fundamental questions related to the structure-properties relationships and its production are still not full understand. Of course, this is related with the complexity of TPVs materials. One of the biggest hindrance in the study of TPVs is the formation of a 3D rubber network, which is not soluble. Therefore, to study the phase morphology and to follow the kinetics of the cross-linking reaction is not straightforward.

Given the results and conclusions of the present research, some future work can be recommended:

- To investigate TPVs morphologies by electron tomography, in order to have a 3D micrograph. To get three-dimensional information on the TPVs morphology would allow clarifying if the EPDM domains are effectively dispersed in the PP matrix. Furthermore it more insight on structures formed during dynamic vulcanisation, such as, lamellar or/and fibrillar;
- Phase morphology could be investigated by means of different techniques such as dynamic stress rheometry and dynamic mechanical analysis, to identify more precisely the co-continuity window and the phase inversion composition;
- To monitor the cross-linking reaction of the EPDM by oscillatory rheological measurement to get information required for modelling the dynamic vulcanisation process;
- To study the morphology development during TPVs production using EPDM pre-mixed with the cross-linking agents;
- To study the properties of TPVs made with low-Mw EPDM;
- To investigate morphology development during dynamic vulcanisation of the TPVs made with a low molecular weight EPDM in a twin- screw extruder.